Imaging of cognitive outcomes in patients with autoimmune encephalitis

Insights from neuropsychological assessments to functional brain networks

DISSERTATION FOR THE AWARD OF THE DEGREE **DOCTOR RERUM NATURALIUM** (DR. RER. NAT.) IN PSYCHOLOGY

PRESENTED TO THE FACULTY OF LIFE SCIENCES
AT HUMBOLDT-UNIVERSITÄT ZU BERLIN

by

JOSEPHINE HEINE

Master of Science in Social, Cognitive & Affective Neuroscience (M.Sc.)

President of Humboldt-Universität zu Berlin
Prof. Dr. Peter Frensch *(acting president)*

Dean of the Faculty of Life Sciences
Prof. Dr. Dr. Christian Ulrichs

Examination committee

Prof. Dr. Isabel Dziobek (Chair), Institute of Psychology, Humboldt-Universität zu Berlin, Berlin, Germany
Prof. Dr. Rasha Abdel Rahman, Institute of Psychology, Humboldt-Universität zu Berlin, Berlin, Germany
Prof. Dr. Carsten Finke, Department of Neurology, Charité – Universitätsmedizin Berlin, Berlin, Germany
Dr. Amit Lampit, Department of Psychiatry, University of Melbourne, Melbourne, Australia
Dr. Mareike Bayer, Institute of Psychology, Humboldt-Universität zu Berlin, Berlin, Germany

The doctoral viva voce is scheduled for March 2, 2022 | https://doi.org/10.18452/2446

Abstract

Autoimmune encephalitis is a recently described inflammatory disease of the central nervous system that gives rise to severe neurological and psychiatric symptoms. In some patients, the pathological antibodies are directed against structures on the neuronal cell surface, such as the N-methyl-D-aspartate receptor *(NMDA receptor encephalitis)* or the leucine-rich glioma inactivated protein 1 *(LGI1 encephalitis)*, causing memory deficits, psychosis, seizures, autonomic dysfunction, or behavioural abnormalities. The trajectory of cognitive dysfunction and the underlying long-term imaging correlates are, however, not yet fully understood.

By using advanced structural and functional neuroimaging combined with cognitive testing and an analysis of clinical data, this thesis shows that cognitive deficits persist beyond the acute phase and that hippocampal damage propagates to widespread functional network abnormalities in these patients. In LGI1 encephalitis, MRI postprocessing revealed that verbal and visual memory deficits are related to focal structural hippocampal lesions, including reduced tissue integrity on diffusion imaging and volume loss across several hippocampal subfields, such as CA2/3 and CA4/dentate gyrus. These hippocampal lesions propagate to brain areas outside the limbic system through aberrant resting-state connectivity of the default mode network (DMN) and the salience network. In NMDA receptor encephalitis, a longitudinal analysis of neuropsychological data describes persistent cognitive deficits, especially in the memory and executive domains, despite good physical recovery several years after the acute disease. Lastly, a transdiagnostic analysis of hippocampal shape changes reveals that the anterior hippocampus is particularly vulnerable to immune-mediated damage across diagnoses.

In conclusion, these results demonstrate that cognitive symptoms in autoimmune encephalitis can persist beyond discharge from acute neurological care. Both discrete structural hippocampal damage and changes in macroscopic functional networks shed light on the pathophysiological basis of these symptoms. These findings help to explain how the brain responds to pathological damage in autoimmune encephalitis and have substantial implications for long-term patient care and the design of future clinical studies.

Keywords

Limbic encephalitis · memory disorders · neuroimmunology · neuroplasticity · hippocampus · brain imaging

Zusammenfassung

Die Autoimmunenzephalitis ist eine kürzlich beschriebene entzündliche Erkrankung des zentralen Nervensystems, die mit schwerwiegenden neurologischen und psychiatrischen Symptomen einhergehen kann. Bei einigen Patientinnen und Patienten richten sich die pathologischen Antikörper gegen Strukturen auf der Nervenzelloberfläche, wie den N-Methyl-D-Asparate-Rezeptor *(NMDA-Rezeptor-Enzephalitis)* oder das Leucine-Rich Glioma-Inactivated Protein 1 *(LGI1-Enzephalitis)*, und rufen dadurch Gedächtnisdefizite, Psychosen, epileptische Anfälle, eine autonome Dysfunktion oder Verhaltensveränderungen hervor. Derzeit ist hingegen noch nicht ausreichend verstanden, welche pathologischen Veränderungen zu den kognitiven Defiziten führen und welche neuropsychologischen und bildgebenden Langzeitoutcomes zu erwarten sind.

Anhand von strukturellen und funktionellen Bildgebungsanalysen im Kontext kognitiver Untersuchungen und der Auswertung klinischer Verläufe zeigt diese Dissertation, dass kognitive Defizite auch nach der akuten Phase der Autoimmunenzephalitis fortbestehen können. Dabei führen Läsionen des Hippocampus zu weitreichenden Veränderungen in funktionellen Hirnnetzwerken. Bei der LGI1-Enzephalitis gehen verbale und visuelle Gedächtnisdefizite mit fokalen strukturellen Läsionen einher, einschließlich verminderter mikrostruktureller Integrität in der Diffusionsbildgebung und Volumenminderung in mehreren hippocampalen Subregionen (z.B. CA2/3 und CA4/Gyrus Dentatus). Durch eine funktionelle Störung der Resting-State-Konnektivität des Default-Mode- und Salienznetzwerkes beeinträchtigen diese Hippocampusläsionen auch Hirnregionen außerhalb des limbischen Systems. Bei Patientinnen und Patienten mit NMDA-Rezeptor-Enzephalitis finden sich in der longitudinalen neuropsychologischen Untersuchung trotz guter allgemeiner Genesung auch noch mehrere Jahre nach der Akutphase persistierende Defizite des Gedächtnisses und exekutiver Funktionen. Zuletzt zeigt eine transdiagnostische Analyse hippocampaler Oberflächenveränderungen, dass der anteriore Hippocampus über verschiedene Erkrankungen hinweg eine erhöhte Vulnerabilität gegenüber immunvermittelten pathologischen Prozessen aufweist.

Diese Ergebnisse legen nahe, dass kognitive Symptome auch noch nach der Entlassung aus der akuten stationären Behandlung fortbestehen können. Sowohl umschriebene strukturelle Hippocampusläsionen als auch Veränderungen in makroskopischen funktionellen Hirnnetzwerken tragen zur pathophysiologischen Erklärung dieser Symptome bei. Zudem erlauben diese Ergebnisse einen Einblick in neuroplastische Veränderungen des Gehirns nach einer Autoimmunenzephalitis und haben weitreichende Implikationen für die Langzeitversorgung und das Design zukünftiger klinischer Studien.

Schlüsselbegriffe

Limbische Enzephalitis · Gedächtnisstörungen · Neuroimmunologie · Neuroplastizität · Hippocampus · Bildgebung

List of articles

This thesis is based on the following publications, which are referred to in the text by their Roman numerals.

I. **Heine, J.,** Pruess, H., Bartsch, T., Ploner, C. J., Paul, F., & Finke, C. (2015). *Imaging of autoimmune encephalitis – Relevance for clinical practice and hippocampal function*. Neuroscience, 309, 68-83. [a]

II. Finke, C., Pruess, H., **Heine, J.,** Reuter, S., Kopp, U. A., Wegner, F., Bergh, F.T., Koch, S., Jansen, O., Münte, T., Deuschl, G., Ruprecht, K., Stöcker, W., Wandinger, K.P., Paul, F., & Bartsch, T. (2017). *Evaluation of cognitive deficits and structural hippocampal damage in encephalitis with leucine-rich, glioma-inactivated 1 antibodies*. JAMA Neurology, 74(1), 50-59. [b]

III. **Heine, J.,** Pruess, H., Kopp, U. A., Wegner, F., Bergh, F.T., Münte, T., Wandinger, K.P., Paul, F., Bartsch, T., & Finke, C. (2018). *Beyond the limbic system: disruption and functional compensation of large-scale brain networks in patients with anti-LGI1 encephalitis.* Journal of Neurology, Neurosurgery & Psychiatry, 89(11), 1191-1199. [c]

IV. **Heine, J**., Ly, L.T., Lieker, I., Slowinski, T., Finke, C., Pruess, H., & Harms, L. (2016). *Immunoadsorption or plasma exchange in the treatment of autoimmune encephalitis: a pilot study.* Journal of Neurology, 263(12), 2395-2402. [d]

V. **Heine, J.,** Kopp, U.A., Klag, J., Pruess, H., Ploner, C., & Finke, C. (under revision). *Long-term cognitive outcome in anti-NMDAR encephalitis*.

VI. **Heine, J.,** Pruess, H., Scheel, M., Brandt, A.U., Gold, S.M., Bartsch, T., Paul, F., & Finke, C. (2020). *Transdiagnostic hippocampal damage patterns in neuroimmunological disorders.* NeuroImage: Clinical, 102515. [e]

Content

Preliminaries

Memory is a peculiar thing – we often only notice it if it no longer works the way it used to. These little slips in memory function reveal how strongly memory processes are linked to our day-to-day experiences. This includes not only the classic abilities to recall a fact read in an article or to remember a name. Predicting the future based on past experiences, daydreaming, making a connection between previously learned pieces of information, or telling a story all rely on intact memory processes. What is more, the coherent encoding and retrieving of autobiographical events create a sense of identity – a narrative that glues together seemingly random events to a personal life story. A large portion of our daily episodic memories are encoded incidentally – i.e. without the conscious effort to memorise. While only a smaller portion undergoes consolidation to long-term storage, some single memories may persist for decades, if not an entire life span.

Many of the most widely known neurological diseases, such as Alzheimer's dementia, cause progressive or largely irreversible memory impairment. In some patients with severe memory deficits, pathological processes can differentially disrupt learning and recollection – resulting in an inability to form new memories (e.g. in anterograde amnesia), to recall previous episodes (e.g. in retrograde amnesia), or both. A new window for clinical memory research has opened with the recent description of a new group of immune-mediated brain diseases. In *autoimmune encephalitis*, antibodies from a patient's own immune system bind to and disrupt the function of neuronal cell surface structures. This leads to an inflammation of the brain tissue. In some cases, the inflammation predominantly affects the medial temporal lobes and causes a circumscribed clinical picture of memory impairment, affective lability, and temporal lobe seizures – the so-called *limbic encephalitis*. Controlling this excess immune response and removing the pathological autoantibodies are some of the main treatment goals. Once the acute brain inflammation has remitted, the recovery phase can take months to years. Many patients experience persistent memory problems or report a selective retrograde amnesia spanning the time of their hospital stay. With this mainly monophasic disease course and partially reversible disruption of memory function, autoimmune encephalitis provides a unique opportunity for insights into the pathology of human cognition.

The presumably first available description of paraneoplastic syndromes, i.e. cancer-related autoimmune encephalitis syndromes, dates back to 1888.[1] The neurologist Hermann Oppenheim describes a case series of three patients presenting with profound neurological symptoms in the presence of tumour, but no macro- or microscopically observable brain pathology. Despite the evident unavailability of antibody testing at that time and the corresponding absence of a secured diagnosis, these case descriptions illustrate one of the major challenges of autoimmune encephalitis. The three described female patients suffered from agnosia, cognitive and language deficits, affective changes, seizures, and progressive paralysis co-occurring with gastric, uterine, and metastatic breast cancer. Surprisingly, histological changes in the meningeal or brain tissue were not observed. Yet, Oppenheim proceeds to deduce a connection between the presence of carcinoma and the focal neurological symptoms, relating them to the presence of yet unknown 'toxic products' in the brain.[2]

Around 130 years later, research has made substantial progress with the continuous discovery of neuronal autoantibodies[3,4] and their pathogenicity.[5] The historical case descriptions were interpreted to be highly suggestive of a paraneoplastic syndrome associated with onconeuronal antibodies.[2] Here, antibodies are directed against proteins inside of the neuron – so-called *intracellular antigens* – and almost always associated with an underlying tumour. The neuronal antigen can be ectopically expressed on the surface of the tumour and thus trigger the immune system to produce antibodies. In the brain, these antibodies cannot directly reach their intracellular target proteins. Here, a cytotoxic T-cell response eventually leads to irreversible damage and the corresponding neurological symptoms.[6]

An autoimmune encephalitis can also be caused by a newly discovered group of antibodies which target receptors or secreted proteins on the outer surface of the neuron – so-called *neuronal surface antigens*. In contrast to the previously described intracellular antigens, an autoimmune encephalitis with antibodies against neuronal surface antigens can occur in the absence of underlying tumours and responds better to immunotherapy. The following sections provide an overview of the disease mechanisms and their implications for studying cognition in this novel group of diseases.

To date, several cell surface structures have been identified as targets in autoimmune encephalitis. Autoantibodies bind to an extracellular epitope of a protein on the outer surface of the cell and can be detected in the patients' cerebrospinal fluid (CSF) and serum using cell-based assays or immunohistochemical staining of rodent brain tissue. One of the most common autoantibodies is directed against the N-methyl D-aspartate (NMDA) receptor, one of the brain's major glutamate receptors and key component of life-long neuroplasticity. In LGI1 encephalitis, antibodies bind to the leucine-rich glioma-inactivated 1 (LGI1) protein. As a part of the voltage-gated potassium channel, this protein orchestrates synaptic transmission between pre- and postsynaptic protein complexes.[4,7] These two subtypes are among the most frequent autoimmune encephalitides and therefore shall be the focus of this thesis.

Apart from these two prominent examples, other autoantibodies have been identified, i.e. against the α-amino-3-hydroxy-5-methyl-4-isoxazolepropionic acid (AMPA) receptor or the γ-aminobutyric acid A ($GABA_A$) receptor. Although the specific symptom presentation and likelihood of tumour association can vary between these subtypes of autoimmune encephalitis, they have in common that all antibodies interfere with protein interactions and normal receptor function. Antibody-mediated processes like cross-linking and internalisation can, for instance, reduce the surface density of NMDA receptors.[8] Decreased levels of these proteins on the cell surface lead to electrophysiological changes in NMDAR-dependent synaptic signalling. To this extend, the antibodies are directly pathogenic.[5] In addition, the erroneous presence of the antibodies in the central nervous system is part of a larger immune response causing immune cell infiltration and inflammation of the brain tissue.

Although the cause of the autoimmune reaction that leads to encephalitis is not fully understood in all cases, several hypotheses have been put forward. Established triggers include the presence of tumours. In NMDA receptor encephalitis, for instance, about 30-40% of the predominantly female patients have an ovarian teratoma, a mostly benign tumour of the ovaries.[9] Pluripotent cells in this germ cell tumour can develop into different types of tissue, including neuronal tissue. It is hypothesized that neuronal receptors in this peripheral tumour are recognised by the immune system, which induces an autoimmune reaction. Alternatively, a preceding viral encephalitis appears to increase the susceptibility to secondary autoimmune mechanisms. This hypothesis is supported by the increased prevalence of NMDA receptor antibodies in patients with herpes simplex encephalitis, presumably due to loss of immune tolerance.[10,11] A genetic predisposition may be another contributing factor.[12] In other cases without preceding viral encephalitis or in which no tumour can be detected, the cause remains to be discovered.

Prevalence & incidence

Recent population-based studies of autoimmune encephalitis estimated an *incidence* of 0.7-1.2/100,000 person-years (2006-2018).[13,14] In line with the discovery of novel antibody targets and the increasing awareness among healthcare professionals involved in the diagnosis, the incidence has increased steadily. NMDA receptor encephalitis, as one of the most common subtypes, has an estimated incidence of 1.5 per million population per year.[15] In 2012, its *prevalence* surpassed that of individual viral causes in young patients in the California Encephalitis Project.[16] Additionally, the prevalence of autoimmune encephalitis was found to have approached that of infectious encephalitides in another study in 2014.[14]

In general, however, autoimmune encephalitis remains a rare neurological disorder. The NMDA receptor (2007)[3,17] and the LGI1 protein (2010)[4] were two of the first described antibody targets on the neuronal cell surface and rank among the most frequent subtypes (*prevalence* of 0.6-0.7/100,000, and 0.6-0.8/100,000, respectively).[14,18] To provide a perspective, a nationwide study reported an annual incidence of 0.83/million for encephalitis associated with antibodies against the LGI1 protein in the Netherlands[18] – i.e. fewer than 15 new cases per year. In comparison, there have been 13,789 stroke events in the Netherlands in 2015.[19] Despite being a relatively rare neurological disorder, it is crucial to identify this treatable cause of brain inflammation, as many patients experience significant improvement once the immunotherapy is started.

Clinical signs & symptoms

Symptom onset is subacute in most patients with autoimmune encephalitis. In NMDA receptor encephalitis, about 70% of the patients experience a prodrome of unspecific symptoms such as fever, headache, or diarrhoea two weeks before the onset of neuropsychiatric symptoms.[20] In LGI1 encephalitis, around 34% of the patients experience preceding faciobrachial dystonic seizures (FBDS):[21] a brief, frequent event typically involving the arm and ipsilateral side of the face with usually intact consciousness.[22] FBDS can be followed by a state of confusion and are specific to LGI1 antibodies. In other cases, symptoms may gradually develop over weeks with subtle memory deficits or behavioural alterations as first signs. The onset of striking symptoms, such as psychosis, hallucinations, memory dysfunction, movement disorders, or new-onset seizures often mark the point in time when patients or their caregivers seek medical attention. From then on, the disease course is rapidly progressive over several days or weeks and should prompt the search for autoantibodies.

Diagnostic criteria have recently been established by an international group of experts based on clinical experiences and a syndrome-based approach.[23] Since the assessment of some clinical criteria may lag over several weeks or may not be readily available to all centres, such as in the case of antibody testing in the cerebrospinal fluid (CSF), the diagnostic approach distinguishes *possible autoimmune encephalitis* and *definite autoimmune limbic encephalitis* criteria. A patient is diagnosed with *possible autoimmune encephalitis* if they fulfill the following criteria:

- *1. A subacute onset of working memory deficits, altered mental status (i.e. decreased or altered level of consciousness, lethargy, or personality change), or psychiatric symptoms*
- *2. At least one of the following: new focal CNS findings, seizures that cannot be explained by a previously known seizure disorder, increased count of white blood cells in the CSF (>5 cells/mm³ so-called CSF pleiocytosis), MRI findings suggestive of encephalitis*
- *3. A reasonable exclusion of alternative causes (e.g. viral encephalitis)*

To date, subtype-specific diagnostic criteria exist only for NMDA receptor encephalitis. A *probable* diagnosis demands the following criteria:

- *1. A rapid onset (<3 months) of at least four of the six following major groups of symptoms: abnormal (psychiatric) behaviour or cognitive dysfunction; speech dysfunction (pressured speech, verbal dysfunction, mutism); seizures; movement disorder, dyskinesias, or rigidity/abnormal postures; decreased level of consciousness; autonomic dysfunction or central hypoventilation*
- *2. At least one of the following laboratory study results: abnormal EEG (focal or diff use slow or disorganised activity, epileptic activity, or extreme delta brush); CSF with pleocytosis or oligoclonal bands*
- *3. A reasonable exclusion of other disorders*

If a systemic teratoma is found, three of the above symptoms are sufficient for the diagnosis. A diagnosis of *definite* NMDA receptor encephalitis additionally requires the detection of IgG GluN1 antibodies in face of at least one of the above symptoms.

The term *limbic encephalitis* refers to a specific clinical syndrome in which patients develop characteristic symptoms that suggest a pathology of the limbic system. These include confusion,

mood changes, memory alterations, and temporal lobe seizures in some cases. The diagnosis of *definite autoimmune limbic encephalitis*[23] is made if a patient:

- *1. has a subacute onset and rapid progression of working memory deficits, seizures, or psychiatric symptoms, suggesting involvement of the limbic system*
- *2. presents with bilateral abnormalities restricted to the medial temporal lobes on brain imaging (i.e. T2-weighted fluid-attenuated inversion recovery (FLAIR) MRI or positron emission tomography (PET))*
- *3. has an elevated white blood cell count (>5 cells/mm³) in the CSF, and/or epileptic or slow-wave activity of the temporal lobes on EEG, and*
- *4. other alternative causes can be excluded.*

A positive autoantibody test is obligatory for the diagnosis if one of the criteria I-III has not been met. Here, several autoantibodies preferentially manifest as limbic encephalitis – e.g. antibodies against LGI1, the AMPA receptor or $GABA_B$ receptor. Accumulating evidence suggests that patients with autoimmune encephalitis benefit from an early start of immunotherapy.[9,24,25] The current recommendation is therefore to initiate preliminary treatment while waiting for further diagnostic results from antibody tests to confirm this diagnosis.[23] Specific diagnostic criteria have furthermore been developed cases in which a diagnosis of autoimmune encephalitis is probable but no currently known antibodies have been detected *(autoantibody-negative)*.[23]

A recent multicentre analysis evaluated the clinical data from 50 patients who received the diagnosis of autoimmune encephalitis between 2007-2016 and who retrospectively fulfill the 2016 diagnostic criteria.[26] Encephalitis was the initially suspected diagnosis in only 32% of these patients. Here, an initial diagnosis of infectious encephalitis was common (18%), and only 7/50 patients received an initial diagnosis of autoimmune encephalitis (14%). Other admission diagnoses covered a wide range of neurologic and psychiatric diseases, such as epilepsy, dementia, transient ischaemic attack, transient global amnesia, dissociative disorder, meningitis, amyotrophic lateral sclerosis, or normal pressure hydrocephalus. A third of the patients were initially admitted to a psychiatric hospital. Even though there have been substantial efforts in conducting research and increasing awareness over the years, this study points out one of the greatest challenges: recognising autoimmune encephalitis is not always straightforward. Unspecific prodromal symptoms, untypical presentations, prominent seizures or psychotic symptoms can complicate and delay a fast diagnosis. The clinical decision making therefore benefits from a precise description of the disease course and symptoms, as well as the evaluation of laboratory tests and treatment options.

Over the past ten years, awareness about autoimmune encephalitis has significantly increased in health care professionals and the available knowledge about diagnosis, treatment options, and prognostic factors has expanded rapidly. Nonetheless, the diagnosis is still delayed in some patients. Besides incomplete awareness in the early years after discovery, one of the reasons is that novel autoantibodies are continuously discovered and the clinical phenotypes of existing autoimmune encephalites are quite heterogeneous. For instance, around 50% of the encephalitis patients with antibodies against the NMDA receptor experience autonomic dysfunction.[9,27] This can be associated with loss of consciousness, breathing dysfunction, or coma, and require admission to an intensive care unit, but is generally uncommon in LGI1 encephalitis. Moreover, some symptoms such as prominent hallucinations or grand-mal seizures may initially divert the attention from an autoimmune origin and misleadingly point to schizophrenia or epilepsy. In a recent analysis, psychiatric abnormalities were the presenting sign in 60% of the 100 patients with autoimmune encephalitis, and a third of them were initially admitted to a psychiatric hospital.[28] Antipsychotic or antiepileptic drugs alone, however, do not lead to a full remission of symptoms as they do not control the excess autoimmune response. These differences in clinical presentation also highlight the need for antibody-specific descriptions of cognitive symptoms, neuroimaging findings, and long-term outcomes in the years after the acute phase.

Another reason is that the diagnostic process can be complicated by normal test results. Although CSF abnormalities are included as a possible diagnostic criterion for autoimmune encephalitis, recent analyses of larger cohorts suggest a varying proportion of inflammatory profiles among autoantibody subtypes. For instance, while a mild increase in white blood cell count (pleiocytosis) is common in NMDA receptor encephalitis and oligoclonal bands can occur during the disease course, around 60% of patients with LGI1 encephalitis show no abnormal CSF findings.[29,30] EEG abnormalities, although common, are mostly unspecific apart from a characteristic delta brush in 30% of NMDA receptor encephalitis patients.[31] Despite severe symptoms during the acute phase of the disease, clinical MRI scans do not necessarily reveal pathological changes in all patients. This *clinico-radiological paradox* – the absence of observable neuroimaging changes in face of clinical symptoms – not only sparks interesting scientific questions but can also hinder the correct diagnosis and prompt initiation of treatment.

Once diagnosed, an immediate initiation of immunotherapy is recommended to control the aberrant immune reaction.[31] The first-line treatment regimen can include high-dose glucocorticoids, intravenous immunoglobulins, and removing the antibodies and other immune

complexes from the patient's blood plasma using therapeutic apheresis. If the screening reveals an underlying tumour, the removal of the tumour is essential for achieving a treatment response. If clinical improvement cannot be achieved under first-line therapy alone, second-line therapy is administered and can include rituximab or cyclophosphamide. Although observational cohort studies that evaluate treatment regimens exist,[e.g. 23] randomised-controlled trials in this very rare disease are yet to be conducted.

Most patients experience a monophasic disease course without relapses. Nonetheless, little is known about the cognitive long-term outcomes in patients with autoimmune encephalitis with cell surface autoantibodies. The pronounced memory deficits during the acute phase are a hallmark symptom. Indeed, many patients report subjective cognitive complaints after discharge from acute hospital care. Frequently mentioned complaints include the difficulty to concentrate, anterograde memory problems, or memory gaps of several months for the time of the acute phase. The latter most strikingly illustrates the disruption of neuronal function. For NMDA receptor encephalitis, the hypothesis has been put forward that the neuronal dysfunction caused by the antibodies is *reversible* rather than a structural, irreversible disruption.[32] In light of the remission of overt symptoms following immunotherapy, this appears to be a logical assumption. It is, however, not fully clear how this temporary, antibody-mediated dysfunction affects the long-term structural and functional integrity of the affected brain structures – and which cognitive sequelae can be expected.

Medial temporal lobe pathology

Of particular interest for this disease is pathological damage to the medial temporal lobe. The three main reasons for this shall be discussed in the following. (I) First, when neuroradiological findings are reported based on clinical MRI scans, they often describe changes to *mesiotemporal brain areas (Figure A)*.

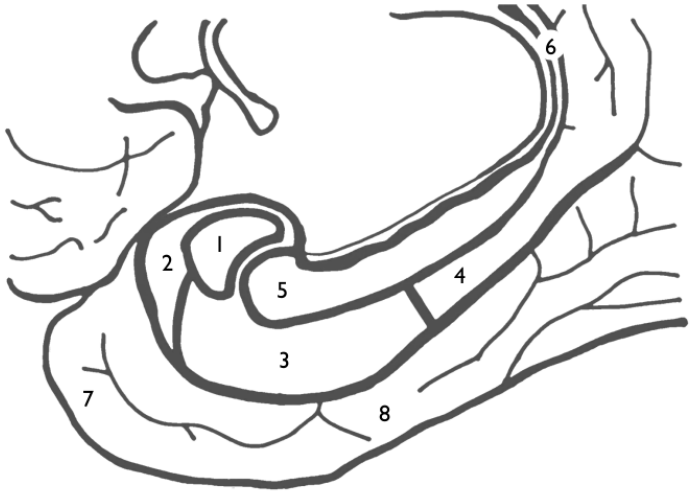

Figure A. Medial temporal lobe (sagittal view)
1 Amygdala
2 Perirhinal cortex
3 Entorhinal cortex
4 Parahippocampal gyrus
5 Hippocampus
6 Fornix
7 Temporal pole
8 Inferior temporal gyrus

The medial temporal lobe (MTL) is involved in major cognitive functions, including associative learning, episodic memory processes, spatial navigation, social cognition, and emotion processing. Anatomically, it comprises a group of brain structures in close proximity to one another: The amygdala *(Fig. A:1)* is located anterior to the head of the hippocampus *(Fig. A:5)*. The hippocampus itself *(Fig. A:5)* stretches from the anterior to posterior portion of the temporal lobe and is surrounded by the perirhinal cortex *(Fig. A:2)*, the entorhinal cortex *(Fig. A:3)*, and the parahippocampal gyrus (*Fig. A:4)* along the longitudinal axis. The fornix *(Fig. A:6)* extends the posterior end of the hippocampus into a curved white matter fibre tract. Clinical imaging findings involving the medial temporal lobes have been reported in previous case series for both LGI1[4] encephalitis and NMDA receptor encephalitis.[17]

(II) Second, prominent cognitive symptoms during the acute phase of autoimmune encephalitis are similar to those of classical patient reports of medial temporal damage. Many of these pioneering case studies paved the way for understanding brain function in contemporary cognitive neuroscience. Due to the nature of these case reports, there is nonetheless an inherent variation concerning the underlying disease, the extent of the lesion, the comprehensiveness of neuropsychological examination, and, if available at the time, imaging technology. For instance, the report of severe amnesia following a bilateral surgical resection of the medial temporal lobe in a patient with intractable epilepsy is a seminal case study in cognitive neurology.[33] As a consequence of this ultima ratio and, at the time, rather experimental therapeutic procedure, the patient (H.M.) developed unpredicted temporally graded retrograde and marked anterograde amnesia. H.M. received a rich neuropsychological characterisation in the years after his surgery. A post-mortem 3D microscopic model revealed that the lesions were less extensive than estimated at the time of surgery, with part of the ventral perirhinal cortex and most of the parahippocampal cortex unaffected.[34] The resected areas, however, still included the cortex of the medial temporal pole, the amygdala, the entorhinal cortex, and the anterior half of the hippocampal formation.

H.M.'s memory deficits were predominantly anterograde in nature and particularly affected the formation of new explicit memory content. In contrast, both retrograde and anterograde memory were affected in a case with more extensive brain damage due to viral encephalitis.[35] Patient D.B.R. developed herpes simplex encephalitis with characteristic symptoms of seizures, fever, and episodes of confusion. He recovered clinically from a three-day coma and was discharged four weeks later with a normal neurological examination, including normal motor and perceptual function. His pronounced retrograde amnesia, however, spanned the first five decades of his life and was largely episodic in nature. Although he recalled some residual semantic facts about his own life and family, the memories lacked spatiotemporal context and personal perspective. A CT scan revealed widespread damage to the orbitofrontal and anterior cingulate

cortex, the insular cortex, the parahippocampal cortex, and almost all of the limbic system, while his basal ganglia, thalamus, and sensorimotor cortices were intact. D.B.R.'s postencephalitic damage thus caused both amnesia for previously learned episodes and impaired the formation of new memories by affecting widespread neo- and allocortical areas.

A last example shall illustrate the significance of lesion extent and location for memory disorders. In this case study, the patient acquired a selective lesion to the hippocampal subfield cornu ammonis 1 (CA1) due to an ischaemic episode. While R.B. performed as well as control participants at recalling past episodic and semantic memories, his focal hippocampal lesion caused a nearly selective anterograde amnesia. In everyday observations, his caregivers noted that he needed assistance in recounting recent activities or asked the same questions within a short time. Neuropsychologically, R.B. was impaired on an associative learning task which required to memorise word pairs over a delay. Despite a perfect copy of a complex geometrical figure, he could only reproduce little of this visual content after a delay. In conclusion, the evidence from these case studies, together with larger group studies in the following years,[e.g.36–38] suggests that mesiotemporal structures are amongst the most vulnerable brain areas when facing pathology. Additionally, a relatively small but selective lesion of a critical brain region can be sufficient to cause memory dysfunction.

(III) The third reason for the interest in mesiotemporal regions in the context of autoimmune encephalitis is that the distribution of the antibody targets mirrors both clinical symptoms and neuroradiological findings. Although NMDA receptors are expressed throughout the cerebrum, their density varies depending on the anatomical region and cortical layer. The hippocampus has by far the highest density of NMDA receptors, with particularly high levels in the stratum oriens and stratum radiatum of area (CA1) and the inner molecular layer of the dentate gyrus (DG).[39] Additionally, a moderate density of NMDA receptors is detected in the stratum lacunosum-moleculare of CA1, the stratum oriens and stratum radiatum of CA3, and in the DG molecular layer. Outside of the hippocampus, the receptor is expressed in the striatum, the insular cortex, the pyriform cortex, the perirhinal cortex, the anterior cingulate and frontal cortex.[39,40] However, extrahippocampal regions like the frontal cortical layers 1-3 still only show around 50% of the NMDA receptor density found in CA1 and the DG.[40] These anatomical variations shed light on why memory deficits and temporal lobe seizures are among the most prominent symptoms during the acute phase.

The case is similar in LGI1 encephalitis. The LGI1 protein forms part of a transsynaptic protein complex and connects two epilepsy-related receptors. By linking the presynaptic ADAM 23 (disintegrin and metalloproteinase domain-containing protein 23) with the postsynaptic ADAM22, LGI1 facilitates interactions between presynaptic voltage-gated potassium channels and postsynaptic AMPA receptors.[7] These play a crucial role in orchestrating neuronal excitation

due to two major mechanisms: On the one hand, voltage-gated potassium channel complexes help returning the depolarized cell back to the resting state after an action potential. On the other hand, AMPA (α-amino-3-hydroxy-5-methyl-4-isoxazolepropionic acid) receptors are, like NMDA receptors, major glutamate receptors of the central nervous system and involved in synaptic plasticity – including long-term potentiation during learning. Reduced LGI1 levels thus lead to abnormal synaptic transmission and seizure activity.[7] The distribution of LGI1 in the brain is even more confined to the hippocampus than that of NMDA receptors. The protein is only expressed weakly in the cerebral cortex (mainly layers V-VI). In contrast, the dentate gyrus and area CA3 of the hippocampus contain very high levels of LGI1, particularly in the pyramidal and granular layers.[41] These hippocampal subregions are described in more detail in the following.

The hippocampal formation

Figure B. Hippocampal formation (coronal view)
1 Cornu ammonis 1 (CA1)
2 Cornu ammonis 2 (CA2)
3 Cornu ammonis 3 (CA3)
4 Cornu ammonis 4 (CA4)
5 Dentate gyrus
6 Subiculum
7 Entorhinal cortex
8 Fimbria
9 Lateral ventricle

The *hippocampal formation* is formed by a set of distinct medial temporal regions. The most prominent part is the allocortical hippocampus proper, consisting of the cornu ammonis subfields and the dentate gyrus *(Fig. B:1-5)*, along with the subiculum *(Fig. B:6)*. These hippocampal subfields show a consistent order of appearance along the long axis[42] and their division is based on their intricate anatomy of distinct cytoarchitectural regions. The entorhinal cortex *(Fig. B:7)* forms the interface between the allocortical hippocampus and the neocortex.

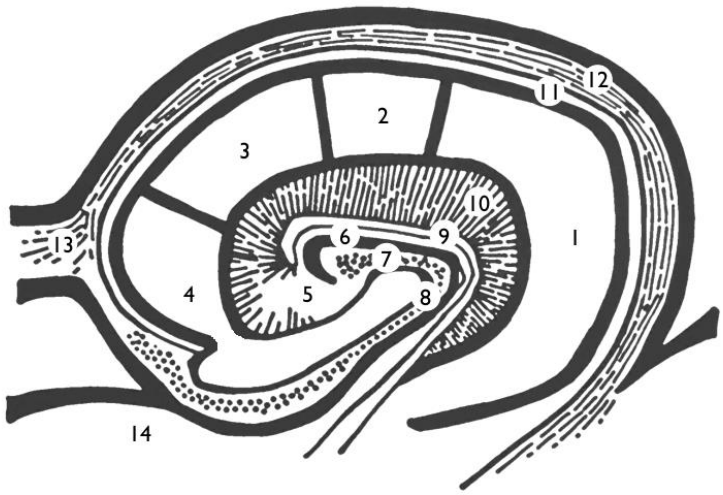

Figure C. Hippocampal subfields (coronal view)
1 Cornu ammonis 1 (CA1)
2 Cornu ammonis 2 (CA2)
3 Cornu ammonis 3 (CA3)
4 Cornu ammonis 4 (CA4)
5 Dentate gyrus:

6 Stratum moleculare
7 Stratum granulosum
8 Hilus (polymorphic layer)

9 Stratum lacunosum
10 Stratum radiatum
11 Stratum oriens
12 Alveus
13 Fimbria
14 Subiculum

CA1 *(Fig. C:1)* is one of the largest areas of the hippocampal head and integrates preprocessed input from the hippocampal circuit. It transitions laterally into the subiculum *(Fig. C:14)*, one of the main hippocampal output regions. CA1 and subiculum play an essential role in spatial processing and memory retrieval. Main functions include detecting novelty or mismatch between new and preprocessed information and maintaining overlapping representations in working memory.[43,44] Similar to CA1, accumulating evidence suggests a functional specialization of other subfields as well. The smaller area CA3 *(Fig. C:3)*, for instance, has been found to be involved in a process called *'pattern completion'*, i.e. the reactivation of an entire hippocampus-dependent memory when it is only partially presented.[43,45] The complementary process, *'pattern separation'*, also involves the dentate gyrus *(Fig. C:5)* and refers to the process of creating discrete representations in memory.[46] The dentate gyrus *(Fig. C:5)* is formed of three layers – the molecular layer *(Fig. C:6)*, the granular layer *(Fig. C:7)*, and the polymorphic layer *(Fig. C:8)* – and one of the two sites in the adult brain in which new neurons are born and subsequently integrated into the hippocampal circuit.[47]

The hippocampal formation forms part of a reciprocal network of medial temporal lobe areas, parahippocampal areas, subcortical nuclei, and neocortical association areas.[48] Information from cortical and subcortical areas enters the hippocampal formation through the entorhinal cortex. Entorhinal layers convey the input to the dentate gyrus *(Fig C:5)* through the perforant pathway. From the dentate gyrus, mossy fibres relay the input to interconnected CA3 neurons *(Fig C:3)*. Further downstream, Schaffer collaterals project to the CA1 *(Fig. C:1)* and output areas of the subiculum *(Fig. C:14)*. This circuit is termed the 'trisynaptic pathway',[43] however, there are also direct projections from the entorhinal cortex to CA3, CA1, and the subiculum. Output is conveyed back to the entorhinal cortex; and to the amygdala, nucleus accumbens, and orbitofrontal cortex within the limbic system; as

well as to the anatomically more remote anterior and posterior cingulate cortices. These pathways process input from olfactory and auditory cortices, the amygdala, and the parahippocampal and perirhinal cortices *(Fig. A:2,4)*. The parahippocampal and perirhinal cortices, in turn, relay visual input to the posterior hippocampus via the entorhinal cortex. Following processing within the hippocampus, the output is sent back from the subiculum, CA1, and parahippocampal gyrus to neocortical areas.

Aims

This doctoral thesis will investigate the neuronal correlates of cognitive impairment in autoimmune encephalitis. By synthesising insights from neuropsychological assessments, structural and functional neuroimaging – including volumetric, diffusion tensor, and functional connectivity analyses – this thesis seeks to unravel mechanisms of hippocampal vulnerability and plasticity in a network perspective of the brain. The aims are as follows:

- *To describe the cognitive and imaging profiles of the two most frequent subtypes of autoimmune encephalitis associated with neuronal cell-surface antigens: NMDA receptor encephalitis and LGI1 encephalitis.*
- *To employ advanced neuroimaging postprocessing methods to trace the origin of cognitive impairment.*
- *To investigate disease-related factors affecting the long-term outcome in autoimmune encephalitis and evaluate treatment options.*
- *To explore the trajectories of recovery using autoimmune encephalitis as a model for mesiotemporal damage.*

And

- *To improve the understanding of the pathophysiological mechanisms underlying memory impairment in neuroimmunological diseases.*

Publication I: Imaging of autoimmune encephalitis – Relevance for clinical practice and hippocampal function

Abstract

The field of autoimmune encephalitides associated with antibodies targeting cell-surface antigens is rapidly expanding and new antibodies are discovered frequently. Typical clinical presentations include cognitive deficits, psychiatric symptoms, movement disorders and seizures and the majority of patients respond well to immunotherapy. Pathophysiological mechanisms and clinical features are increasingly recognized and indicate hippocampal dysfunction in most of these syndromes. Here, we review the neuroimaging characteristics of autoimmune encephalitides, including N-methyl-D-aspartate (NMDA) receptor, leucine-rich glioma inactivated 1 (LGI1), contactin-associated protein-like 2 (CASPR2) encephalitis as well as more recently discovered and less frequent forms such as dipeptidyl-peptidase-like protein 6 (DPPX) or glycine receptor encephalitis. We summarize findings of routine magnetic resonance imaging (MRI) investigations as well as 18F-fluoro-2-deoxy-D-glucose (FDG)–positron emission tomography (PET) and single photon emission tomography (SPECT) imaging and relate these observations to clinical features and disease outcome. We furthermore review results of advanced imaging analyses such as diffusion tensor imaging, volumetric analyses and resting-state functional MRI. Finally, we discuss contributions of these neuroimaging observations to the understanding of the pathophysiology of autoimmune encephalitides.

Keywords

Hippocampus, Autoimmune encephalitis, limbic encephalitis, imaging, MRI, PET

Introduction

The first description of an autoimmune encephalitis dates back to 1888, when Hermann Oppenheim described a patient with neurological symptoms but no underlying brain pathology.[1] In the 1960s, postmortem brain sections of patients with subacute encephalitis presenting with mood and behavioral changes revealed inflammatory changes most pronounced in limbic structures, e.g. hippocampus and amygdala, resulting in the term limbic encephalitis.[49,50] At this time, the relationship between limbic encephalitis and systemic cancer was already established and first hypotheses of an autoimmune-mediated pathogenesis were put forward,[51] leading to the discovery of specific neuronal antibodies targeting intracellular neuronal antigens (e.g. Hu, Yo, Ri, Ma2, Tr, CV2) in tumor patients.[52–54] These onconeuronal antibodies are associated with classic paraneoplastic disorders such as limbic encephalitis and paraneoplastic cerebellar degeneration that respond poorly to tumor removal and immunotherapy. Antibodies are not directly pathogenic and neuronal damage rather seems to be mediated by cytotoxic T cells.[55,56]

In recent years, autoimmune encephalitides with antibodies directed against cell-surface proteins were increasingly recognized (Fig. 1). In contrast to classic paraneoplastic disorders, they occur with and without underlying tumor and frequently respond well to immunotherapy.[55,57] By targeting ion channels, receptors, or associated proteins such as N-methyl-D-aspartate (NMDA) or GABA receptors, the associated antibodies directly interfere with synaptic transmission and neuronal plasticity. Owing to the variety of antibodies directed against different cell surface proteins, autoimmune encephalitides manifest with a wide range of symptoms and neuroimaging features. Frequently, patients present with cognitive deficits including memory disturbances and imaging shows an affection of the hippocampus, a structure critically involved in the formation of memory.[58–60] Comprehensive reviews have covered pathophysiology, clinical presentation and treatment strategies of these disorders (e.g.[6,56,61–63]). Here, we provide an overview of the neuroimaging characteristics of autoimmune encephalitides with antibodies against cell-surface antigens (Table 1). We summarize observations from clinical routine MR and PET imaging and their relation to clinical characteristics and disease prognosis. Furthermore, we describe results of studies using advanced neuroimaging techniques, e.g. diffusion tensor imaging and resting-state functional magnetic resonance imaging (MRI), which shed light on pathophysiological mechanisms and which may also help in the evaluation of disease prognosis. We start by describing imaging findings in more frequent autoimmune encephalitis variants, e.g. NMDAR or leucine-rich glioma inactivated 1 (LGI1) encephalitis, and continue to include recently discovered antibodies where fewer studies or only case reports are available.

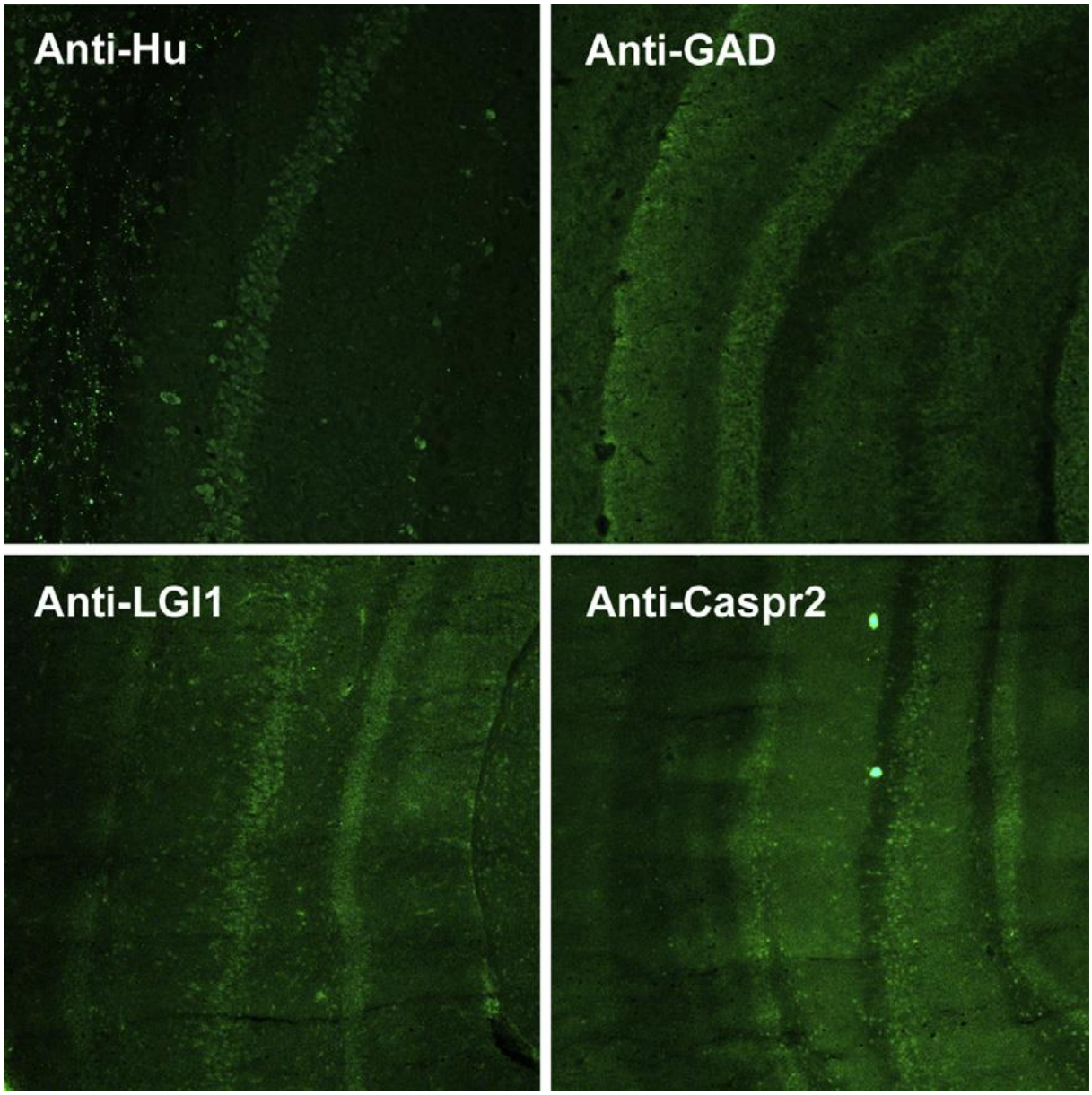

Figure 1. Antibody-positive patient serum and CSF samples display distinct staining patterns in the hippocampus. Using indirect immunofluorescence on hippocampus sections, patient serum was diluted 1:100 and incubated on rat brains overnight, followed by visualization of specifically bound antibodies with fluorescently labeled secondary anti-human antibodies. Although all patients with limbic encephalitis had strong antibody binding in the hippocampus, the immunohistochemistry pattern in different hippocampal layers varied depending on the target epitope, such as anti-Hu, anti-GAD, anti-LGI1, and anti-CASPR2.

Early studies on limbic encephalitis

Before the recent surge in discovery of antibodies against neuronal cell-surface antigens, studies investigating limbic encephalitis frequently combined analysis of patients with and without antibodies or paraneoplastic and non-paraneoplastic manifestations.[64–67] In patients with paraneoplastic limbic

encephalitis, uni- or bilateral T2 hyperintense lesions in the medial temporal lobes including the hippocampus were observed in the majority of patients and were accompanied by extra-limbic cortical and subcortical alterations in up to 40%.[64–68] Gadolinum contrast-enhancement as an indicator of an increased blood–brain barrier permeability was observed in 15–25% of the patients.[64–66] In a serial MRI study of limbic encephalitis in patients with onconeuronal antibodies, voltage-gated potassium channel (VGKC) antibodies or without detectable antibodies, swelling of medial temporal lobe structures was observed initially and followed by progressive atrophy, while hyperintensity persisted in most patients.[67] This post-inflammatory atrophy of the hippocampus contributes to persistent memory impairment and the neurological disability seen in patients in due course of the disease, representing a large part of the chronic disease burden.[69] 18F-fluoro-2-deoxy-D-glucose (FDG)–positron emission tomography (PET) imaging significantly increases the sensitivity for abnormalities in limbic encephalitis and can show medial temporal lobe hypo or hypermetabolism even in normally appearing temporal lobe structures on MRI.[70,71] Additionally, FDG–PET more often shows extra-limbic abnormalities (mainly hypermetabolism), e.g. in the brainstem, cerebellum or cerebral cortex, and seems to correlate more closely with clinical symptoms than MRI.[66] Accordingly, serial MRI and PET imaging in an anti Ma2-positive seminoma and teratoma patient revealed an increasing hypermetabolism in the left medial temporal lobe on PET, which was paralleled by a significant increase in anti-Ma2 antibody titers while left medial temporal lobe hyperintensity on MRI remained unchanged.[70]

Antibody target	NMDA receptor	LGI1
Patients with reported neuroimaging*	~ 800	~ 90
Magnetic resonance imaging (MRI)	Abnormalities in 23–50% of patients that typically are discrete and nonspecific (small white matter lesions in frontal, parietal & mediotemporal areas; thalamic, cerebellar and brainstem involvement in some patients, less frequently basal ganglia abnormalities) **Resting-state fMRI:** Disrupted hippocampal functional connectivity **Diffusion tensor imaging:** Widespread white matter damage **Overlap with demyelinating syndrome:** Multifocal T2/FLAIR hyperintense lesions **Follow-up:** Hippocampal atrophy and impaired hippocampal microstructural integrity	**FBDS stage:** Typically unremarkable, T2/FLAIR hyperintense signal alterations and contrast-enhancing basal ganglia lesions in single cases **Limbic encephalitis stage:** Uni- or bilateral T2/FLAIR hyperintensities of mediotemporal lobes in most patients; basal ganglia signal changes in some patients **Follow-up:** Frequently progression to hippocampal or whole brain atrophy, also affecting patients with formerly unremarkable MRI
Contrast-enhanced MRI	Mostly transient or faint T1 contrast enhancement of the cortex, meninges and basal ganglia in ~25% of the patients with non-contrast MRI abnormalities Mild contrast enhancement of cortical and subcortical lesions in patients with overlapping demyelinating Syndromes	**Limbic encephalitis stage:** Mild, ill-defined contrast enhancement of T2-hyperintense brain areas in ~30% of the patients Reduction of contrast-enhanced caudate nucleus and globus pallidus lesion at follow-up in one case
Positron emission tomography (FDG-PET)	Increased frontotemporal-occipital gradient (frontotemporal glucose hypermetabolism, occipital hypometabolism) Other patients reported with altered metabolism in frontal, temporal and occipital lobes, in the basal ganglia, cerebellum and brainstem; lateralized effects in some patients	**FBDS stage:** Uni- or bilateral glucose hypermetabolism of basal ganglia in single cases **Limbic encephalitis stage:** Altered basal ganglia glucose metabolism (mostly hypermetabolism) in 63–70% and altered mediotemporal metabolism (mostly hypermetabolism) in 70–75% of the cases
Single photon emission tomography (SPECT)	Increased or decreased perfusion in the medial frontal and temporal cortex in single case studies	**FBDS stage:** Hypo- or hyperperfusion in the medial temporal lobe in single cases

*Table 1. *Estimated based on provided cohort descriptions, corrected for repeatedly reported patients*

Antibody target	CASPR2	AMPA receptor
Patients with reported neuroimaging*	~ 50	18
Magnetic resonance imaging (MRI)	Normal MRI in majority of patients with Morvan's syndrome, T2/FLAIR hyperintensities in frontal and mesiotemporal areas and nonspecific periventricular white matter lesions in some patients Hyperintense medial temporal lobe signal in ~25% of patients with limbic encephalitis, neuromyotonia or Morvans's syndrome; **Follow-up:** In 3/3 patients no progression to hippocampal atrophy or sclerosis	Mesiotemporal T2/FLAIR hyperintensities in 90% of the patients, extending to anterior septal nuclei, insula, frontal, occipital or cerebellar regions in some cases **Follow-up:** Bilateral MTL abnormalities developing to hippocampal and amygdalar sclerosis in some patients, progression from unilateral to bilateral involvement over time
Contrast-enhanced MRI	-	Mild, transient contrast enhancement of the left hippocampus in one case
Positron emission tomography (FDG-PET)	Focal and generalized hyper- and hypometabolism despite normal MRI in Morvan's syndrome involving basal ganglia, orbitofrontal, anterolateral and mediotemporal regions	Hypermetabolism predominantly in left hippocampus in one case More widespread bilateral hypometabolism involving the caudate nucleus, frontal, temporal and occipital areas in one case
Single photon emission tomography (SPECT)	-	-

Table 1. (continued)

Antibody target	$GABA_A$ receptor	$GABA_B$ receptor	Dopamine D2 receptor
Patients with reported neuroimaging*	8	~ 65	12
Magnetic resonance imaging (MRI)	MRI abnormal in all patients with extensive multifocal or diffuse cortical and subcortical T2/FLAIR signal alterations Rapid progression from focal mediotemporal and frontal T2/FLAIR abnormalities to atrophy and extensive bilateral lesions in some patients	Uni- or bilateral T2/FLAIR signal increases of the medial temporal lobe, including hippocampus and amygdala, in the majority of the patients Single cases reported with frontal and temporal leukencephalopathy, hippocampal laminar necrosis, brainstem encephalitis, cerebellar lesions, basal ganglia lesions, longitudinally extensive myelitis, **Follow-up:** Progression hippocampal atrophy or frontotemporal atrophy	T2/FLAIR signal increase in caudate, putamen, globus pallidus and substantia nigra in 50% of the patients **Follow-up:** Basal ganglia atrophy and gliosis in 2 patients
Contrast-enhanced MRI	-	Contrast enhancement of cortical and subcortical lesions in frontal and temporal regions, brainstem, cerebellum and basal ganglia in single cases	-
Positron emission tomography (FDG-PET)	-	Mediotemporal hypermetabolism corresponding to T2 signal increases in two patients; diffuse cortical hypometabolism in one case	-
Single photon emission tomography (SPECT)	-	Hypoperfusion in thalamus, cerebellum, frontal, parietal and mediotemporal areas together with hyperperfusion in middle and superior temporal, precentral & postcentral cortex in one case	-

Table 1. (continued)

Antibody target	DPPX	GAD	Glycine receptor
Patients with reported neuroimaging*	20	~ 50	~ 60
Magnetic resonance imaging (MRI)	Normal MRI in major abnormalities in 4 of 13 patients; patchy periventricular and subcortical white matter T2/FLAIR signal increases and nonspecific white matter changes in single cases	Characteristic T2/FLAIR hyperintensities in the medial temporal lobe; higher FLAIR intensity values than in patients with VGKC or NMDAR antibodies; Cerebellar atrophy in ataxia patients **Follow-up:** Hippocampal sclerosis in some patients	Normal brain MRI in ~70% of patients; observed abnormalities include T2/FLAIR hyperintense white matter lesions, temporal lobe signal alterations and atrophy; small as well as longitudinally extensive spinal lesions in some patients
Contrast-enhanced MRI	-	-	T2 lesions were non-enhancing in one case; no contrast enhancement in another patient with unremarkable MRI
Positron emission tomography (FDG-PET)	-	-	.
Single photon emission tomography (SPECT)	-	-	-

Table 1. (end)

NMDA receptor antibody encephalitis

Encephalitis with antibodies against the N-methyl-D-aspartate receptor (NMDAR) ranks among the most frequent forms of autoimmune encephalitis.[72] The disease typically affects young women and is associated with an ovarian teratoma in 40–60% of patients.[9,20] Patients present with a typical clinical syndrome: Following a prodromal phase with low-grade fever, headache and fatigue, patients develop psychiatric symptoms including anxiety, psychosis, delusions, and hallucinations. With further progression, the disease may include abnormal movements such as orofacial dyskinesia and dystonia, autonomic instability, epileptic seizures and disorders of consciousness.[3,9,73] Immunotherapy and tumor removal lead to substantial improvement in about 80% of the patients, especially when treated at an early disease stage.[9] However, many patients suffer from persistent cognitive deficits, i.e. memory impairment and executive dysfunction.[74]

Although numerous imaging descriptions exist, large cohort studies reported MRI abnormalities only in 23– 50% of the patients.[9,20,73] This clinico-radiological paradox constitutes one of the main challenges in NMDAR encephalitis neuroimaging. If imaging abnormalities become evident, they are typically mild and unrelated to clinical symptoms. They may involve the frontal, parietal and medial temporal cortex,[3,17,73] but have also been reported to affect the cingulate gyrus,[75] thalamus,[76] cerebellum[77–79] and brainstem.[17,77] Basal ganglia imaging changes were observed in a 21-year-old male NMDAR encephalitis patient with T2/fluid-attenuated inversion recovery (FLAIR) hyperintense signal and FDG–PET hypometabolism of the caudate head and lentiform nuclei.[80] These MRI signal alterations were, among other symptoms, associated with bradykinesia and dysarthria and resolved following immunotherapy. In another patient with NMDAR antibodies, progressive striatal necrosis was documented,[81] while in most reported patients with prominent movement disorders no MRI changes were seen.[82–86]

Serial MRI and long-term follow-up indicate that severe disease courses can result in predominantly hippocampal or mild global atrophy.[3,20,76,87–91] Interestingly, brain atrophy was partially reversible and accompanied by clinical recovery in two patients with follow-up for 5 and 7 years.[88] A recent investigation of 40 patients after the acute stage of the disease found bilateral hippocampal atrophy that affected the input and output subregions of the hippocampal circuit.[92] Additionally, hippocampal microstructural integrity was impaired in patients, and both hippocampal volumetric and microstructural integrity measures correlated with memory performance, disease severity and duration. These data thus emphasize the importance of a rapid and adequate immunotherapy to prevent persistent hippocampal damage.

FDG–PET can reveal pathological changes even when MRI and CT scans are normal. Metabolic abnormalities (hypo- or hypermetabolism) have been observed throughout the brain, including the frontal, temporal and occipital lobes as well as basal ganglia, cerebellum and brainstem.[73,75,77,93–95] A characteristic pattern was described in an FDG–PET imaging study of six NMDAR encephalitis patients

with relative frontal and temporal glucose hypermetabolism alongside occipital hypometabolism.[94] This increased frontotemporal-occipital gradient was associated with disease severity and normalized following recovery in two patients. Similar PET imaging findings were reported in other studies,[75,77,96,97] although distinct patterns with occipital hypermetabolism,[73] widespread cortical hypometabolism[78,89] or more lateralized effects[95,98] have been described as well. In accordance with frequent abnormal movements in NMDAR encephalitis, altered basal ganglia metabolism was described in several patients.[93,95,99] For example, sequential PET imaging in a 25-year-old woman with marked limb rigidity showed an increased striatal metabolism in parallel to the diffuse cortical metabolic hypoactivity that normalized upon clinical recovery.[93] Single photon emission tomography (SPECT) revealed either increased[77,87] or decreased perfusion in the medial frontal and temporal cortex in single patients.[77,88,100]

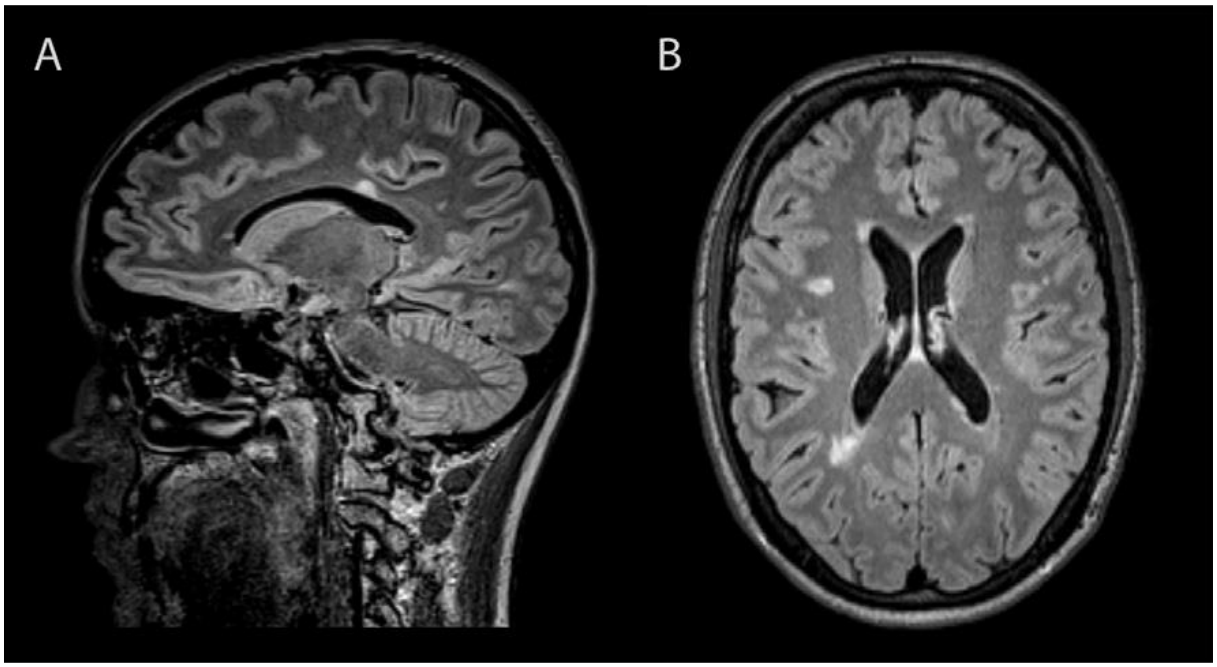

Figure 3. Overlapping demyelinating syndrome in two patients with NMDAR encephalitis. (A) FLAIR-hyperintense lesions in the corpus callosum of a 20-year-old female patient with NMDAR encephalitis, one lesion with a "Dawson finger" aspect typical for multiple sclerosis. Further demyelinating lesions were observed in the periventricular white matter with two of the lesions showing contrast- enhancement. Lesions were detected on a routine follow-up MRI, however the patient had suffered from fatigue during the last six months before MRI. Shortly after MRI, she developed hypoesthesia of both lower legs and bladder dysfunction. A treatment with IV steroids was initiated and symptoms partially remitted. (B) FLAIR hyperintense lesions in the periventricular white matter of a 26-year old female patient with NMDAR encephalitis. In total, 14 supratentorial lesions were detected and two lesions showed contrast enhancement. MRI was performed because the patient had reported intermittent double vision. The patient was treated with IV steroids and double vision remitted.

Diffusion tensor imaging analyses detected widespread white matter changes, i.e. reduction of fractional anisotropy and increase of mean diffusivity, that correlated with individual disease severity.[101] This observation suggests that white matter damage contributes to the pathophysiology of NMDAR encephalitis and may be mediated by antibodies binding to oligodendrocytic NMDARs.[102] Apart from these observations of white matter damage, an overlap of NMDAR encephalitis with demyelinating syndromes has been described[79,103,104] (Fig. 3). A recent assessment of clinical and radiological data of 691 NMDAR encephalitis patients found 23 patients with clinical or MRI features of demyelination.[104] These patients suffered from episodes of neuromyelitis optica spectrum disorder (NMOSD), brainstem or multifocal demyelinating syndromes which preceded, occurred simultaneously with or followed manifestation of NMDAR encephalitis. In some of these patients, antibodies against AQP4 and MOG were detected in addition to NMDAR antibodies. MRI showed new extensive or multifocal T2/FLAIR hyperintense lesions in various brain regions and the spinal cord which contrasted with the typical MRI result in NMDAR encephalitis with no or only small lesions.

While the clinical diagnosis was challenging, lesions resolved after treatment in some patients. In a 28-year-old woman with antibodies against both NMDAR and MOG who was followed up for 5 years, recurring T2/FLAIR lesions in the deep gray matter and white matter were reported.[105] These lesions co-occurred with neuropsychiatric symptoms when oral prednisone therapy was discontinued and resolved after IV methylprednisolone treatment. Another patient with multiple sclerosis was tested positive for NMDAR antibodies when she developed severe and persisting cognitive impairment.[106] In children with NMDAR antibodies, three distinct clinicoradiologic syndromes, i.e. brainstem encephalitis; leukoencephalopathy following herpes simplex encephalitis; and CNS demyelination, were identified and responded well to immunotherapy.[79] It is therefore important for clinicians to consider such an overlap syndrome in NMDAR encephalitis patients with atypical symptoms and/or spinal or cerebral demyelinating lesions. Conversely, patients with NMOSD or multiple sclerosis with atypical symptoms should be tested for NMDAR antibodies.

Besides structural changes in gray and white matter, functional connectivity was found to be disrupted in NMDAR encephalitis.[101] In a resting-state functional MRI analysis, functional connectivity of the left and right hippocampus with the anterior default mode network was significantly reduced in patients and correlated with individual memory impairment (Fig. 2). Remarkably, administration of the NMDA antagonist ketamine resulted in similar functional connectivity alterations and clinical symptoms, e.g. memory impairment and executive dysfunction.[107] Considering the usually unremarkable structural routine MRI in NMDAR encephalitis, the results of these imaging analyses constitute a possible future avenue to address the clinico-radiological paradox of the disease.

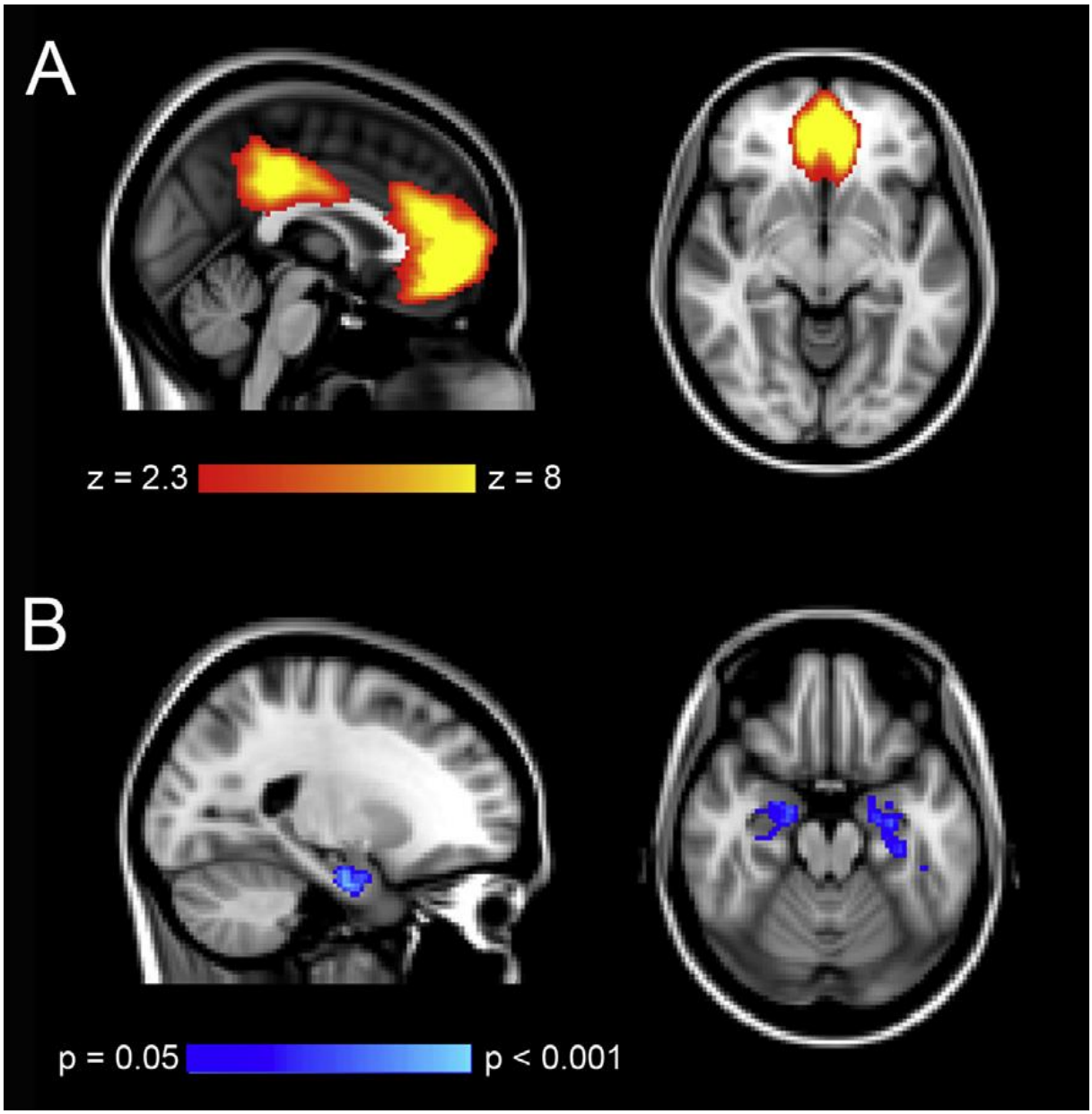

Figure 2. Reduced functional connectivity of the hippocampus in NMDAR encephalitis. Resting-state functional MRI analysis revealed reduced hippocampal functional connectivity in patients with NMDAR encephalitis. (A) The anterior default mode network (DMN) was identified in patients and controls. The DMN is a functional brain network with increased activity during rest and internally focused tasks. It comprises multiple components, including a distinct medial temporal lobe subnetwork that is involved in memory processing. (B) In patients, functional connectivity between the DMN and both the left and the right hippocampus was significantly reduced in comparison to controls ($p<0.05$, corrected). The strength of hippocampal functional connectivity correlated with memory performance in patients demonstrating that dysfunction of hippocampal NMDARs is a key pathophysiological mechanism in NMDAR encephalitis-associated memory deficits (not shown). Reproduced with permission from John Wiley and Sons[101].

In line with these clinical and imaging observations, an animal model of NMDA receptor encephalitis has been established. Animals with intraventricular infusion of patients' cerebrospinal fluid developed progressive memory deficits and anhedonic behavior. Interestingly, post-mortem analysis showed a widespread labeling of NMDA antibodies in the hippocampus, whereas the density of total and synaptic NMDAR clusters and total NMDAR protein concentration decreased in this area. These findings suggest a transient antibody-associated impairment of hippocampal NMDAR function, thus providing a link between hippocampal dysfunction in immune-mediated neuroinflammatory diseases and cognitive deficits. The experiments also provide a rationale for therapeutic approaches by reducing NMDAR antibodies and immune-active cells in these disease states, thereby improving neurological function.[108]

Taken together, these imaging studies indicate that the hippocampus, which contains the highest density of NMDARs in the human brain, appears to be the most affected brain structure in NMDAR encephalitis. This observation is in line with the prominent memory impairments of patients. However, PET imaging highlights that, in contrast to classic limbic encephalitis, almost all brain structures can be affected by the disease, frequently exhibiting a characteristic metabolic pattern. Metabolic or structural alterations of the basal ganglia as demonstrated by MRI and PET are furthermore associated with movement disorders in some patients. Diffusion tensor imaging suggests that white matter damage likewise contributes to the clinical phenotype of the disease. An overlap syndrome should be considered in NMDAR encephalitis patients with atypical symptoms or demyelinating lesions.

VGKC-complex antibody encephalitis

Antibodies directed against the VGKCs were detected in patients with limbic encephalitis, neuromyotonia and Morvan's syndrome.[24,109] Recent research has shown that these antibodies – rather than directly acting on VGKCs – target proteins associated with the VGKC complex, i.e. LGI1 and contactin-associated protein-like 2 (CASPR2).[4,110] Imaging studies of autoimmune encephalitis with VGKC-associated antibodies that did not differentiate between LGI1 and CASPR2 antibodies reported pathological changes in the medial temporal lobes with varying degrees of atrophy and cognitive outcomes.[24,66] In a study of 42 VGKC encephalitis patients, medial temporal lobe structures were uni- or bilaterally enlarged and hyperintense on T2/FLAIR images in 79% of patients, involving both the hippocampus and the amygdala.[111] These signal alterations showed diffusion restriction in the T2 hyperintense areas in 42% of patients and contrast enhancement in 28% of patients. Only two patients had extra-limbic manifestation in the perisylvian cortex and the caudate nucleus. On follow-up, almost 50% of patients developed hippocampal sclerosis, with an increased risk for patients with restricted diffusion and contrast enhancement. Using an automated volumetric analysis, Wagner et al.[112] found increased volumes of amygdala and hippocampus for patients investigated during the first 12 months of the disease. At follow-up 6–12 months later, the volumes had normalized with a trend for smaller

hippocampi in patients. FDG–PET imaging in a 67-year-old patient revealed successive mediotemporal hypermetabolism together with hippocampal T2 hyperintensity and swelling, initially affecting the right hemisphere and three months later the left hemisphere.[113] At follow-up two years later, hypometabolism of both medial temporal regions had developed, accompanied by right hippocampal atrophy and persistent swelling of the left hippocampus.

Limbic encephalitis with VGKC-associated antibodies has only rarely been described in children. A case study of a 13-year-old girl reported a progression from bilateral swelling with T2/FLAIR signal increase of the amygdala and hippocampus, together with signal increase in the left claustrum and insula, to bilateral hippocampal atrophy within seven months.[114] This case emphasizes that VGKC-associated limbic encephalitis is not restricted to adult patients and may show the same characteristic temporal evolution with rapid progression to hippocampal atrophy in children.

LGI1 antibody encephalitis

Patients with LGI1 encephalitis present with subacute memory disturbances which are accompanied by various neuropsychiatric symptoms, such as disorientation, confusion, temporal lobe seizures and behavioral abnormalities indicating affection of limbic structures. Patients are typically older than 40 years and men are more frequently affected than women.[4,110] LGI1 encephalitis is only rarely associated with systemic tumors and the overall prognosis is good when immunotherapy is initiated at an early disease stage. Importantly, LGI1 limbic encephalitis is frequently preceded by faciobrachial dystonic seizures (FBDS) – short, jerky and highly stereotyped dystonic episodes that typically affect one arm and the ipsilateral side of the face and occur at a high frequency (median 50/day). Recognition of FBDS is of high clinical importance, since early immunotherapy can prevent progression to limbic encephalitis.[115] MRI at the stage of FBDS is typically unremarkable, although in single cases T2 hyperintense signal alterations, diffusion restriction and contrast-enhancing lesions of the basal ganglia have been reported.[115,116] Increased T2/FLAIR signal in the left caudate, putamen and rectus and cingulate gyrus was accompanied by left basal ganglia hypermetabolism in FDG–PET in a patient with a right-sided FBDS.[117] In a patient with frequent bilateral FBDS but no cognitive deficits, bilateral striatal hypermetabolism was observed with FDG–PET in the absence of MRI basal ganglia abnormalities[118] (Fig.4).

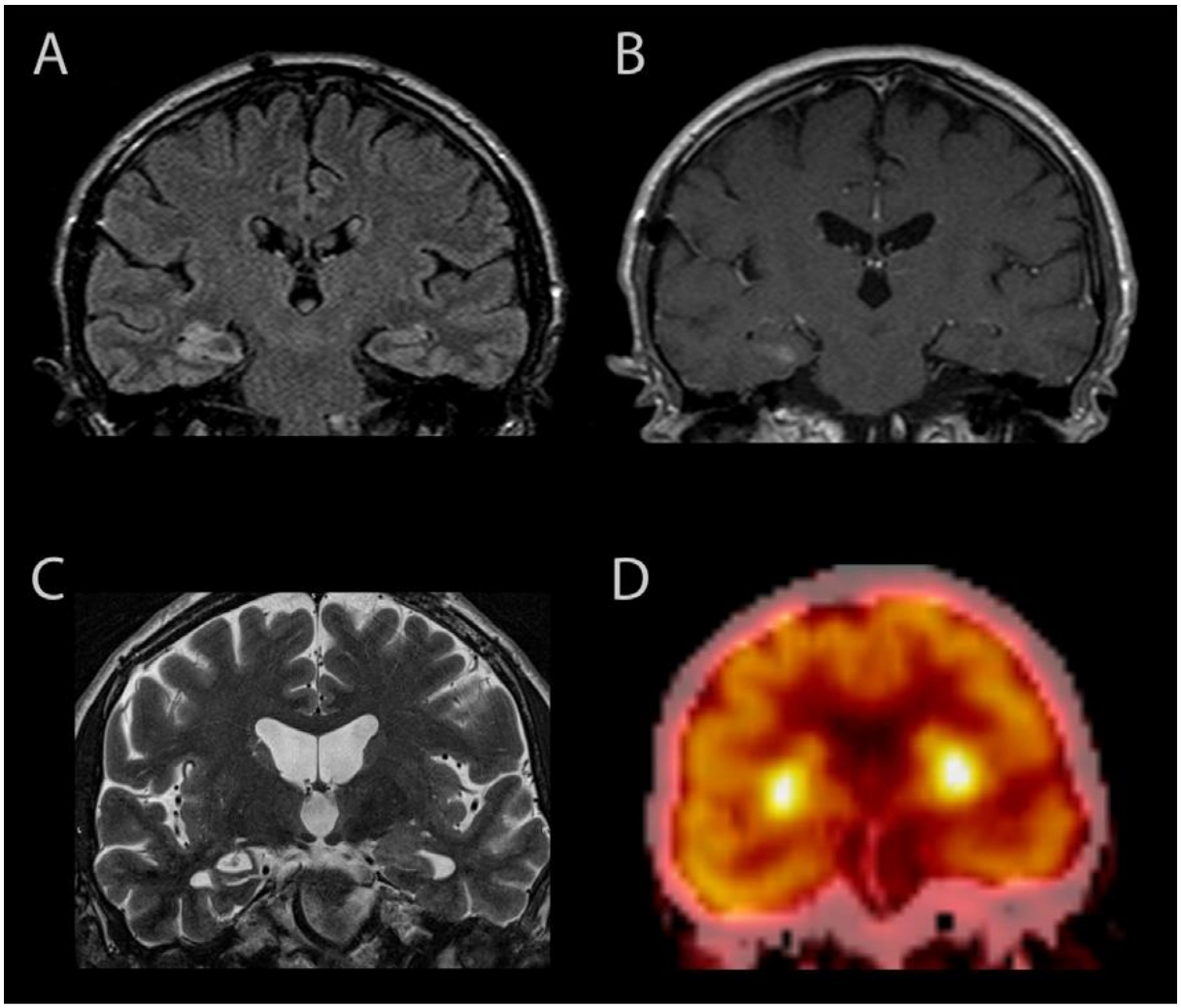

Figure 4. MRI and FDG–PET imaging in LGI1 encephalitis. (A–C) 60- year-old male patient with LGI1 encephalitis: FLAIR-hyperintense signal alterations in the hippocampus bilaterally (right >left; A), with contrast enhancement on the right side (B). The patient presented with frequent faciobrachial dystonic seizures (FBDS), followed by confusion, agitation, and severe memory impairment. Following immunotherapy with IV steroids, plasma exchange and IV immunoglobulins FBDS ceased while memory impairment persisted. Follow-up MRI 17 months later showed bilateral (right>left) atrophy of the hippocampus as well as moderate global atrophy (C). (D) FDG–PET showing bilateral hypermetabolism in the basal ganglia in a 92-year-old patient that presented with up to 100 FBDS/day but without cognitive deficits. FBDS stopped after two courses of IV immunoglobulin therapy. MRI was unremarkable except mild global atrophy and microangiopathic leukoencephalopathy and especially showed no abnormalities of basal ganglia or medial temporal lobes.[118]

At the limbic encephalitis stage of the disease, uni- or bilateral T2/FLAIR hyperintensities of the medial temporal lobes are detected in the majority of patients and can likewise be accompanied by basal ganglia signal changes[4,22,110,115] (Fig. 4). Patients frequently progress to develop hippocampal atrophy at later follow-up investigations and remain with permanent general cognitive and mnestic

impairments[111,115,119–121] (Fig. 4). Importantly, volumetric analysis detected hippocampal and whole brain atrophy also in post-recovery FBDS patients without MRI abnormalities in the medial temporal lobes during the acute illness, indicating that FBDS can cause significant atrophy despite unremarkable clinical routine imaging.[115] Time to administration of immunotherapy was correlated with time to clinical recovery in these patients, thus again highlighting the need for early immunotherapy in patients with FBDS. It is likely that an early immunotherapy will also be associated with less severe hippocampal and whole brain atrophy in larger longitudinal samples.

FDG–PET at the limbic encephalitis disease stage revealed altered basal ganglia glucose metabolism in 63–70% of patients (hypermetabolism in 11/18; hypometabolism in 1/18) and altered temporal metabolism in 70–75% of patients (hypermetabolism in 11/18; hypometabolism in 2/18) in two recent studies.[22,122] Normal mediotemporal glucose metabolism was correlated with better clinical outcome, whereas basal ganglia metabolism was unrelated to disease course.[122] A recent analysis of cerebral glucose metabolism in four LGI1 encephalitis patients in comparison to matched healthy controls found hypermetabolism in the basal ganglia as well as in the cerebellum, the occipital lobe and the precentral gyrus and hypometabolism in the anterior cingulate - but interestingly no significant alteration of medial temporal lobe metabolism.[75] This latter finding might partially be related to the disease stage of the investigated patients, since longitudinal PET investigations show waxing and waning of temporal PET metabolism mirroring the clinical course of the disease.[123,124]

In summary, LGI1 encephalitis presents with the typical imaging correlates of limbic encephalitis, i.e. T2/FLAIR hyperintense signal alterations in the medial temporal lobes including the hippocampus which frequently progress to hippocampal atrophy. Additionally, prominent basal ganglia involvement is observed in many patients using MRI and FDG–PET imaging. This finding might provide an important clue to the pathophysiology of FBDS in the current debate on whether these episodes represent seizures or extrapyramidal movements.[125] It has recently been proposed that the concomitant MRI and PET abnormalities in contralateral cortical and extrapyramidal areas might explain the overlap of epileptic (cortical) and movement disorders (subcortical) features in FBDS, thus blurring the traditional borders between these two entities.[117]

CASPR2 antibody encephalitis

Patients with CASPR2 antibodies develop Morvan's syndrome or, less frequently, limbic encephalitis.[110] Morvan's syndrome is characterized by encephalopathy with prominent psychiatric symptoms, insomnia, dysautonomia and neuromyotonia and almost exclusively affects male patients.[126,127] MRI was normal in 23 of 25 patients with Morvan's syndrome, while right frontal T2 hyperintensity was observed in one and bilateral hippocampal T2 high signal with consecutive atrophy in another patient (Fig. 5). Focal and generalized hyper- and hypometabolism were found in all four patients examined with PET,

despite normal MRI.[127] In a 64-year-old patient with VGKC antibodies and Morvan's syndrome, FDG–PET revealed increased basal ganglia metabolism while only nonspecific periventricular white matter lesions were seen on MRI.[128] Cognitive function improved and cerebral glucose metabolism normalized in this patient following 15 months of immunotherapy with plasma exchange, cyclophosphamide and azathioprine. In a 66-year-old patient with Morvan's syndrome and VGKC antibodies, PET demonstrated reduced FDG uptake bilaterally in the orbitofrontal cortex and anterolateral temporal regions, as well as in the left medial temporal lobe, while MRI was normal.[129]

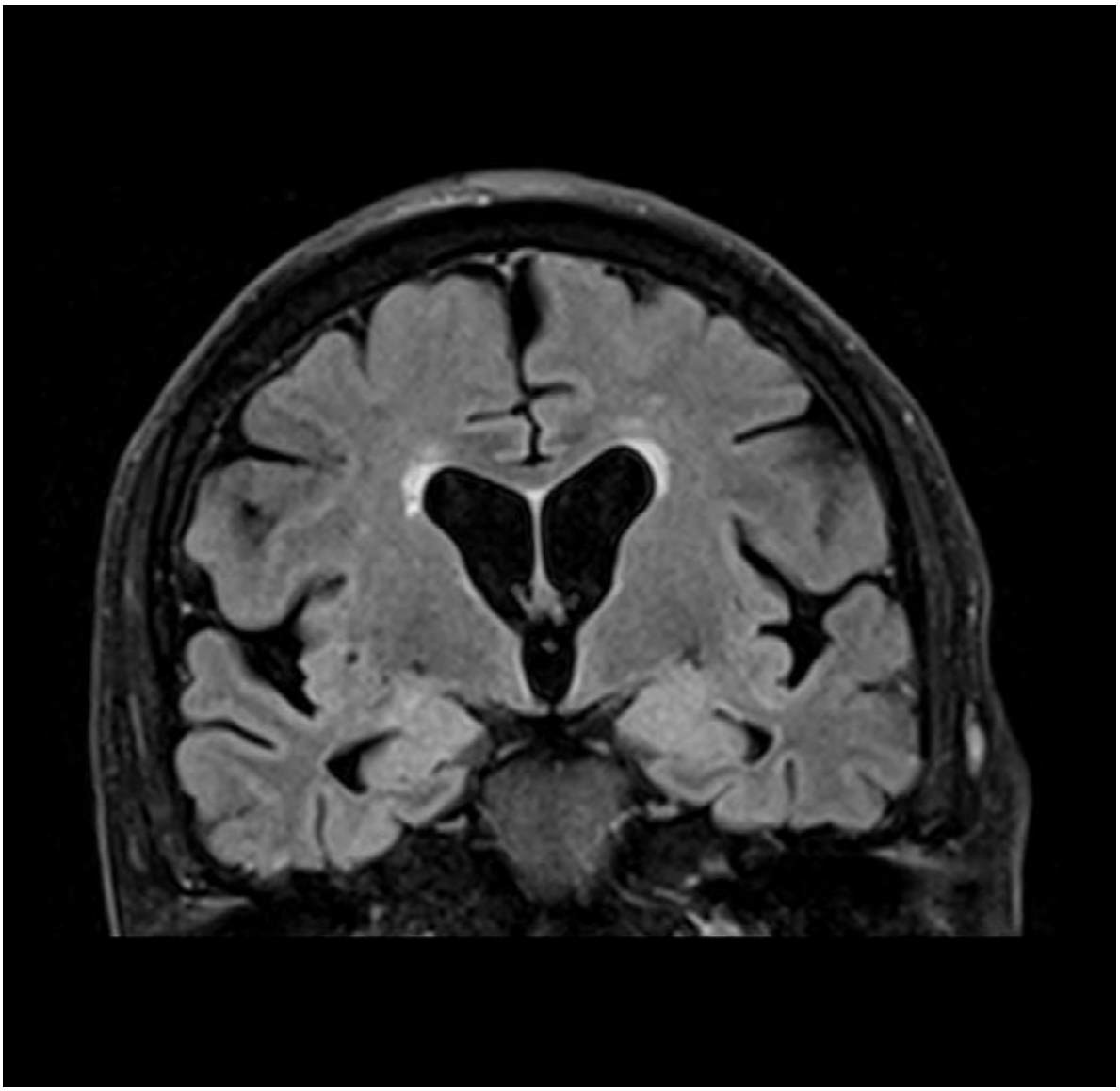

Figure 5. Medial temporal lobe abnormalities in CASPR2 encephalitis. A 71-year-old male patient with CASPR-2 antibodies presented with complex partial seizures, memory deficits and affective disturbance. MRI revealed symmetric FLAIR hyperintensities in the medial temporal lobes. Following extensive immunotherapy with IV steroids, plasma exchange, IV immunoglobulins and rituximab, a mild improvement of symptoms was observed.

In a sample of CASPR2-positive patients suffering from Morvan's syndrome, neuromyotonia or limbic encephalitis, five of 19 patients had MRI hyperintense signal alterations in the medial temporal lobes, but all five patients with Morvan's syndrome had normal MRI.[110] Lancaster et al.[126] observed T2 hyperintensities in the medial temporal lobes in two CASPR2 antibody-positive patients, diffuse cortical and subcortical atrophy in one patient and normal MRI in two patients. In a 67-year-old patient with Morvan's syndrome, multiple small T2-hyperintense white matter lesions mostly in the periventricular region, consistent with chronic small vessel changes, were observed.[130] In a 55-year-old patient with epilepsy, dysarthria, and paroxysmal kinesigenic dystonia, acute right subcortical infarction was reported with however uncertain relation to CASPR2 antibody-positivity.[131] Another study that only investigated limbic encephalitis patients with T2/FLAIR-hyperintense medial temporal lobe structures found normal MRI at follow-up 11–58 months later in three patients with CASPR2 antibodies.[120] In contrast to LG11-positive patients, patients with CASPR2 antibodies did not develop hippocampal atrophy or sclerosis.[111,120]

AMPA receptor antibody encephalitis

Encephalitis with antibodies against the a-amino-3-hydroxy-5-methyl-4-isoxazolepropionic acid (AMPA) receptors most frequently affects female patients and is associated with different tumors in 70% of the cases.[132] It typically manifests as limbic encephalitis with seizures, memory impairment and psychiatric symptoms. Accordingly, T2/FLAIR hyperintense signal alterations were observed in the medial temporal lobes in eight of nine patients in the first reported case series.[132] In two of these patients, abnormalities extended into anterior septal nuclei and insular, frontal, occipital or cerebellar regions. Most patients responded well to immunotherapy, with the long-term outcome depending on the management of relapses. Bataller and colleagues[133] described a 67-year-old woman with confusion, hypersomnia, visual hallucinations, and memory deficits. Mild bilateral FLAIR hyperintensities in the medial temporal lobe were observed on MRI examination. In accordance with the good therapy response in AMPAR encephalitis, her memory impairment alleviated with decreasing antibody titers. Exclusive bilateral mediotemporal T2/FLAIR signal increases were also reported in three patients whose most prominent symptom was short-term memory impairment.[134] While two initially showed bilateral abnormalities, one patient with left hemispheric involvement became affected bilaterally over time. In the latter case, laminar necrosis-like pattern in the left hippocampal sectors cornu ammonis (CA) 1 and CA2 was observed. All three patients developed hippocampal and amygdalar sclerosis on follow-up. A similar pattern was found in a 33- year-old female patient with progressive anterograde and retrograde amnesia.[135] Left-sided hippocampal edema and hyperintensities on T2/FLAIR images evolved into bilateral affection and finally bilateral hippocampal atrophy. FDG–PET imaging revealed hypermetabolism predominantly in the left hippocampus which persisted after resolution of CSF

pleocytosis and hippocampal oedema. Antiepileptic therapy was potentiated with the presumption of ongoing temporal seizures, resulting in memory improvement and normalization of left hippocampal glucose metabolism. A fulminant disease course was reported in a 30-year-old pregnant woman. She developed behavioural changes and memory impairment followed by ataxia, nystagmus, quadriparesis, impaired consciousness and status epilepticus.[136] MRI showed FLAIR hyperintensities bilaterally in the medial temporal lobes, insula and caudate nucleus. Remarkably, follow-up MRI 5 days later revealed severe diffuse cortical atrophy. At a second follow-up on day 37, FLAIR changes had resolved, but cortical atrophy persisted. An FDG–PET performed on day 52 showed widespread bilateral hypometabolism of frontal, temporal, and occipital lobes and the caudate. In contrast, Graus et al.[137] reported two women with rapidly progressive confusion, personality changes, agitation and aggressive behaviour with completely normal MRI. Both patients fully recovered with corticosteroid therapy.

$GABA_A$ receptor antibody encephalitis

Gamma-aminobutyric acid A ($GABA_A$) receptor antibodies were recently identified in patients with cognitive deficits and prominent seizures.[138] Six patients with high titers of $GABA_AR$ antibodies in serum and CSF developed a rapidly progressive encephalopathy that eventually resulted in refractory seizures and status epilepticus in five patients. Seizures were preceded or accompanied by cognitive deficits and psychiatric symptoms, including memory impairment, depression, psychosis, confusion and mutism. Further symptoms included opsoclonus, ataxia, chorea and hemiparesis. MRI was abnormal in all patients, showing extensive multifocal or diffuse cortical and subcortical T2/FLAIR signal alterations. For example, a 16-year-old girl presented with multiple T2/FLAIR-hyperintense lesions involving the left temporal lobe and frontal parasagittal regions. Follow-up MRIs revealed considerable progression with increasing size of existing lesions, manifestation of new lesions and diffuse atrophy together with increased ventricular size. MRI performed six months after symptom onset showed resolution of the abnormalities and normalization of ventricular size. In a 51-year-old male patient, MRI changes progressed within 14 days from focal T2/FLAIR signal abnormalities to an extensive involvement of cortical and subcortical regions of both hemispheres. Two of the patients died of sepsis during treatment of refractory status epilepticus and four patients substantially recovered. Twelve patients with low serum titres of GABAAR antibodies presented with a broader spectrum of diseases including stiff-person syndrome, opsoclonus-myoclonus syndrome and (limbic) encephalitis with seizures. MRI abnormalities included high T2/FLAIR signal in fronto-temporal regions and medial temporal lobes, multifocal lesions and cortical atrophy, as well as normal results in five patients. Ohkawa et al.[139] reported two patients with invasive thymoma and serum $GABA_AR$ antibodies who developed cognitive deficits and psychiatric symptoms. MRI of both patients showed extensive bilateral multifocal lesions involving the temporal lobes.

$GABA_B$ receptor antibody encephalitis

Gamma-aminobutyric acid B ($GABA_B$) receptors are expressed throughout the brain, particularly in hippocampus, thalamus, and cerebellum. $GABA_B$ encephalitis typically manifests as limbic encephalitis and is associated with small cell lung cancer or neuroendocrine tumours in 50% of patients.[140] Accordingly, in the majority of patients, uni- or bilateral T2/FLAIR increases in the medial temporal lobes are observed with normal MRI results in some patients.[134,140,141] Höftberger et al.[142] categorized their patient sample according to clinical presentation. Out of 17 patients with limbic encephalitis, MRI showed uni- or bilateral increased T2/FLAIR signal in hippocampus and amygdala in nine patients, increased pial enhancement in one patient and was normal in seven patients. Brain MRI was also normal in a patient with status epilepticus. In a patient with ataxia, MRI showed frontal and temporal leukoencephalopathy and another patient with opsoclonus-myoclonus syndrome had increased signal in T2/FLAIR and contrast enhancement in cortex and white matter of both frontal and temporal lobes and cingulum. Follow-up MRI investigations revealed progressive hippocampal atrophy and signal increase on T2/FLAIR-weighted images demonstrating evolution of hippocampal sclerosis. In two patients, T1-weighted not-enhanced images indicated hippocampal laminar necrosis.[134]

The clinical spectrum was expanded by Jeffery et al.,[143] who reported a patient with multiple myeloma and $GABA_BR$ antibody-associated encephalopathy and myelopathy. Spinal MRI in this patient revealed longitudinally extensive T2 signal abnormalities in the thoracic spinal cord characteristic of paraneoplastic myelopathy. Other rare manifestations of $GABA_B$ autoimmunity include cerebellar ataxia in a 64-year-old malignant melanoma patient with normal MRI[144] and brainstem encephalitis in a 63-year-old patient with oesophageal carcinoma and T2-hyperintense lesion in pons, medulla oblongata and right cerebellar peduncle.[145] A 33-year-old woman presented with opsoclonus-myoclonus syndrome, followed by a severe episode of limbic encephalitis. Serial MRI studies showed extensive T2/FLAIR hyperintense lesions in the frontal and temporal lobes and the cingulate gyrus which developed into marked fronto-temporal atrophy at follow-up one year later.[146] The first paediatric case, a 3-year-old boy, presented with opsoclonus, ataxia, chorea and refractory seizures accompanied by brainstem, cerebellum and basal ganglia involvement upon diffusion-weighted imaging and T2/FLAIR sequences.[147] FDG–PET imaging revealed hypermetabolism in the medial temporal lobes in two out of five patients that was congruent with increased T2/FLAIR signal in MR imaging and diffuse cortical hypometabolism in a third patient.[148] In a case study of a 62-year old female patient presenting with limbic encephalitis, 123I-IMP SPECT detected hypoperfusion in thalamus, cerebellum and frontal, parietal, and mediotemporal areas as well as hyperperfusion in middle and superior temporal, precentral and postcentral cortex despite unremarkable MR imaging.[149] Remarkably, repeat SPECT imaging following methylprednisolone pulse therapy showed normalization of perfusion in almost all brain regions.

Dopamine-D2 receptor antibody encephalitis

Dopamine-D2 receptor antibodies have recently been characterized in children with basal ganglia encephalitis.[150] Twelve children with this encephalitis presented with Parkinsonism, dystonia, chorea, as well as psychiatric symptoms including emotional lability and psychosis. MRI was abnormal in 50% of these patients, showing T2/FLAIR signal increases in the caudate, putamen, globus pallidus and substantia nigra. Patients with D2-encephalitis may remain with residual motor, cognitive, and psychiatric deficits despite a good response to immunotherapy in some cases. At follow-up examination, basal ganglia atrophy and gliosis was seen in two patients and corresponded to their persistent cognitive and psychiatric symptoms.[150]

Dipeptidyl-peptidase-like protein 6 (DPPX) antibody encephalitis

DPPX is a cell-surface auxiliary subunit of the Kv4.2 potassium channel family and antibodies targeting DPPX were detected in four patients with agitation, confusion, myoclonus, tremor and seizures.[151] In three patients, these symptoms were preceded by severe diarrhoea of unclear aetiology, causing substantial weight loss. Cerebral MRI showed only nonspecific periventricular and subcortical white matter T2/FLAIR increased signal in a 61-year-old man and non-specific white matter changes and nonacute right frontal infarction in a 58-year-old woman.[151] A recent study reported 20 patients with DPPX antibodies with various neurological symptoms including amnesia, psychosis, seizures, eye movement disorders, ataxia, and dysphagia as well as signs of central hyperexcitability including myoclonus, exaggerated startle, diffuse rigidity, and hyperreflexia.[152] Additionally, patients suffered from dysautonomic symptoms such as diarrhoea, gastroparesis or bladder dysfunction. Despite the severe neurological deficits, MRI was normal in nine of 13 patients with available MRI and showed only nonspecific abnormalities in the remaining four patients. In three patients with DPPX antibodies and a distinct syndrome characterized by trunk stiffness, hyperekplexia and cerebellar ataxia, cerebral MRI likewise was normal except for one patient with mild cerebellar atrophy 17 years after disease onset.[153]

GAD antibody encephalitis

Glutamate decarboxylase is an intracellular synaptic antigen concentrated in presynaptic terminals that can be exposed to antibodies during synaptic vesicle fusion and reuptake.[61] The presence of high titres of GAD antibodies has been associated with different neurological syndromes including stiff-person syndrome, cerebellar ataxia and limbic encephalitis.[154] In patients with limbic encephalitis, characteristic T2/FLAIR hyperintensities in the medial temporal lobes are observed (Fig. 6), accompanied by anterograde amnesia and language deficits, while disorientation and confusion seem to be less common

compared to other antibodies.[154,155] On follow-up MRI, regression of encephalitic mediotemporal signal was observed, although some patients developed hippocampal sclerosis[155]. In GAD-antibody-positive patients with cerebellar ataxia, MR imaging showed isolated atrophy of the cerebellum.[156,157] Using an observer-independent postprocessing method, Wagner et al.[158] found that limbic encephalitis patients with GAD antibodies had significantly higher hippocampal FLAIR intensity values than patients with VGKC and NMDAR antibodies.

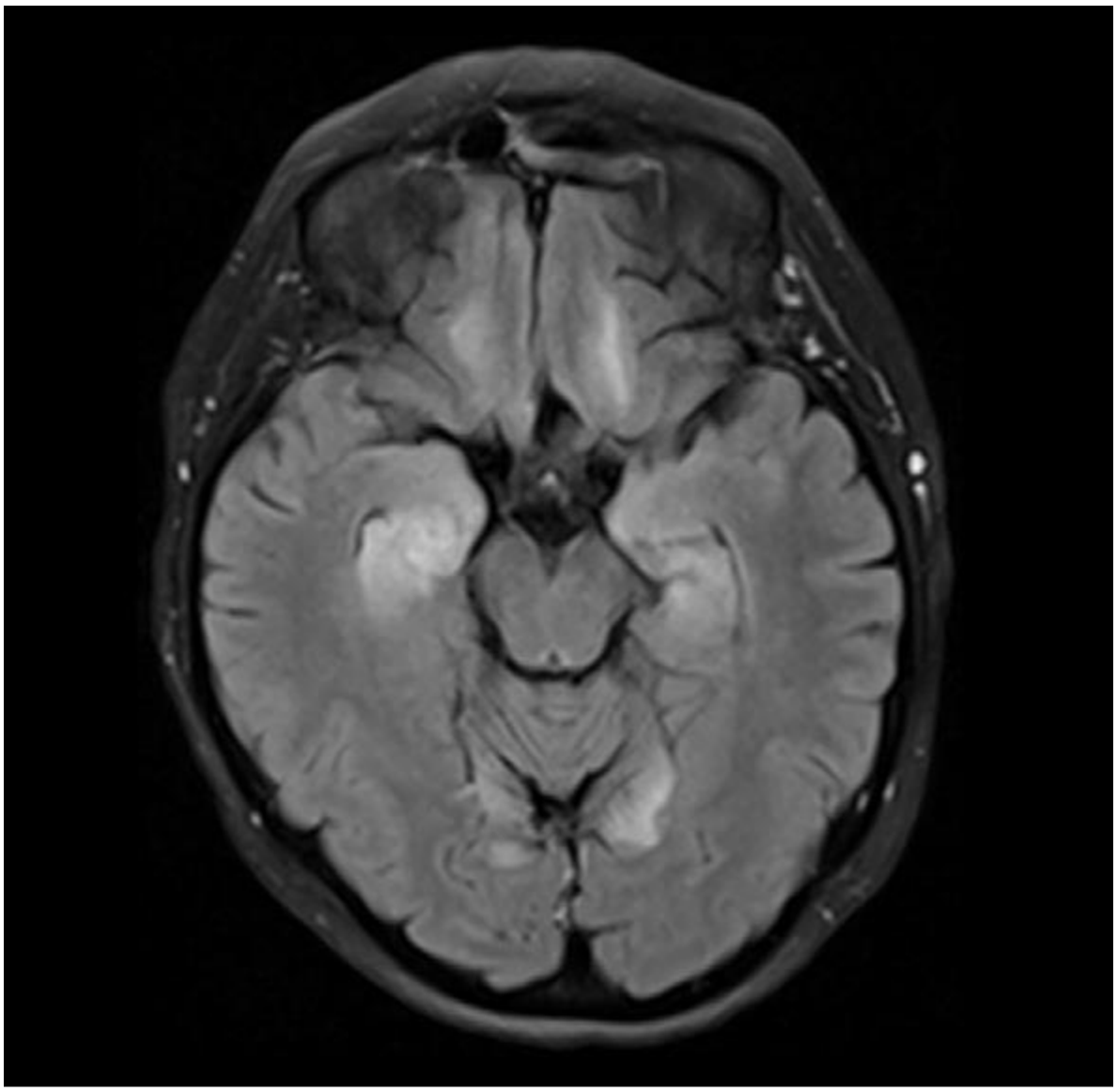

Figure 6. Medial temporal lobe abnormalities in GAD encephalitis. GAD antibodies were detected in a 53-year-old female patient with generalized seizures, gait ataxia, downbeat nystagmus and cognitive deficits. MRI showed FLAIR hyperintensities in the medial temporal lobes that progressed at follow-up, now extending into insular and frontal cortex. Oncological work-up revealed a gall bladder carcinoma. Immunotherapy with IV steroids, plasma exchange, rituximab and cyclophosphamide resulted in remission of seizures and cerebellar symptoms, while anterograde memory impairment persisted.

This observation might be linked to a more severe affection of the hippocampus and worse mnestic and seizure outcome in GAD encephalitis. In a volumetric analysis, amygdala volume was significantly increased in patients with GAD antibody- positive limbic encephalitis when analysed within the first twelve months after disease onset and normalized during follow-up. In contrast, hippocampal volumes did not differ significantly from a control group.[112]

Glycine receptor antibody encephalitis

Antibodies against the glycine receptor have recently been described in adult and pediatric patients with progressive encephalomyelitis, rigidity and myoclonus (PERM) or stiff person syndrome.[159–162] Glycine receptors are mainly located in the caudal pontine brainstem and spinal cord, and patients present with the respective brainstem and autonomic signs. In addition, cognitive deficits such as disorientation and memory impairment, and psychiatric symptoms including visual hallucinations, depression or anxiety can be present. Tumours, mainly thymomas and lymphomas, are found in some of the patients. In the largest study so far, brain MRI was unremarkable in 26/36 patients while two patients had signal alterations in the temporal lobes, two had other FLAIR lesions and the remaining patients had unspecific white matter lesions or small vessel disease.[161] Interestingly, spinal MRI showed smaller lesion in four patients and, longitudinally, extensive lesions in one, but the majority of patients (18/23) had no abnormalities.[161] In a study of 11patients, MRI changes were found in a 62-year-old male patient with generalized cerebral and cerebellar atrophy and a 42-year-old male patient with non-enhancing T2 abnormalities in the bilateral superior colliculi, superior cerebellar peduncle, left brachium pontis, bilateral occipital white matter.[160]

Conclusions and future directions

In the last few years, a variety of new antibodies targeting cell-surface proteins associated with distinct clinical syndromes have been discovered. Despite the wide range of different antibody targets, many of these syndromes present with features of limbic encephalitis and corresponding T2/FLAIR hyperintense signal alterations in the medial temporal lobes including the hippocampus. This includes patients with antibodies directed against LGI1, GABAB receptors, AMPA receptors or (the intracellular synaptic antigen) GAD and a subset of patients with CASPR2 antibodies. These findings are contrasted by the frequently normal MRI in NMDAR and DPPX encephalitis, extensive multifocal or widespread diffuse abnormalities in $GABA_AR$ encephalitis and basal ganglia lesions in Dopamine D2R encephalitis. It must be noted, however, that the current analysis is based on studies using a wide range of MRI protocols with different MRI sequences and image resolutions, which likely influences the detection rate of imaging abnormalities. Moreover, some advanced imaging methods (resting-state fMRI, diffusion

tensor imaging) have so far only been used in NMDAR encephalitis. Future extension of these methods to other autoimmune encephalitis subtypes and advances in imaging methods and analyses as well as the use of multimodal imaging approaches will facilitate the discrimination between different encephalitis variants and will help to identify characteristic imaging profiles of these disorders.

Neuroimaging serves several purposes with regard to autoimmune encephalitides. First, it takes a central role in their diagnosis, given that the corresponding imaging characteristics are now increasingly recognized. While MRI T2/FLAIR hyperintensities in the medial temporal lobes might point to limbic encephalitis caused by $GABA_BR$, AMPAR or GAD antibodies, basal ganglia hypermetabolism in FDG–PET imaging may support the diagnosis of LGI1 encephalitis. As mentioned above, imaging abnormalities in routine MRI and FDG PET are not specific and clinical MR imaging can also return completely normal results, e.g. in NMDAR, DPPX or GlyR encephalitis. Advanced imaging techniques, e.g. automated volumetric analyses, quantification of signal alterations, or the application of new sequences or imaging methods, e.g. resting-state functional MRI will help to bridge the gap between clinical and radiological findings.

Second, neuroimaging can contribute to the pathophysiological understanding of autoimmune encephalitides. The detection of widespread white matter damage in NMDAR encephalitis led to the hypothesis of an involvement of oligodendrocyte NMDA receptors in the pathogenesis of the disease and is particularly interesting with regard to the discovery of overlapping demyelinating syndromes in patients with NMDAR encephalitis. Moreover, a reduced functional connectivity of the hippocampus is a neural substrate of persisting memory deficits in these patients. In LGI1 encephalitis, further analysis of concurrent signal alterations in the medial temporal lobes and the basal ganglia in MRI and PET imaging might help to identify the nature of FBDS. And longitudinal analyses of amygdala and hippocampus volumes in patients with limbic encephalitis are starting to identify distinct volumetric courses depending on the associated antibody, thus pointing to different pathogenetic mechanisms, including different levels of inflammation and neuronal cytotoxicity.

Third, imaging parameters may serve as prognostic markers. To date, this is typically based on visual inspection, e.g. on the extent and intensity of signal alterations in the medial temporal lobes. Future studies will increasingly use quantitative, observer-independent analyses that provide more robust and reliable measures and allow for a better comparison between patient populations. Moreover, modern imaging techniques will enable the development of new imaging markers and – in association with longitudinal study designs – further improve the predictive value of neuroimaging in autoimmune encephalitis.

Publication II: Evaluation of Cognitive Deficits and Structural Hippocampal Damage in Encephalitis With Leucine-Rich, Glioma-Inactivated 1 Antibodies

Key Points

Question What are the neuroimaging characteristics and the cognitive long-term outcome in encephalitis with leucine-rich, glioma-inactivated 1 (LGI1) antibodies?

Findings In this cross-sectional study of 30 patients with anti-LGI1 encephalitis, significant bilateral atrophy of the hippocampus and its subfields, as well as significantly impaired hippocampal microstructural integrity, was observed. This structural damage was correlated with persistent verbal and visuospatial memory deficits; early immunotherapy was associated with better memory outcome.

Meaning Anti-LGI1 encephalitis is associated with pronounced structural damage of the hippocampus that causes persisting impairments of verbal and visuospatial memory.

Abstract

Importance Limbic encephalitis with leucine-rich, glioma-inactivated 1 (LGI1) antibodies is one of the most frequent variants of autoimmune encephalitis with antibodies targeting neuronal surface antigens. However, the neuroimaging pattern and long-term cognitive outcome are not well understood.

Objective To study cognitive outcome and structural magnetic resonance imaging (MRI) alterations in patients with anti-LGI1 encephalitis.

Design, Setting, and Participants A cross-sectional study was conducted at the Departments of Neurology at Charité-Universitätsmedizin Berlin and University Hospital Schleswig-Holstein, Kiel, Germany. Data on 30 patients with anti-LGI1 encephalitis and 27 healthy control individuals matched for age, sex, and educational level were collected from June 1, 2013, through February 28, 2015.

Main Outcomes and Measures Clinical assessment, cognitive testing, and high-resolution MRI data, including whole-brain, hippocampal and basal ganglia volumetry; white matter integrity (diffusion tensor imaging); gray matter density (voxel-based morphometry); and hippocampal microstructural integrity (mean diffusivity and fractional anisotropy).

Results Of the 30 patients included in the study, 19 were male (63%); mean (SD) age was 65.7 (12.3) years. Patients with anti-LGI1 encephalitis had incomplete recovery with significant and persisting verbal (mean [SE] Rey Auditory Verbal Learning Test [RAVLT], delayed recall: patients, 6.52 [1.05]; controls, 11.78 [0.56], P < .001) and visuospatial (Rey-Osterrieth Complex Figure Test [ROCF], delayed recall: patients, 16.0 [1.96]; controls, 25.86 [1.24]; P < .001) memory deficits. These deficits were accompanied by pronounced hippocampal atrophy, including subfields cornu ammonis 2/3 (CA2/3) and CA4/dentate gyrus (DG), as well as impaired hippocampal microstructural integrity. Higher disease severity correlated with larger verbal memory deficits (RAVLT delayed recall, r = −0.40; P = .049), decreased volumes of left hippocampus (r = −0.47; P = .02) and left CA2/3 (r = −0.41; P = .04) and CA4/DG (r = −0.43; P = .03) subfields, and impaired left hippocampal microstructural integrity (r = 0.47; P = .01). In turn, decreased volume of the left CA2/3 subfield (RAVLT delayed recall, r = 0.40; P = .047) and impaired left hippocampal microstructural integrity (RAVLT recognition, r = −0.41; P = .04) correlated with verbal memory deficits. Basal ganglia MRI signal abnormalities were observed in only 1 patient, but a longer duration of faciobrachial dystonic seizures correlated with a reduction of pallidum volume (r = −0.71; P = .03). In contrast, no abnormalities of cortical gray matter or white matter were found. The latency between disease onset and initiation of immunotherapy was significantly correlated with verbal (RAVLT recall after interference, r = −0.48; P = .02) and visuospatial (ROCF delayed recall, r = −0.46; P = .03) memory deficits.

Conclusions and Relevance Anti-LGI1 encephalitis is associated with cognitive deficits and disability as a result of structural damage to the hippocampal memory system. This damage might be prevented by early immunotherapy.

Introduction

Encephalitis associated with leucine-rich, glioma-inactivated 1 (LGI1) antibodies belongs to a newly discovered group of autoimmune encephalitides with antibodies targeting neuronal surface antigens.[4,110] Patients with LGI1 antibodies develop limbic encephalitis and typically present with memory impairment, confusion, behavioral changes, and temporal lobe seizures. Faciobrachial dystonic seizures (FBDS), presenting as short, stereotyped dystonic movements of the face and the ipsilateral arm and/or leg, frequently precede the onset of anti-LGI1 encephalitis.[22] Early recognition and immunosuppressive treatment of FBDS can prevent progression to limbic encephalitis and development of cognitive deficits.[115,122]

Characteristic imaging features of autoimmune encephalitides associated with different antibodies are increasingly recognized[74]. For example, advanced imaging analyses, including resting-state functional magnetic resonance imaging (MRI), diffusion tensor imaging (DTI), and volumetry, have revealed

reduced hippocampal functional connectivity, widespread white matter damage, and hippocampal atrophy in encephalitis associated with N-methyl-d-aspartate receptor (NMDAR) antibodies despite normal results of clinical MRIs in most of these patients.[92,101] Thus, these advanced analyses can provide relevant clinical and pathophysiologic information in autoimmune encephalitis. In anti-LGI1 encephalitis, results of clinical MRI at the stage of FBDS are frequently unremarkable, although basal ganglia abnormalities have been observed in some patients.[115–117,163] During the limbic encephalitis stage of the disease, most patients develop T2 hyperintense signal alterations of the medial temporal lobes.[4,22,110] However, to our knowledge, no previous study has examined imaging correlates of anti-LGI1 encephalitis and their association with cognitive deficits and clinical outcome in detail.

In the present study, we investigated the effect of anti-LGI1 encephalitis on clinical and cognitive outcomes as well as the structure and function of the hippocampus and the basal ganglia in a cohort of 30 patients. We report (1) findings of routine clinical MRI; (2) neuropsychological outcome; (3) results of whole-brain, hippocampal, and basal ganglia volumetry; assessment of white matter integrity using DTI; gray matter morphology using voxel-based morphometry; and hippocampal microstructural integrity; and (4) correlation of structural imaging markers and onset of treatment with clinical and cognitive outcomes.

Methods

Patient Cohort

Thirty patients (11 women, 19 men; mean [SD] age, 65.7 [12.3] years) with anti-LGI1 encephalitis from 2 centers using a unified study protocol were included in this study (eTable 1 in the Supplement) (Charité-Universitätsmedizin Berlin, Germany, 19 patients; University Hospital Schleswig-Holstein Kiel, Germany, 11 patients). Patients were recruited after the acute stage of limbic encephalitis (latency after disease onset: median, 23.3 months; interquartile range [IQR], 6.4-35.4 months). Three patients were not eligible for MRI studies, and imaging analyses were therefore restricted to 27 patients. Fludeoxyglucose F 18–positron emission tomography data on 4 patients were previously published.[75,118] The imaging and neuropsychology control group comprised 27 healthy individuals without a history of psychiatric or neurologic disease. The control participants were individually matched to patients with respect to study site, sex, educational level, and age (9 women, 18 men; mean [SD] age, 64.3 [2.3] years). There were no significant differences between patients and controls regarding age and years of formal education. The study was conducted from June 1, 2013, through February 28, 2015. The study was approved by the ethics committees of the Charité-Universitätsmedizin and the University Hospital Schleswig-Holstein. All participants provided written informed consent, and all received financial compensation.

Clinical Assessment

Neurologic disability and dependence in daily activities were scored using the modified Rankin Scale (mRS)[164] by 3 experienced neurologists (C.F., H.P., and T.B.). The scale is scored as 0, no symptoms; 1, no significant disability, able to carry out all usual activities despite some symptoms; 2, slight disability, able to look after own affairs without assistance but unable to carry out all previous activities; 3, moderate disability, requires some help but able to walk unassisted; 4, moderately severe disability, unable to attend to own bodily needs without assistance and unable to walk unassisted; 5, severe disability, requires constant nursing care and attention, bedridden, incontinent; and 6, death due to the condition. Latency from disease onset to treatment was calculated as the time between the onset of the first symptoms (eg, FBDS or autonomic seizures) and initiation of the first immunotherapy, and follow-up time was defined as the interval between the onset of the first symptoms and the time of the study (eTable 1 in the Supplement).

Neuropsychological Assessment

Patients and controls were tested using a comprehensive neuropsychological test battery on verbal episodic memory (Rey Auditory Verbal Learning Test [RAVLT], 25 participants), with learning and recall trials scored from 0 to 15 (sum score, 0-75);[165] visuospatial memory (Rey-Osterrieth Complex Figure [ROCF], 23 participants), with copy and recall trials scored from 0 to 36;[166] and working memory (forward and backward digit span test, 26 participants). We assessed attention and executive functions using the Trail-Making Test A and B (n = 11)[167] and a computerized test battery (simple response time [subtest alertness], n = 25; Go/No-Go and dual-task performance [subtest divided attention], n = 24), naming and conceptual knowledge (Regensburg Word Fluency Test, n = 22),[168] and interference (Stroop test, 16 participants). To estimate the premorbid general intellectual ability, 25 patients performed the German equivalent of the National Adult Reading Test, scored from 0 to 37.[169] General reasoning abilities were evaluated using the German version of the Raven's Progressive Matrices (Leistungsprüfsystem, subtest logical thinking, 15 participants), scored from 0 to 40.[170] The Montreal Cognitive Assessment test was administered for cognitive screening in 11 patients.

Antibody Testing

Serum samples and cerebrospinal fluid of the patients were tested for LGI1 antibodies by indirect immunofluorescence using a biochip mosaic containing, as antigenic substrates, frozen sections of rat hippocampus, rat and monkey cerebellum, and formalin-fixed HEK293 cells that expressed recombinant membrane-bound LGI1 (Euroimmun AG; Lübeck, Germany) (Figure 1).

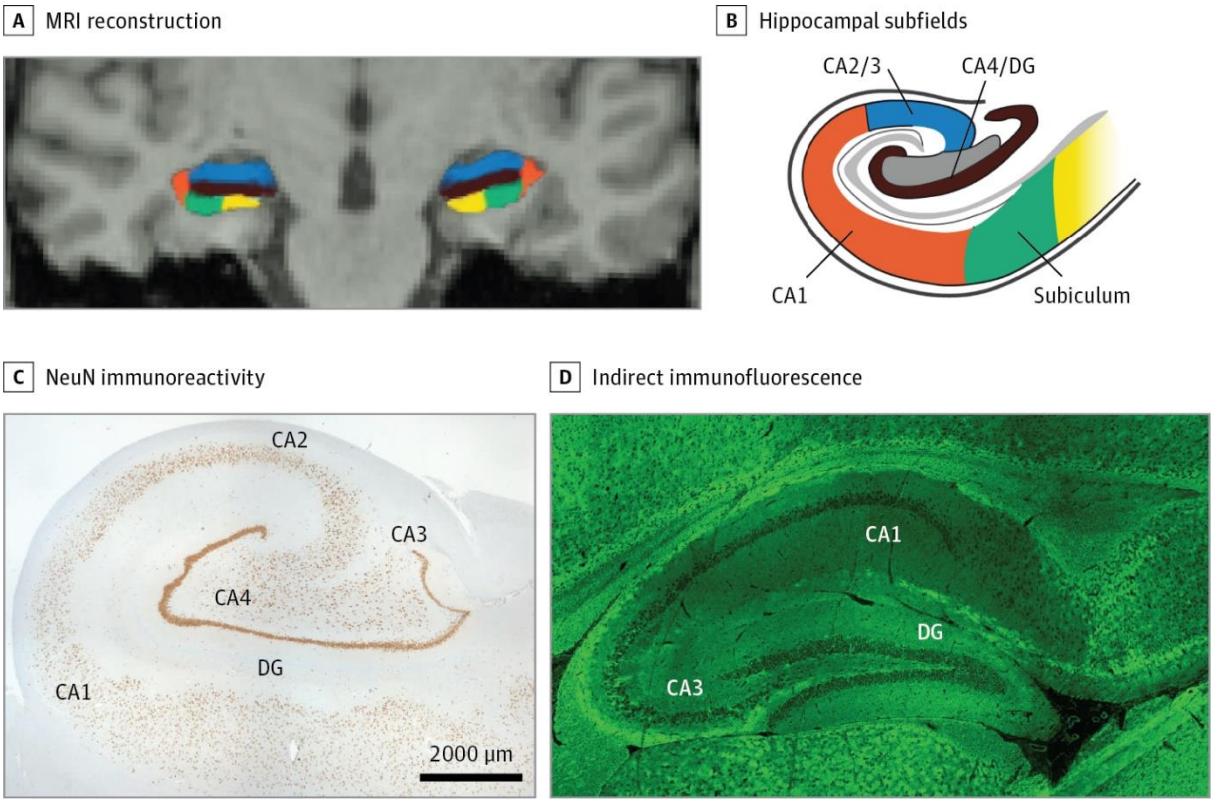

Figure 1. Hippocampal Subfield Anatomy and Pathophysiology in Encephalitis With Leucine-Rich, Glioma-Inactivated 1 (LGI1) Antibodies. A, Magnetic resonance imaging (MRI) reconstruction of the hippocampus with a representative subfield segmentation. B, Schematic overview showing the different hippocampal subfields. C, NeuN immunoreactivity showing histologic subfield morphology. D, Detection of anti-LGI1 autoantibodies with indirect immunofluorescence. Patient serum with antibodies against LGI1 was incubated with frozen sections of mouse hippocampus. Bound antibodies were visualized using a fluorescence-labeled secondary antibody. CA indicates cornu ammonis; DG, dentate gyrus.

MRI Analyses

Detailed information about MRI acquisition and analysis is available in the Methods in the Supplement. Imaging data were acquired at both study sites using 3-T MRI scanners. For the clinical study, previous brain MRIs (4-9 serial MRIs in all patients) were reevaluated with specific regard to hippocampal and basal ganglia signal changes by a neuroradiologist or experienced neurologist (C.F. and T.B.) blinded to the patient's diagnosis. Whole-brain DTI analysis using tract-based spatial statistics, hippocampal microstructural integrity analysis, and voxel-based morphometry were performed as described previously[92,101] using the FMRIB Software Library (FSL, version 5.0; http://fsl.fmrib.ox.ac.uk/fsl/fslwiki) (Figure 1). Volumes of the basal ganglia, whole hippocampus, and hippocampal subfields were determined using FreeSurfer, version 5.1 (http://surfer.nmr.mgh.harvard.edu/). FreeSurfer has been

shown[171,172] to provide reliable and valid subcortical volumes, including hippocampal subfield segmentation, and to be more accurate than other automated methods in comparison with manual tracing. All volumes were adjusted within subject for intracranial volume.

Statistical Analysis

Psychometric test results were compared between groups using unpaired, 2-tailed t tests for independent samples or, if required, the Welch t-test. Multivariate analyses of variance, with group as factor, age as covariate, and the 6 subfield volumes as dependent variables, were performed to analyze left and right hippocampal subfield volumes. Separate multivariate analyses of variance were used to assess whole left and right hippocampal volume and hippocampal mean diffusivity (MD). Bivariate correlation analyses were performed using parametric Pearson correlation for interval or ratio-scaled data and nonparametric Spearman rank correlation for ordinal data.

Results

Clinical Features

Clinical, laboratory, and electrophysiologic data of all patients are provided in the Table and eTable 1 in the Supplement. Sixteen of 30 patients (53%) experienced unilateral or bilateral FBDS. In addition, 5 patients (17%) reported pilomotor and/or autonomic seizures (eg, shivers or flushing),[173,174] and 1 patient (3%) experienced both FBDS and autonomic seizures (in total, 6 patients [20%]). All except 1 patient with isolated FBDS developed limbic encephalitis with typical clinical features (ie, amnesia, confusion, behavioral and mood disturbances, sleep disturbances, and/or complex partial or generalized seizures). In summary, 28 of 30 patients (93%) experienced FBDS and/or other types of seizures. Immunotherapy was initiated in 29 patients (97%) (Table). Most patients initially received intravenous corticosteroids followed by plasma exchange and/or immunoglobulins (first-line treatment) and long-term immunosuppression (second-line treatment: azathioprine, cyclophosphamide, rituximab, or methotrexate sodium). Clinical outcome was moderate, with a median mRS score of 2 (IQR, 1-2). One patient died of infectious complications.

Table. Clinical Features of 30 Patients With Anti-LGI1 Encephalitis

Characteristic	No. (%)
Sex	
Male	19 (63)
Female	11 (37)
Age, mean (SD), y	65.7 (12.3)
Time after disease onset, median (IQR), mo	23.3 (6.4-35.4)
Tumors present[a]	3 (10)
Clinical diagnosis of limbic encephalitis	29 (97)
Time from symptom onset to immunotherapy, median (IQR), mo	1.6 (0.8-4.4)
Amnesia	30 (100)
Confusion, irritability	18 (60)
Behavioral and mood disturbances	11 (37)
Sleep disturbances	6 (20)
Modified Rankin Scale score, mean (SD)[b]	1.7 (1.1)
Death[c]	1 (3)
Unilateral or bilateral faciobrachial dystonic seizures[d]	16 (53)
Pilomotor and/or autonomic seizures	6 (20)
Complex partial or generalized seizures	12 (40)
Electroencephalogram (n = 27)	
Epileptiform activity	7 (26)
Focal or generalized slowing	12 (44)
Antiepileptic treatment[e]	26 (87)
Acute immunotherapy	29 (97)
IV corticosteroids	27 (90)
Plasma exchange	10 (33)
Immunoglobulins	11 (37)
Long-term immunosuppression	
Oral corticosteroids	20 (67)
Azathioprine	10 (33)
Rituximab	5 (17)
Methotrexate sodium	1 (3)
Cyclophosphamide	1 (3)
Acute clinical imaging	
Hippocampal/MTL T2/FLAIR hyperintensities[f]	22 (73)
Follow-up clinical imaging (n = 26)	
Hippocampal atrophy	25 (96)
Hippocampal sclerosis	13 (50)
Hyponatremia[g]	21 (70)
Antibodies against LGI1	
During acute phase[h]	30 (100)
During follow-up	20 (67)

Abbreviations: FBDS, faciobrachial dystonic seizures; FLAIR, fluid-attenuated inversion recovery; IQR, interquartile range; IV, intravenous; LGI1, leucine-rich, glioma inactivated 1; mRS, modified Rankin Scale; MTL, medial temporal lobe.

[a] One neuroendocrine tumor of the jejunum, 1 breast cancer, and 1 esophageal adenocarcinoma.

[b] Explained in the Clinical Assessment subsection of the Methods section.

[c] One patient died of infectious complications (sepsis and multiorgan failure).

[d] Sixteen of 30 patients (53%) experienced unilateral or bilateral FBDS before the onset of the acute limbic phase of the encephalitis. All but 1 patient with FBDS developed limbic encephalitis.

[e] Including carbamazepine, levetiracetam, valproic acid, clonazepam, pregabaline, and phenytoin.

[f] Transient diffusion restriction of bilateral posterior cortex in 1 patient (3%) and no specific abnormalities in 7 patients (23%).

[g] Hyponatremia (sodium level <135 mEq/L); mean (SD) sodium level, 129.3 (4.5) mEq/L; the remaining patients showed a low-normal serum sodium concentration of 137.6 (1.5) mEq/L (to convert to mmol/L, multiply by 1).

[h] In serum and cerebrospinal fluid, titer range 1:10-1:1000.

Table. Clinical Features of 30 Patients With Anti-LGI1 Encephalitis.

Cognitive outcome

Patients with anti-LGI1 encephalitis showed pronounced episodic verbal memory deficits. Performance in the patients, reported as mean (SE), was significantly impaired across all 5 learning trials of the RAVLT compared with that of the healthy controls (patients, 40.64 [2.88] vs controls, 54.59 [1.67], t(50) = −4.27; P < .001) during the retrieval after the interference list (patients, 6.88 [0.99] vs controls, 11.70 [0.48], t(50) = −4.48; P < .001) and delayed recall (patients, 6.52 [1.05] vs controls, 11.78 [0.56], t(50) = −4.51; P < .001), as well as in the recognition of target words (patients, 10.24 [0.76] vs controls, 13.69 [0.34], t(50) = −3.46; P = .001) (Figure 2 and Figure 1 and Table 2 in the Supplement). Moreover, patients showed significant visuospatial memory deficits (ROCF: immediate recall, patients, 16.62 [2.14] vs controls, 25.16 [1.21], t(27) = −3.64; P = .001; delayed recall, patients, 16.0 [1.96] vs controls, 25.86 [1.24], t(48) = −4.17; P < .001) and impaired working memory (digit span forward, patients, 6.92 [0.47] vs controls, 8.12 [0.35], t(50) = −2.04; P = .047; digit span backward, patients, 5.73 [0.58] vs controls, 7.42 [0.43], t(50) = −2.42; P = .02). Furthermore, patients had impairments of executive function and attention as well as impaired semantic and phonemic fluency (Table 2 in the Supplement).

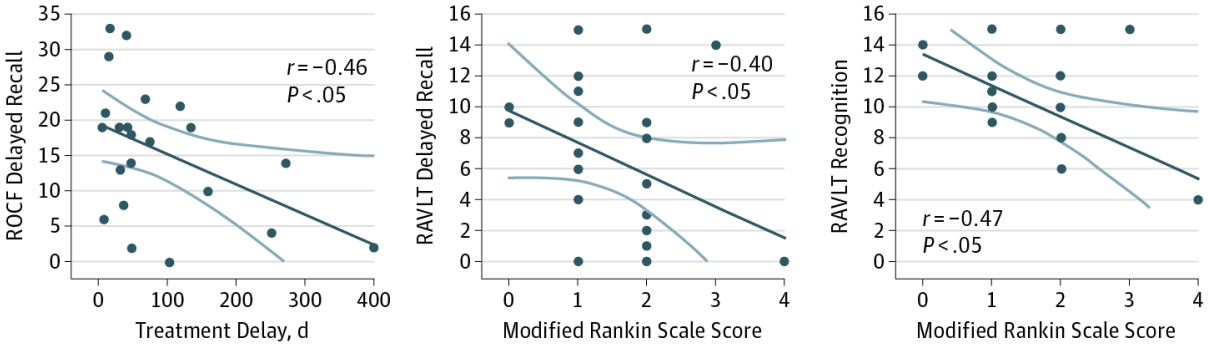

Figure 2. Cognitive Deficits in Encephalitis With Leucine-Rich, Glioma-Inactivated 1 (LGI1) Antibodies. Delayed treatment and a higher disease severity (modified Rankin Scale score) were associated with more severe visual and verbal memory impairments. RAVLT indicates Rey Auditory Verbal Learning Test; ROCF, Rey-Osterrieth Complex Figure.

Clinical Imaging

Visual inspection of the acute routine MRI revealed unilateral or bilateral hippocampal T2/fluid-attenuated inversion recovery (FLAIR) hyperintensities in 22 of 30 patients (73%), transient diffusion restriction of bilateral posterior cortex in 1 patient (3%), and was normal or showed no specific abnormalities in 7 patients (23%) (median, 17 [IQR, 13-119] days after symptom onset) (Figure 3 and Table). One patient with normal MRI results exclusively showed FBDS that did not progress to limbic encephalitis. Follow-up routine MRI data were available for 26 patients and showed hippocampal

atrophy in 25 patients (96%) on visual inspection (Figure 3). In 13 of 26 patients (50%), hippocampal atrophy was accompanied by T2/FLAIR signal increase and loss of internal laminar architecture indicating hippocampal sclerosis.

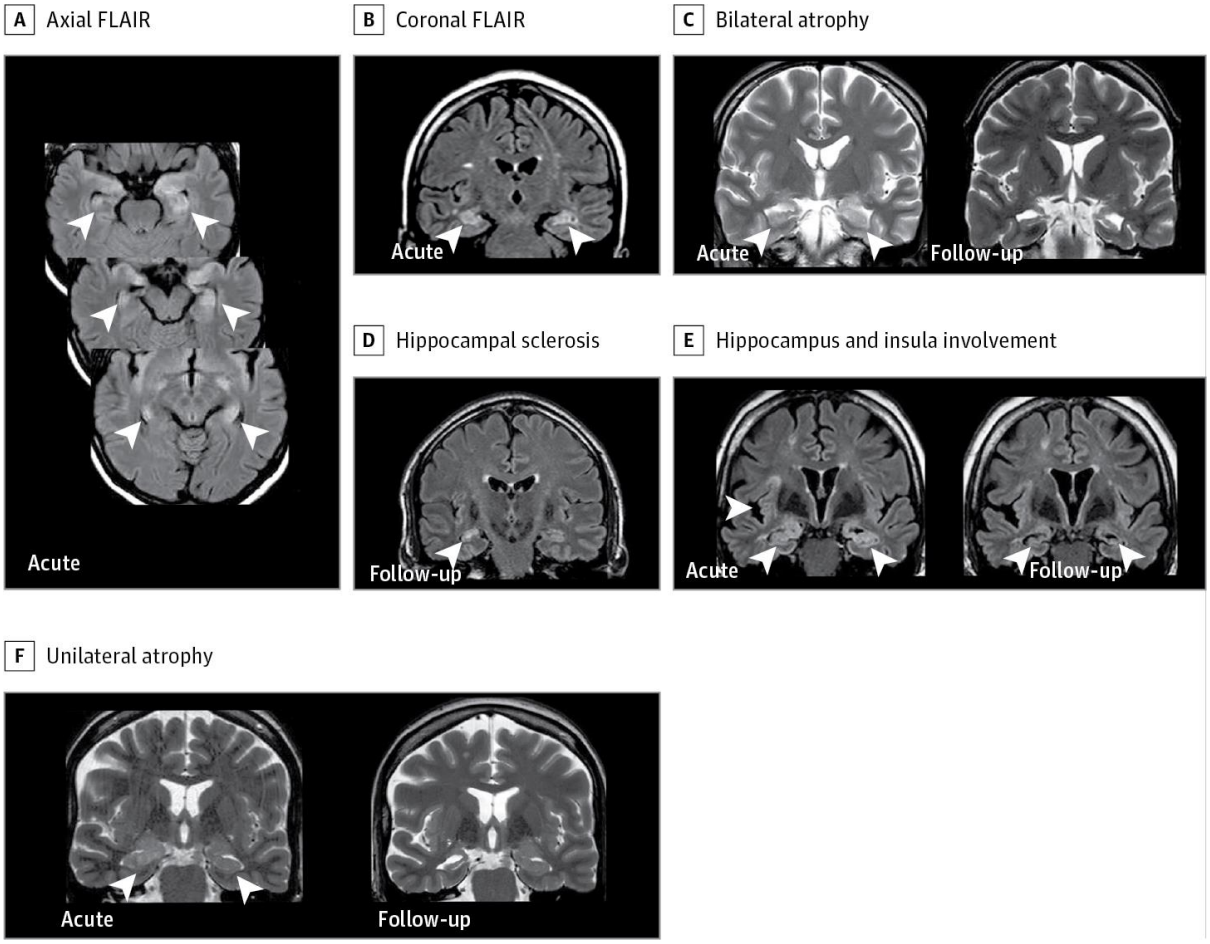

Figure 3. Clinical Magnetic Resonance Imaging (MRI) Findings in Encephalitis With Leucine-Rich, Glioma-Inactivated 1 (LGI1) Antibodies. Representative MRIs of patients with anti-LGI1 encephalitis during the acute stage (median, 17 days after onset) and during follow-up (median, 23.3 months after onset). A, Axial fluid-attenuated inversion recovery (FLAIR) imaging shows signal hyperintensities in both hippocampi and amygdalae during the acute phase. B, Coronal FLAIR image of another patient showing swelling and signal hyperintensity in both hippocampi. C, T2-weighted imaging showing hippocampal edema and enlargement during the acute phase evolving into bilateral hippocampal atrophy. D, Follow-up stage in one patient showing the transition into hippocampal sclerosis of the right hippocampus with gliosis and increased signal in T2. E, Swelling and hippocampal enlargement in one patient showing also an involvement of the right insula and transformation into hippocampal atrophy (follow-up image). F, T2-weighted imaging showing hippocampal edema and enlargement during the acute phase evolving into unilateral hippocampal atrophy. Arrowheads indicate hippocampal and insula imaging changes.

Serial acute routine and follow-up MRI (T1, T2, FLAIR, and diffusion-weighted imaging; 4-9 MRIs per patient) revealed no signal abnormalities in the basal ganglia except for a small, punctuate T2 hyperintensity in the left pallidum in 1 patient.

Hippocampal Volumetry

Patients had a significantly reduced whole bilateral hippocampal volume in comparison with controls (Table 2 in the Supplement). A multivariate analysis of variance of the left and right hippocampal volumes and their corresponding subfields revealed a significantly reduced volume of the right hippocampus in the patient group (Figure 1, Figure 4, and Figure 2 in the Supplement). Significant reductions of hippocampal subfield volumes in patients were observed bilaterally for cornu ammonis 2/3 (CA2/3), CA4/dentate gyrus (DG), presubiculum, and subiculum (Figure 4 and Table 2 in the Supplement).

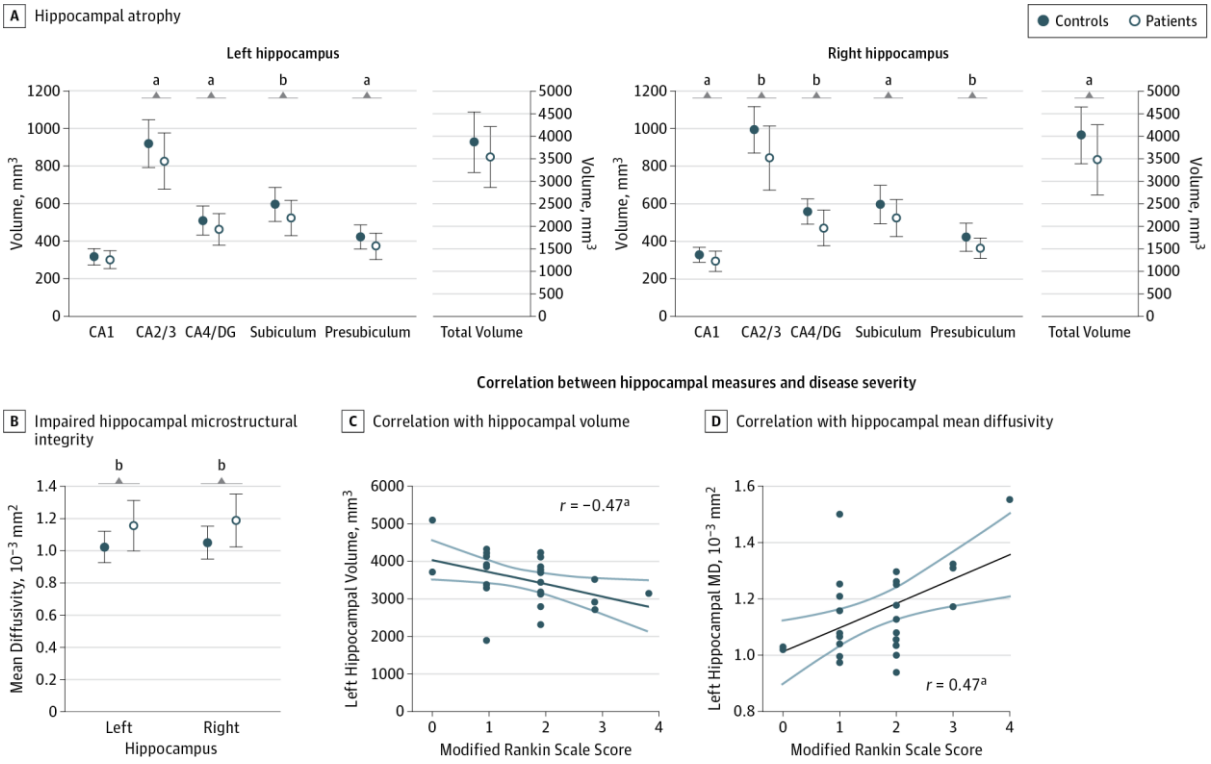

Figure 4. Hippocampal Volumetry and Microstructural Integrity Analyses. A, Reduced volumes of the left and right hippocampus and their corresponding subfields. Error bars indicate SD. B, Mean diffusivity (MD) of the left and right hippocampus is increased in patients with encephalitis with leucine-rich, glioma-inactivated 1 (LGI1) antibodies. C, Higher disease severity (modified Rankin Scale Score) is associated with lower hippocampal volumes. D, Higher disease severity (modified Rankin Scale Score) is associated with more severely impaired microstructural integrity of the hippocampus. [a]*P < .05.* [b]*P < .01.*

A decreased volume of the left CA2/3 subfield correlated significantly with deficits in the recall of the verbal memory material after interference (r = 0.40, P = .048) and delay (r = 0.40, P = .047) as well as during recognition (r = 0.42, P = .04) (Figure 4 and Figure 2 in the Supplement). Impaired recognition was also associated with a decreased volume of the left subiculum (r = 0.42, P = .04). Patients with lower CA4/DG volumes were additionally more prone to commit intrusion errors during the recognition part of the RAVLT (r = −0.59, P = .03).

Hippocampal Microstructural Integrity

Patients had increased MD of both the left and right hippocampus (diffusivity left: patients, 1.155 [0.030] × 10−3; controls, 1.028 [0.019] × 10−3, F(1,34) = 12.99; P = .001; right: patients, 1.186 [0.031] × 10−3; controls, 1.045 [0.019] × 10−3, F(1,34 = 14.78); P < .001) (Figure 4 and eTable 2 in the Supplement). The MD of the left hippocampus was negatively correlated with recognition performance of verbal episodic memory material on the RAVLT (r = −0.41, P = .04). Increase of right hippocampal MD correlated significantly with the number of intrusion errors during the RAVLT recognition (r = 0.57, P = .03). No significant hippocampal fractional anisotropy differences were observed.

Basal Ganglia Volumetry

Basal ganglia volumes were not significantly different between the patients and controls (eTable 2 in the Supplement). Right pallidum volume was negatively correlated with duration of FBDS (ie, days that FBDS persisted: r = −0.71, P = .03), with longer FBDS duration associated with smaller pallidum volume. The same trend was observed for all investigated basal ganglia volumes (all r < −0.30).

Voxel-based Morphometry & DTI

Voxel-based morphometry analysis revealed no differences in cortical gray matter volume between the patient and control groups. No abnormalities in white matter microstructure were observed in the patient group compared with the control group with regard to the diffusion parameters fractional anisotropy, MD, axial diffusivity, and radial diffusivity.

Immunotherapy & Clinical Outcome

The latency between disease onset and initiation of immunotherapy was correlated with worse verbal and visuospatial episodic memory performance (RAVLT recall after interference: r = −0.48, P = .02;

intrusions during recognition: r = 0.62, P = .03; ROCF: immediate recall, r = −0.64, P = .02; and delayed recall, r = −0.46, P = .03) (Figure 2). Higher mRS scores were associated with worse verbal memory performance (RAVLT delayed recall: r = −0.40, P = .049; recognition: r = −0.47, P = .02) (Figure 2) and a higher susceptibility to errors on the Stroop task (r = 0.66, P = .03). Moreover, higher disease severity as indicated by higher mRS scores was accompanied by a volume decrease in left CA2/3 (r = −0.41, P = .04), left CA4/DG (r = −0.43, P = .03), left subiculum (r = −0.47, P = .01), and left hippocampus (r = −0.47, P = .02), as well as an increased MD of the left hippocampus (r = 0.47, P = .01) (Figure 4).

Patients with second-line therapy had significantly worse verbal memory performance (mean [SE] RAVLT delayed recall: 4.07 [1.30] vs 8.15 [1.43], F(1,25) = 4.48; P = .04) and higher disease severity (mRS: 2.00 [0.26] vs 1.31 [0.21], F(1,25) = 4.30; P = .048) in comparison with patients with first-line therapy only. Hippocampal volume (3441.0 [162.6] vs 3568.3 [203.7], F(1,25) = 0.28; P = .60) and integrity (0.00117 [0.00004] vs 0.00116 [0.00003], F(1,25) = 0.62; P = .81) were equally affected in both groups. Antibody titers and time to follow-up were not significantly correlated with memory performance or structural hippocampal findings.

Discussion

We observed that patients with anti-LGI1 encephalitis had markedly impaired verbal and visuospatial memory in association with significantly reduced hippocampal volumes and impaired hippocampal microstructural integrity. Patients with more severe clinical outcomes had more structural hippocampal damage that in turn predicted worse memory performance. Patients with delayed treatment had worse verbal and visuospatial memory performance. Longer FBDS duration correlated with smaller pallidum volume.

Clinical & Cognitive Outcomes

Patients with anti-LGI1 encephalitis presented with typical clinical symptoms (ie, FBDS and limbic encephalitis) complemented by hyponatremia and characteristic hippocampal MRI signal changes.[4,110,120,122,175] Twenty percent of the patients in our cohort had autonomic (eg, shivers, flushing) or pilomotor seizures.[173,174] Tumors were identified in 3 patients (10%). This observation is in line with findings from the cohorts of Lai et al[4] (6 of 51 patients [12%] with 5 different tumors) and Shin et al.[122] (1 of 14 patients [7%]) but contrasts with several studies[22,110,115] that found no tumor associations.

Most patients with anti-LGI1 encephalitis respond to immunotherapy.[57,115,122,176] Almost all of our patients received first- and second-line treatment. Despite this therapy, patients developed substantial verbal and spatial memory deficits.[110,120] These neuropsychological deficits were correlated with disease

severity, with higher mRS scores predisposing to worse performance. Memory deficits were more pronounced in patients who received second-line therapy, which likely relates to the higher disease severity in these individuals. Patients with later treatment had significantly worse memory outcomes. These results add to the observation[115] that early identification and immunosuppressive treatment of FBDS can prevent the subsequent development of cognitive deficits and mirror reports[177–179] of a significant correlation between treatment delay and cognitive outcome in NMDAR encephalitis and other autoimmune encephalitides. Consequently, testing for neuronal antibodies should be performed at a low threshold even in patients with normal findings on routine MRI. Our data furthermore suggest that pilomotor and autonomic seizures can be early symptoms of limbic encephalitis, which is in line with previous case reports[180–182] of patients with limbic encephalitis. Although an objective diagnosis of such seizures frequently cannot be achieved, we propose that antibody testing should be considered in patients presenting with paroxysmal shivering, flushing, or pilomotor erection. Despite possible severe adverse effects, all patients in the present study tolerated immunosuppression well, which is in line with findings from previous studies.[57,122]

Neuroimaging

The hippocampus shows a selective vulnerability to metabolic and cytotoxic insults and is the major pathogenetic target in limbic encephalitis.[38,48,74,92,101] In our cohort, 97% of patients experienced memory deficits. Unilateral or bilateral hippocampal hyperintense signal alterations were found on acute and follow-up routine MRI of most patients, but the results of acute imaging were normal or showed no specific alterations in 23% of the patients. On follow-up, almost all patients had developed hippocampal atrophy or sclerosis, suggesting that hippocampal inflammation was present in the acute phase but not detectable by routine MRI.[111,183] Volumetric analyses confirmed these observations and revealed bilateral hippocampal atrophy, thus extending previous observations of smaller whole hippocampal volumes in 8 patients with anti-LGI1 encephalitis[115] and in 15 patients with voltage-gated potassium channel-complex antibodies (3 of 15 with LGI1 antibodies).[112] Furthermore, we observed bilateral volume reductions of all hippocampal subfields except CA1, a finding that contrasts with predominant CA1 abnormalities in other memory disorders, such as transient global amnesia.[58] Pronounced volume loss was observed in CA2/3 and CA4/DG, and patients with more severe disease courses had lower volumes of left whole hippocampus, CA2/3, CA4/DG, and subiculum. Moreover, CA2/3 volume was significantly correlated with several measures of verbal memory performance. This observation is in line with a predominant expression of LGI1 in CA3,[41] a hippocampal subfield that has been implicated in memory encoding[184,185] as well as in pattern completion and pattern separation (ie, hippocampal mechanisms to recover an entire memory from a partial cue and to create distinct, nonoverlapping memory representations).[186,187] During the recognition phase of the verbal learning test (RAVLT), patients were required to distinguish target words from highly similar interference and

lure items. Patients recognized fewer target words and were more likely to misclassify interference and lure words as targets, indicating a failure in creating and retrieving nonoverlapping representations in memory. Thus, it is conceivable that impaired pattern separation and completion contribute to the memory deficits in patients with anti-LGI1 encephalitis.

Microstructural integrity of the hippocampus was assessed based on analysis of hippocampal MD, which reflects the mean motion of water molecules that is limited by intact membranes and tissue cytoarchitecture. Thus, MD increases are considered a measure of neuronal disintegration and corresponding structural damage.[188] In anti-LGI1 encephalitis, hippocampal MD proved to be a sensitive marker of hippocampal damage: MD of both hippocampi was significantly increased and correlated with disease severity and memory deficits in patients. These findings are in line with observations of correlations between increased hippocampal MD and worse memory performance in healthy individuals,[189,190] patients with Alzheimer disease,[191] and patients with anti-NMDAR encephalitis.[92]

In contrast, we observed basal ganglia signal alterations in only 1 patient, and basal ganglia volumes were not reduced in comparison with those in healthy controls. However, longer individual FBDS duration correlated with reduced pallidum volume. This result adds to observations of basal ganglia positron emission tomography and MRI abnormalities and suggests a role for basal ganglia in FBDS pathophysiology.[22,115,117,163,192] We did not observe basal ganglia T1 and T2 hyperintensities that were recently reported in 42% of patients with anti-LGI1 encephalitis and FBDS.[163] This difference in basal ganglia MRI findings might be due to the transient nature of these signal alterations and the different timing of MRI in both studies. For example, T1 hyperintensities were detected a median of 26.5 days after FBDS onset with a median duration of 11 weeks, but T2 hyperintensities were seen after 15 days and lasted only 1 week.[163] Thus, longitudinal studies are needed to reveal the exact time course of these basal ganglia signal changes. Another recent study[192] reported hypermetabolism in the primary motor cortex contralateral to the limb affected by FBDS that normalized when the patients recovered. Using whole-brain voxel-based morphometry and DTI, we found no reduction of gray matter density and whole-brain white matter integrity. Specifically, we detected no structural damage in the motor cortex, corroborating the transient nature of motor cortex involvement in contrast to the severe and persistent hippocampal damage.

Taken together, our MRI analyses provide a characteristic pattern of imaging alterations in anti-LGI1 encephalitis that reveal a more focal and less widespread pathophysiology in comparison with other autoimmune encephalitides.[74] The results particularly contrast with findings in anti-NMDAR encephalitis. The most prominent difference is widespread white matter damage in patients with anti-NMDAR encephalitis that was not observed in those with anti-LGI1 encephalitis despite the typical older age and the presence of microvascular white matter lesions on routine imaging in some of these patients.[101] Furthermore, although whole hippocampal volumes are reduced in both disorders,

hippocampal subfields are differentially affected (bilateral atrophy of CA2/3, CA4/DG, subicular complex in anti-LGI1 encephalitis, and CA4/DG and subicular complex in anti-NMDAR encephalitis).[92]

Limitations

This study has limitations inherent to its exploratory and multicenter design. Patients were studied at 2 centers, and some neuropsychological tests were performed only in 1 center. However, major tests assessing memory, attention, and executive function were identical in both centers. Furthermore, a large number of imaging and neuropsychological analyses were performed. Given the exploratory nature of this study, no correction for multiple comparisons was performed across tests. However, corrections for multiple comparisons were performed for individual analyses where applicable (eg, voxel-based morphometry and DTI analyses) (eMethods in the Supplement).

Conclusions

We show that patients with anti-LGI1 encephalitis develop persistent and severe verbal and visuospatial memory deficits in addition to impairments of working memory, attention, and executive functions. Advanced imaging analyses revealed a characteristic pattern of bilateral hippocampal atrophy with predominant effects on the subfields CA2/3, CA4/DG, and the subicular complex and bilaterally impaired hippocampal microstructural integrity. Patients with more severe disease courses had a larger amount of hippocampal damage that in turn predicted worse memory performance. Duration of FBDS was associated with reduced pallidum volume. On clinical evaluation, we observed that 20% of patients presented with pilomotor or autonomic seizures—subtle clinical symptoms that need to be considered as possible signs of limbic encephalitis. Routine MRI during the acute disease stage revealed hippocampal hyperintensities in most patients but was unremarkable in 23% of the patients. Our data show that delayed immunotherapy is associated with more severe memory impairment and thus highlight the need for early diagnosis and rapid treatment in patients with anti-LGI1 encephalitis.

Supplementary material

Supplementary methods (eMethods)

MRI Acquisition

Imaging data was acquired at both sites using 3T MRI Scanners. At Charité University Hospital, a Siemens Tim Trio scanner equipped with a 12-channel phased-array head coil (Siemens, Erlangen,

Germany) at the Berlin Center for Advanced Neuroimaging was used. At University Hospital Schleswig-Holstein in Kiel, MRI data was acquired using a 32-channel head coil on a Philips Achieva scanner (Philips, Best, The Netherlands). At both sites, a high-resolution three-dimensional T1-weighted magnetization-prepared rapid gradient echo (MPRAGE) sequence (matrix size = 240x240, 176 slices, voxel size = 1x1x1 mm^3) and a single-shot echo-planar imaging sequence for the acquisition of DTI data (voxel size = 2x2x2 mm^3, 61 slices, 64 diffusion directions, b value = 1000s/mm^2) were acquired. For clinical assessment, T2-weighted turbo spin echo sequences and a 3D isotropic T2-weighted fluid-attenuated inversion recovery (FLAIR) were collected.

Analyses of clinical MRIs

For the clinical study, available previous brain MRIs from other institutions were re-evaluated by a neuroradiologist or neurologist experienced in the assessment of hippocampal signal abnormalities and blinded to the patient's diagnosis. Signal characteristics were assessed using T2-weighted or FLAIR images and were classified as "normal" or "hyperintense". Hippocampal volume was assessed by visual inspection and in comparison classified as "normal", "enlarged" or "atrophic". In follow-up images, T2/FLAIR signal increase and loss of internal laminar architecture in the cornu ammonis were used as criteria for diagnosing Ammon's horn sclerosis. All patients MRI's were also carefully evaluated with regard to signal changes in the basal ganglia in the acute, subacute and follow-up state to detect possible transient imaging changes. All patients had serial MRIs (4-9 MRIs) over the course of the disease. Signal abnormalities in the basal ganglia were longitudinally assessed with regard to hypo- or hyper intensities and volume changes in T1, T2, FLAIR and diffusion-weighted imaging.

Diffusion Tensor Imaging & Hippocampal Microstructural Integrity

Differences in white matter integrity between patients and controls were investigated with diffusion tensor imaging[193]. The FMRIB Diffusion Toolbox as implemented in FSL[194] was used to assess fractional anisotropy (FA), mean diffusivity (MD), axial diffusivity (AD) and radial diffusivity (RD). Preprocessing steps included eddy current correction and brain extraction. Subsequently, a tensor model was fitted to the raw diffusion data. The FA images were aligned to a 1x1x1 standard space, non-linearly registered to the group-specific template and narrowed to the FA skeleton. Cross-subject non-parametric permutation testing (5000 permutations) was conducted on a voxel-wise basis using the randomise tool as implemented in FSL. In order to account for deviations in imaging acquisition, we included 'study site' as a covariate of no interest in the model. Threshold-free cluster enhancement was applied (TFCE, $p < 0.05$, family-wise error corrected). Similarly, MD, AD and RD maps were determined using tract-based spatial statistics (TBSS).

In order to assess the microstructural integrity of the hippocampus and its relation to cognitive outcome, we conducted a region-of-interest analysis of the FA and MD maps in patients and controls. The left and right hippocampi were individually segmented from the brain extracted T1-weighted images using FSL FIRST, with the quality of the automated segmentation being controlled by visual inspection.[195] An affine linear ratio cost function transformation was used to register individual FA maps to the T1-weighted images. The resultant transformation matrices were then used for registration of MD maps. Finally, hippocampal masks were used for calculation of the mean individual hippocampal FA and MD values.

Voxel-based morphometry

The evaluation of differences in the local grey matter volume between patients and controls was carried out using FSL VBM[196]. MPRAGE images were brain extracted, segmented, aligned to MNI152 standard space using nonlinear registration and a study-specific template was created. Next, all native grey matter images were nonlinearly reregistered to this study-specific template. Further steps included modulation to correct for local expansion or contraction and smoothing with an isotropic Gaussian kernel (σ = 3mm). The final voxel-wise statistical analysis was performed with 'study site' as a covariate of no interest in the model and comprised non-parametric permutation testing with 5000 permutations and threshold-free cluster enhancement (TFCE) using FSL randomise ($p < 0.05$, FWE-corrected).

Hippocampal & Basal Ganglia Volumetry

The Freesurfer image analysis suite (http://surfer.nmr.mgh.harvard.edu/)[197] was used to perform hippocampal and basal ganglia volumetry. Following motion correction and brain extraction, the images were segmented into subcortical white matter and grey matter volumetric structures including the hippocampal formation, caudate nucleus, putamen, globus pallidus and nucleus accumbens. Automated subfield segmentation of the hippocampus was performed using Bayesian inference and a probabilistic atlas of the hippocampal formation.[172,198] The following subfield volumes were calculated: cornu ammonis CA1, CA2/3, CA4/dentate gyrus (DG), presubiculum, subiculum, and fimbria (Fig. 1). Volumes of the basal ganglia, whole hippocampus and hippocampal subfields were adjusted for intracranial volume (ICV) using the following formula: $Volume_{adjusted} = Volume_{observed} - \beta$ *(slope from ICV vs. regional volume regression)* $x\ (ICV_{observed} - ICV_{sample\ mean})$.

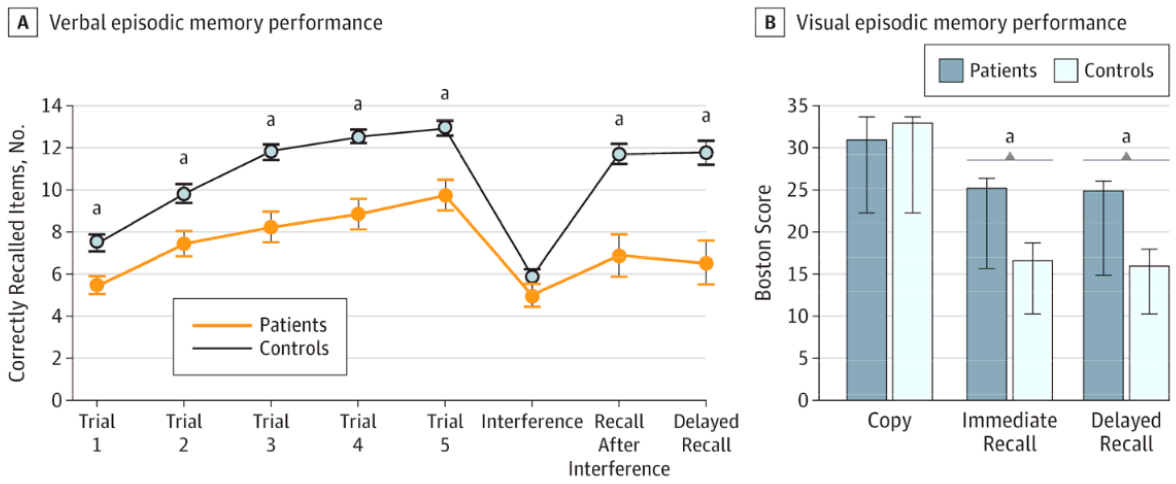

eFigure 1. Cognitive Deficits in LGI1 Encephalitis

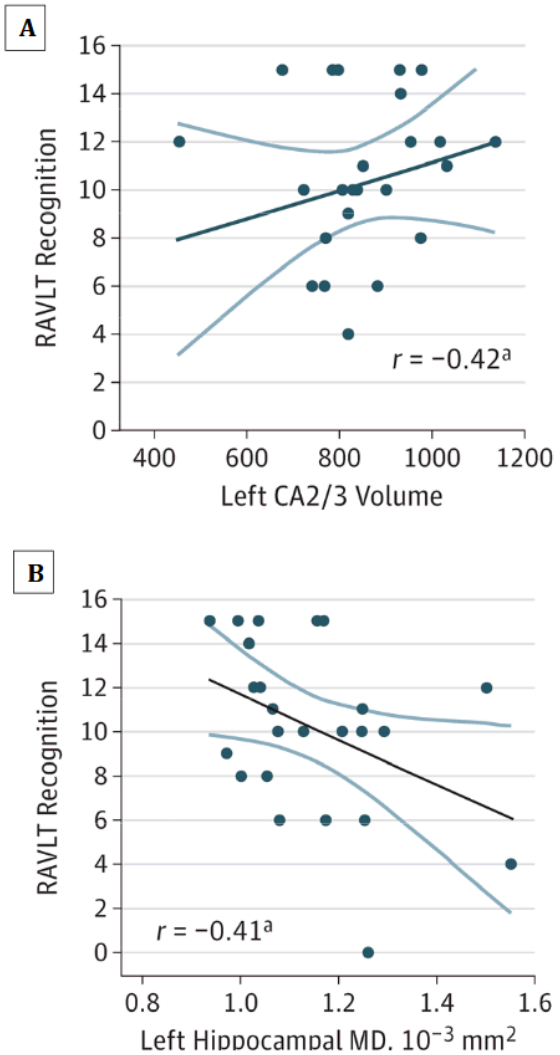

eFigure 2. Hippocampal Volumetry and Microstructural Integrity Analysis

ID	**1**	**2**	**3**
Sex	F	M	M
Age	69	48	66
Acute routine imaging	T2/FLAIR acute: hyperintensities hippocampus and amygdalae bilaterally, Follow-up after 4 months: mild right-sided hippocampal atrophy with T2/FLAIR signal increase, Mild SAE	T2/FLAIR acute: right hippocampal hyperintensities, Follow-up after 4 months: right hippocampal atrophy	T2/FLAIR acute: bilateral (left > right) hippocampal hyperintensities, Follow-up after 10 months: Left hippocampal atrophy and T2/FLAIR signal increase
EEG	Normal EEG	Predominant alpha rhythm with repeated episodes of rhythmic bilateral theta activity	Predominant alpha rhythm with epileptiform activity
FBDS or pilo-motor/ auto-nomic seizures	FBDS	Pilomotor seizures, shivers running through the body	-
Other seizures	-	One complex-focal seizures with secondary generalization	One complex focal seizure
Limbic encephalitis symptoms	Memory deficits, sleep disturbances	Memory deficits	Memory deficits, confusion, sleep disturbances
Hyponatremia (<135 mmol/l)	Yes	No	Yes
Lowest sodium level (mmol/l)	129	137	129
Tumour	Neuroendocrine tumor grade 2, Jejunum (Mib-1, 5%)	No	No
Antiepileptic therapy	Levetiracetam (3000 mg/d)	Levetiracetam (2000 mg/d)	Levetiracetam (1000 mg/d)
Immunotherapy	Plasma exchange, IV Methylprednisolone (x3), Prednisolone (30 - 70 mg/d), Methotrexate 15 mg/week	Immunoglobulins, IV Methylprednisolone	IV Methylprednisolone, Plasma exchange, Azathioprine (60 mg/d)
mRS*	1	1	2
Antibody titre*	1:100 (S), Neg (CSF)	1:100 (S)	1:10 (S)

*eTable 1. Clinical and Laboratory Characteristics of Anti-LGI1 Encephalitis Patients. *at the time of study, ***clinical MRI*

ID	**4**	**5**	**6**
Sex	M	M	M
Age	75	75	70
Acute routine imaging	T2/FLAIR acute: no hyperintensities in hippocampi, Follow-up after 30 months: Bilateral hippocampal atrophy, Extensive SAE, mild global atrophy	T2/FLAIR acute: normal, Follow-up after 12 months: mild bilateral hippocampal atrophy	T2/FLAIR acute: left hippocampal hyperintensities, Follow-up after 5 years: mild left hippocampal atrophy, Mild SAE
EEG	Normal EEG	Normal EEG	Moderate generalized slowing with right frontotemoral slowing
FBDS or pilo-motor/ auto-nomic seizures	FBDS	FBDS	FBDS
Other seizures	-	-	-
Limbic encephalitis symptoms	Memory deficits	Memory deficits, confusion	Memory deficits, confusion, sleep disturbances, reduced vigilance, delirium
Hyponatremia (<135 mmol/l)	No	No	Yes
Lowest sodium level (mmol/l)	-	136	130
Tumour	No	No	No
Antiepileptic therapy	Valproic acid (600 mg/d)	Levetiracetam (1000 mg/d)	Levetiracetam (3000 mg/d)
Immunotherapy	IV Methylprednisolone, Plasma exchange	IV Methylprednisolone (x4), Immunoglobulins (x3), Prednisolone (60 mg/d), Azathioprine (60 mg/d)	IV Methylprednisolone, Plasma exchange (x2), Prednisolone (100mg/d), Azathioprine (100mg/d)
mRS*	2	1	2
Antibody titre*	Neg (S)	1:100 (S)	1:10 (S)

eTable 1. (continued)

ID	**7**	**8**	**9**
Sex	M	F	F
Age	76	68	73
Acute routine imaging	T2/FLAIR acute: normal hippocampi, periventricular leukoencephalopathy, Follow-up after 24 months: Bilateral hippocampal atrophy, Mild global atrophy	T2/FLAIR acute: mild bilateral hyperintensities in hippocampus, Follow-up after 30 months: mild right hippocampal atrophy	T2/FLAIR acute: left hippocampal hyperintensities, Follow-up after 14 months: bilateral (left >> right) hippocampal atrophy
EEG	n/a	Predominant alpha rhythm with hemispheric focus of slowed activity during hyperventilation, no epileptiform activity	n/a
FBDS or pilo-motor/ auto-nomic seizures	-	FBDS and short shivers of whole body	-
Other seizures	-	-	Generalised
Limbic encephalitis symptoms	Memory deficits, sleep disturbances	Memory deficits, confusion	Memory deficits, confusion
Hyponatremia (<135 mmol/l)	Yes	No	Yes
Lowest sodium level (mmol/l)	134	140	133
Tumour	No	No	No
Antiepileptic therapy	-	Levetiracetam	Levetiracetam (1000 mg/d)
Immunotherapy	Immunoglobulins, IV Methylprednisolone (x3), Prednisolone (70 mg/d), Azathioprine (150mg/d)	IV Methylprednisolone , Plasma Exchange	IV Methylprednisolone (x2), Prednisolon (60mg/d), Azathioprine (150mg/d), Rituximab (2 x 1000 mg)
mRS*	3	1	3
Antibody titre*	1:32 (S)	1:320 (S)	IgG 1:100 (12/04/13), IgG 1:32 (07/06)

eTable 1. (continued)

ID	**10**	**11**	**12**
Sex	M	M	M
Age	54	38	68
Acute routine imaging	T2/FLAIR acute: bilateral hyperintensities in hippocampi, Follow-up after 10 months: bilateral (left > right) hippocampal atrophy with T2/FLAIR signal increase and mild global atrophy, Mild SAE	T2/FLAIR acute: normal	T2/FLAIR acute: right hippocampal hyperintensities, Follow-up after 10 months: right hippocampal atrophy, Mild SAE
EEG	n/a	Normal EEG	Diffuse theta and delta activity with intermittent sharp waves
FBDS or pilo-motor/ auto-nomic seizures	FBDS	-	FBDS
Other seizures	-	Complex focal seizures	-
Limbic encephalitis symptoms	Memory deficits, confusion, pavor nocturnus	Memory deficits, irritability, anxiety, depressive symptoms, sleep disturbances	Memory deficits, confusion, agitation, confusion, pseudobulbar affect with pathological crying
Hyponatremia (<135 mmol/l)	Yes	No	Yes
Lowest sodium level (mmol/l)	n/a	138	118
Tumour	No	No	No
Antiepileptic therapy	Levetiracetam	Levetiracetam (1250 mg/d)	Levetiracetam (3000 mg/d)
Immunotherapy	Immunoglobulins (x3), IV Methylprednisolone (x3)	IV Methylprednisolone, Prednisolone (80 mg/d)	IV Methylprednisolone, Prednisolone (80 mg/d)
mRS*	-	0	2
Antibody titre*	Neg (S)	1:100 (CSF)	1:10 (S)

eTable 1. (continued)

ID	**13**	**14**	**15**
Sex	M	M	M
Age	60	63	71
Acute routine imaging	T2/FLAIR acute: hyperintensities right hippocampus, Follow-up after 12 months: bilateral (right > left) hippocampal atrophy with T2/FLAIR signal increase and mild global atrophy	T2/FLAIR acute: hyperintensities right hippocampus; residual hyperintensities left hippocampus, Follow-up after 3 months: left > right hippocampal atrophy	T2/FLAIR acute: bilateral hyperintensities in hippocampi, Follow-up after 3 months: mild bilateral hippocampal atrophy, Mild SAE
EEG	Moderate generalized slowing	Bilateral fronto-temporal slowing and epileptiform discharges	Moderate generalized slowing
FBDS or pilo-motor/ auto-nomic seizures	Shivers	FBDS	FBDS
Other seizures	-	-	-
Limbic encephalitis symptoms	Memory deficits, confusion, apathy, suicidality	Memory deficits, confusion, delusions, aggressiveness; later apathy, depressive symptoms, somnolence	Memory deficits
Hyponatremia (<135 mmol/l)	Yes	Yes	Yes
Lowest sodium level (mmol/l)	127	134	129
Tumour	No	No	No
Antiepileptic therapy	-	Valproic acid (1800 mg/d), Levetiracetam	-
Immunotherapy	IV Methylprednisolone, Plasma exchange, Immunoglobulins Prednisolone (20 mg/d)	IV Methylprednisolone, Plasma exchange, Immunoglobulins, Rituximab (2 x 1000 mg)	IV Methylprednisolone, Immunoglobulins, Prednisolone (80mg/d), Rituximab (2 x 1000mg)
mRS*	2	3	1
Antibody titre*	Neg (S)	Pos (S), Pos (CSF)	1:100 (S)

eTable 1. (continued)

ID	**16**	**17**	**18**
Sex	M	F	F
Age	75	74	95
Acute routine imaging	T2/FLAIR acute: normal hippocampi, extensive SAE involving white matter, basal ganglia and brain stem; mild global atrophy, Follow-up after 4 months: mild bilateral hippocampal atrophy, Extensive SAE	T2/FLAIR acute: bilateral hyperintensities in hippocampi, Follow-up after 3 months: bilateral hippocampal atrophy with persisting hyperintensities	T2/FLAIR acute: Mild generalized atrophy and SAE, FDG-PET: bilateral striatal hypermetabolism
EEG	Normal EEG	Moderate slowing, no epileptiform activity	Normal EEG
FBDS or pilo-motor/ auto-nomic seizures	FBDS	-	FBDS
Other seizures	-	complex focal seizures	-
Limbic encephalitis symptoms	Memory deficits	Memory deficits	(No limbic encephalitis)
Hyponatremia (<135 mmol/l)	Yes	Yes	No
Lowest sodium level (mmol/l)	128	134	137
Tumour	No	No	No
Antiepileptic therapy	Levetiracetam , Clonazepam (0.75 mg/d)	Valproic acid, Levetiracetam (2000 mg/d)	Pregabalin
Immunotherapy	IV Methylprednisolone, Prednisolone (80mg/d)	No immunosuppressive treatment due to severe complications (pneumonia, sepsis), Deceased in 4/2014 due to multi-organ failure	Immunoglobulins (x2)
mRS*	1	4**	0**
Antibody titre*	1:32 (S), Neg (CSF)	1:320 (S), 1:100 (CSF)**	1:320 (S)

eTable 1. (continued)

ID	**19**	**20**	**21**
Sex	M	F	M
Age	62	61	61
Acute routine imaging	T2/FLAIR acute: bilateral hyperintensities in hippocampi (left > right)	T2/FLAIR acute: bilateral hyperintensities in hippocampi, fornices, amygdalae, Follow-up after 4 months: hippocampal atrophy with T2/FLAIR signal increase (predominantly left-sided) (i.e., hippocampal sclerosis), SAE, other imaging features: peri-ventricular (non-active) subclinical lesions suggestive for multiple sclerosis	T2/FLAIR acute: no hyperintensities in hippocampi, Follow-up after 9 years: hippocampal atrophy with T2/FLAIR signal increase (hippocampal sclerosis), SAE
EEG	Normal EEG	Periodic rhythmic theta-activity temporal left, suspicious for focal EEG-seizures	Alpha rhythm, left fronto-temporal focus without epileptiform activity
FBDS or pilo-motor/ auto-nomic seizures	FBDS	-	FBDS
Other seizures	Complex focal seizures	Complex focal seizures	Generalised tonic-clonic seizure
Limbic encephalitis symptoms	Memory deficits, confusion, executive dysfunction, agitation, delusions	Memory deficits, confusion, psychosis	Memory deficits, fluctuating consciousness, optic & acustic hallucinations, confusion, delirium, psychosis, apathy followed by aggressiveness
Hyponatremia (<135 mmol/l)	Yes	Yes	Yes
Lowest sodium level (mmol/l)	126	126	124
Tumour	No	No	No
Antiepileptic therapy	Valproic acid (2000 mg/d), Levetiracetam (1500 mg/d)	Levetiracetam (3000 mg/d)	Valproic acid (1500 mg/d), Levetiracetam (1500 mg/d), Phenytoin (400 mg/d)
Immunotherapy	IV Methylprednisolone, Immunoglobulins, Plasma exchange	IV Methylprednisolone (x2) Plasma exchange (x2) Rituximab (4 x 375 mg/m^2) Cyclophosphamid	IV Methylprednisolone, Prednisolone (50 mg/d) , Azathioprine (150 mg/d)
mRS*	4**	3	2
Antibody titre*	1:320 (S), 1:10 (CSF)**	Neg (S), Neg (CSF)	1:32 (S). Neg (CSF)

eTable 1. (continued)

ID	**22**	**23**	**24**
Sex	F	M	M
Age	73	66	79
Acute routine imaging	T2/FLAIR acute: hyperintensities left hippocampus, Follow-up after 12 months: left hippocampal atrophy with T2/FLAIR signal increase (i.e., hippocampal sclerosis), SAE	T2/FLAIR acute: hyperintensities hippocampi (predominantly left), Follow-up after 12 months: left hippocampal atrophy with moderate T2/FLAIRsignal increase (i.e., hippocampal sclerosis), SAE	T2/FLAIR acute: hyperintensities hippocampi (predominantly right), Follow-up after 12 months: bilateral hippocampal atrophy with T2/FLAIR signal increase right (i.e., hippocampal sclerosis), SAE
EEG	Continuous theta and delta activity with fronto-temporal dominance	Predominant alpha rhythm with inconstant left temporoparietal theta-delta-focus ; no epileptiform activity	Slow alpha rhythm wit intermittent generalized slowing
FBDS or pilo-motor/ auto-nomic seizures	FBDS	Pilomotor seizures	FBDS
Other seizures	Complex focal seizures	Generalised tonic-clonic seizure	-
Limbic encephalitis symptoms	Memory deficits, confusion, impaired consciousness	Memory deficits, affect lability, confusion	Memory deficits, delirium, apathy
Hyponatremia (<135 mmol/l)	Yes	No	Yes
Lowest sodium level (mmol/l)	112	n/a	130
Tumour	No	No	No
Antiepileptic therapy	Levetiracetam (1500 mg/d)	Valproic acid (1200 mg/d)	Levetiracetam (2000 mg/d), Carbamazepine (600 mg/d), Lorazepam (3 mg/d)
Immunotherapy	IV Methylprednisolone (x2), Prednisolone (30 mg/d), Azathioprine (25 mg/d)	IV Methylprednisolone (x2), Prednisolone (20 mg/d) Azathioprine (150 mg/d)	Immunoglobulins, IV Methylprednisolone, Prednisolone
mRS*	2	2	2
Antibody titre*	1:10 (S), Neg (CSF)	Neg (S), Neg (CSF)	Neg (S)

eTable 1. (continued)

ID	**25**	**26**	**27**
Sex	F	F	F
Age	38	70	70
Acute routine imaging	T2/FLAIR acute: hyperintensities hippocampi and amygdalae, insula right, Follow-up after 12 months: bilateral hippocampal atrophy with T2/FLAIR signal increase (i.e., hippocampal sclerosis)	T2/FLAIR/DWI acute: no hippocampal hyperintensities; transient bilateral posterior cortical diffusion lesions, Follow-up: normal	T2/FLAIR acute: hyperintensities hippocampi and amygdalae, SAE
EEG	Predominant alpha rhythm with paroxysmal dysrhythmia and left frontotemporal theta-delta focus with epileptiform discharges	Alpha rhythm, left frontotemporal focus with intermittent sharp-waves	Predominant alpha rhythm with increased beta-activity, no epileptiform activity
FBDS or pilo-motor/ auto-nomic seizures	-	-	FBDS
Other seizures	Absence-like seizures, one generalized tonic-clonic seizure	-	-
Limbic encephalitis symptoms	Memory deficits, confusion	Memory deficits	Memory deficits, confusion, personality changes, depressive symptoms including suicidality
Hyponatremia (<135 mmol/l)	No	No	Yes
Lowest sodium level (mmol/l)	138	138	126
Tumour	No	No	Mammary Carcinoma (highly differentiated)
Antiepileptic therapy	Levetiracetam (2500 mg/d), Valproic acid (1800 mg/d)	Levetiracetam (1000 mg/d)	-
Immunotherapy	IV Methylprednisolone, Prednisolone (25mg/d), Immunoglobulins, Plasma exchange (x2), Immunoadsorption, Rituximab (4x375 mg/m2)	IV Methylprednisolone (x2), Prednisolone, Azathioprine	IV Methylprednisolone , Prednisolone 80mg
mRS*	1	1	1
Antibody titre*	Neg (S)	Neg (S), Neg (CSF)	1:10 (S)

e*Table 1. (continued)*

ID	**28**	**29**	**30**
Sex	M	M	F
Age	48	74	51
Acute routine imaging	T2/FLAIR acute: hyperintensities hippocampi and amygdalae, Follow-up after 7 months: mild bilateral hippocampal atrophy with T2/FLAIR signal increase (i.e., hippocampal sclerosis), gliotic changes after brain trauma 1995	T2/FLAIR acute: bilateral hyperintensities hippocampi and amygdalae, Follow-up after 14 months: mild bilateral hippocampal atrophy (l>r) with mild T2/FLAIR signal increase (i.e., hippocampal sclerosis) general atrophy, SAE	T2/FLAIR acute: hyperintensities hippocampus and amygdalae right, Follow-up after 9 months: mild right-sided hippocampal atrophy with T2/FLAIR signal increase (i.e., hippocampal sclerosis) , mild SAE
EEG	Mild generalized slowing, no epileptiform actitvity	Normal EEG	Predominant alpha rhythm, diffuse and paroxysmal dysrhythmia, no epileptiform actitvity
FBDS or pilo-motor/ auto-nomic seizures	Pilomotor seizures	-	Pilomotor seizures, flushing
Other seizures	-	Complex focal and generalized tonic-clonic seizures	-
Limbic encephalitis symptoms	Memory deficits, confusion	Memory deficits, confusion	Memory deficits, affect lability
Hyponatremia (<135 mmol/l)	Yes	Yes	Yes
Lowest sodium level (mmol/l)	114	n/a	122
Tumour	No	Adenocarcinoma of the esophagus (highly differentiated)	No
Antiepileptic therapy	Levetiracetam (2000 mg/d)	Valproic acid (1500 mg/d)	Levetiracetam (1000 mg/d)
Immunotherapy	IV Methylprednisolone , Prednisolone	IV Methylprednisolone, Prednisolone, Azathioprine	Prednisolone (80 mg/d)
mRS*	0	1	1
Antibody titre*	1:10 (S)	Neg (S)	Neg (S)

eTable 1. (end)

	Patient group (mean±SEM)	Control group (mean±SEM)	Test statistic	p-value
Volumes (in mm³)				
Bilateral hippocampus	3502.3 ± 127.4 mm³	3921.4 ± 128.5 mm³	F(1,34)=5.37	p=0.025
Left hippocampus	3530.5 ± 127.6 mm³	3843.1 ± 131.4 mm³	F(1,34)=2.80	p=0.100
Left CA1	300.9 ± 8.9 mm³	315.0 ± 8.5 mm³	F(1,34)=1.28	p=0.263
Left CA2/3	826.0 ± 28.3 mm³	916.7 ± 24.3 mm³	F(1,34)=5.70	p=0.021
Left CA4/DG	461.5 ± 15.7 mm³	507.6 ± 14.6 mm³	F(1,34)=4.46	p=0.040
Left presubiculum	372.6 ± 13.3 mm³	421.0 ± 12.4 mm³	F(1,34)=6.88	p=0.011
Left subiculum	522.3 ± 17.6 mm³	592.8 ± 17.5 mm³	F(1,34)=7.80	p=0.007
Right hippocampus	3474.1 ± 147.1 mm³	3999.7 ± 126.1 mm³	F(1,34)=7.09	p=0.010
Right CA1	293.6 ± 10.2 mm³	326.3 ± 8.0 mm³	F(1,34)=6.14	p=0.017
Right CA2/3	841.3 ± 32.4 mm³	990.5 ± 24.1 mm³	F(1,34)=13.17	p=0.001
Right CA4/DG	470.0 ± 17.9 mm³	555.7 ± 12.8 mm³	F(1,34)=14.61	p<0.001
Right presubiculum	365.3 ± 10.3 mm³	423.3 ± 14.3 mm³	F(1,34)=10.40	p=0.002
Right subiculum	523.0 ± 18.5 mm³	593.3 ± 19.5 mm³	F(1,34)=6.59	p=0.013
Bilateral caudate nucleus	3671.2 ± 164.1 mm³	3488.9 ± 115.2 mm³	F(1,34)=0.83	p=0.367
Left caudate nucleus	3579.4 ± 164.6 mm³	3453.3 ± 120.5 mm³	F(1,34)=0.38	p=0.539
Right caudate nucleus	3763.1 ± 167.8 mm³	3524.4 ± 118.9 mm³	F(1,34)=1.35	p=0.251
Bilateral putamen	5059.5 ± 157.2 mm³	5040.7 ± 127.3 mm³	F(1,34)=0.01	p=0.927
Left putamen	5197.2 ± 176.6 mm³	5180.2 ± 142.2 mm³	F(1,34)=0.006	p=0.941
Right putamen	4921.7 ± 146.1 mm³	4901.3 ± 121.6 mm³	F(1,34)=0.12	p=0.915
Bilateral pallidum	1507.6 ± 42.1 mm³	1594.1 ± 40.5 mm³	F(1,34)=2.20	p=0.144
Left pallidum	1589.3 ± 55.3 mm³	1679.2 ± 44.8 mm³	F(1,34)=1.59	p=0.212
Right pallidum	1425.8 ± 32.9 mm³	1509.0 ± 39.9 mm³	F(1,34)=2.58	p=0.114
Microstructural integrity				
MD left hippocampus (*10⁻³)	1.155 ± 0.030	1.028 ± 0.019	F(1,34)=12.99	p=0.001
MD right hippocampus (*10⁻³)	1.186 ± 0.031	1.045 ± 0.019	F(1,34)=14.78	p<0.001
FA left hippocampus	0.1314 ± 0.004	0.1344 ± 0.004	F(1,34)=0.28	p=0.597
FA right hippocampus	0.1332 ± 0.004	0.1331 ± 0.003	F(1,34)=0.001	p=0.975
Neuropsychological assessment				
RAVLT sum score	40.64 ± 2.88	54.59 ± 1.67	t(50)=-4.27	p<0.001
RAVLT recall after interference	6.88 ± 0.99	11.70 ± 0.48	t(50)=-4.48	p<0.001
RAVLT delayed recall	6.52 ± 1.05	11.78 ± 0.56	t(50)=-4.51	p<0.001
RAVLT recognition	10.24 ± 0.76	13.69 ± 0.34	t(50)=-3.46	p=0.001
ROCF copy	32.96 ± 0.85	30.89 ± 1.24	t(49)=1.14	p=0.262
ROCF immediate recall	16.62 ± 2.14	25.16 ± 1.21	t(27)=-3.64	p=0.001
ROCF delayed recall	16.0 ± 1.96	25.86 ± 1.24	t(42)=-4.17	p<0.001
Digit span forward	6.92 ± 0.47	8.12 ± 0.35	t(50)=-2.04	p=0.047
Digit span backward	5.73 ± 0.58	7.42 ± 0.43	t(50)=-2.42	p=0.019
MoCA	23.36 ± 1.22	28.46 ± 0.51	t(20)=-3.86	p=0.001
Premorbid intelligence*	27.08 ± 1.52	30.52 ± 1.08	t(46)=-1.82	p=0.075
Logical reasoning	22.07 ± 2.25	26.87 ± 1.67	t(28)=-1.72	p=0.097
Phasic alertness (ms)	311.4 ± 17.0	268.0 ± 8.8	t(48)=2.32	p=0.025

Divided attention: auditory (ms)	638.21 ± 53.46	570.15 ± 21.48	t(46)=1.25	p=0.217
Divided attention: visual (ms)	940.91 ± 69.43	822.19 ± 25.31	t(46)=1.71	p=0.094
Stroop test (s)	165.00 ± 19.03	149.43 ± 13.68	t(23)=0.68	p=0.502
Stroop test errors	1.18 ± 0.66	0.43 ± 0.23	t(23)=1.19	p=0.247
Trail making test A (s)	58.55 ± 11.31	33.46 ± 2.70	t(20)=2.16	p=0.043
Trail making test B (s)	174.0 ± 34.25	87.0 ± 11.95	t(20)=2.40	p=0.026
Go/NoGo false alarms	1.63 ± 0.69	0.35 ± 0.11	t(43)=2.14	p=0.038
Go/NoGo misses	0.90 ± 0.41	0.00 ± 0.00	t(43)=2.56	p=0.014
Semantic fluency (animals)	21.86 ± 1.23	26.52 ± 1.34	t(45)=-2.53	p=0.015
Phonemic fluency "s"	12.00 ± 1.86	18.36 ± 1.63	t(20)=-2.57	p=0.018
Phonemic fluency "k"	13.00 ± 2.08	21.27 ± 2.16	t(20)=-2.75	p=0.013

*eTable2. Hippocampal Volumes, Microstructural Integrity and Neuropsychological Scores. *NART equivalent*

Publication III: Beyond the limbic system: disruption and functional compensation of large-scale brain networks in patients with anti-LGI1 encephalitis

Abstract

Objective Hippocampal inflammation in anti-LGI1 encephalitis causes memory deficits, seizures and behavioural abnormalities. Recent findings suggest that extralimbic brain areas are additionally affected and that patients also suffer from non-limbic cognitive symptoms. Moreover, up to 60% of patients show no structural MRI abnormalities in the acute disease stage. We therefore investigated whether functional connectivity analyses can identify brain network changes underlying disease-related symptoms.

Methods We studied 27 patients and a matched healthy control group using structural and functional MRI. Intrinsic functional networks were analysed using Independent Component Analysis and Dual Regression. Cognitive testing covered working memory, episodic memory, attention and executive function.

Results Our analysis revealed functional connectivity alterations in several large-scale networks, including the default mode network (DMN) which showed an aberrant structure-function relationship with the damaged hippocampus. In addition, connectivity in the sensorimotor, salience and higher visual networks was impaired independent of hippocampal damage. Increased connectivity in ventral and dorsal DMN regions significantly correlated with better memory performance. In contrast, stronger connectivity of the insula with the salience network and DMN was linked to impaired memory function.

Conclusions Anti-LGI1 encephalitis is associated with a characteristic pattern of widespread functional network alterations. Increased DMN connectivity seems to represent a compensatory mechanism for memory impairment induced by hippocampal damage. Network analyses may provide a key to the understanding of clinical symptoms in autoimmune encephalitis and reveal changes of brain function beyond apparent structural damage.

Introduction

Limbic encephalitis with neuronal autoantibodies targeting the leucine-rich glioma-inactivated 1 (LGI1) protein affects one of the brain's major hubs for higher-order cognition: the hippocampus. Patients consequently suffer from pronounced memory deficits, seizures and neuropsychiatric

abnormalities.[4,110,199] While the term limbic encephalitis suggests a pathology limited to limbic brain structures such as the hippocampus and amygdala, recent clinical and imaging findings indicate an involvement of a wider network of brain areas.[21,163,192,200]

In anti-LGI1 encephalitis, faciobrachial dystonic seizures (FBDS) frequently precede the onset of limbic encephalitis.[18,25,115] Imaging analyses during this early disease stage revealed alterations of basal ganglia metabolism using FDG-PET[22,163] and transient T1 and T2 basal ganglia hyperintensities contralateral to the side of FBDS.[163] Another recent study linked hypermetabolism of the primary motor cortex and frontal cortex EEG changes to contralateral FBDS.[192]

During the limbic encephalitis stage of the disease, hippocampal T2/FLAIR hyperintense signal alterations are observed in most patients and frequently evolve into permanent hippocampal atrophy with persistent cognitive dysfunction.[18,200–202] These imaging findings correspond to the predominant expression of LGI1 in the hippocampus[41,110] and underpin hippocampal vulnerability in anti-LGI1 encephalitis. However, previous studies reported a range of 20%–60% of patients without structural MRI abnormalities in this disease stage despite an impaired memory function,[22,74,192,200] and whole brain analyses of grey and white matter integrity revealed no extrahippocampal damage in patients with anti-LGI1 encephalitis.[200] In contrast, recent FDG-PET studies provide first evidence for altered metabolism in the prefrontal cortex, anterior cingulate, parietal cortex and cerebellum.[75,192] In addition, the majority of patients present with extralimbic (non-memory) cognitive impairments, such as deficits of attention and executive dysfunction. Together, these findings illustrate the currently insufficient understanding of the relationship between affected brain regions and clinical symptoms in anti-LGI1 encephalitis.

Given these findings, we hypothesised that patients with anti-LGI1 encephalitis suffer from disruptions of large-scale functional networks, induced either by hippocampal damage or by more widespread antibody-mediated LGI1 dysfunction, thereby contributing to extralimbic clinical manifestations. We therefore used resting state functional MRI and Independent Component Analysis (ICA) to study the relationship of intrinsic connectivity alterations and cognitive symptoms. This data-driven analysis allows the identification of functional networks, that is, consistently detectable ensembles of distributed brain regions whose spontaneous activation patterns exhibit a high degree of temporal correlation.[203] These functional networks link to higher-order information processing to predict and respond to environmental demands.[204] For this reason, they are of major interest in the study of neurological and psychiatric diseases, including autoimmune encephalitis.[101] Corresponding to the clinical picture, we were primarily interested in resting-state networks (RSN) implicated in cognition and motor functions, that is, the default mode network (DMN), the salience network (SN), the frontoparietal (FPN) and the sensorimotor network.

Methods

Participants

Twenty-seven patients with anti-LGI1 encephalitis (9 women/18 men; mean age 65.8 years (SD 11.4, range 38–80); mean of 14.8 years of formal education (SD 2.4)) were studied at Charité University Hospital Berlin (n=16) and the University Hospital Schleswig-Holstein in Kiel (n=11). Data of 26/27 patients have been reported previously.[200] Diagnosis was established based on the proposed criteria of characteristic clinical presentation, cerebrospinal fluid findings, neuroimaging changes and autoantibody detection.[23] Disease symptoms during the acute stage and clinical MRI findings are summarised in table 1. The modified Rankin Scale (mRS) was used to assess symptom severity. Follow-up time was defined as the time span between the onset of first symptoms and the study MRI. Clinical and neuropsychological data as well as structural MRI analyses of these patients have previously been reported.[200] At the time of study MRI, patients received immunosuppressive drugs (n=5), anticonvulsive medication (n=5) or both (n=7; see online supplementary table 1). All patients were seizure-free. The control group consisted of 27 healthy individuals without history of neurological and psychiatric disease was similar to patients with regard to age (mean 64.3 years (SD 12.0); p=0.66), sex and education (mean 13.4 years (SD 12.0); p=0.07). Healthy controls were matched at each study site, providing the same ratio of patients to healthy controls at each location. All participants provided informed written consent.

Neuropsychological assessment

Cognitive testing comprised (1) verbal short-term memory (digit span test; Wechsler Memory Scale—Revised), (2) verbal and non-verbal episodic memory (Rey Auditory Verbal Learning Test (RAVLT), Rey-Osterrieth Complex Figure Test (ROCF) & Boston Scoring System), (3) a test of tonic and phasic alertness as well as (4) executive functions (semantic fluency, Stroop test, computerised Go/No-Go test of the TAP battery).

Image acquisition

MRI was performed at the Berlin Center for Advanced Neuroimaging (BCAN) at Charité University Hospital Berlin using a 3T Tim Trio scanner (Siemens, Erlangen, Germany) equipped with a 12-channel phased array head coil. At the University Hospital in Kiel, MR images were acquired on a 3T Achieva scanner (Philips, Amsterdam, the Netherlands) with a 32-channel head coil. The neuroimaging protocol included structural and functional scans. We acquired a resting-state functional MRI scan using an echoplanar imaging sequence (EPI; TR=2250/3000 ms, TE=30 ms, 260/200 volumes, matrix

size=64×64/80×80, 37/40 axial slices aligned to the bicommissural plane, slice thickness=3.4/3.5 mm, voxel size=3.4×3.4×3.4/3×3×3.5 mm^3). For this resting-state sequence, participants were asked to lie still and keep their eyes closed. The acquisition time was ~10 min. The high-resolution T1-weighted structural scan (1×1×1 mm^3) was collected using a magnetization-prepared rapid gradient echo sequence (MPRAGE; matrix size=240×240, 176 slices). Diffusion tensor imaging (DTI) data were acquired using a single-shot EPI sequence (voxel size 2×2×2 mm^3, 61 slices, 64 diffusion directions, b value=1000 s/mm^2).

Age (mean ± SD)	65.8 ± 11.4 years	
Sex	18 male, 9 female	
mRS score (median [range])	2 [0-4]	
Follow-up time (mean ± SD)	25.9 ± 16.7 months	
EEG abnormalities	20/27 (74%)	
Symptoms		
Cognitive		
Memory impairment	27/27 (100%)	
Disorientation, confusion	20/27 (74%)	
Affective symptoms	7/27 (26%)	
Behavioral abnormalities	7/27 (26%)	
Sleep disturbance	6/27 (22%)	
Seizures	26/27 (96%)	
FBDS	13/26 (50%)	
Pilomotor/autonomic	6/26 (23%)	
Complex focal	6/26 (23%)	
Generalized tonic-clonic	5/26 (19%)	
MRI abnormalities	Acute phase	Follow up [1]
Mild global atrophy	1/27 (4%)	6/27 (22%)
Periventricular white matter lesions	1/27 (4%)	1/27 (4%)
Basal ganglia T1/2 hyperintensities	0	0
Hippocampal hyperintensities		
(T2/FLAIR)	8/27 (30%)	5/27 (19%)
Unilateral	13/27 (48%)	9/27 (33%)
Bilateral		
Conversion to hippocampal atrophy		
Unilateral	-	9/27 (33%)
Bilateral	-	15/27 (56%)

Table 1. Patient characteristics (mRS = modified Rankin Scale, FBDS = faciobrachial dystonic seizures; [1] Time of study MRI)

Functional connectivity analysis

fMRI analysis was performed using the ICA and Dual Regression approach as implemented in the fMRIB Software Library (FSL 5.0 https://fsl.fmrib.ox.ac.uk/fsl/fslwiki). ICA is a data-driven method that decomposes a multivariate fMRI signal into single components with maximally independent spatial and temporal patterns. Resting state scans from the two study sites were preprocessed independently to account for differences in image acquisition. All scans were brain extracted, slice time corrected and underwent high-pass temporal filtering with a cut-off of 100 s. To correct for motion artefacts and ensure consistent mapping between voxels of individual scans, we performed FSL MCFLIRT motion correction. Both absolute (patients, 0.39±0.19 mm vs controls, 0.43±0.29 mm, p=0.61) and relative head motion (0.14±0.06 mm vs 0.16±0.08 mm, p=0.27) were not significantly different between groups. Next, all images were smoothed by a Gaussian Kernel of 6 mm full-width at half-maximum. After preprocessing, the functional scan was first aligned to the individual's high resolution T1-weighted image (linear boundary-based registration), which was subsequently registered to the MNI152 standard space using nonlinear registration with 12 DOF and 10 mm warp resolution. FSL MELODIC V.3.14[205] was used to identify RSNs from the control group data. The estimation of the ICs was restricted to control group fMRI data to create a group ICA template unbiased towards disease-related changes. Voxel-wise between group comparisons were performed using dual regression.[206] During this step, a grey matter mask derived from all subjects using FSL FAST[207] restricted the analysis to cortical areas. To account for possible influences of the different MR scanners, 'acquisition site' was added as a covariate to the general linear model (GLM) for permutation testing using the FSL tool randomise.[208] Correlational analyses were likewise modelled in the GLM and tested for associations with disease severity (mRS), disease duration and cognitive scores. All statistical parametric maps were corrected for multiple comparisons using threshold-free cluster enhancement.[209] The threshold was set to $p<0.05$. Images were created using MRIcron (http://people.cas.sc.edu/rorden/mricron/index.html) and Caret software (http://www.nitrc.org/projects/caret/). We additionally assessed hippocampal, whole brain and total grey matter volume and analysed white matter tracts using DTI and grey matter morphology using voxel-based morphometry (VBM) as described previously[200] to account for structural changes underlying functional alterations. Last, we performed an interaction analysis of hippocampal volume and functional connectivity to investigate differences in structure-function relationships between patients and controls.

Statistical analyses

Statistical analyses were carried out using SPSS V.22.0 (SPSS). Cognitive results are reported with mean and standard error (SE). Between-group differences were analysed using independent samples t-tests.

Results

Neuropsychological assessment

In comparison to healthy controls, patients were cognitively impaired in several neuropsychological domains (table 2). Patients had a significantly impaired working memory when compared with healthy controls (digit span test) and a substantial impairment in both verbal and visual learning and episodic memory (RAVLT/ROCF). Executive dysfunction became evident as increased error rate on the Go/No-Go test and a decreased semantic fluency. In contrast, the patients' response times were normal on the Go/No-Go test and not different from those of healthy controls on tests of tonic and phasic alertness.

	Patient	**Controls**	**t**	**p**
Memory				
Working memory				
Digit span	12.63 (±0.93)	15.54 (± 0.69)	t(51)=-2.51	0.015*
Verbal episodic memory (RAVLT)				
Supraspan	5.38 (±0.42)	7.48 (±0.41)	t(51)=-3.57	0.001**
Sum score	39.46 (±3.01)	54.59 (±1.67)	t(51)=-4.44	<0.001**
Interference	4.67 (±0.63)	5.88 (±0.36)	t(51)=-1.69	(0.102)
Delayed recall	6.27 (±1.04)	11.78 (±0.56)	t(51)=-4.72	<0.001**
Visual episodic memory (ROCF)				
Delayed recall	15.63 (± 1.91)	25.86 (± 1.24)	t(43)=-4.35	<0.001**
Attention				
Tonic alertness (median, ms)	309.24 (±16.35)	281.58 (±11.09)	t(43)=1.43	(0.160)
Phasic alertness (median, ms)	308.23 (±19.49)	269.12 (±45.49)	t(45)=1.89	(0.065)
Executive function				
Go/No-Go (median, ms)	608.20 (±24.88)	583.38 (±63.65)	t(37)=0.97	(0.338)
Go/No-Go (errors)	3.00 (±1.09)	0.35 (±0.11)	t(37)=2.77	0.008**
Semantic fluency	21.35 (±6.15)	26.52 (±6.72)	t(46)=-2.78	0.008**
Hippocampal volume				
Left	3566 (±127) mm^3	3858 (±130) mm^3	t(52)=1.60	(0.115)
Right	3448 (±152) mm^3	4015 (±122) mm^3	t(52)=2.91	0.005**

*Table 2. Cognitive results and hippocampal volumes (RAVLT = Rey Auditory Verbal Learning Test, ROCF = Rey-Osterrieth Complex Figure Test; mean (± standard error); * p<0.05, ** p<0.01)*

Structural MRI analyses

During the acute phase, hippocampal T2/FLAIR hyperintensities on routine MRI were seen in the majority of patients (21/27 patients (77.7%); unilateral in 8/27 patients (29.6%); bilateral in 13/27 patients (48.1%)), while in 6 patients (22.3%) no hippocampal abnormalities were present (table 1).

At the time of resting-state data acquisition (follow-up), initial hyperintensities evolved into unilateral (in 33.3%) or bilateral (55.6%) visually detectable hippocampal atrophy, while 11.1% of the patients showed no hippocampal atrophy. Volume measures revealed a significantly reduced right hippocampal volume (table 2). Furthermore, patients and controls did not differ on global measures of whole brain volume (1.223×106±0.33×106 mm^3 vs 1.191×106±0.29×106 mm^3, p=0.697) and total grey matter volume (0.567×106±0.01×106 mm^3 vs 0.591×106±0.01×106 mm^3, p=0.172) at follow-up. VBM analysis revealed no further cortical volume change and there was no evidence of structural white matter damage as assessed using DTI.

Functional connectivity MRI analyses

Following the investigation of structural integrity, we identified nine canonical RSNs, including the DMN, FPN, SN, sensorimotor network, auditory network as well as the primary and higher visual networks (figure 1A–I).[210,211] Aberrant functional connectivity was observed across several networks. We observed significantly increased functional connectivity in patients relative to controls in the dorsal and ventral DMN, the higher visual network and the sensorimotor network, while connectivity in the SN was reduced in patients (figure 2). Furthermore, connectivity within the dorsal and ventral DMN and the SN correlated with patients' memory performance (figure 3). No correlations were observed with follow-up time in any of the examined networks (median 25.9 months, range 1.0–118.2). These results are presented in more detail in the following paragraphs.

Dorsal DMN

Within the dorsal DMN, cingulate and medial prefrontal cortex (mPFC) connectivity was bilaterally increased in patients (p=0.01; figure 2A). Higher connectivity was additionally observed between the dorsal DMN and more remote areas in the left precuneus and frontal cortex. Regarding memory function, higher DMN connectivity with left temporal areas and the cingulate cortex correlated with better working memory performance (digit span test, r=0.66, p=0.012; figure 3A).

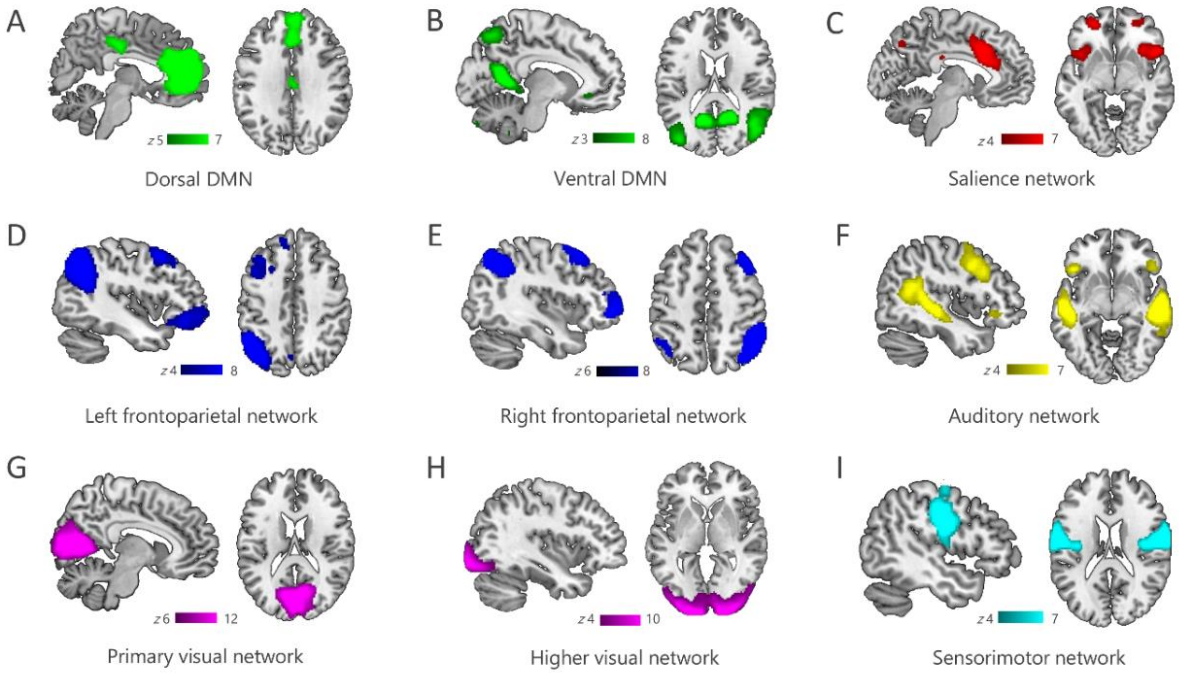

Figure 1. Functional networks. Resting-state networks identified using Independent Component Analysis included the dorsal and ventral fractions of the DMN (A,B), the salience network (C), the lateralised frontoparietal networks (D,E), auditory and visual networks (F,G,H) as well as a sensorimotor network (I). DMN, default mode network.

Ventral DMN

Patients had significantly higher precuneus connectivity within the ventral DMN ($p<0.001$; figure 2B). Moreover, patients showed increased connectivity of the ventral DMN with distributed frontal areas, including the insula, but also inferior temporal and right lateral occipital regions. These connectivity changes were associated with higher disease severity (mRS, $r_s=0.81$, $p=0.031$). Correlation analyses additionally revealed a negative association between insular involvement and verbal memory performance: The higher the insular connectivity with this network, the fewer words were recalled on the verbal learning test (RAVLT supraspan, $r=-0.46$, $p=0.026$). In contrast, a coactivation of left temporal areas was—as previously observed in the dorsal DMN—positively correlated with verbal memory performance (RAVLT interference, $r=0.92$, $p=0.005$, figure 3B).

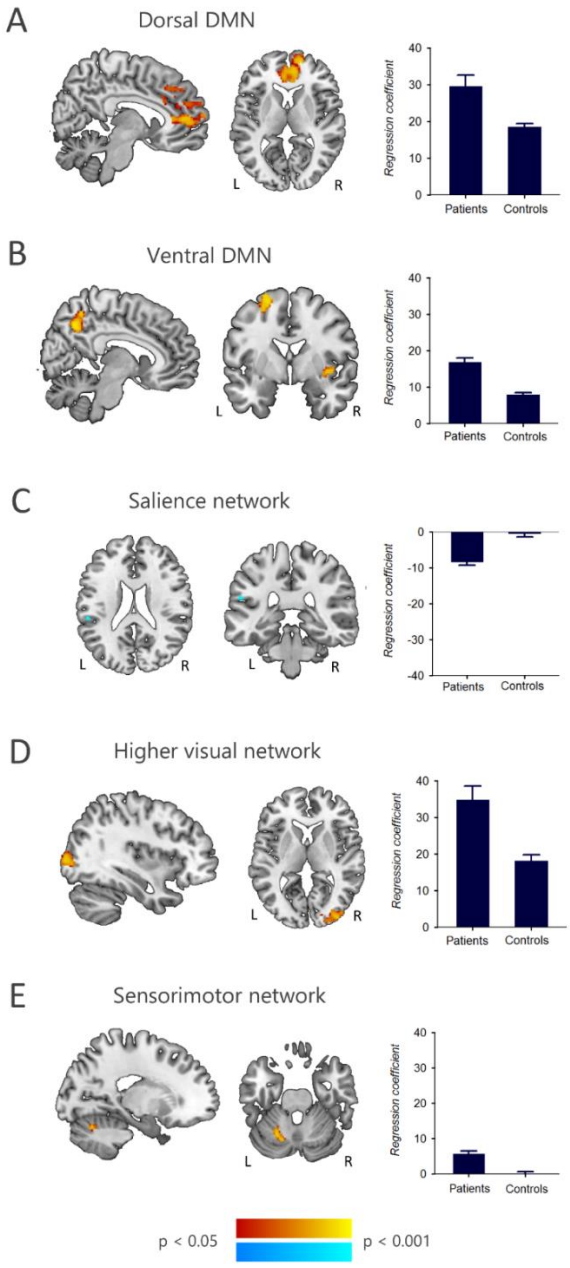

Figure 2. Patients with anti-LGI1 encephalitis show aberrant functional connectivity in several large-scale networks. Five resting-state networks showed significant group differences between patients and controls: (A) In patients with anti-LGI1 encephalitis, functional connectivity was increased between the dorsal DMN and the aCC/pCC, the left precuneus and the mPFC and left precentral gyrus in the frontal cortex. (B) In the ventral DMN, patients had higher connectivity with distributed frontal areas (insula, left superior and right inferior frontal gyrus), the inferior temporal and right lateral occipital cortex. (C) Decreased connectivity was observed between the salience network and two clusters in the left parietal opercular and postcentral cortex. Moreover, (D) patients exhibited higher connectivity in the right lateral occipital cortex within the visual network and (E) the left cerebellum within the sensorimotor network (p<0.05; corrected for multiple comparisons). aCC/pCC, anterior/posterior cingulate cortex; DMN, default mode network; LGI1, leucine-rich glioma-inactivated 1; mPFC, medial prefrontal cortex.

Salience network

We observed decreased functional connectivity between the SN and left parietal areas in patients (p=0.029; figure 2C). A negative association was observed between cognitive performance and insular connectivity, that is, one of the major SN hubs. Specifically, higher connectivity of the left insula within the network related to worse working memory performance (digit span test, r=−0.72, p=0.032) and higher connectivity of the insula bilaterally was associated with poorer verbal learning performance (RAVLT sum score, r=−0.90, p=0.007) and poorer verbal episodic memory (RAVLT delayed recall, r=−0.88, p=0.002; figure 3B). A poor outcome in the memory domain was also related to the involvement of external DMN areas. Working memory performance was worse for higher connectivity between the SN and parietal default mode areas (digit span test, r=−0.72, p=0.032; figure 3A). In the same way, poor episodic memory performance was associated with increased SN connectivity with the temporal cortex, parietal cortex and subcortical structures, including the hippocampus (RAVLT sum score, r=−0.88, p=0.007, delayed recall, p=0.002; figure 3B). Unlike in the DMNs, a coactivation of lateral temporal areas correlated with higher disease severity (mRS, r_s=0.73, p=0.031).

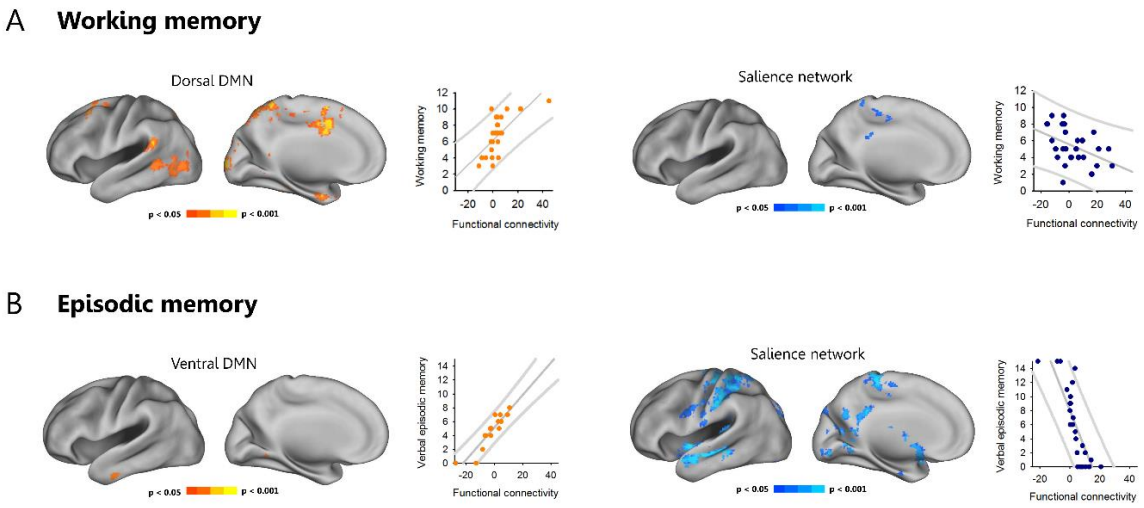

Figure 3. Correlations with memory performance. Alterations in functional connectivity significantly correlated with memory performance in patients with anti-LGI1 encephalitis (p<0.05; corrected for multiple comparisons). (A) Better working memory performance was associated with higher connectivity between the dorsal DMN and the left middle/superior temporal and parahippocampal gyrus, the left temporal pole as well as the cingulate cortex (digit span test, p=0.012). Likewise, episodic memory function was better with increased connectivity between the ventral fraction of the DMN and the left inferior temporal gyrus and fusiform cortex (RAVLT interference, p=0.005). This points to a potential functional compensatory mechanism. (B) In contrast, cognitive impairment was associated with aberrant SN connectivity: Higher insular connectivity and coactivation of temporal (hippocampus, middle and superior temporal gyrus) and parietal default mode areas (posterior

cingulate cortex, precuneus, superior parietal lobule and right angular gyrus) predicted both impaired working memory (p=0.032) and impaired episodic memory (RAVLT sum score, p=0.007; delayed recall, p=0.002). DMN, default mode network; LGI1, leucine-rich glioma-inactivated 1; RAVLT, Rey Auditory Verbal Learning Test; SN, salience network.

Sensorimotor and visual networks

Additionally, patients showed a higher connectivity of the sensorimotor network with left cerebellum (p=0.01) and of the visual network with right lateral occipital cortex (p=0.01). We observed no association of the sensorimotor network changes with the duration or frequency of FBDS events. No alterations were observed in the left and right frontoparietal networks, the auditory network and the primary visual network.

Relationship between hippocampal structure and functional network changes

An interaction analysis revealed an aberrant structure-function relationship between left hippocampal volume and ventral DMN connectivity in patients compared with controls (p=0.029; figure 4). Specifically, patients showed increased connectivity in the retrosplenial cortex in association with smaller hippocampal volumes while the opposite effect was present for controls.

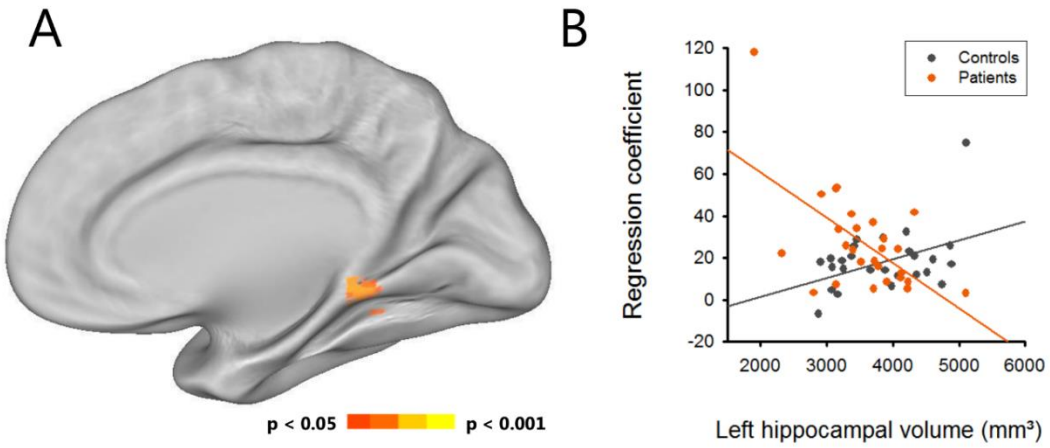

Figure 4. Aberrant structural-functional relationship in anti-LGI1 encephalitis. (A) Interaction analysis revealed an inversed relationship between left hippocampal volume and retrosplenial cortex connectivity in the ventral default mode network. (B) In anti-LGI1 encephalitis, patients showed a negative slope of the regression, with smaller left hippocampus volume relating to higher retrosplenial connectivity.

Discussion

We observed functional connectivity alterations in several major networks in patients with anti-LGI1 encephalitis, suggesting that the disease is not confined to the limbic system, but rather affects a wide range of brain regions and functional systems. Affected networks include not only the DMN, which is highly interconnected with the hippocampus, but also the SN, the sensorimotor network and the higher visual network. Increased connectivity of the ventral and dorsal DMN was associated with better memory performance, suggesting a compensatory role of these network changes. The characteristic connectivity alterations in anti-LGI1 encephalitis may expedite the correct diagnosis after implementation in future routine imaging algorithms.

The most prominent connectivity changes were observed in the DMN. The DMN comprises a set of brain areas that activate in the absence of an experimental task and that are related to self-referential processing.[212] The network consists of a dorsal subsystem engaged in self-relevant mental simulations and a ventral subsystem implicated in episodic memory processing.[213,214] The hippocampus, the major disease target in anti-LGI1 encephalitis,[200,201] is part of the ventral DMN and also highly interconnected with dorsal DMN regions. In line with this, working memory and episodic memory deficits constitute the major domains of cognitive impairment in anti-LGI1 encephalitis.[18,200] Here, we correspondingly observed connectivity alterations in both DMN subsystems: Patients with anti-LGI1 encephalitis showed significantly increased functional connectivity between the precuneus and other ventral DMN regions as well as between the mPFC/ACC and other dorsal DMN areas. Interaction analyses revealed a disturbed structure-function relationship in patients, with an inverse association between left hippocampal volume and ventral DMN connectivity in the retrosplenial cortex. Our results suggest that focal structural hippocampal damage can induce functional connectivity alterations that propagate to distant brain regions. In addition, functional connectivity alterations can occur independent of hippocampal damage and might be the result of global LGI1 antibody-mediated effects. Indeed, although predominantly expressed in the CA3 and dentate gyrus subfields of the hippocampus, LGI1 is also found to a weaker extend throughout the inner layers of the cerebral cortex.[41]

Increased ventral and dorsal DMN connectivity was moreover associated with significantly better memory performance. In the dorsal DMN, increased connectivity with the cingulate cortex and further areas was related to better working memory performance while for the ventral DMN, left temporal lobe connectivity was positively correlated with episodic memory performance. Such increased functional connectivity associated with better clinical symptoms or task performance has previously been established as potential functional compensatory mechanism in response to structural damage,[215] and has been observed in other neurological disorders with structural hippocampal damage. For example, patients with Alzheimer's disease showed increased connectivity in the ventral and dorsal DMN associated with better cognitive performance at early disease stages that was lost at follow-up with cognitive deterioration.[214] In patients with hippocampal sclerosis, increased connectivity within

the DMN similarly related to better memory performance[216]. Thus, strengthened ventral and dorsal DMN connectivity may provide a compensatory mechanism for structural hippocampal damage in patients with anti-LGI1 encephalitis (figure 5). Interestingly, these findings contrast with the connectivity changes in anti-N-methyl-D-aspartate receptor (NMDAR) encephalitis, another autoimmune encephalitis with (less severe) hippocampal atrophy, in which both hippocampi were decoupled from the DMN, with stronger decoupling relating to worse memory performance.[92,217] In addition to this hippocampal dysfunction, patients with anti-NMDAR encephalitis exhibit a characteristic pattern of whole-brain functional connectivity alterations—including reduced functional connectivity in the sensorimotor network, the visual network and the ventral attention network—likely reflecting the ubiquitous expression of NMDA receptors throughout the human brain.[217] This pattern is clearly distinguishable from the connectivity changes in anti-LGI1 encephalitis and indicates that functional connectivity analyses can identify unique and disease-specific connectivity profiles in autoimmune encephalitis.

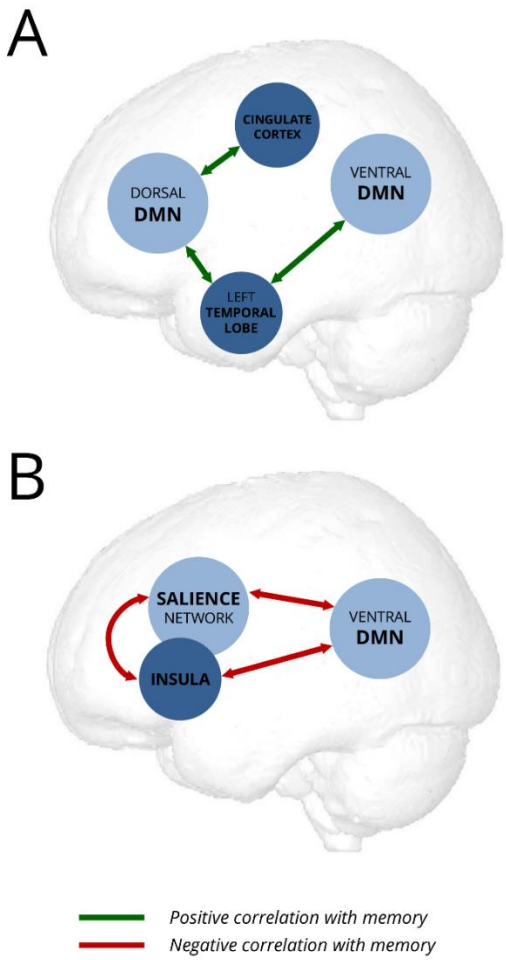

Figure 5. Schematic model of potential compensatory (A) and maladaptive (B) changes of resting-state functional connectivity in anti-LGI1-encephalitis. DMN, default mode network.

Marked connectivity changes of the insula are another main finding of this study. Insular activity has been related to a wide spectrum of functions, including autonomic control, emotion processing and higher-level cognition.[218] Together with the dorsal anterior cingulate, the insula is a main hub of the SN, a functional network centrally involved in detecting relevant external stimuli and switching between the central executive network and the DMN to guide behaviour.[219] In the present analysis, the ventral DMN exhibited increased connectivity with the right insula. This increased connectivity was associated with impaired verbal episodic memory. Interestingly, the same principle applied to the SN: The higher the connectivity between insula and DMN regions, the worse patients performed on working memory and episodic memory tests. These results suggest that aberrant coupling of the insula and the SN with the DMN contributes to cognitive deficits in anti-LGI1 encephalitis (figure 5). In addition, around 26% of our patients experienced affective and/or behavioural symptoms including anxiety, mood changes and psychosis. Aberrant SN interactions have been reported across various neuropsychiatric diseases, including frontotemporal dementia and schizophrenia.[220] The observed connectivity changes of the insula might therefore also be linked to neuropsychiatric features in LGI1 encephalitis.[202,221,222] Furthermore, our observations extend previous reports of T2/FLAIR-hyperintense signal alterations in the insula in patients with anti-LGI1 encephalitis.[18,111,200,223] Interestingly, insular involvement was also linked to episodic bradycardia in three patients with anti-LGI1 encephalitis.[224] Together, these findings suggest a role for insula dysfunction in the pathophysiology of anti-LGI1 encephalitis that is linked to autonomic control as well as cognitive and behavioural function.

The cognitive deficits in anti-LGI1 encephalitis are not restricted to limbic dysfunction, that is, hippocampal damage-induced memory impairment. Indeed, attention, verbal fluency and executive functions can be equally affected.[200,225] Given the here reported aberrant interaction between the salience and the DMN, network models of cognitive function may provide a key to the understanding of the widespread cognitive dysfunction in autoimmune encephalitis. The insula as key node of the SN, for example, monitors and detects behaviourally relevant (salient) events. When a salient stimulus is detected, the right insula mediates the switch from the internally directed DMN to the externally directed frontoparietal executive network (FPN) to facilitate access to attentional and executive processing.[218] The FPN core regions, that is, lateral prefrontal cortex and posterior parietal cortex, support attentional processes and goal-directed behaviour during working memory updating, retrieval of episodic memories, shifting of attention and inhibiting motor responses.[226] For neurological diseases, accumulating evidence suggests that disrupted saliency mapping contributes to cognitive dysfunction.[220] This line of research may elucidate the increased error susceptibility (as seen on the Go/No-Go task) in patients with anti-LGI1 encephalitis and, more generally, also help to explain cognitive impairments in patients with normal structural MRI.

Interestingly, our network analysis also identified increased connectivity between the sensorimotor network and the cerebellum in patients. A recent FDG-PET analysis reported hypermetabolism of the

sensorimotor cortex in patients with anti-LGI1 encephalitis that, together with contralateral frontal EEG changes and results from polymyographic recordings, are suggestive of a motor cortex origin of FBDS[192]. Another FDG-PET study observed hypermetabolism in the precentral gyrus, basal ganglia and cerebellum in patients with LGI1 encephalitis with FBDS.[75] Here, precentral hypermetabolism was associated with higher disease severity at follow-up, suggesting that sensorimotor network integrity may serve as a predictor for disease-related disability. Although the sensorimotor network was altered in patients, the connectivity changes observed in our study did not significantly correlate with FBDS frequency, likely related to the fact that only three patients were still experiencing FBDS at the time of functional imaging. Transient FBDS-related changes in motor areas, such as the basal ganglia T1/T2 hyperintensities observed in 30%–40% of patients in previous studies, responded well to or dissolved completely following immunotherapy.[21,163] We therefore assume that FBDS-related motor cortex connectivity abnormalities are most pronounced during the FBDS stage itself. Taken together, functional connectivity alterations and metabolic changes of the sensorimotor system constitute another extralimbic manifestation of LGI1 encephalitis.

The target antigen of anti-LGI1 encephalitis was only recently discovered.[4] Due to delayed diagnosis, some of the patients did not receive immediate immunotherapy in the hospitals of their first presentation. Variable disease courses are thus a natural limitation of this study. In addition, we believe that future longitudinal studies will help to better understand the influence of therapeutic strategies on structural and functional brain changes in anti-LGI1 encephalitis and to establish causal inferences on compensational or maladaptive functional connectivity.

In the present study, we observed that structural hippocampal damage is associated with a characteristic pattern of widespread functional network alterations in anti-LGI1 encephalitis. Connectivity changes correlated with memory performance and disease severity, corroborating the clinical relevance of our observations and suggesting successful compensatory mechanisms. Our results moreover suggest that resting state functional MRI and data-driven functional connectivity analyses might become useful clinical tools that can track disease-related changes in the brain and inform treatment monitoring. Finally, our findings offer an explanation why cognitive impairments are not restricted to memory dysfunction but can extend to attention and executive deficits, and they shed light on cases with cognitive deficits despite an unremarkable MRI.

Supplementary material

Patient No.	Immunosuppressive medication	Anticonvulsive medication
1	Methotrexate	-
2	Prednisolone	Levetiracetam
3	Azathioprine	-
4	-	-
5	-	-
6	Azathioprine	Levetiracetam
7	Azathioprine	Carbamazepine
8	-	-
9	-	Levetiracetam
10	-	-
11	-	Oxcarbazepine
12	-	Levetiracetam
13	-	-
14	Azathioprine	Levetiracetam
15	Azathioprine	Levetiracetam
16	Azathioprine, prednisolone	-
17	Prednisolone	Levetiracetam
18	-	Levetiracetam
19	-	-
20	-	-
21	Prednisolone	Levetiracetam, Lamotrigine
22	-	-
23	-	Levetiracetam
24	-	-
25	Prednisolone	-
26	-	-
27	Azathioprine	-

Supplementary Table 1. Medication at time of study MRI

Publication IV: Immunoadsorption or plasma exchange in the treatment of autoimmune encephalitis: a pilot study

Abstract

Therapeutic apheresis has emerged as a major treatment option for autoantibody-associated inflammatory diseases of the nervous system. This includes patients with autoimmune encephalitides caused by antibodies against neuronal proteins. Plasma exchange (PE) and immunoadsorption (IA) constitute two possibilities to eliminate pathogenic antibodies from patients' plasma, but their efficacy and safety has not been prospectively assessed in larger patient groups of autoimmune encephalitides. In a prospective observational case control study, we, therefore, investigated the disease courses and treatment effects of 21 patients with autoimmune encephalitis associated with NMDAR, LGI1, CASPR2, GAD, mGluR5 and Hu antibodies. Patients were randomly assigned to receive PE (n = 11) or IA (n = 10). Symptoms were evaluated using the modified Rankin Scale (mRS). Side effects or adverse events were recorded. Both interventions, IA ($p = 0.014$) and PE ($p = 0.01$), resulted in significant reduction of the median mRS. With IA, 60 % of the patients improved clinically by at least 1 mRS score, none worsened. PE led to a comparable symptom reduction in 67 % of the cases. During 83 PE sessions, three adverse events were documented, while no side effects occurred under IA. Symptom improvement was significantly associated with younger age ($r = -0.58$), but not with disease duration. Therapeutic apheresis was most effective for neuronal surface antigens (83.3 %), followed by intracellular-synaptic antigens (66.7 %). Both IA and PE resulted in moderate to marked clinical improvement, with a low rate of adverse events. Apheresis is well tolerated and effective also as first-line therapy in autoimmune encephalitis, particularly in patients with antibodies targeting neuronal surfaces.

Keywords

Autoimmune encephalitis, Immunotherapy, Autoimmunity, Plasma exchange, Immunoadsorption

Introduction

Over the past years, autoimmune encephalitides have emerged as a distinct neuropathology and constitute a heterogeneous group of inflammatory central nervous system (CNS) diseases.[227] Antibodies target intracellular antigens (such as Hu or Ma2) or proteins and receptors on the cell

surface and membrane (e.g. NMDAR, LGI1, CASPR2). Following a subacute onset of disorientation and memory deficits, symptoms often progress to seizures, psychosis, sleep disorder and agitation, while the specific disease course, symptomatology[20,126] and neuroimaging[74,101] depend on the antibody type.

Case studies and retrospective analyses have established a multimodal treatment protocol for autoimmune encephalitides, comprising high-dose corticosteroids, intravenous immunoglobulins (IVIG), and plasmapheresis (PE) or immunoadsorption (IA) as first-line therapy. Rituximab or cyclophosphamide may be added as second-line treatment in patients without response to first-line therapy or relapsing symptoms. Immunotherapy is most effective when administered early after symptom onset.[9,177]

Several antibodies are pathogenic by disrupting the structure and function of their antigens. In the case of anti-NMDAR encephalitis, antibodies mediate internalization of NMDAR clusters.[8] Since recovery and symptom remission are accompanied by a decline in titres,[228] reducing the number of autoantibodies is a primary treatment approach. PE and IA both provide an opportunity for the extracorporeal elimination of circulating antibodies. While the treated plasma volume is replaced by a human albumin solution or fresh frozen plasma (FFP) in PE, IA follows a more selective approach: the patients' plasma is passed to an adsorber column to remove immunoglobulins and immune complexes and thereupon re-infused into the blood circuit.

Therapeutic apheresis has been shown to result in moderate to marked clinical improvement across several inflammatory autoantibody associated diseases of the central and peripheral nervous system, such as Guillain-Barré syndrome[229] and multiple sclerosis.[230,231] With regard to autoimmune encephalitides, symptom remission following a treatment regimen that included PE has been reported in patients with anti-NMDAR[9,17,232] and voltage-gated potassium channel complex antibodies.[233] In a recent retrospective study in anti-NMDAR encephalitis, the combined treatment with PE and intravenous steroids was found to be more effective than intravenous steroids alone.[234] Likewise, immunoadsorption promoted recovery with no[235] or few adverse events.[236]

As previously pointed out, IA may be of similar efficacy and safety compared to the non-selective approach of PE. Data comparing these two apheresis approaches are still scarce in autoimmune encephalitis. In the present study, we, therefore, prospectively analyzed the treatment courses of 21 patients treated with PE or IA and provide information on clinical features, symptom outcome, and safety.

Patients & methods

Patients

Twenty-one patients with autoimmune encephalitis and indication for IA/PE were enrolled in the prospective observational case control study at the Clinic of Neurology at Charité University Hospital Berlin between 2013 and 2015. All patients had an established diagnosis of autoimmune encephalitis based on the typical clinical features, antibody detection, CSF findings, abnormalities in magnetic resonance imaging and the exclusion of relevant differential diagnoses. The study comprised 13 female and 8 male patients with an age range of 16–76 years (mean = 49.0 years, SD = 16.0 years) with antibodies against glutamic acid decarboxylase (GAD, n = 6), N-methyl-d-aspartate receptors (NMDAR, n = 5), the leucine-rich glioma inactivated 1 protein (LGI1, n = 4), contactin-associated protein-like 2 (CASPR2, n = 2), and metabotropic glutamate receptor 5 (mGluR5, n = 1). Three patients had anti-Hu antibodies. Demographic and clinical features of the patients were derived from the review of medical records (Table 1).

Apheresis treatments

In the majority of patients, the decision for the treatment with PE or IA was made after unsuccessful or incomplete recovery from therapy with high-dose cortisone (3–5 days à 1000 mg IV methylprednisolone) and intravenous immunoglobulins (2 g/kg body weight over 5 days). Eleven patients were randomly assigned to receive a series of 5–12 PE sessions (median: 7). Ten patients were treated with IA (3–7 sessions, median: 5.5). All patients received a central venous catheter placed in an internal jugular vein as vascular access. IA treatments were performed using a single-use TR-350 tryptophan adsorber (ASAHI Kasei Medical Tokyo, Japan) and the tubing system PA-420 (Beldico, Belgium). Plasma was separated using a polyethylene OP-05W plasma separator together with Octo Nova SW430.2 technology (DIAMED, Cologne, Germany). Angiotensin-converting enzyme inhibitors were paused 48 h prior to IA to reduce the risk of IA-associated bradykinin release syndrome. For each patient, plasma volume was estimated according to Sprenger's formula.[237] A total of the 1.5-fold plasma volume was treated for PE and 2000–2500 ml per treatment for IA. Treatment was administered every other day. In PE, a 4 % human albumin (HA) solution (diluted from a 5 % HA stock solution, Albutein 5 % Grifols, Frankfurt, Germany) was used as a replacement solution. FFP was used only in patients at risk of bleeding. During treatment, patients were anticoagulated with systemic unfractionated heparin and their vital signs were monitored, including blood pressure, heart rate, and body temperature.

	Ab	Sex	Age	Tumour	MRI
Immunoadsorption					
1	NMDAR	F	35	Ovarian teratoma	Mild frontotemporal white matter glioses
2	LGI1	F	70	Small intestinal neuroendocrine tumour	Left mesiotemporal hyperintensities, supratentorial leukoencephalopathy
3	LGI1	M	60	-	Bilateral mesiotemporal hyperintensities
4	LGI1	M	64	-	Bilateral mesiotemporal hyperintensities
5	CASPR2	M	71	-	Bilateral mesiotemporal hyperintensities, periventricular leukencephalopathy
6	GAD	M	36	-	Moderate global atrophy with mesiotemporal accentuation
7	GAD	F	46	Uterine myoma	Unremarkable
8	GAD	F	54	-	-
9	Anti-Hu	M	58	Small-cell lung carcinoma	-
10	mGluR5	F	31	-	Unremarkable
Plasma exchange					
11	NMDAR	F	22	Ovarian teratoma	Unremarkable
12	NMDAR	F	18	Ovarian teratoma (unilaterally malignant)	Unremarkable
13	NMDAR	F	21	Ovarian teratoma	Unremarkable
14	NMDAR	F	16	-	Unremarkable
15	LGI1	M	62	-	Predominantly left mesiotemporal hyperintensities extending to insular cortex
16	CASPR2	M	54	-	Unremarkable
17	GAD	F	52	Gallbladder carcinoma	Frontal & mesiotemporal hyperintensities extending to insular cortex
18	GAD	F	76	-	Mild global atrophy, leukencephalopathic opercular lesion
19	GAD	F	74	Benign osteoma of the humerus	Bilateral mesiotemporal and cerebellar hyperintensities
20	Anti-Hu	M	48	Testicular carcinoma	Left mesiotemporal hyperintensities
21	Anti-Hu	F	61	Mamma carcinoma	-

Table 1. Patient characteristics. Ab=antibody; MRI=magnetic resonance imaging; EEG=electroencephalography; ICU=intensive care unit; IV=intravenous; IVIG=intravenous immunoglobulin; mRS=modified Rankin Scale; NMDAR=N-methyl-d-aspartate receptor; LGI1=leucine-rich, glioma-inactivated 1 protein; CASPR2=contactin-associated protein-like 2; GAD=glutamic acid decarboxylase; mGluR5=metabotropic glutamate receptor 5.

	EEG	ICU	Preceding immunotherapy	Cycles	mRS pre	mRS post	Follow-up immuno-suppression
Immunoadsorption							
1	(Not evaluable due to fluctuation of vigilance)	Yes	IVIG	7	2	1	-
2	Left temporal seizure pattern (after stopping Keppra)	-	-	6	3	2	Methylprednisolone Rituximab
3	-	-	IV steroids	6	3	2	Methylprednisolone Rituximab
4	Increased cerebral excitablity	-	IV steroids, IVIG	5	4	3	Rituximab
5	unremarkable	-	IV steroids, IVIG	5	3	3	Methylprednisolone
6	unremarkable	-	IV steroids	6	1	1	Rituximab
7	Focal abnormal activity in left temporal lobe	-	-	5	3	2	Rituximab
8	unremarkable	-	-	7	3	2	Rituximab
9	unremarkable	-	IV steroids	5	3	3	-
10	Pathological alpha activity with left hemispheric functional disturbance	-	-	3	2	1	Rituximab
Plasma exchange							
11	-	Yes	-	10	3	1	Methylprednisolone Rituximab
12	-	Yes	-	8	4	2	Rituximab
13	Increased cerebral excitability	Yes	IV steroids, IVIG	6	3	1	Rituximab
14	Moderate generalised slowing	Yes	IV steroids, IVIG	6	3	1	Methylprednisolone Rituximab
15	unremarkable	Yes	IV steroids, IVIG	9	4	3	-
16	-	-	IV steroids, IVIG	5	3	2	Methylprednisolone Rituximab
17	Occipital discontinuous patterns with moderately increased cerebral excitability	Yes	IV steroids	10	4	3	Cyclophosphamide Methylprednisolone Rituximab
18	unremarkable	-	-	7	4	4	Rituximab
19	-	-	IV steroids	5	3	2	Rituximab
20	Left frontotemporal seizure pattern	-	IV steroids, IVIG	12	1	1	Cyclophosphamide
21	-	-	IVIG	5	4	4	Cyclophosphamide

Table 1. (end)

Statistical analysis

Treatment efficacy was evaluated using the modified Rankin Scale (mRS) score before and after the treatment series. A reduction of one point was considered as clinically relevant. The statistical significance of the treatment-related mRS changes was determined using the Wilcoxon signed-rank test for each treatment group. A p value <0.05 was considered significant. The effect size r was calculated based on the z value using the formula $r = z/\sqrt{N}$. Differences between categorical variables were analyzed using the χ^2 test, and the results of the Fisher's exact test are reported accordingly. Furthermore, we applied the Mann–Whitney test as a non-parametric equivalent to the independent samples t test. Spearman correlations were calculated for non-parametric ranked data and reported with 95 % confidence intervals (CI). Statistical analysis was performed using IBM SPSS Statistics 22. All figures were created using SigmaPlot 11.0. Error bars show the standard error of the mean.

Results

Symptom severity as baseline characteristic did not differ between patients treated by IA versus patients treated by PE (U = 81.0, p = 0.18, r = 0.36). The median disease duration, defined as the time span between symptom onset and IA/PE treatment, was 14.1 months for IA (range 1–98.6 months, CI [5.3, 48.6]) and 4.7 months for PE (range 0.2–84.3 months, CI [1.7, 9.0]; U = 25.5, p = 0.04, r = −0.45).

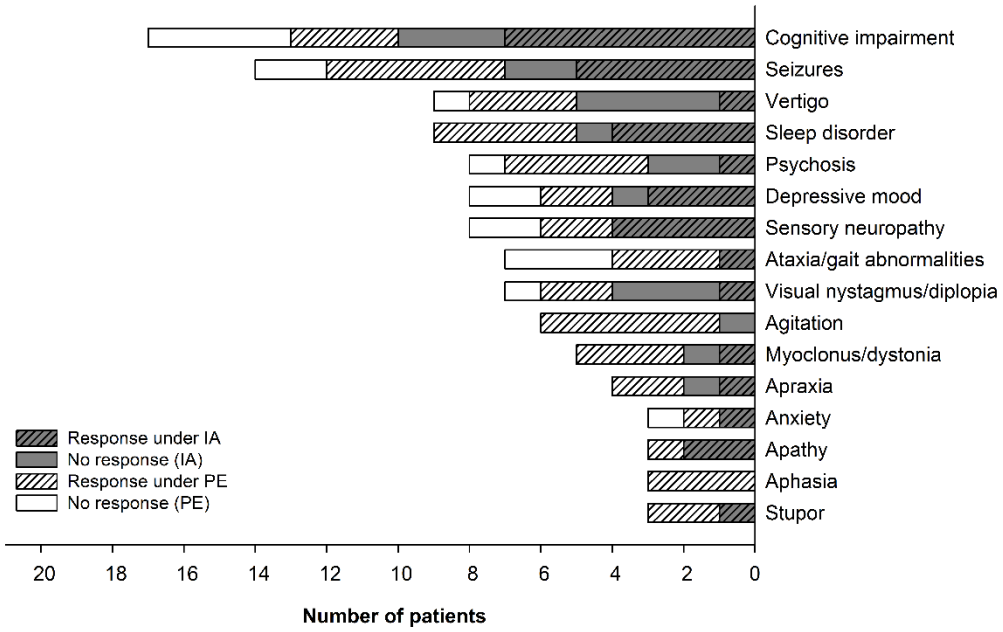

Figure 1. Frequent symptoms and their responsiveness to treatment

Across both groups, patients with and without previous IVIG/high-dose corticosteroids benefitted from the treatment. Apathy (100 %), aphasia (100 %), stupor (100 %), sleep disorder (88.9 %), agitation (83.3 %), myoclonus/dystonia (80 %), sensory neuropathy (75 %), apraxia (75 %), and seizures (71.4 %) were the symptoms which responded best to therapeutic apheresis in our sample (Fig. 1). Treatment-related improvement was observed in 83.3 % of the patients with neuronal cell surface antibodies (NMDAR, LGI1, CASPR2, mGluR5), 66.7 % of the patients with intracellular-synaptic (GAD) and none of the cases with intracellular antigens (anti-Hu). The effect of antigen type on treatment responsiveness was statistically significant (p = 0.032, Fisher's exact test). Post-hoc analyses revealed a significant difference between the response rates of cell surface and intracellular antigens (p = 0.022, Fisher's exact test). Furthermore, patients with a history of tumour resection improved more often (75 %) than patients with a non-paraneoplastic autoimmune encephalitis (50 %; not significant: p = 0.659; Fisher's exact test). The magnitude of the mRS decrease was significantly associated with age (r S = −0.58, p = 0.014, CI [−0.81, −0.03]; Fig. 2a), but not with the duration of the disease until the time point of treatment (r S = −0.31, p = 0.17, CI [−0.70, 0.15]; Fig. 2b).

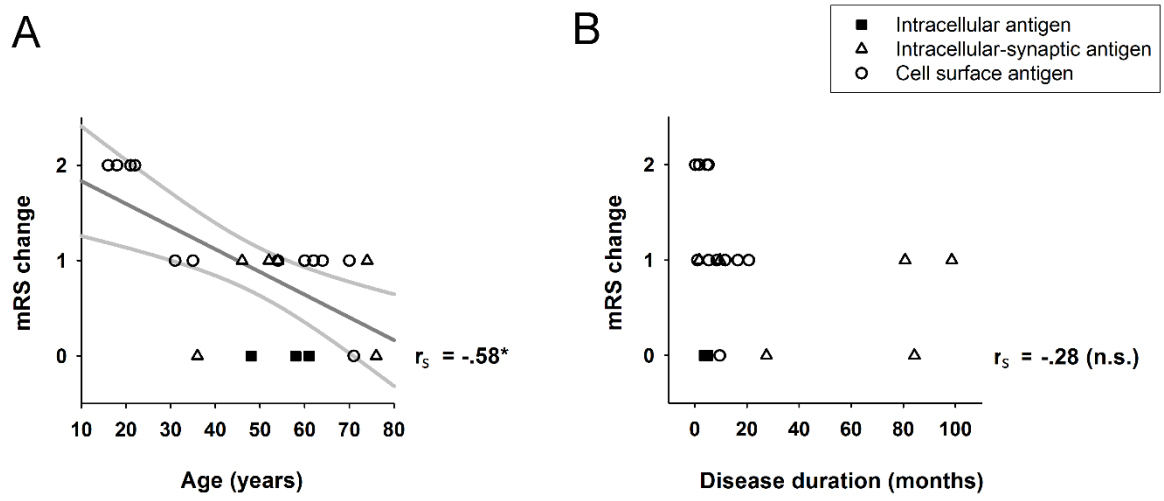

Figure 2. (A) Treatment-related decline of symptom severity (reduction in points on the modified Rankin Scale, mRS) was significantly associated with age at treatment onset (Spearman correlation with 95% confidence intervals; r_S=-.52, p=.014). (B) In contrast, treatment delay (time between the onset of first symptoms and administration of IA/PE) was not significantly associated with a worsened outcome (r_S=-.31, p=.17), indicating that therapeutic apheresis can be useful for the management of a broader spectrum of disease courses (n.s. = not significant).

Immunoadsorption

Out of the ten patients treated with IA (Table 1), three had received high-dose corticosteroids, one intravenous immunoglobulins and two patients had been treated with both prior to IA. In the four remaining patients, IA was the first immunotherapy. The adsorption was well tolerated by all patients, and relevant adverse events (beyond the common transient symptoms of nausea, hypotension or mild hematoma associated with the vascular access) were not observed during the 55 performed sessions. Before IA, patients had a median mRS score of 3 (range 1–4, CI [2.3, 3.2], mean = 2.8). Clinically relevant improvement was observed in 60 % of the patients (Fig. 3). All treatment-responding patients decreased by one mRS point (median = 2, range 1–3, CI [1.8, 2.6], mean = 2.1). None of the patients worsened. The symptom improvement proved to be statistically significant ($T = -2.45$, $p = 0.014$, $r = -0.78$).

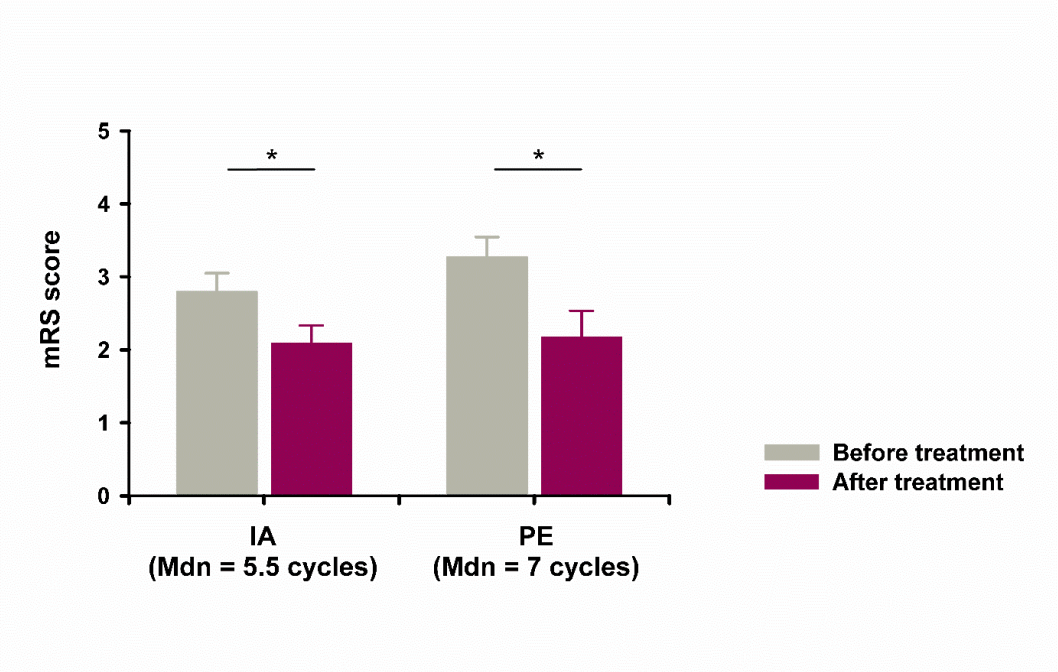

Figure 3. Symptom severity assessment with using the modified Rankin Scale (mRS) before and after treatment. The two groups did not differ in their symptom severity before treatment (p = .18, r = .36). Both the immunoadsorption (IA, p=.014, r=-.78) and the plasma exchange patient group (PE, p=.01, r=-.75) improved significantly after treatment (Wilcoxon signed rank test).

Plasma exchange

Eleven patients were treated with PE (Table 1). Five patients received PE after incomplete or absent recovery following both IVIG and high-dose corticosteroids. Another two patients had received high-dose corticosteroids only, one patient had a previous treatment attempt with IVIG only, and the remaining three patients had no previous treatment. During the 83 administered PE sessions, no

adverse events occurred in the majority of the 11 patients. In one case, catheter-associated infection led to the cessation of treatment. After management of infection and interim IVIG, PE was resumed and she experienced marked symptom improvement. Anaemia was documented in one case. The completion of PE was feasible and the patient improved clinically. A third patient showed a marked fibrinogen decrease and changed from human serum albumin to FFP. A subsequent allergic reaction towards FFP and normalization of the fibrinogen level prompted a return to human serum albumin. Clinical improvement remained absent in this case. 67 % of the PE patients showed a clinically relevant improvement. Four patients decreased by one point on the mRS and five patients, all cases of anti-NMDAR encephalitis, improved substantially by two mRS points (Fig. 3). The median mRS score decreased significantly from 3 (range 1–4, CI [2.5, 3.5], mean = 3.27) to 2 (range 1–4, CI [1.4, 2.6], mean = 2.18; T = −2.59, p = 0.01, r = −0.75). Three patients did not respond to the therapy, none of them worsened.

Discussion

In this prospective observational analysis, we evaluated the treatment outcome under IA or PE in 21 patients with autoimmune encephalitis. 60 % of the patients receiving IA showed a clinically relevant improvement of at least one mRS score. This outcome is comparable to previous findings showing response rates ranging from 47 to 85 % in recent studies of autoimmune encephalitis[235,236] and an earlier study of paraneoplastic neurological syndromes.[238] Three principal mechanisms of action have been proposed to underlie treatment effects in IA:[239] Autoantibodies are instantly removed from the plasma, their redistribution is induced and provokes succeeding immunomodulatory changes. Out of the 11 patients treated with PE in our study, 67 % showed moderate to marked symptom regression. Case studies have reported successful treatment with PE in autoimmune encephalitis.[240,241] In other neurological diseases, response rates to PE range from 42 to 60 % in CNS inflammatory demyelinating disease[230,242] to symptom improvement in all patients in a study of myasthenia gravis and Guillain-Barré syndrome.[229]

We did not observe severe adverse events during IA. In the course of the 83 PE treatments, a fibrinogen decrease and allergic reaction to FFP were observed in one patient during two sessions, another patient developed anaemia and a catheter infection occurred in a further case. As no allo-proteins are substituted in IA, our evaluation suggests good tolerability by reducing the risk for allergic reactions. Similarly, side effects were observed less frequently in IA compared to PE in myasthenic crisis.[243] Beside the potential adverse effects of substitution with foreign plasma, IA precludes the—albeit extremely rare—risk of pathogen transmission.[244]

In this patient sample, both treatment options were administered with a comparable number of sessions [median 7 (PE) vs. 5.5 (IA)] and lead to a clinically and statistically significant symptom amelioration. Since both groups did not differ in their mRS scores before the treatment, results of this pilot study suggest that IA and PE constitute two treatment options of equivalent efficacy. This equivalent efficacy was demonstrated despite the fact that IA was performed less frequently and in patients with longer disease duration.

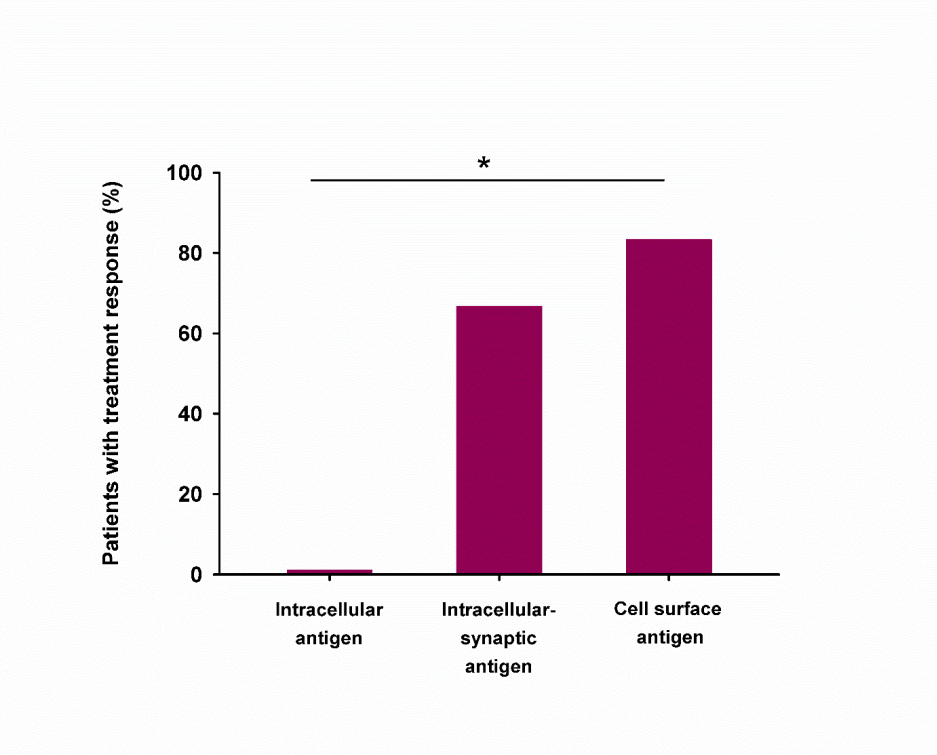

Figure 4. Treatment-related improvement was observed more often for neuronal cell surface (NMDAR, LGI1, CASPR2, mGluR5) than for intracellular-synaptic antigens (GAD). None of the patients with intracellular antigens (anti-Hu) improved. The effect of antigen type on treatment responsiveness was statistically significant (p=.032, Fisher's exact test). Post-hoc analyses revealed a significant difference between the response rates of cell surface and intracellular antigens (p=.022, Fisher's exact test).

Notably, clinical improvement following therapeutic apheresis was achieved in all cases of anti-NMDAR, mGluR5 and LGI1 encephalitis, and in one of two patients with CASPR2 encephalitis. These findings are in line with observations from a previous study in which 64 % of the patients with cell surface antigens showed symptom improvement[236]. No benefit was seen for intracellular antigens (Fig. 4). Our findings suggest that therapeutic apheresis is particularly effective in patients with antibodies against proteins or receptors on the cell surface, and should be considered as a treatment option in GAD encephalitis. In the same way, the observed association between better treatment outcomes and younger age may be driven by the distinct patient characteristics of the particular encephalitides: In our

study, all patients with a remarkable improvement of two mRS points suffered from anti-NMDAR encephalitis, which is in turn predominantly observed in younger women[9].

Moreover, it is currently unclear whether treatment effects of therapeutic apheresis are limited to an early treatment onset. As there was no association between treatment delay and response in our patients, we propose that therapeutic apheresis can be useful for the management of a broader spectrum of patients. A later treatment was previously not found to be a significant limitation for treatment response in CNS inflammatory demyelination.[242,245] Nevertheless, early tumour removal in paraneoplastic encephalitides has an important impact on the clinical outcome of the immunotherapy protocol.[20]

Autoimmune encephalitides are relatively rare, and severe courses with autonomic instability or poor patient cooperation can potentially complicate a successful administration of therapeutic apheresis. Nonetheless, future prospective and randomized study designs can help to find the ideal number of apheresis sessions and elaborate on antibody titres, neuropsychological and clinical long-term outcomes.

Ethical standards

All participants or next of kin gave informed written consent for participation. The study was approved by the Ethics Committee of the Charité University Hospital Berlin and conducted in accordance with the principles of the Declaration of Helsinki (1964) and its later amendments.

Immunoadsorption or plasma exchange in the treatment of autoimmune encephalitis: a pilot study. Heine, J., Ly, L.T., Lieker, I., Slowinski, T., Finke, C., Prüss, H., & Harms, L. (2016). 263(12), 2395-2402.
https://doi.org/10.1007/s00415-016-8277-y

Publication V: Long-term cognitive outcome in anti-NMDA receptor encephalitis

Abstract

Objective. Cognitive dysfunction is a core symptom of NMDAR encephalitis, but detailed studies on prevalence and characteristics of cognitive deficits as well as the potential for recovery are missing. Here, we performed a prospective longitudinal study to assess cognitive long-term outcome and identify clinical predictors.

Methods. Standardized comprehensive neuropsychological assessments were performed in 43 patients with NMDAR encephalitis 2.3 years and 4.9 years (median) after disease onset. Cognitive assessments covered executive functions, working memory, verbal/visual episodic memory, attention, as well as subjective cognitive complaints, depression, and anxiety levels. Cognitive performance of patients was compared to that of 30 healthy participants matched for age, sex, and education.

Results. All patients had persistent cognitive deficits 2.3 years after disease onset, with moderate or severe impairment in more than 80% of patients. Core deficits were impairments of memory and executive function. After 4.9 years, a significant improvement of cognitive function was observed, but moderate to severe deficits persisted in 2/3 of patients, despite favorable functional neurological outcomes (median mRS=1). Delayed treatment, higher disease severity and older age were identified as predictors for impaired cognitive outcome. Linear regression analyses showed a domain-specific recovery process. Improvements of cognitive function were observed for up to 9 years after disease onset.

Interpretation. Cognitive deficits are the main contributor to long-term morbidity in NMDAR encephalitis and persist beyond functional neurological recovery. Nonetheless, cognitive improvement is possible for several years after the acute phase and should be supported by continued cognitive rehabilitation. Cognition should be included as outcome measure in future clinical studies.

Keywords

autoimmune encephalitis, NMDA receptor, NMDAR, neuropsychology, long-term outcome, cognitive deficits, cognitive outcome

Introduction

Cognitive dysfunction is a core symptom in patients with anti-NMDA receptor (NMDAR) encephalitis.[9,246] Impairments of cognitive function substantially affect the quality of life, potential academic and occupational achievements and social interactions of the frequently young patients.[177] Here, we present the first comprehensive longitudinal study of the cognitive sequelae of NMDAR encephalitis in adults based on detailed neuropsychological assessments.

Following the first description of NMDAR antibodies 13 years ago,[3] clinical studies have started to examine the long-term prognosis in patients with NMDAR encephalitis. Large-scale studies assessed neurological outcomes based on the modified Rankin Scale (mRS)[9,17] and cognitive screening results - such as the mini-mental state examination (MMSE)[17] - for a follow-up period of up to 24 months. With a definition of good outcome as mRS score ≤ 2, which characterizes a status of relative independence in most activities of daily living while still experiencing slight disabilities,[247] about 80% of the patients showed full recovery or improved to mild deficits within two years of follow-up. Considering the severe disease courses in many patients, that frequently requires intensive care unit admission and can include autonomic instability, status epilepticus, or coma,[248] neurological long-term outcome thus appears to be relatively favourable. However, clinical outcome measures like the mRS focus on physical impairment and largely neglect cognitive dysfunction - despite its substantial and permanent impact on daily functioning. Patients with NMDAR encephalitis often report self-observed residual deficits in the post-acute phase that span several cognitive domains and manifest in poor memory,[177,249,250] difficulties to concentrate on everyday tasks,[177,249–251] increased fatiguability,[249,251] and social withdrawal.[249] Neuropsychological studies revealed impairments in the majority of these patients with deficits encompassing episodic and working memory,[101,177,246,249–254] as well as executive function.[101,177,246,249–253] In addition, deficits of attention,[177,246,249–253] language deficits,[250,251] and visuospatial dysfunction[249] can occur. Considering the typically young age of onset in NMDAR encephalitis, promoting cognitive recovery is essential for preserving the patients' potential at school, at university, or at the workplace. Previous small case series point to a potential recovery in some patients and domains, while others remained with persistent impairment.[246,251–253] However, cross-sectional study designs, short follow-up times, small sample sizes, and differences in testing protocols and analyses impede coherent conclusions.

We therefore performed a comprehensive longitudinal neuropsychological and clinical assessment in 40 patients with NMDAR encephalitis at two time points. The aims of this study were to: (1) systematically investigate the cognitive outcome in a large sample of NMDAR encephalitis patients; (2) describe the trajectory of cognitive deficits in a 2-year follow-up; (3) explore the relationship between clinical neurological and cognitive recovery; (4) identify clinical predictors of cognitive long-term outcome; and (5) evaluate the time courses of recovery of cognitive function across the major cognitive domains.

Methods

Participants

We prospectively enrolled 43 adult patients with NMDAR encephalitis to participate in two follow-up study visits between January 2011 and December 2018 (table 1). We consecutively recruited all available patients from university hospitals in Germany without clinical selection criteria, i.e. consecutive patients were enrolled irrespective of their clinical disease course. Three age-, sex- and education-matched patients with deviant follow-up spans (0.8 years, 1.1 years, and 3.35 years) were excluded from analysis to avoid potential bias due to heterogeneous follow-up times.

All study visits comprised clinical evaluation, comprehensive neuropsychological assessment and MRI data acquisition conducted at the Department of Neurology at Charité – Universitätsmedizin Berlin and the Berlin Center for Advanced Neuroimaging (BCAN). All patients were tested NMDAR antibody-positive in CSF during the acute disease phase and fulfilled the current diagnostic criteria.[23] Clinical details are provided in Table 1. Neurologic disability was assessed using the modified Rankin Scale (mRS). Patients were frequency matched to a group of 30 healthy controls without history of neurological or psychiatric disease with regard to sex, age, and education (see table 1). This study was approved by the Ethics Committee of Charité – Universitätsmedizin Berlin. Written informed consent was obtained from all participants in accordance with the Declaration of Helsinki.

Study participation	**Patients (1st study visit)**	**Patients (2nd study visit)**	**Controls**
Sex (% female)	35 f / 5 m (88%)	35 f / 5 m (88%)	25 f / 5m (83%)
Age (mean ± SD, range)	28.5 ± 7.2 years (15-45 years)	30.7 ± 7.2 years (17-48 years)	30.1 ± 8.3 years (16-52 years)
Years of education (mean ± SD, range)	13.5 ± 2.0 years (10-18 years)	14.0 ± 1.7 years (10-18 years)	14.4 ± 2.0 years (10-18 years)
mRS (median, range)	1 (0-3)	1 (0-1)	-
Time since disease onset (median, range) [a]	2.3 (0.3-7.0) years	4.9 (2.3-9.4) years	-
Subjective complaints	29/40 (73 %)	20/40 (50%)	0/30 (0%)
Anticonvulsant medication [b]	6/40 (15%)	2/40 (5%)	-
Antipsychotic medication [b]	0/40	0/40	-
Time between study visits (median, range)	2.1 (1.7-4.6) years		-
Disease course			
Age at onset (mean ± SD, range)	25.9 ± 7.1 years (15-44 years)		
Maximum mRS (median, range) [c]	4 (2-5)		
Prodromal symptoms	**22/40 (55 %)**		
Affective/personality change	19/40 (48 %)		
Flu-like symptoms	12/40 (30 %)		

Acute phase symptoms	
Neuropsychiatric	39/40 (98 %)
Cognitive	38/40 (95 %)
Seizures	29/40 (73 %)
Sleep disorder	20/40 (50 %)
Movement disorder	17/40 (43 %)
Autonomic dysfunction	13/40 (33 %)
Status epilepticus	3/40 (8 %)
Acute neurological care	**40/40 (100 %)**
Days in acute neurological care (median, range)	83 (15-410)
Intensive care unit	**23/40 (58 %)**
Days in intensive care (median, range)	19 (1-252)
Tumor [d]	10/40 (25 %)
Relapse [e]	7/40 (17.5 %)
Acute phase treatment	
First-line therapy	**39/40 (98 %)**
Intravenous methylprednisolone (IVMP)	32/39 (82 %)
Therapeutic apheresis	26/39 (67 %)
Intravenous immunoglobulins (IVIG)	24/39 (62 %)
Oral prednisolone	15/39 (38 %)
Second-line therapy	**19/40 (48 %)**
Rituximab	17/40 (43 %)
Cyclophosphamide	6/40 (15 %)
Azathioprine	5/40 (13 %)
Anticonvulsants	32/40 (80 %)
Antipsychotics	23/40 (58 %)
Treatment delay (median, range) [f]	31 (1 – 770) days
Acute phase MRI abnormalities	**18/40 (45 %)**
White matter lesions	12/40 (30 %)
Medial temporal hyperintensity (T2w)	3/40 (8 %)
Mild global atrophy	3/40 (8 %)
Basal ganglia hyperintensity (T1w)	1/40 (3 %)
Acute phase EEG abnormalities	25/40 (63 %)
Depression (BDI-II) [g]	8 (0-24)
Anxiety (BAI) [h]	12 (0-27)

Table 1. Clinical characteristics of the patient group. a Time span between symptom onset and study date; b Anticonvulsant medication included levetiracetam, valproate, lamotrigine, and oxcarbazepine exclusively (n=4) or in combination (n=2). No significant difference in cognitive performance between patients with and without anticonvulsant medication was observed at 1st (cognitive composite score: median 3.5 (range 1-5) vs. 3.5 (1-5)) and 2nd study visit (scores 1 & 4 vs 2.5 (0-4); Fig. S2); c Highest disability score at any time point during the disease course; d Tumors included 9 ovarian teratomas and 1 testicular teratoma; e Relapses occurred

before enrolment (n=5) or between study visits (n=2) at a median of 21 months from onset (range 7-44 months). Visits were scheduled with an interval >9 months from acute relapse to ensure that patients had recovered from their relapse. Frequent symptoms were new-onset cognitive deterioration, acute psychiatric symptoms (aggression, hallucinations, delusions), or seizures (Fig. S3); f Time span between symptom onset and initiation of first-line immunotherapy; g Scoring: 0-8 no depression, 9-13 minimal depression, 14-19 mild depression, 20-28 moderate depression, 29-63 severe depression; h Scoring: 0-7 minimal anxiety, 8-15 mild anxiety, 16-25 moderate anxiety, 26-63 clinically relevant anxiety (SD: standard deviation; mRS: modified Rankin Scale; BDI-II: Beck Depression Inventory Revision; BAI: Beck Anxiety Inventory).

Neuropsychological assessment

All participants underwent an extensive neuropsychological test battery covering the five cognitive domains of [1] executive functions, [2] working memory, [3] verbal and [4] visual episodic memory, and [5] attention. We assessed [1] executive functions using a Go/No-Go[167] and Stroop[255] paradigm (Farbe-Wort-Interferenztest; FWIT). In a semantic fluency test, participants were moreover asked to name as many animals as possible within one minute (Regensburger Wortflüssigkeitstest; RWT).[168] Working memory [2] was examined with the forward and backward conditions of the digit span test (Wechsler Adult Intelligence Scale, WAIS-IV).[256] Tests of episodic memory included [3] a word-list learning paradigm (Verbaler Lern- und Merkfähigkeitstest,[165] German version of the Rey Auditory Verbal Learning Test; RAVLT) for the verbal and [4] the Rey-Osterrieth Complex figure test (ROCF, 36-point scoring system) for the visual domain. Both tests include a short-term and delayed recall. Lastly, we examined [5] attention using a cued and non-cued reaction time task (subtests phasic and tonic alertness) as well as a dual-task paradigm with simultaneous auditory and visual cues (subtest divided attention) from the Testbatterie für Aufmerksamkeitsprüfung (TAP).[167] Response times and error rates were recorded. We additionally included an estimate of premorbid intelligence levels (Mehrfachwahl-Wortschatz-Intelligenztest, MWT).[169] Parallel test versions were used for longitudinal testing as appropriate. Details about subjective cognitive deficits, mental and physical state were recorded using structured interviews. In addition, patients performed a self-report depression (Beck Depression Inventory; BDI-II)[257] and anxiety screening (Beck Anxiety Inventory; BAI).[258]

Statistical analyses

Cross-sectional analyses. First, we investigated the overall frequency of cognitive impairment at first and second follow-up study visit. Raw test scores of each patient were z-standardized with regard to the mean and standard deviation of the control group. Performance on a neuropsychological test was considered impaired when a patient performed ≤ 1 SD below controls (see Fig. S1 for -1.5 SD). A

deficit at the domain-level was detected when patients showed impairments in at least one test of the respective domain. Besides determining the prevalence of cognitive impairment, this allowed us to identify cognitively affected patients. Furthermore, a composite score of cognitive dysfunction was defined as the number of affected domains. Demographic variables were compared using independent two-sample t-tests. The Shapiro-Wilk test was used to assess the normality of the data. We used lme4[259] in R for a linear mixed effects analysis of the relationship between cognitive performance and study visit. By modelling intercepts for subjects and time since onset as random effects, we accounted for baseline differences between individuals and variation in timing of the neuropsychological assessments after the acute phase. P-values are two-tailed and adjusted for multiple comparisons using the Benjamini-Hochberg correction. Statistical analyses were carried out using IBM SPSS Statistics 22 and R 3.6.1.

Longitudinal analyses. Second, we assessed the longitudinal evolution of cognitive performance using McNemar tests for the proportion of affected patients in each domain. Additionally, we analyzed the longitudinal development of deficits in cognitively impaired patients as identified in the cross-sectional analysis of the first study visit. Changes in cognitive performance were tested using the Wilcoxon signed-rank test for repeated measurements.

Regression analyses. Multiple linear regression analysis was used to identify clinical predictors for cognitive outcome. The following variables were included as predictors for long-term cognitive performance: (1) time between disease onset and initiation of treatment (treatment delay; days); (2) total duration of hospitalization in acute neurological care (days); (3) intensive care unit (ICU) treatment; (4) maximal mRS score during the acute disease phase; and (5) age of onset (years).

Temporal evolution of recovery. To explore the temporal dynamics of recovery from cognitive impairment, we performed linear regression and correlation analyses between recovery time (time between disease onset and last study visit) and longitudinal change in cognitive performance (change in composite score, change in performance across domains (SD)).

Results

Clinical symptoms and subjective cognitive complaints

The patient group was typical of NMDAR receptor encephalitis with respect to acute phase symptoms, demographic characteristics, and disease course variables, including ICU admission, administered first and second-line therapies, and MRI and EEG abnormalities. Further clinical characteristics are provided in table 1. Detailed antibody titres and CSF findings are presented table S1. Despite moderate to severe

disability during the acute phase (median maximum mRS of 4, range 2-5), the neurological outcomes were favourable: Patients showed no or only mild physical disability at the time of first study visit (median of 2.3 years after symptom onset: median mRS 1, range 0-3), with further improvement at second study visit (4.9 years after symptom onset: median mRS 1, range 0-1). Spontaneous speech production was unremarkable in all patients regarding form and content, with no indication of disordered speech or language. None of the patients reported pain or other potentially compromising physical or psychological stressors during the testing session.

Subjective complaints were reported by 73% of the patients at first and 50% at second study visit in a structured medical history interview. Perceived deficits were reported for memory and sustained attention, compromising daily activities such as reading, driving, or memorizing new information. Increased fatiguability was noted during cognitively demanding tasks in everyday situations. Initially, 11/40 (28%) of the patients reported no complaints despite impaired test performance. Longitudinally, 10/40 patients (25%) reported an improved, 28/40 (70%) unchanged, and 2/40 (5%) deteriorated subjective cognition compared to their first study visit.

Cognitive deficits at first study visit

At first study visit 2.3 years after disease onset, all patients had cognitive deficits, with 50% of the patients showing severe cognitive impairment (i.e. a composite score of 4-5 affected domains; Fig. 1). Another 32.5% of patients were moderately affected (2-3 affected domains), and only 17.5% of the patients had just mild deficits (0-1 affected domains). This contrasts with a favorable functional neurological outcome in the majority of patients, with 55% of the patients showing no or only mild disability (mRS 0-1), 45% having moderate impairments (mRS of 2-3) and none of the patients showing severe disability (mRS of 4-5).

In a linear mixed model accounting for the timing of the first study visit and baseline differences between individuals, patients showed a significantly lower performance on test of executive function ($p=0.02$; affected in 80% of the patients), working memory ($p<0.001$; affected in 75% of the patients), and verbal memory ($p=0.002$; 72.5%; Fig. 2; table S2; n=40). Visual memory and attention were affected in 40% and 55% of the patients, respectively, but showed no significant difference. Premorbid intelligence estimates were comparable to those of controls (table S3).

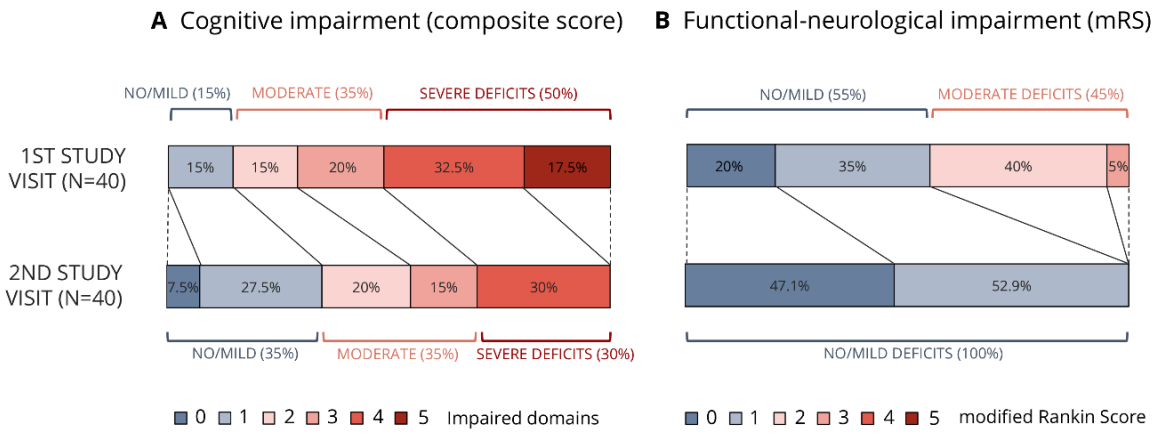

Fig 1. Dissociation of cognitive and functional-neurological outcomes in NMDAR encephalitis. (A) Cognitive impairment at first and second study visit (n=40). The composite score of cognitive impairment represents the number of affected domains on tests of working memory, verbal and visual episodic memory, executive function, and attention (% of patients). At first study visit (2.3 years after disease onset), 50% of the patients showed severe impairments (4-5 domains affected) and only 17.5% had no or mild residual cognitive deficits (0-1 domain affected). At second study visit (4.9 years after disease onset), 30% of patients remained with severe cognitive deficits (4-5 domains affected), moderate deficits (2-3 domains affected) persisted in 35% of the patients, and 35% had fully recovered or recovered with only minimal residual impairments. (B) In contrast, there was no or only mild functional-neurological impairment (mRS 0-1) in 55% of patients and moderate impairment (mRS 2-3) in 45% of patients at first study visit. At second study visit, all patients had either fully recovered or had only mild neurological disability.

Cognitive deficits at second study visit

Improvements of cognitive performance were observed in all patients at second study visit. Here, none of the patients showed deficits across all five domains anymore. The proportion of severely affected patients decreased significantly from 50% to 30% at second study visit (p=0.021; Fig. 1). Another 35% of patients remained moderately affected (2-3 domains affected) and 35% of the patients had recovered completely or remained with only minimal deficits (0-1 domains affected). Improvement between first and second study visit was observed across almost all domains – albeit with high rates of patients with persisting deficits at second study visit (Fig. 2A). For example, although the number of patients with executive impairment decreased significantly from 80% to 60% between first and second study visit (Fig. 2B; p=0.039), patients remained significantly below the level of the control group on tests of executive function (p=0.035) when accounting for the timing of study visit and individual baseline differences. Similarly, working memory (p=0.007), and verbal memory (p=0.029) continued to be affected in the overall sample, although the number of affected patients generally decreased (first vs.

second study visit; working memory: 75% vs. 55%, p=0.146; verbal episodic memory: 72.5% vs. 40%, p=0.210). Visuospatial memory dysfunction (40% vs. 20%; p=0.092) and attention (55% vs. 35%, p=0.581) were less common already at first study visit, but also improved in some patients.

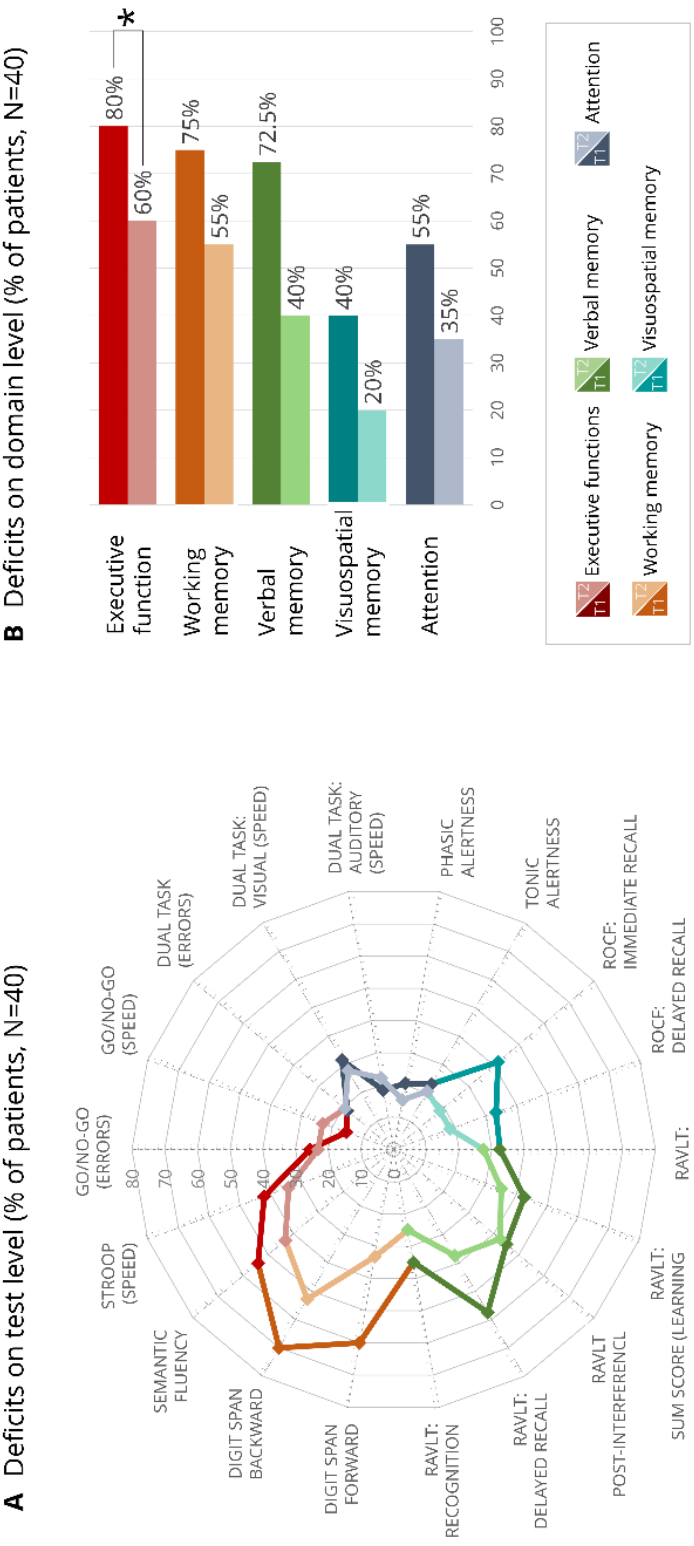

Fig 2. Cognitive impairment at first and second study visit on test and domain-level (n=40). (A) Polar plot showing the percentage of patients with deficits on a test-by-test basis. Cognitive domains are colour-coded (see legend). Dark colours represent the first (T1) and light colours the second study visit (T2). (B) Cognitive impairment on the domain-level. Bar charts depict percentage of patients with impairment in the respective cognitive domain. Dark colours represent the first (T1) and light colours the second study visit (T2). Cognitive recovery was most pronounced for executive function (80% vs. 60%, p=0.039), working memory (75% vs. 55%, p=0.146) and verbal episodic memory (72.5% vs. 40%, p=0.210). However, residual cognitive deficits were common at second study visit (median 4.9 years after disease onset), despite this substantial improvement.

Longitudinal development in patients with cognitive deficits

Next, we analyzed the longitudinal evolution of cognitive deficits for patients with deficits at first study visit (table 2). Improvements were seen across all cognitive domains, and no deterioration occurred on any of the performed tests. Significant improvement of executive function was demonstrated by better performance in the Go/No-Go test (Wilcoxon signed-rank test: p=0.016, effect size: r=-0.76) and the semantic fluency task (p=0.04, r=0.50; Fig. 3A). Working memory was significantly enhanced for repetition (p=0.029, r=0.46) and manipulation of the material (p=0.001, r=0.62; Fig. 3B). Verbal memory deficits improved on the immediate (p=0.009, r=0.73), post-inference (p=0.032, r=0.50), and delayed recall (p=0.016, r=0.50; Fig. 3C). Visual memory improved on the immediate (z=2.36, p=0.018, r=0.59), but not the delayed condition. In the domain of attention, better performance was reflected in shorter response times (p=0.018, r=-0.90; Fig. 3E) and lower error rates (p=0.04, r=-0.82) in the dual-task paradigm. Further analysis of the deficit pattern at first and second study visit showed a strong coexistence of impairments of working memory, verbal memory, and executive function (Fig. 3F).

Domain	**Test**	**Controls**	**1st study visit**	**2nd study visit**	**Longitudinal evolution**			
					N	Test statistic	Effect size [c]	Change
Executive functions	*Go/No-Go (median RT)*	502.3 ± 63.9 ms	612.3 ± 17.8 ms	559.5 ± 52.2 ms	6	z=-1.57, p=0.116	r=-0.64	→
	Go/No-Go (errors)	0.6 ± 0.7	2.6 ± 0.7	1.0 ± 0.9	**10**	**z=-2.40, p=0.016 ***	**r=-0.76**	↘
	Stroop (RT)	97.7 ± 12.7 s	138.9 ± 19.2 s	126.4 ± 29.2 s	14	z=-1.35, p=0.177	r=-0.36	→
	Semantic fluency	29.1 ± 5.7	20.4 ± 2.9	23.3 ± 4.5	**16**	**z=2.01, p=0.044 (*)**	**r=0.50**	↗

Working memory	*Digit span forward*	8.6 ± 1.4	5.8 ± 0.8	6.7 ± 1.5	**23**	**z=2.19, p=0.029 ***	**r=0.46**	↗
	Digit span backward	8.1 ± 1.8	4.9 ± 1.1	6.2 ± 1.2	**26**	**z=3.18, p=0.001 ****	**r=0.62**	↗
Verbal memory	*RAVLT 1 (immediate recall)*	8.9 ± 2.5	4.8 ± 1.1	6.6 ± 1.5	**13**	**z=2.62, p=0.009 ****	**r=0.73**	↗
	RAVLT sum score (learning)	60.8 ± 6.9	44.5 ± 6.2	48.8 ± 7.9	17	z=1.73, p=0.084	**r=0.42**	→
	RAVLT 6 (post-interference)	13.8 ± 1.2	7.5 ± 2.3	9.4 ± 2.6	**18**	**z=2.14, p=0.032 ***	**r=0.50**	↗
	RAVLT 7 (delayed recall)	13.5 ± 1.6	8.5 ± 2.0	10.7 ± 3.2	**23**	**z=2.41, p=0.016 ***	**r=0.50**	↗
	RAVLT recognition [a]	14.8 ± 0.3	11.0 ± 1.6	12.6 ± 1.8	14	z=1.80, p=0.071	**r=0.48**	→
Visual memory [b]	*ROCF immediate recall*	28.9 ± 2.8	20.1 ± 4.2	26.4 ± 6.1	**15**	**z=2.36, p=0.018 ***	**r=0.61**	↗
	ROCF delayed recall	29.6 ± 2.8	18.9 ± 4.0	24.8 ± 5.8	12	z=1.88, p=0.060	r=0.54	→
Attention	*Tonic alertness (median RT)*	257.7 ± 28.7 ms	336.1 ± 53.0 ms	304.4 ± 42.4 ms	9	z=-1.72, p=0.086	r=-0.57	→
	Phasic alertness (median RT)	269.1 ± 28.3 ms	362.6 ± 60.1 ms	335.0 ± 59.3 ms	8	z=-1.12, p=0.263	r=-0.40	→
	Dual-task: Auditory (median RT)	611.1 ± 49.6 ms	771.2 ± 85.9 ms	619.4 ± 36.8 ms	**7**	**z=-2.37, p=0.018 ***	**r=-0.90**	↘
	Dual-task: Visual (median RT)	729.0 ± 64.5 ms	868.8 ± 44.3 ms	782.4 ± 90.0 ms	11	z=-1.96, p=0.050	r=-0.59	→
	Dual task (errors)	1.7 ± 1.7	10.3 ± 6.1	6.3 ± 5.0	**6**	**z=-2.01, p=0.044 (*)**	**r=-0.82**	↘

*Table 2. Longitudinal evolution of cognitive deficits. In patients with deficits on the respective tests at first study visit, Wilcoxon-signed rank tests show significant improvement of memory, executive functions, and attention. Scores are presented with mean ± standard deviation. a Corrected for errors. b No patient showed deficits in visuospatial skills. c Rosenthal's r was used as effect size estimate for the Wilcoxon signed-rank test. * p<0.05. ** p<0.01. (*) not significant after Benjamini-Hochberg correction. (RAVLT: Rey Auditory Verbal Learning Test; ROCF: Rey-Osterrieth Complex Figure Test; RT: Response time).*

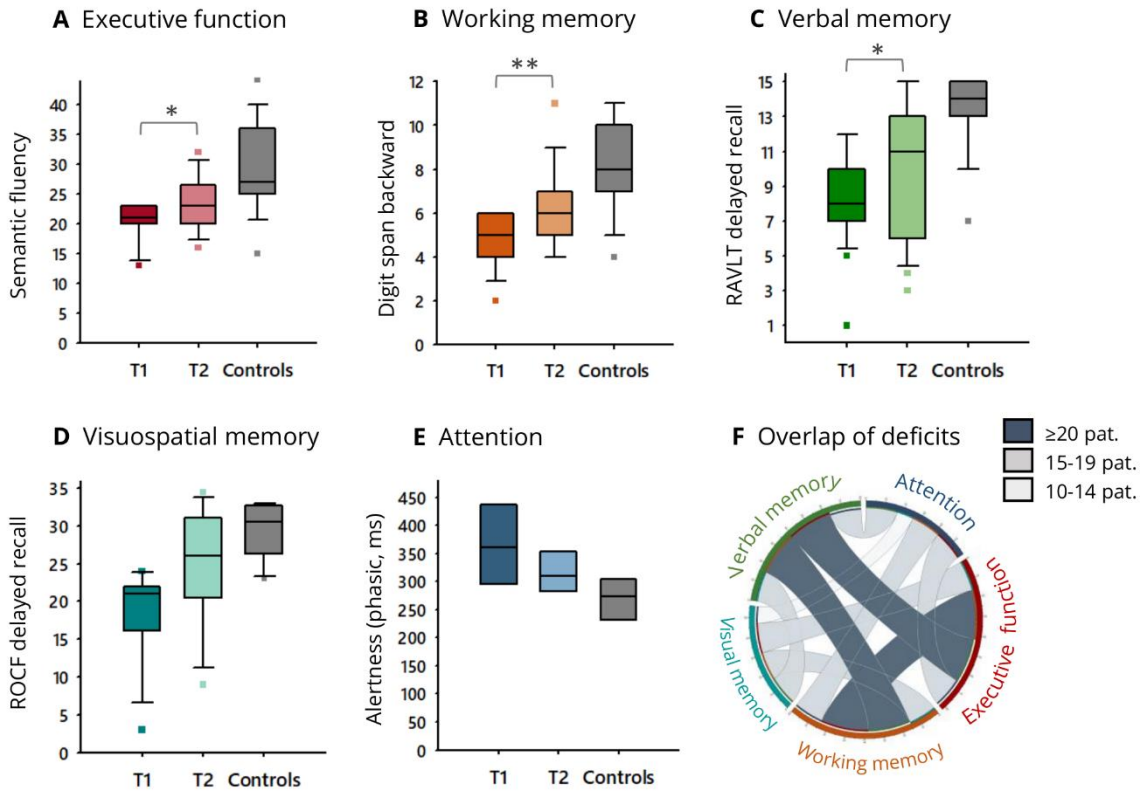

*Fig 3. Longitudinal development of deficits in representative cognitive tests. (A-E). Patients with deficits of executive function (z=2.01, p=0.04), working memory (z=3.18, p=0.001), and verbal memory (z=2.41, p=0.02) at first study visit improved significantly between the two study visits. *p<0.05, **p <0.01. (F) Overlap of deficits. Circular plot showing a strong coexistence of deficits in working memory, verbal memory, and executive function. The strength of the connection between domains represents the number of patients presenting with the respective overlap at first study visit.*

Depression and anxiety screening

Depression and anxiety screenings revealed no or minimal affective symptoms for most patients (table 1) at first study visit. The depression inventory indicated moderate depressive symptoms in 12% of the patients, mild symptoms in 20%, minimal signs in 12% and no depression in 56%. No association was observed between depressive symptoms and cognitive outcome. Anxiety screening suggested clinically relevant anxiety in 8% of the patients, moderate anxiety in 20%, mild symptoms in 32% and no or minimal anxiety symptoms in 40%. Stronger symptoms were associated with slower response times on tests of attention (r=0.43, p=0.036).

Predictors of long-term cognitive outcome

Multiple regression analyses identified several clinical predictors for cognitive outcomes at a median of 4.9 years after the acute phase. Treatment delay significantly predicted long-term executive and memory function, i.e. patients with delayed onset of first-line immunotherapy performed worse on test of inhibition (b=.371, t=2.25, p=0.031) and verbal episodic memory (b=-.436, t=-2.81, p=0.008). Long hospitalization times, i.e. a longer duration of the acute phase, significantly predicted working memory outcomes (b=-.474, t=-2.79, p=0.009) at our last study visit. Similarly, the disease severity during the acute phase (maximum mRS) predicted visual memory (b=-.525, -3.07, p=0.004) and the overall cognitive outcome (composite score; b=.536, t=2.90, p=0.006). The need for ICU admission was associated with a worse visual memory outcome (b=-.610, t=-3.70, p=0.001). Lastly, a younger age of onset was associated with a better executive performance at last study visit (b=.345, t=2.20, p=0.035).

Temporal evolution of recovery

Regarding overall cognitive performance, recovery was quantified as the number of recovered domains between first and second study visit. The greatest potential for improvement was observed in patients with severe disease courses, i.e. severe cognitive (composite score at first study visit; r_s=0.45, p=0.003) and neurological impairment (maximum mRS; r_s=0.37, p=0.02). Nevertheless, these patients also remained with more severe residual deficits at second study visit (composite scores; r_s=0.53, p<0.001).

Finally, we analyzed how long cognitive recovery can be observed after disease onset. Indeed, improvement of cognitive function was significantly associated with the timepoint of study visit, i.e. cognitive improvement was more pronounced early after the acute phase (composite score; r_s=-0.41, p=0.009). To explore this further, we analysed the recovery patterns in individual cognitive domains (Fig. 4). Time-dependent recovery was particularly pronounced for attention (r=0.435, p=0.031), with greater early after the acute phase. However, importantly, these analyses also demonstrate continued improvement of cognitive function for an extended time period of up to 8-9 years after disease onset in some patients (Fig. 4). There was no correlation between the time-point of disease onset with respect to first description with cognitive outcome (composite score: r_s=-.136, p=0.698) or neurological disability (mRS: r_s=-.040, p=0.830) at last study visit, i.e. patients who developed NMDAR encephalitis more recently did not a better long-term outcome.

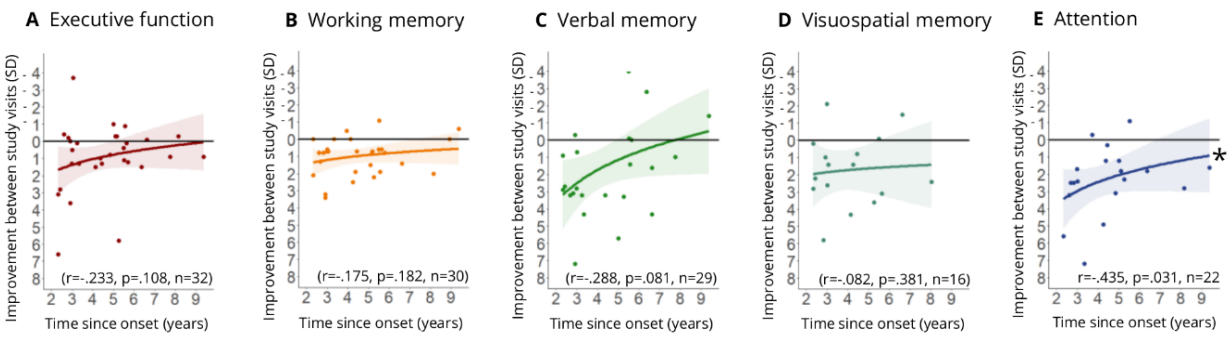

Fig 4. Cognitively impaired NMDAR encephalitis patients show extended period of cognitive improvement and domain-specific recovery patterns. Data points show the observed improvement between the first and the second study visit for each patient (y-axis) in relation to the time between last study visit and disease onset (x-axis). Affected patients show a time-dependent recovery for working memory, verbal memory, and attention, with greater gains earlier after the acute phase (semi-log regression plot with 95% confidence interval). Improvement of cognitive function, however, is still observed for an extended time period of up to 8-9 years in some patients.

Discussion

In this comprehensive longitudinal study of cognitive outcome following NMDAR encephalitis, we observed the following main findings: (i) All patients exhibit cognitive deficits after the acute disease stage (median 2.3 years after disease onset), with severe deficits in 50% of patients; (ii) Core cognitive deficits were impairments of working memory, verbal episodic memory, and executive function; (iii) At further follow-up more than 4 years after disease onset, cognitive performance had significantly improved; however, one third of patients remained with severe deficits, while one third was moderately affected and one third had fully recovered; (iv) Improvement of cognitive function was seen across all domains; however, working memory, episodic memory, attention and executive functions remained significantly impaired; (v) These persistent cognitive deficits were observed despite a favourable functional neurological outcome; (vi) Predictors for impaired cognitive long-term outcome were delayed treatment, older age and higher disease severity, i.e. higher maximum mRS, longer intensive care unit treatment, and longer overall disease duration; Importantly, (vii) the temporal dynamics of cognitive recovery are domain-specific, and improvements of cognitive function were observed for up to 8-9 years after disease onset.

Cognitive impairment is the main contributor to long-term morbidity in NMDAR encephalitis

All NMDAR encephalitis patients had cognitive deficits about 2 years after disease onset, with more than 80% showing moderate or even severe impairment. This contrasts with the favorable functional neurological outcome in previous observations of large and well-characterized cohorts of NMDAR encephalitis patients.[9,260] Upon further follow-up at a median of 4.9 years after disease onset, patients improved in all cognitive domains, albeit with persisting deficits of memory and executive function. In contrast, all patients had achieved a favorable functional neurological outcome with no or only minor residual disability (mRS 0-1).

These findings highlight that cognitive impairment is the main contributor to long-term morbidity in NMDAR encephalitis. The dissociation between good functional neurological and poorer cognitive outcome extends and corroborates findings from earlier small case series that suggested variable cognitive long-term outcomes in NMDAR encephalitis despite substantial improvement or full recovery of other neuropsychiatric symptoms.[177,246,253] Similarly, a recent investigation of long-term cognitive outcome in children with NMDAR encephalitis observed a dissociation between persisting cognitive deficits and good functional outcome 31 months after disease onset.[261]

The high rate of patients with moderate and severe cognitive deficits several years after the disease illustrates the substantial negative impact of the disease on the patients' long-term health. Importantly, these long-lasting cognitive impairments substantially limit the success and participation in occupational and social environments of these typically young patients and thus substantially impact their quality of life. It is therefore important that clinicians are sensitive to cognitive alterations and address complaints in their patients, even when other major neuropsychiatric symptoms have remitted. Our findings show that standardized cognitive testing is essential to assess outcome in the post-acute phase of patients with NMDAR encephalitis. Therefore, cognitive measures should also be included in clinical studies in addition to measures of functional neurological outcome.

Core cognitive deficits: memory impairment and executive dysfunction

Our data illustrate that the cognitive profile of NMDAR encephalitis in adults is characterized by deficits of verbal episodic memory, working memory and executive function. This predominant mnestic-executive presentation corresponds with the distribution of NMDARs, with highest receptor densities in the hippocampus (cornu ammonis 1 [CA1] region and dentate gyrus) and the frontal cortex (cortical layers I-III).[39,40] NMDARs regulate synaptic transmission and plasticity[262] involved in long-term potentiation[263] and long-term depression[264] during memory encoding and consolidation. Memory impairment as well as executive dysfunction are, therefore, likely consequences of frontal and medial

temporal NMDAR dysfunction. In line with this hypothesis, decoupling of the hippocampus and the medial prefrontal cortex correlates with severity of memory deficits in NMDAR encephalitis patients.[101] At the same time, structural hippocampal damage (i.e. reduced hippocampal volume and decreased microstructural integrity)[92] is associated with memory impairment. Dysfunction of NMDARs in the frontal cortex is a likely correlate of the frequent impairment of executive function. Indeed, administration of the NMDAR antagonist ketamine not only causes memory deficits,[265] but also leads to increased error rates and stronger perseverance in the Wisconsin Card Sorting Test,[266] a standard test of executive function. In addition, extensive white matter damage[101,267,268] and whole-brain functional connectivity changes[101,217] contribute to cognitive deficits beyond memory and executive dysfunction. Interestingly, the cognitive deficit profile of NMDAR encephalitis seems to be different in children, where predominant impairment of sustained attention was observed.[261]

Predictors for long-term cognitive outcome

Our regression analyses showed that delayed immunotherapy and higher disease severity during the acute phase are predictors of impaired cognitive long-term outcome. Specifically, patients with delayed treatment start had more severe deficits of verbal memory and executive function, i.e. cognitive processes related to inhibitory and attentional control, mental flexibility, problem solving and action planning. These results highlight the need for a rapid diagnostic work-up and treatment of patients with NMDAR encephalitis, as a failure to do so can cause a significant negative impact on academic achievements and social interactions of patients. In addition, impaired working memory and visual memory outcome were predicted by higher disease severity, assessed as need for longer hospitalization, need for ICU treatment, and higher acute phase mRS. These findings corroborate previous exploratory observations in a small cross-sectional study on cognitive outcome in NMDAR encephalitis.[177] Furthermore, our results are in line with findings from large cohort studies that identified later treatment and more severe disease symptoms (assessed as need for ICU treatment) as predictors of general disability (mRS).[9,27] Overall, the identified clinical predictors can help to guide clinical management decisions to achieve good cognitive long-term outcomes and prevent long-term impairments in the core cognitive deficit domains of NMDAR encephalitis, i.e. memory and executive function.

Long-term recovery of cognitive function

The temporal dynamics of cognitive recovery are domain-specific and continued improvements of cognitive function were observed for several years after disease onset. Despite noticeable subjective memory and concentration complaints at first study visit, many patients reported either subjective

cognitive improvement or stable abilities at second study visit. In correlation analyses, we observed that greater improvement occurs in the early recovery phase. Nonetheless, our analysis showed that recovery can continue for years, with improvement in working memory, verbal episodic memory and attention for up to 9 years after symptom onset. These results can help to counsel patients and relatives that improvement of cognitive function is domain-specific and can be expected to continue for several years after disease onset. Vice versa, these data can be used to define the temporal boundaries of the recovery period and thereby suggest a domain-specific time point at which cognitive deficits can be considered persistent. Furthermore, our results highlight that current cognitive rehabilitation approaches may be insufficient for most patients, given their typical limitation to several weeks or at most a few months, calling for longer and individually adapted rehabilitation regimens.

Implications for clinical management

Our results have several implications for the clinical management of patients with NMDAR encephalitis: (i) All patients should receive dedicated neuropsychological testing after the acute disease stage and clinical studies should include cognitive performance as outcome measures; (ii) The high risk for cognitive long-term deficits should be considered in the decision making process for the initiation and escalation of immunotherapy, as late treatment and severe disease symptoms are associated with worse cognitive outcome; (iii) Patients and relatives should be counseled about the risk for cognitive long-term impairments, but also about the continued recovery for several years; (iv) Finally, our results call for continued and dedicated cognitive rehabilitation in patients with NMDAR encephalitis to support the observed recovery process over several years. Targeting mnemonic and executive functions - ideally in individually tailored cognitive interventions[249] - may be particularly helpful to achieve a favourable long-term outcome. In a study of pediatric NMDAR encephalitis, attention deficits and fatigue had a persisting impact on the school performance, so that one third of the children did not return to their previous school level.[261] Ameliorating the impact of autoimmune encephalitis on cognitive performance should therefore be one of the main treatment goals to preserve long-term educational and occupational potential in these patients. In the current dataset, we did not see improved functional neurological and cognitive outcomes in patients with a more recent disease onset. However, given the observed association between shorter treatment delay and better cognitive outcome, a further increased awareness and treatment of the disease will hopefully lead to improved cognitive outcomes.

Limitations

Neuropsychological testing is often difficult to perform during the acute phase of the disease when cognitive symptoms are most pronounced. Here, severe neuropsychiatric symptoms, decreased levels of consciousness or drug effects can impede structured cognitive testing. Comprehensive assessments, such as in this study, are therefore limited to the recovery phase after the peak of the disease. There are, nonetheless, several case studies that describe cognition in severely impaired patients using individually adapted neuropsychological protocols.[269–271] In addition, given the rarity of the disease and long-distance travel arrangements of our patients, a certain variability in the timing of study visits was unavoidable. Study visits were, however, unrelated to other medical consultations and this variability was statistically accounted for using linear mixed effects analyses. Although we controlled the impact of practice effects at second study visits using parallel versions or randomization of trials wherever applicable, we cannot fully exclude the impact of familiarity with the task design.

Conclusion

In conclusion, this study presents comprehensive longitudinal data for the cognitive outcome in NMDAR encephalitis. All patients had cognitive deficits about 2 years after disease onset, mainly affecting memory and executive function. After 4 years, moderate or severe cognitive deficits persisted in 2/3 of patients despite good functional neurological outcome, indicating that cognitive function is an important outcome measure in addition to the functional neurological scales. Impaired cognitive outcome was predicted by delayed treatment and higher disease severity. However, continued improvement of cognitive function was observed for up to 9 years after disease onset. Our results demonstrate that cognitive deficits are frequent and severe long-term sequelae following NMDAR encephalitis. These deficits show a slow and incomplete recovery and persist beyond recovery of other neuropsychiatric symptoms of the disease. As a consequence, our findings call for rapid diagnosis and treatment at disease onset as well as for continued and customized cognitive rehabilitation to improve the long-term outcome.

Supplementary material

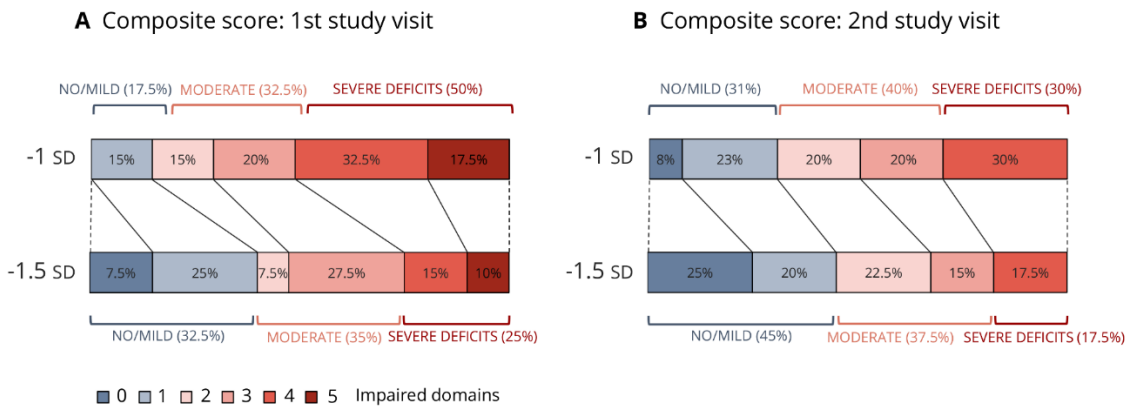

Supplementary Fig. 1. Composite score of cognitive deficits at different thresholds of impairment (n=40).

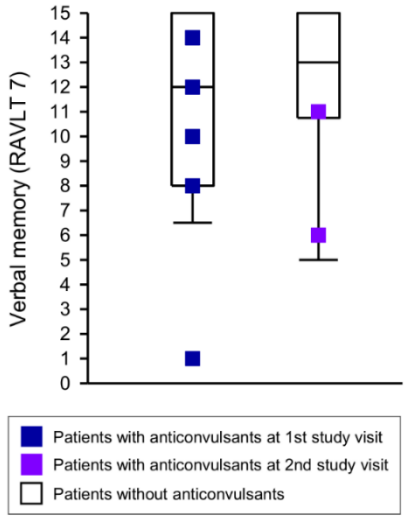

Supplementary Fig. 2. Effect of anticonvulsant medication on test outcomes. Patients with and without anticonvulsant medication did not differ significantly in their overall cognitive performance (composite score: U=-.098, p=0.93) or verbal memory (U=-.770, p=0.47) at first study visit. At second study visit, only two patients received anticonvulsants.

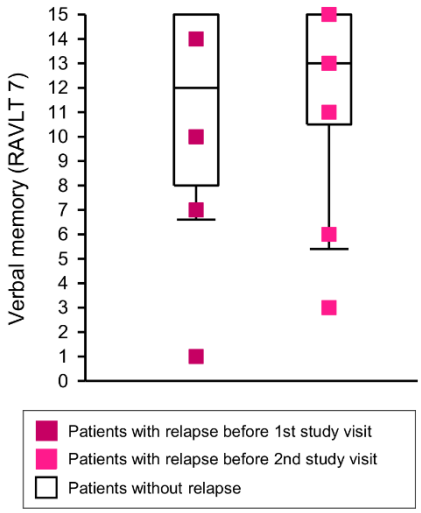

Supplementary Fig. 3. Effect of relapses on test outcomes. Patients with and without relapse did not differ significantly in their overall cognitive performance (composite score: U=-.357, p=0.751) or verbal memory (U=-1.54, p=0.133) at first and second study visit (composite score: U=-1.70, p=0.102; verbal memory: U=-.51, p=0.626)

Acute phase CSF titre	n
1:3.2 *to* 1:4	5/40 (12.5%)
1:10 *to* 1:16	7/40 (17.5%)
1:32 *to* 1:50	11/40 (27.5%)
1:100	7/40 (17.5%)
1:320 *to* 1:360	2/40 (5%)
1:2560	1/40 (2.5%)
Positive *(unspecified)*	7/40 (17.5%)

Supplementary table S1. IgG anti-GluN1 antibody titres during the acute phase. n: number of patients.

	Patients *(median, IQR)*	Controls *(median, IQR)*	Fixed effects estimate (*b*, 95% CI)	p
1st study visit				
Executive function *(semantic fluency)*	23 (21,29)	27 (25,30)	*b*=-3.19 [-6.06,-0.34]	p=0.020 *
Working memory *(digit span backward)*	6 (5,7)	7 (6,9)	*b*=-1.88 [-2.7,-1.04]	p<0.001 **
Verbal memory *(RAVLT delayed recall)*	12 (8,15)	14.5 (13,15)	*b*=-2.49 [-5.21,0.21]	p=0.002 **
Visual memory *(ROCF delayed recall)*	26 (22,31)	29 (25.5,32)	*b*=-1.50 [-5.80,2.84]	p=0.300
Attention *(phasic alertness, RT in ms)*	233 (212,260.5)	247 (224.8,264.8)	*b*=5.35 [-76.2,87.8]	p=0.856
2nd study visit				
Executive function *(semantic fluency)*	24 (21,28)	27 (25,30)	*b*=-2.88 [-5.75,-0.03]	p=0.035 *
Working memory *(digit span backward)*	6 (5,7)	7 (6,9)	*b*=-1.20 [-2.05,-0.35]	p=0.007 **
Verbal memory *(RAVLT delayed recall)*	13 (10.8,15)	14.5 (13,15)	*b*=-1.63 [-4.32,1.09]	p=0.029 *
Visual memory *(ROCF delayed recall)*	28.5 (24,31.9)	29 (25.5,32)	*b*=-0.04 [-4.32,4.28]	p=0.962
Attention *(phasic alertness, RT in ms)*	250 (229.5,281)	247 (224.8,264.8)	*b*=14.65 [-67.54,96.29]	p=0.267

Supplementary table S2. Cross-sectional comparison between patients and controls and first and second study visit (linear mixed effects analyses, n=40). (RAVLT: Rey Auditory Verbal Learning Test; ROCF: Rey-Osterrieth Complex Figure Test; RT: Response time, CI confidence interval)

	Test	Controls	1st study visit	2nd study visit
Executive functions	*Go/No-Go (median RT)*	525.5 ± 58.3 ms	502.4 ± 60.2 ms	540.0 ± 49.6 ms
	Go/No-Go (errors)	0.9 ± 1.1	0.8 ± 1.0	1.0 ± 1.2
	Stroop (RT)	97.9 ± 16.2 s	113.0 ± 21.8 s	108.0 ± 22.2 s
	Semantic fluency	27.7 ± 4.2	24.4 ± 4.1	24.8 ± 4.2
Working memory	*Digit span forward*	8.5 ± 1.5	7.3 ± 1.8	7.3 ± 1.4
	Digit span backward	7.7 ± 1.6	5.8 ± 1.3	6.5 ± 1.2
Verbal memory	*RAVLT 1 (immediate recall)*	8.4 ± 2.2	7.9 ± 2.1	8.0 ± 1.9
	RAVLT sum score (learning)	61.3 ± 7.1	55.9 ± 9.8	56.3 ± 8.8
	RAVLT 6 (post-interference)	13.5 ± 1.6	11.2 ± 3.3	11.5 ± 2.6
	RAVLT 7 (delayed recall)	13.6 ± 1.6	11.1 ± 3.1	11.9 ± 2.8
	RAVLT recognition[a]	14.5 ± 0.7	13.5 ± 1.7	13.9 ± 1.3
Visual memory	*ROCF immediate recall*[b]	28.0 ± 3.8	26.1 ± 5.3	27.7 ± 4.9
	ROCF delayed recall[b]	27.7 ± 4.3	26.1 ± 5.2	27.6 ± 4.6
Attention	*Tonic alertness (median RT)*	247.5 ± 21.9 ms	252.0 ± 40.9 ms	270.3 ± 35.2 ms
	Phasic alertness (median RT)	250.9 ± 25.5 ms	253.6 ± 46.5 ms	267.7 ± 39.7 ms
	Dual-task: Auditory (median RT)	587.2 ± 80.3 ms	563.5 ± 100.5 ms	585.2 ± 82.0 ms
	Dual-task: Visual (median RT)	733.1 ± 66.7 ms	733.0 ± 97.6 ms	738.8 ± 80.0 ms
	Dual task (errors)	2.3 ± 1.8	3.2 ± 2.8	2.8 ± 2.3
(Premorbid) intelligence estimate	*Vocabulary (MWT)*	30.5 ± 3.0	30.0 ± 3.6	-

Supplementary table S3. Cognitive test results at first and second study visit (n=40). Scores are presented with mean ± standard deviation. a Corrected for errors. b None of the participants showed deficits in visuospatial skills during the copy condition. (RAVLT: Rey Auditory Verbal Learning Test; ROCF: Rey-Osterrieth Complex Figure Test; MWT: Mehrfachwahl-Wortschatz-Intelligenztest (German equivalent of the National Adult Reading Test; RT: Response time)

Publication VI: Transdiagnostic hippocampal damage patterns in neuroimmunological disorders

Abstract

Hippocampal damage and associated cognitive deficits are frequently observed in neuroimmunological disorders, but comparative analyses to identify shared hippocampal damage patterns are missing. Here, we adopted a transdiagnostic analytical approach and investigated hippocampal shape deformations and associated cognitive deficits in four neuroimmunological diseases.

We studied 120 patients (n=30 in each group), including patients with multiple sclerosis (MS), neuromyelitis optica spectrum disorder (NMOSD), anti-NMDAR and anti-LGI1 encephalitis. A control group was matched to each patient sample from a pool of 79 healthy participants. We performed an MRI-based vertex-wise hippocampal shape analysis, extracted hippocampal volume estimates and scalar projection values as a measure of surface displacement. Cognitive testing included assessment of verbal memory and semantic fluency performance.

Our cross-sectional analyses revealed characteristic patterns of bilateral inward deformations covering up to 32% of the hippocampal surface in MS, anti-NMDAR encephalitis, and anti-LGI1 encephalitis, whereas NMOSD patients showed no deformations compared to controls. Significant inversions were noted mainly on the hippocampal head, were accompanied by volume loss, and correlated with semantic fluency scores and verbal episodic memory in autoimmune encephalitis and MS. A deformation overlap analysis across disorders revealed a convergence zone on the left anterior hippocampus that corresponds to the CA1 subfield.

This convergence zone indicates a shared downstream substrate of immune-mediated damage that appears to be particularly vulnerable to neuroinflammatory processes. Our transdiagnostic morphological view sheds light on mutual pathophysiologic pathways of cognitive deficits in neuroimmunological diseases and stimulates further research into the mechanisms of increased susceptibility of the hippocampus to autoimmunity.

Keywords

Hippocampal shape, neuroinflammation, autoimmune encephalitis, neuromyelitis optica spectrum disorder, multiple sclerosis, memory disorders

Introduction

The hippocampus is a frequent target in many neuroimmunological diseases despite their distinct pathophysiological mechanisms. Accumulating evidence suggests a selective vulnerability of the hippocampus, and particularly its subfield CA1, to inflammatory processes.[48] Consequently, largely overlapping cognitive deficits are observed in neuroimmunological disorders, including impairments of episodic memory, spatial navigation and affective processing.[177,200,272] Here, we directly compared hippocampal damage and associated cognitive deficits in four distinct neuroimmunological disorders using the same imaging analysis protocol in order to explore the hypothesis of selective vulnerability and to identify shared hippocampal damage patterns.

Previous imaging studies have identified characteristic hippocampal damage patterns leading to cognitive deficits in neuroimmunological disorders. In multiple sclerosis, for example, MRI analyses revealed a hippocampal volume reduction associated with impaired verbal and visuospatial memory performance.[273] Anti-NMDA receptor (NMDAR) encephalitis is a recently discovered autoimmune encephalitis with autoantibodies targeting the NR1 subunit of the NMDA receptor.[10] The hippocampus contains the highest density of NMDARs and, consequently, volume loss, impaired microstructural integrity and disrupted functional connectivity of the hippocampus are characteristic imaging findings that correlate with the severity of memory impairment.[92] Autoimmune encephalitis with LGI1 antibodies manifests as limbic encephalitis with bilateral hippocampal inflammation detectable in 60-85% of patients.[18,25,200] At later disease stages, almost all patients develop atrophy and impaired microstructural integrity of the hippocampus that relates to marked memory deficits.[111,200] In contrast, the majority of imaging studies observed no volume reduction or microstructural changes of the hippocampus in patients with neuromyelitis optica spectrum disorder (NMOSD).[274,275]

However, to date, there have been no comparative approaches that characterize hippocampal damage patterns across different neuroimmunological diseases. Considering the shared cognitive symptoms, such transdiagnostic approaches can identify common downstream mechanisms that give rise to mutual clinical presentations and may therefore help to improve the pathophysiological understanding of neuropsychiatric symptoms.[276] In addition, volumetric analyses only assess global hippocampal changes, while shape analyses can identify the exact spatial distribution of atrophy by providing discrete information about the location of pathological changes on a brain structure's surface. Indeed, shape deformations were shown to provide a sensitive marker of hippocampal pathology that can track disease progression in patients with memory disorders.[277–279]

We therefore performed a comprehensive vertex-based shape analysis of the hippocampus in patients with four different neuroimmunological disorders, i.e. multiple sclerosis (MS), neuromyelitis optica spectrum disorder (NMOSD), anti-NMDA receptor (NMDAR) encephalitis and anti-LGI1 encephalitis. The aims of this study are to (1) describe the spatial patterns of pathological changes on the

hippocampal surface, (2) provide comparative data and identify shared transdiagnostic damage patterns for these disorders, (3) and complement previous volumetric analyses by morphological assessments.

Materials & methods

Participants

We included one hundred twenty patients with four different neuroimmunological disorders, i.e. patients with NMDAR encephalitis (n=30), LGI1 encephalitis (n=30), relapsing remitting multiple sclerosis (RRMS; n=30) and aquaporin-4 antibody positive NMOSD (n=30). All patients were recruited from the outpatient clinics of the NeuroCure Clinical Research Center and the Department of Neurology of Charité - Universitätsmedizin Berlin between 2012-2017, except for eleven LGI1 encephalitis patients that were recruited at the University Hospital Schleswig-Holstein in Kiel.

NMDAR encephalitis and LGI1 encephalitis patients were studied after the acute stage of the disease and were diagnosed based on the proposed criteria of characteristic clinical presentation, cerebrospinal fluid findings, neuroimaging changes and autoantibody detection (IgG NMDAR antibodies in CSF and IgG LGI1 antibodies in CSF or serum).[23] Patients with multiple sclerosis fulfilled the 2017 revised McDonald criteria and were on stable immunomodulatory therapy for at least three months, with no acute relapse for at least three months prior to enrolment and without corticosteroid therapy in the last 30 days. All NMOSD patients fulfilled the 2015 international consensus diagnostic criteria for NMOSD and were tested positive for AQP4 antibodies; no patient was MOG-antibody seropositive. Demographic and clinical descriptions of the study groups are provided in table 1. Lesion segmentations for the characterization of MS and NMOSD patients was performed on 3D FLAIR images using the semiautomatic Lesion Segmentation Toolbox (LST)[280] for SPM. We created an individual control group for each clinical sample by performing a 1:1 matching (regarding age and sex) between patients and healthy control participants drawn from a pool of seventy-nine healthy volunteers.

All participants gave informed written consent. The study was approved by the Ethics Committee of Charité – Universitätsmedizin Berlin and conducted in accordance with the Declaration of Helsinki.

	NMDA	LGI1	RRMS	NMOSD
Sex				
Patients	26 f, 4 m	9 f, 21 m	18 f, 12 m	27 f, 3 m
Controls	26 f, 4 m	9 f, 21 m	18 f, 12 m	27 f, 3 m
Age				
Patients (mean (±SD))	28.0 (±7.6) yrs	65.6 (±9.1) yrs	43.3 (±6.4) yrs	45.5 (±11.1) yrs
Controls (mean (±SD))	29.0 (±8.1) yrs	62.8 (±10.3) yrs	41.8 (±8.4) yrs	44.0 (±12.5) yrs
	t(58)=-0.42, p=.68	t(58)=0.52, p=.61	t(58)=0.63, p=.53	t(58)=0.41, p=.68
Disease duration[a]	21.0 months	23.3 months	163.5 months	47.0 months
Median (range)	(2.0-82.0)	(0.2-118.2)	(17.0-346.0)	(10.0-336.0)
Disease severity[b]	mRS	mRS	EDSS	EDSS
Median (range)	2 (0-3)	2 (0-4)	2 (1-5)	4 (0-6.5)
Clinical MRI				
T2 lesion count	-	-	34 (3-126)	9 (0-68)
Median (range)				
T2 lesion volume	-	-	9.3 ± 7.4 ml	2.1 ± 2.3 ml
Mean (SD)				
Acute phase MRI (No. of affected patients)	13/30 patients with abnormal MRI: Unilateral T2/FLAIR hyperintensities (temporal (5), basal ganglia (1), thalamus (1)), T2-hyperintense white matter lesions (periventricular (6), frontal/opercular (4)), mild global atrophy (1)	25/30 patients with abnormal MRI: Unilateral T2/FLAIR hyperintensities (left hippocampus (4), right hippocampus (5), right insula (1)), Bilateral T2/FLAIR hyperintensities (hippocampus (11), amygdala (5)), subcortical arteriosclerotic encephalopathy (3), periventricular leukencephalopathy (1), mild global atrophy (2)	-	-
Acute phase seizures	22/30 patients (complex-focal (2), generalized tonic-clonic (6), status epilepticus (1), unknown type (13))	FBDS: 16/30 patients Seizures: 13/30 patients (pilomotor (4), complex-focal (5), generalized tonic-clonic (4))	-	-

Therapy delay				
Median (range)	37 (1-1,096) days	49 (7-400) days	-	-
Memory score	RAVLT sum score	RAVLT sum score	SRT-LTS	SRT-LTS
Mean (±SD)	54.1 (±10.1)	38.0 (±12.4)	57.1 (±14.4)	56.3 (±9.2)
Norm (percentile)	40th %ile	20th %ile	52th %ile	58th %ile
Fluency score	RWT score	RWT score	WLG score	WLG score
Mean (±SD)	22.7 (±3.4)	21.5 (±4.9)	24.8 (±7.4)	26.7 (±5.6)
Norm (percentile)	35th %ile	57th %ile	31th %ile	57th %ile
BDI-II[c]				
Median (range)	8 (0-17)	8 (1-22)	6.5 (0-26)	11.5 (0-29)

Table 1. Sample characteristics. [a] Disease duration is calculated as the time span between symptom onset and time of MRI. [b] Disease severity was assessed using the modified Rankin Scale (mRS) and the Expanded Disability Status Scale (EDSS) at the study date. [c] Scoring: 0-8 no depression, 9-13 minimal depression, 14-19 mild depression, 20-28 moderate depression, 29-63 severe depression. (BDI-II: Beck Depression Inventory – Revision; RAVLT: Rey Auditory Verbal Learning Test; SRT-LTS: Selective Reminding Test – long-term storage; RWT: Regensburg Word Fluency Test; WLG: Word List Generation Test).

MRI data acquisition

A 3-dimensional, high-resolution T1-weighted sequence (Magnetization Prepared Rapid Acquisition Gradient Echo; MPRAGE, voxel size 1x1x1mm³) and a 3D FLAIR/T2 sequence (Fluid-Attenuated Inversion Recovery; voxel size 1x1x1mm³) were acquired for each participant on a 3T Siemens Tim Trio scanner (Siemens, Erlangen, Germany) at the Berlin Center for Advanced Neuroimaging. Eleven LGI1 encephalitis patients and matched controls were examined at the University Hospital Schleswig-Holstein in Kiel on a 3T Philips Achieva scanner using the same sequence. Study site was accounted for as a covariate in the general linear model.

Surface-based analyses and statistics

The segmentation of the left and right hippocampi was performed using FMRIB's Integrated Registration and Segmentation Tool (FIRST) as implemented in FSL (www.fmrib.ox.ac.uk). As detailed previously,[195] the FIRST algorithm automatically segments the hippocampus based on shape models and voxel intensities. A deformable mesh model is used to create a surface mesh for each hippocampus. Each mesh is composed of a set of triangles with a fixed number of vertices, i.e. apices of adjoining triangles, for each structure. This allows for comparisons of corresponding vertices between groups. The segmentations were visually examined to confirm the accuracy of the results. For between-group comparisons, we performed separate T-tests for the left and right hippocampi using FSL randomize

with threshold-free cluster enhancement (TFCE). Contrasts were designed to test for both atrophy and growth to allow for the detection of changes in both directions. Vertex-wise T-statistics were corrected for multiple comparisons and the presented maps survived TFCE with a $q<0.05$ FDR correction.

Next, we extracted summary statistics for the scalar projection values and volumes using the FSL-Utils toolbox. During the analysis, the surface locations of each individual's hippocampus are projected onto the cohort average surface, which reflects the mean surface position across patients and control participants. This allows a quantification of the distance between an individual's hippocampal surface and the cohort average hippocampal surface at all vertices. Scalar values represent this perpendicular distance of a vertex. As a reference, we collected volume estimates of the hippocampi, which were corrected for intracranial volume (ICV) using the following formula: $volume_{adjusted} = volume_{raw} - \beta\ (ICV_{raw} - ICV_{mean})$; with β referring to the slope of the linear regression of a participant's ICV on their raw hippocampal volume. ICV measures were determined using FSL Sienax.[281] Descriptive statistics are presented with mean and standard error. Group-based analyses between patients and controls were performed using multivariate analyses of variances and receiver operating characteristics (ROC) for continuous data of the left and right hippocampus. P-values <0.05 were considered significant. The Shapiro-Wilk test was used to assess the normality of the data.

Between-group similarity analysis

Finally, the pattern similarity of affected hippocampal surface areas was compared between diseases. To this end, the results of the normalized shape analysis were binarized for each disease group, with 1 coding a significantly affected vertex and 0 coding a non-affected surface vertex. We determined the contingency coefficient phi (Φ) for the extracted matrices using the Chi-Square test for categorical data. Φ constitutes a measure of correlation between two binary variables and allows a quantification of pattern similarity between diseases. Figures showing surface renderings were created using SurfIce (https://www.nitrc.org/projects/surfice/) and FSL FIRST3Dview.

Association with cognitive performance

Cognitive performance of patients was assessed for the purpose of correlational analyses. We assessed verbal fluency using a 1-minute semantic fluency task (category 'animals'; Regensburg Word Fluency Test (NMDA/LGI1 patients); and the identical Word List Generation subtest of the Brief Repeatable Battery of Neuropsychological Tests (BRB-N; RRMS/NMOSD patients). Verbal learning and memory were tested using two equivalent multiple-trial list-learning paradigms (German version of the Rey

Auditory Verbal Learning Test (RAVLT; NMDA/LGI1 patients); Selective Reminding Test (SRT; RRMS/NMOSD patients). Depressive symptoms were assessed in all participants using the Beck Depression Inventory (BDI-II). Correlational analyses were performed using Pearson/Spearman correlation coefficients in IBM SPSS Statistics 22.

Results

Hippocampal deformations were observed in NMDAR encephalitis, LGI1 encephalitis and relapsing remitting multiple sclerosis (RRMS), but not in NMOSD (Fig.1; see Fig.S1 for FDR threshold information). Volumetric results were in line with these observations (Table 2).

		Patients (mean ± SEM)	**Controls (mean ± SEM)**	**F**	**p-value**	**Partial η^2**
NMDA	*Left*	3463.8 (± 92.8) mm^3	3993.3 (± 68.9) mm^3	F(1,58)=21.0	<0.001**	0.266
	Right	3600.3 (± 87.1) mm^3	3917.7 (± 89.6) mm^3	F(1,58)=6.5	0.014*	0.100
LGI1	*Left*	3162.3 (± 109.5) mm^3	3621.0 (± 96.7) mm^3	F(1,58)=9.9	0.003**	0.145
	Right	3188.5 (± 105.7) mm^3	3771.9 (± 88.4) mm^3	F(1,58)=17.9	<0.001**	0.236
RRMS	*Left*	3464.9 (± 70.3) mm^3	3942.4 (± 80.8) mm^3	F(1,58)=19.9	<0.001**	0.255
	Right	3472.1 (± 103.0) mm^3	3914.3 (± 80.6) mm^3	F(1,58)=11.5	0.001**	0.166
NMOSD	*Left*	3824.8 (± 70.0) mm^3	3788.3 (± 84.4) mm^3	F(1,58)=0.1	(0.740)	0.002
	Right	3835.1 (± 80.1) mm^3	3802.9 (± 75.5) mm^3	F(1,58)=0.1	(0.771)	0.001

Table 2. Hippocampal volumes. Volumes were estimated using automated segmentation and corrected for intracranial volume.

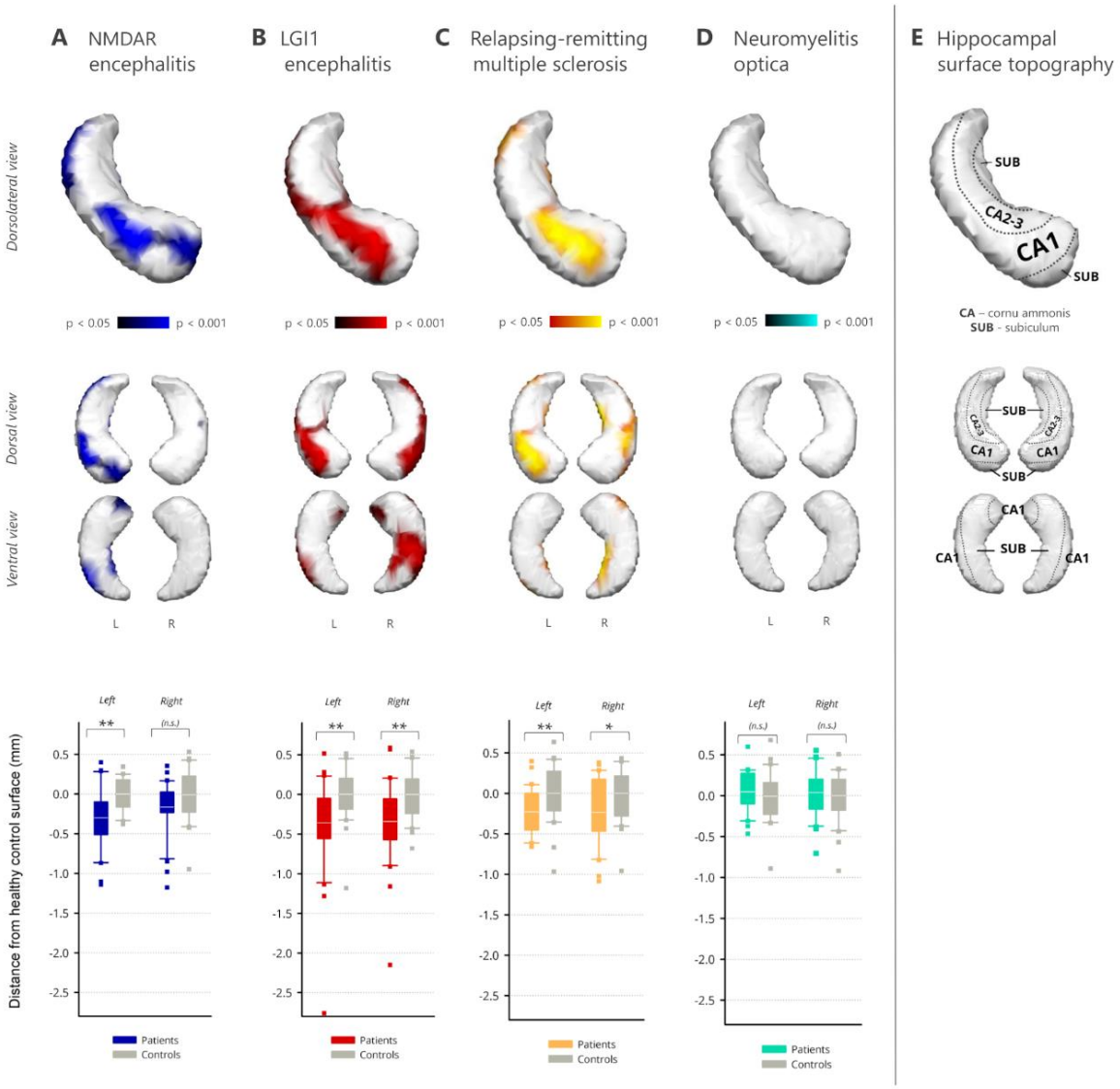

*Figure 1. Hippocampal shape deformations. Upper panels: Coloured regions show significant inward deformation of the hippocampal surface (p<.05; multiple-comparison corrected). Top row: Surface deformations of the left hippocampus are shown in a dorsolateral perspective. Bottom row: Deformations of the left and right hippocampus are shown in ventral and dorsal view. Lower panel: Scalar projection values of the hippocampus show the average displacement of the hippocampal surface with respect to the control groups (in mm; *p<0.05; **p<0.01).*

NMDAR encephalitis

In NMDAR encephalitis, an inward deformation of the surface was noted on the head of the left hippocampus (Fig.1A). Atrophic regions extended medially and laterally along the hippocampal axis, corresponding to subfields CA1-3 and subiculum (p<0.001). The same pattern was observed for the

right hippocampus, but only two smaller clusters survived correction for multiple comparisons (p=0.034).

We next determined the magnitude of displacement from the mean surface across the whole structure (Table 3). Surface deformations were -0.30mm for the left hippocampus and -0.16mm for the right hippocampus in the patient group. When compared to controls, this mean displacement of the hippocampal surface was significant for the left hippocampus ($F(1,58)=13.88$, $p<0.001$), but did not reach statistical significance for the right hippocampus ($F(1,58)=3.71$, $p=0.059$; Fig.1A).

		Total displace-ment	**Patients (mean ± SEM)**	**Controls (mean ± SEM)**	**F**	**p-value**	**Partial η^2**
NMDA	*Left*	-0.30 mm	-0.15 (± 0.07) mm	0.15 (± 0.04) mm	F(1,58) = 13.9	< 0.001**	0.193
	Right	-0.16 mm	-0.08 (± 0.06) mm	0.08 (± 0.06) mm	F(1,58) = 3.7	0.059	0.060
LGI1	*Left*	-0.36 mm	-0.18 (± 0.11) mm	0.18 (± 0.06) mm	F(1,58) = 8.1	0.006**	0.123
	Right	-0.34 mm	-0.17 (± 0.09) mm	0.17 (± 0.06) mm	F(1,58) = 9.6	0.003**	0.142
RRMS	*Left*	-0.22 mm	-0.11 (± 0.05) mm	0.11 (± 0.06) mm	F(1,58) = 8.4	0.005**	0.126
	Right	-0.24 mm	-0.12 (± 0.07) mm	0.12 (± 0.06) mm	F(1,58) = 6.3	0.015*	0.098
NMOSD	*Left*	0.06 mm	0.03 (± 0.04) mm	-0.03 (± 0.06) mm	F(1,58) = 0.6	(0.456)	0.010
	Right	0.04 mm	0.02 (± 0.05) mm	-0.02 (± 0.06) mm	F(1,58) = 0.3	(0.613)	0.004

Table 3. Scalar projection values of the hippocampus. Total displacement values show the magnitude of the disease-related inversion of the hippocampal surface (averaged across the whole structure). Scalar values for the individual patient and control groups represent the distance to the mean surface in the analysis that is created from both groups.

Correlational analyses revealed an association of the surface deformations with verbal learning performance: the stronger the inward movement of the surface cluster in the patient group, the fewer words were learned during word list learning (RAVLT sum score; r=.335, p=.035, n=30). We observed no association with word fluency (r=-.033, p=.432, n=30), depression screening scores (r_s=-.100, p=.356, n=16), treatment delay (r=.150, p=.237, n=25), time since onset (r=.021, p=.455, n=30), or functional outcome (mRS; r_s=-.120, p=.265, n=30). In addition, both hippocampi showed a significantly reduced volume (*left*: -13.3%, $F(1,58)=20.98$, $p<0.001$; *right*: -8.1%, $F(1,58)=6.45$, $p=0.014$; Table 2).

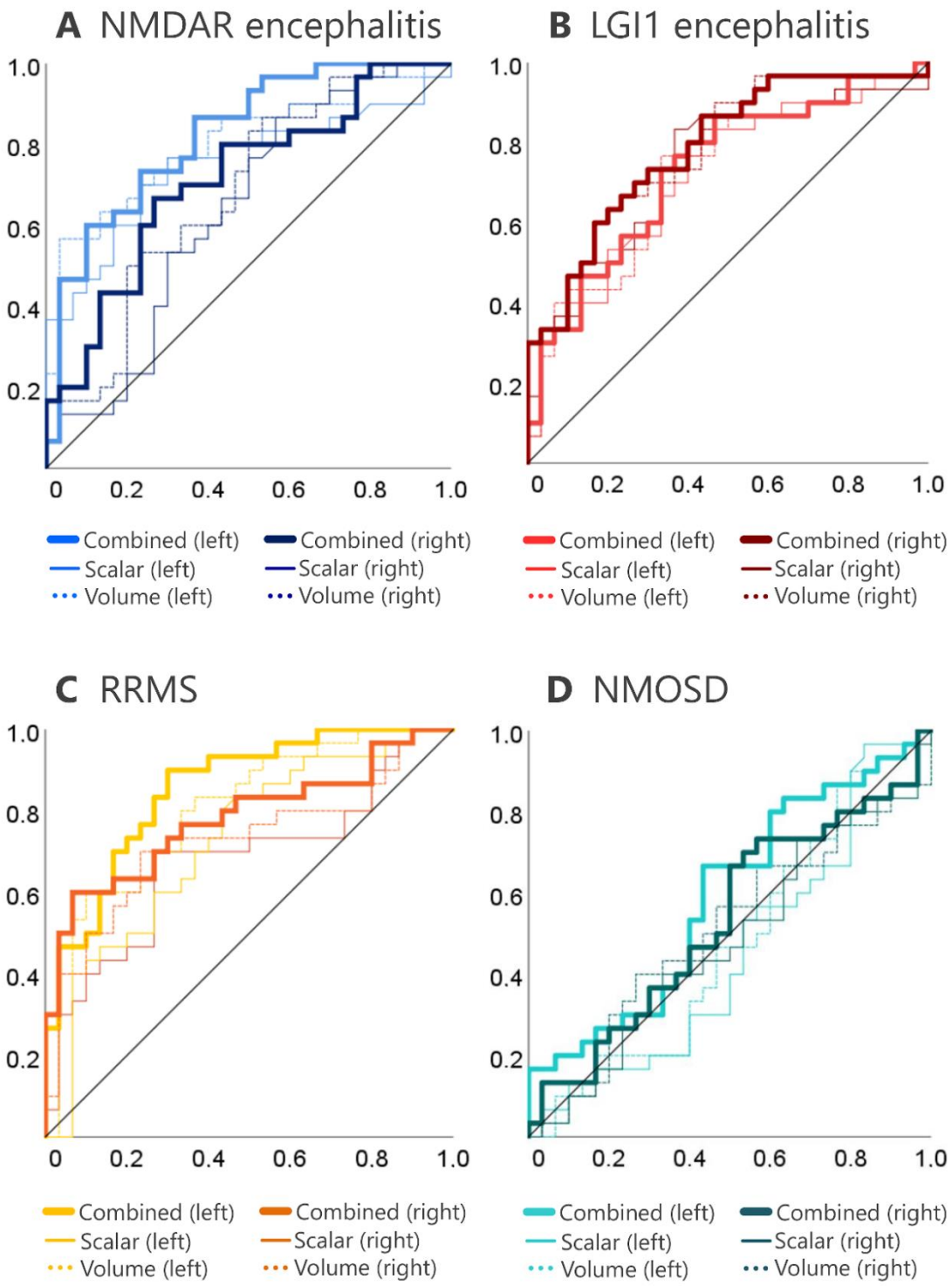

Figure 2. Receiver operating characteristics (ROC) for hippocampal scalar values, hippocampal volumes, and their combined classification performance. Sensitivity and specificity of the derived displacement measure are plotted on the x and y axes. The average scalar values of the left and right hippocampi (solid lines) show comparable diagnostic performance to that of conventional volumetric measures (dotted lines). Combining shape and volume information yielded the best classification performance across all diseases.

ROC analyses revealed that surface deformations of the left hippocampus significantly differentiated between patients and controls (area under the curve (AUC) ± standard error = .751±.065, p=.001; Fig.2A; Table 4). This fair to good diagnostic performance was comparable to that of volume measurements (AUC=.803±.058, p<.001). ROC performance for the right hippocampus was poor for both scalar displacement values (AUC=.636±.073, p=.070) and volumes (AUC=.678±.070, p=.018). Interestingly, the combination of shape and volume measures improved the classification performance for both the left (AUC=.823±.053, p<.001, excellent) and right hippocampus (AUC=.712±.067, p<.005, fair to good) as compared to any of the measures alone.

		Volume	**Scalar**	**Volume + Scalar**
NMDA	*Left*	.678 (±.070), p<.001	.751 (±.065), p=.001	.823 (±.053), p<.001
	Right	.636 (±.073), p=.018	.678 (± .070), p=.070	.712 (±.067), p<.005
LGI1	*Left*	.723 (±.066), p=.003	.721 (±.066), p=.003	.731 (±.065), p=.002
	Right	.781 (±.059), p<.001	.738 (±.066), p=.002	.786 (±.059), p<.001
RRMS	*Left*	.802 (±.057), p<.001	.723 (±.067), p=.003	.853 (±.048), p<.001
	Right	.724 (±.068), p=.003	.678 (±.071), p=.018	.781 (±.061), p<.001
NMOSD	*Left*	.474 (±.076), p=.734	.452 (±.076), p=.520	.589 (±.074), p=.237
	Right	.502 (±.076), p=.976	.479 (±.075), p=.779	.533 (±.076), p=.657

Table 4. Receiver operating characteristics (ROC).

LGI1 encephalitis

LGI1 encephalitis was characterized by a significant bilateral inward movement of the hippocampal surface. Affected regions encompassed the anterior hippocampus bilaterally in the area of CA1-3 (*left*, p=0.005; *right*, p=0.004). Atrophy was more extensive on the right hippocampus, where it extended laterally into area CA1 towards the tail and covered almost the whole ventral posterior surface, corresponding to the subfields CA1 and subiculum (Fig.1B).

We observed a significant surface displacement of -0.36mm for the left (F(1,58)=8.13, p=0.006) and -0.34mm for the right hippocampus (F(1,58)=9.63, p=0.003; Fig.1B). Inward movement of the surface cluster correlated with decreased word fluency (r=.444, p=.017, n=23), but not with depression screening scores (r_s=-.371, p=.117, n=12), functional outcomes (mRS; r_s=-.146, p=.221, n=30), or duration since onset (r=.210, p=.142, n=28). A longer treatment delay was, however, associated with a stronger inward deformation (r=-.422, p=.020, n=24).

While overall left hippocampal surface displacement correlated with worse verbal memory outcome (r=.348, p=.041, n=26), no such correlation was observed in controls (RAVLT sum score; r=.032, p=.874, n=30), suggesting that the association between surface displacement and cognition is a feature of disease pathology and not a physiological association. Volumetry revealed bilateral atrophy (*left*: -12.7%, F(1,58)=9.86, p=0.003; *right*: -15.5%, F(1,58)=17.94, p<0.001).

Surface deformations significantly differentiated between patients with LGI1 encephalitis and controls in the ROC analyses (*left*: AUC=.721±.066, p=.003; *right*: AUC=.738±.066, p=.002; Fig.2B; Table 4). Diagnostic performance was of comparable precision in the volumetric approach (*left*: AUC=.723±.066, p=.003; *right*: AUC=.781±.059, p<.001), and improved when both measures were combined (*left*: AUC=.731±.065, p=.002; *right*: AUC=.786±.059, p<.001).

Relapsing-remitting multiple sclerosis (RRMS)

In RRMS, a significant bilateral inward deformation of the hippocampal surface was observed (Fig.1C). Atrophic regions covered the anterior hippocampi in areas corresponding to the subfields CA1-3 and were more pronounced on the left side (*left*, p=0.001; *right*, p=0.002). Further significant clusters were noted towards the tail of the left hippocampus. On the right hippocampus, inward deformations also encompassed the whole medial surface and extended towards the tail in the subicular area.

We noted surface deformations of -0.22mm for the left hippocampus (F(1,58)=8.35, p=0.005) and -0.24mm for the right hippocampus (F(1,58)=6.34, p=0.015; Fig.1C). Patients with a stronger inward movement of the affected surface area generated fewer words on the word list generation test (r=.540, p=.010, n=18). Additionally, a stronger inward deformation was associated with a longer disease duration (r=-.583, p<.001, n=30) and higher load of T2-hyperintense lesions (r=-.457, p=.006, n=30). We observed no association with verbal learning (r=.035, p=.445, n=18), depression screening scores (r_s=.238, p=.103, n=30), or functional outcomes (EDSS; r_s=.165, p=.192, n=30).

Both hippocampi showed a significantly decreased volume (*left*: -12.1%, F(1,58)=19.9, p<0.001; *right*: -11.3%, F(1,58)=11.5, p=0.001). Deformations of the hippocampal surface significantly differentiated between patients with RRMS and controls (Fig.2C; Table 4). This diagnostic performance was better for the left (AUC=.723±.067, p=.003) than for the right hippocampus (AUC=.678±.071, p=.018) and slightly inferior to that of the volumetric estimates (*left*: AUC=.802±.057, p<.001; *right*: AUC=.724±.068, p=.003). The combination of shape and volume information achieved the best classification performance (*left*: AUC=.853±.048, p<.001, excellent; *right*: AUC=.781±.061, p<.001, fair to good).

Neuromyelitis optica spectrum disorder (NMOSD)

No shape differences were observed for the left (p=0.26) and right (p=0.53) hippocampus in NMOSD patients (Fig.1D). Mean displacement was -0.06mm for the left and -0.04mm for the right hippocampus, with no significant group difference (*left*: F(1,58)=0.56, p=0.46; *right*: F(1,58)=0.26, p=0.61; Fig.1D).

Volumetric analyses showed no hippocampal atrophy (*left*: F(1,58)=0.11, p=0.740; *right*: F(1,58)=0.09, p=0.771). Accordingly, the ROC classifier performed at chance level when testing surface deformations (*left*: AUC=.452±.076, p=.520; *right*: AUC=.479±.075, p=.779), volumes (*left*: AUC=.474±.076, p=.734; *right*: AUC=.502±.076, p=.976; Fig.2D; Table 4), and the combination of shape and volume information (*left*: AUC=.589±.074, p=.237; *right*: AUC=.533±.076, p=.657).

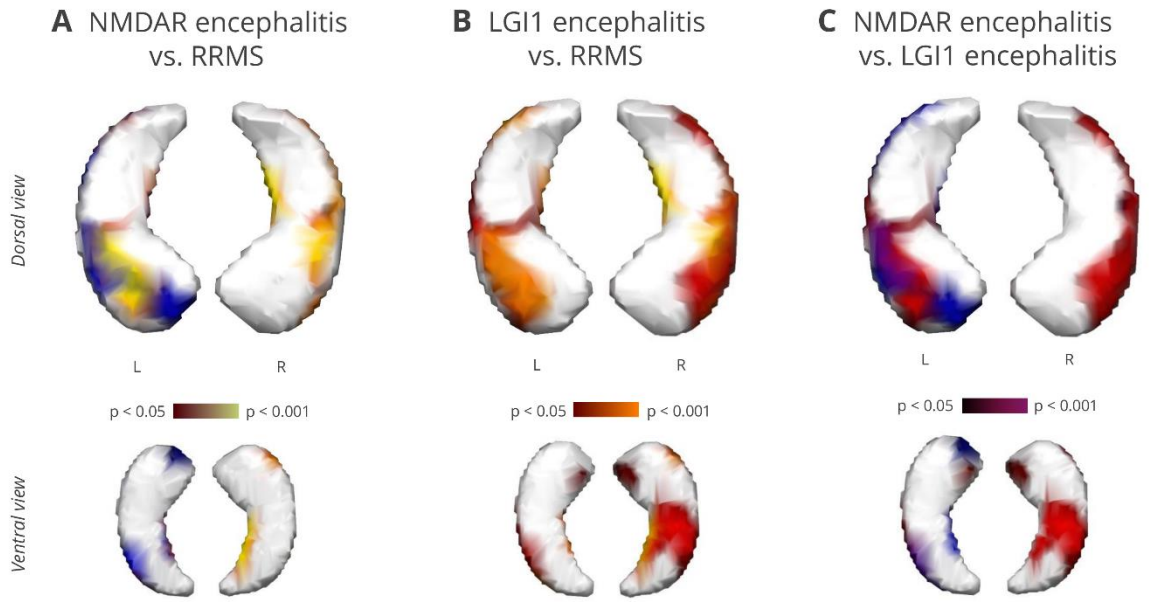

Figure 3. Pairwise overlaps of surface deformations in ventral (upper panel) and dorsal view (lower panel). (A) Multiple sclerosis (yellow) and NMDAR encephalitis (blue) overlapped strongly on the left hippocampus (Φ=.440; contingency coefficient). More than 70% of the affected vertices in multiple sclerosis were also affected in NMDAR encephalitis. (B) LGI1 encephalitis (red) and multiple sclerosis (yellow) overlapped with moderate contingency on the left (Φ=.386) and right (Φ=.260) hippocampus. Surface deformations overlap around 50% on both sides. (C) Overlap of NMDAR (blue) and LGI1 encephalitis (red) was stronger for the left (Φ=.268) than for the right hippocampus (Φ=.108). Around 50% of the surface inversions overlapped.

Overlap of surface deformations

In the next step, we quantified the surface deformation overlaps across the NMDAR encephalitis, LGI1 encephalitis and RRMS patient groups (Fig.3). Binarized coding of the surface area revealed significant overlaps in each of the pair-wise comparisons with varying contingencies (2-sided, exact significance).

NMDAR encephalitis vs. RRMS

Surface deformations on the *left hippocampus* affected 32.0% of the vertices in NMDAR encephalitis and 20.8% in the multiple sclerosis group. Lesion patterns in both disorders correlated strongly (Φ=.440, p<.0001): 72% of the surface vertices that were affected in multiple sclerosis were also affected in NMDAR encephalitis. Vice versa, 47% of the vertices showing inversion in NMDAR encephalitis overlapped with multiple sclerosis. On the *right hippocampus*, 26.5% of the surface vertices were significantly inverted in multiple sclerosis. Only 0.02% of the vertices were affected in NMDAR encephalitis when thresholded to a significance level of p<.05. Accordingly, the overlap was significant but with low contingency for the right side (Φ=.205, p<.0001; Fig.3A) and only 7% of the vertices affected in multiple sclerosis were also deformed in NMDAR encephalitis.

LGI1 encephalitis vs. RRMS

Left-sided deformations covered 27.6% of the surface vertices in LGI1 encephalitis. We observed a significant overlap with moderate contingency (Φ=.386, p<.0001): Out of the vertices affected in LGI1 encephalitis, 46% overlapped with multiple sclerosis. Vice versa, 62% of the inverted surface vertices in multiple sclerosis were also affected in LGI1 encephalitis (Fig.4). On the *right hippocampus*, LGI1 encephalitis affected 38.2% of the surface vertices. As observed in the previous comparison, the right-sided overlap was significant, with an albeit lower correlation (Φ=.260, p<.0001; Fig.3B). Furthermore, 41% of the inverted vertices in LGI1 encephalitis were also inverted in multiple sclerosis; and 59% vice versa.

NMDAR encephalitis vs. LGI1 encephalitis

In NMDAR and LGI1 encephalitis, affected areas overlapped significantly, but contingency was weaker than for the previous comparisons (*left:* Φ=.268, p<.0001; *right:* Φ=.108, p<.0001; Fig.3C). For the left hippocampus, 45% of the inverted vertices in NMDAR encephalitis overlapped with LGI1 encephalitis; and 52% vice versa. Overlaps on the right hippocampus were negligible due to the small affected area in NMDAR encephalitis.

Common deformation zone in NMDAR encephalitis, LGI1 encephalitis and RRMS

Regions that were affected across NMDAR encephalitis, LGI1 encephalitis and RRMS overlapped in a convergence zone on the left anterior hippocampus corresponding to the surface area of CA1 (Fig.4). Deformations in this overlap area correlated with cognitive performance, i.e. with verbal memory in NMDAR encephalitis (r=.342, p=.032, n=30) and verbal fluency in LGI1 encephalitis (r=.395, p=.031, n=23).

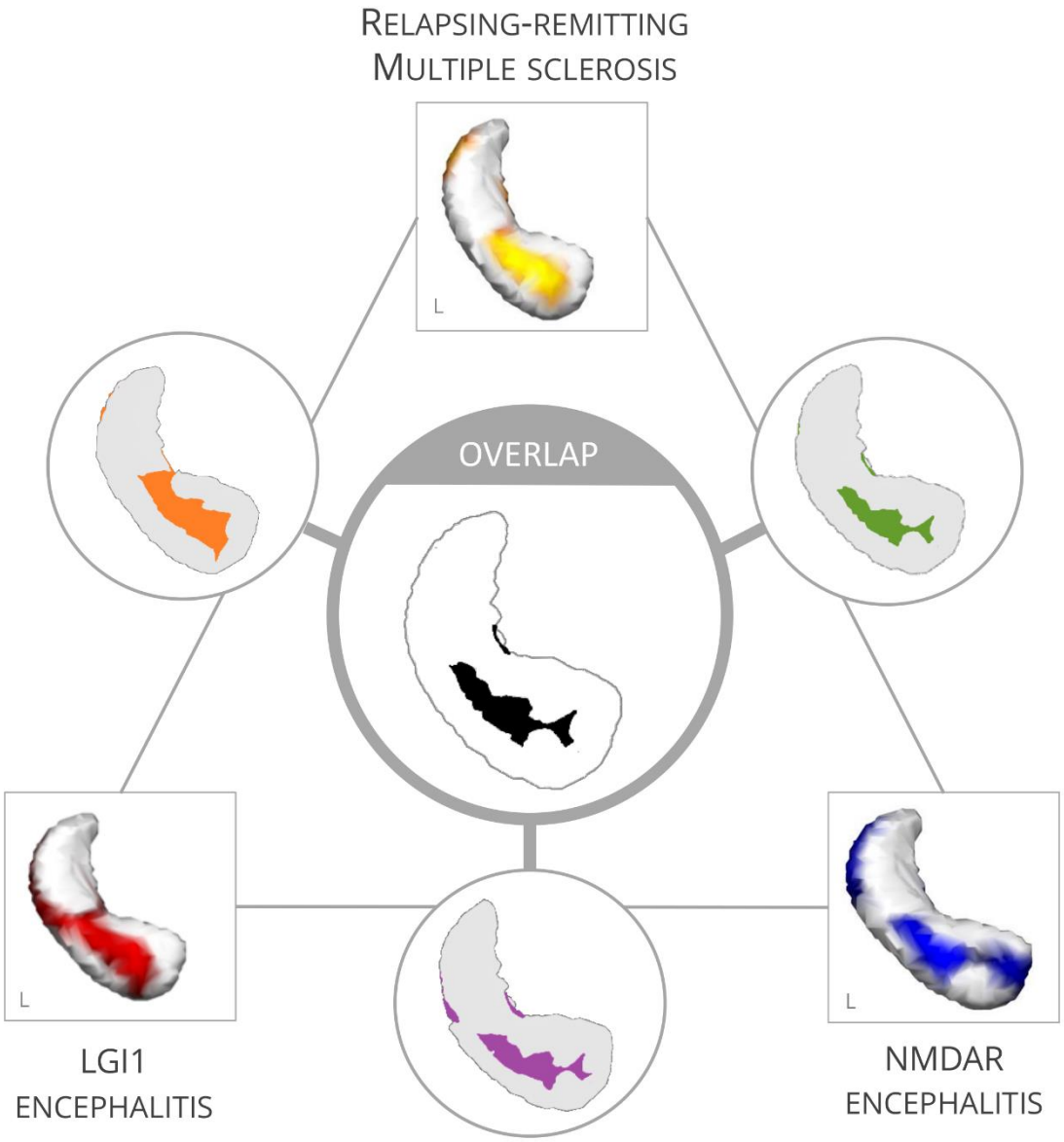

Figure 4. Overlap analyses reveal an area of the left anterior hippocampus that is affected across diseases and sensitive to cognitive alterations.

Discussion

In this study, we performed transdiagnostic hippocampal shape analyses in four neuroimmunological diseases using a unified imaging protocol. Our analysis revealed a characteristic pattern of bilateral inward deformations of the hippocampal surface in multiple sclerosis, NMDAR encephalitis and LGI1 encephalitis, but not in NMOSD. Surface deformations discriminated significantly between patients of these three disorders and controls. Higher inward deformation of the hippocampal surface predicted decreased semantic fluency in multiple sclerosis and impaired verbal memory performance in both NMDAR and LGI1 encephalitis. Analysis of deformation overlaps revealed a convergence zone in the left anterior hippocampus that corresponds to the CA1 subfield of the hippocampus and that appears to be particularly vulnerable to neuroinflammatory processes.

In NMDAR encephalitis, the most frequent subtype of autoimmune encephalitis,[10] deformations were mainly observed in surface areas that correspond to the CA1-3 subfields and subiculum. Given that an inversion of the surface likely reflects volume loss of underlying tissue, it is not surprising that the location of shape deformations resembles those subfields that also showed volume loss in volumetric analyses.[74,92] Indeed, NMDAR patients had lower volumes of the subiculum as well as CA1 and CA2-3 areas. This is in line with the finding that the hippocampus, specifically CA1, contains the highest density of NMDARs in the brain.[39] Furthermore, recent studies observed functional decoupling of the hippocampus from major brain networks such as the default mode network, which was related to impaired memory performance in NMDAR encephalitis patients.[101,217] The pathogenic effects of antibodies in NMDAR encephalitis are thus not only reflected in focal hippocampal damage, but also result in functional network alterations.

LGI1 encephalitis showed the most extensive shape deformations in this comparative study, covering up to 32% of the hippocampal surface area. Previous studies have shown that almost all LGI1 encephalitis patients develop hippocampal atrophy that arises from volume loss in several subfields, including the CA1, CA2-3 areas, the dentate gyrus and subiculum.[200,201] The absence of further cortical grey matter loss suggests that long-term structural damage is localized to the hippocampus,[200,201] while functional connectivity alterations can involve brain-wide networks.[282] Shape deformations in our study were located in the surface areas approximately corresponding to the cornu ammonis and subicular subfields. The inward movement of the bilateral surfaces correlated with impaired verbal learning and fluency, suggesting that shape alterations may represent a complementary explanation of cognitive deficits in LGI1 encephalitis.

For MS patients, our analyses show a bilateral inward deformation of the hippocampal surface associated with decreased word fluency. Beyond conventional MRI measures such as white matter lesion count or volume that do not sufficiently explain cognitive deficits, there is increasing evidence for hippocampal damage in MS.[283,284] Indeed, hippocampal demyelination and neuronal loss are common

and can affect all hippocampal subfields.[285,286] MRI studies observed bilateral volume loss as well as impaired microstructural integrity of the hippocampus.[273,287–289] Additionally, recent studies showed alterations of structural and functional connectivity of the hippocampus, as well as aberrant activation during memory encoding.[285,290,291] Local pathology due to inflammatory and degenerative changes may thus interact with damage to connected white matter tracts and cortical regions[285,290] – eventually inducing widespread deficits that also affect processing speed and executive function. Hippocampal shape changes occurred bilaterally in our study and were pronounced on the left side. This cluster on the left anterior hippocampus approximately identifies as CA1 subfield but also extends to the areas of the subfields CA2-3. Importantly, previous volumetric subregion analyses revealed a similar pattern: Progressive CA1 atrophy was related to slowed processing speed, verbal and visuospatial memory deficits.[273,288,292] This atrophy expanded to other subfields with progression to secondary progressive multiple sclerosis.[273] In addition, smaller CA2-3 volumes were observed in multiple sclerosis patients with depression.[288] Together, these results point to a critical involvement of distinct hippocampal subregions in the pathophysiology of cognitive and affective symptoms in MS.

In contrast, we observed no shape deformations of the hippocampus in NMOSD patients. This result is in line with previous observations of normal hippocampal volumes and intact microstructural integrity in NMOSD.[275,293] Other studies, however, found decreased hippocampal volumes in a cognitively impaired sample of Chinese patients,[294] as well as in NMOSD patients with depression and anxiety symptoms.[295] Whether this observation is limited to NMOSD patients with pronounced cognitive impairment or affective symptoms, or reflects differences in disease phenotypes related to ethnicity, remains an open question. Similarly, evidence for the contribution of damage to further subcortical and cortical regions to cognitive deficits in NMOSD remains inconsistent. While some studies found no cortical lesions,[274] no cortical demyelination[296] or subcortical volume loss,[275] others observed decreased thalamic volumes.[297] In our study, we focused on AQP4 antibody-positive NMOSD patients and the apparent sparing of the hippocampus may be related to the distribution of AQP4 in periventricular and hypothalamic areas.[298] It thus remains an important open question whether hippocampal damage patterns are different in AQP4-negative NMOSD patients, and how they differ from NMOSD patients with antibodies against the myelin oligodendrocyte glycoprotein (MOG).

Shape deformations shared by NMDAR encephalitis, LGI1 encephalitis and multiple sclerosis converged on the anterolateral surface of the hippocampus, a surface area mainly covering the CA1 subfield. CA1 relays input from the CA3-DG circuitry and entorhinal cortex downstream to the subicular output areas and back to the entorhinal cortex, i.e. the hippocampal-neocortical interfaces. CA1 neurons are critically involved in memory formation and consolidation and dysfunction of these neurons leads to severe memory impairment, including input integration, mismatch and novelty detection, as well as intermediate and long-term autobiographical memory retrieval.[48,299] A selective vulnerability of the CA1 subfield has not only been described in limbic encephalitis[38] and MS,[273] but also in other

neurological disorders such as transient global amnesia, epilepsy and ischemia.[38,300] Conceivable mechanisms for CA1 vulnerability include its high inherent degree of plasticity, local differences in antioxidant enzymes as well as calcium- and glutamate-related excitotoxicity of CA1 neurons affecting the metabolic homeostasis.[48] Interestingly, the transdiagnostic pattern of anterolateral hippocampal deformations observed in our study is also a prominent finding in Alzheimer's disease.[278,301] Mainly left-sided CA1 shape changes furthermore predicted dementia onset in healthy elderly subjects and patients with mild cognitive impairment (MCI).[277,302] In face of the overlapping nature of cognitive symptoms across neurological diseases, it has been suggested that the same ensemble of disrupted brain regions causes a clinical phenotype to arise regardless of conventional diagnostic demarcations.[276] In line with this transdiagnostic approach, our data support the notion that damage to CA1 and its surface area is one of the main contributors to deficits of memory formation and consolidation in neuroimmunological disorders, as well as in a wide range of other neuropsychiatric diseases.

Shape changes in our samples additionally extended to surface areas that can be approximately identified as belonging to hippocampal subfields CA2 and CA3. The CA3 subregion is involved in associative memory and pattern completion,[303] a computational process in which entire memory representations can be recalled in response to the presentation of one of its parts. Together with the dentate gyrus, CA3 also plays a role in creating non-overlapping memory representations, a process referred to as pattern separation.[186] CA3 volume loss is observed both in autoimmune encephalitides[92,200,201] and MS, particularly when depressive symptoms are present.[288] Besides the autoimmune pathology, glucocorticoid receptor activation in response to disease-related behavioural stress may additionally contribute to CA2-3[304] and CA1[48] vulnerability.

In contrast to volumetric approaches, surface analyses provide detailed information about the location of pathological changes of the hippocampus. These analyses have been shown to discriminate between patients with neuropsychiatric disorders and controls and to reliably track disease progression. For example, morphological changes of the hippocampal surface successfully differentiated patients with MCI and patients with Alzheimer's disease (AD) from healthy controls,[278,301] with superior performance compared to volumetric measures.[278] In schizophrenia, left-right asymmetry of hippocampal shape was observed in patients even in the absence of volume loss.[305,306] In line with this, we show that the combination of shape and volume information yields a better classification performance than any of the measure alone. Together with previous findings in neuropsychiatric diseases, our results suggest that shape may be a sensitive marker of – even early – damage.

Although shape analyses have made substantial contributions, some limitations need to be considered. The nature of shape analyses limits the findings of this study to the outer surface of the hippocampus. Considering the intricate hippocampal anatomy, this technique allows no assumptions about inner structures, e.g. the dentate gyrus. However, results from our and previous studies suggest that a

combination of different approaches including shape, volumetric and microstructural integrity analyses provides more detailed pathophysiological insights and yields an improved discriminatory power. In addition, despite assessing the same underlying construct and using an equivalent multiple-trial list-learning approach, minor differences in test versions used for verbal memory need to be taken into account. Future longitudinal studies may explore whether the deformations are transient or chronic, and to which extend they might serve as predictors for long-term functional outcomes.

Conclusion

In conclusion, we show that hippocampal shape deformations are common and highly overlapping across neuroimmunological diseases and contribute to cognitive symptoms. Our comparative approach reveals a convergence zone on the left anterolateral surface, mainly corresponding to subfield CA1 that appears to be most vulnerable to neuroinflammation - despite the distinct pathomechanisms in multiple sclerosis and autoimmune encephalitides. In this way, it improves the understanding of cognition networks in health and disease and stimulates further basic research into the mechanisms of increased susceptibility to autoimmunity of this anatomical region. This morphological view provides unique spatial information about the pattern of hippocampal lesions, transcending traditional global measures of hippocampal volume.

Supplementary material

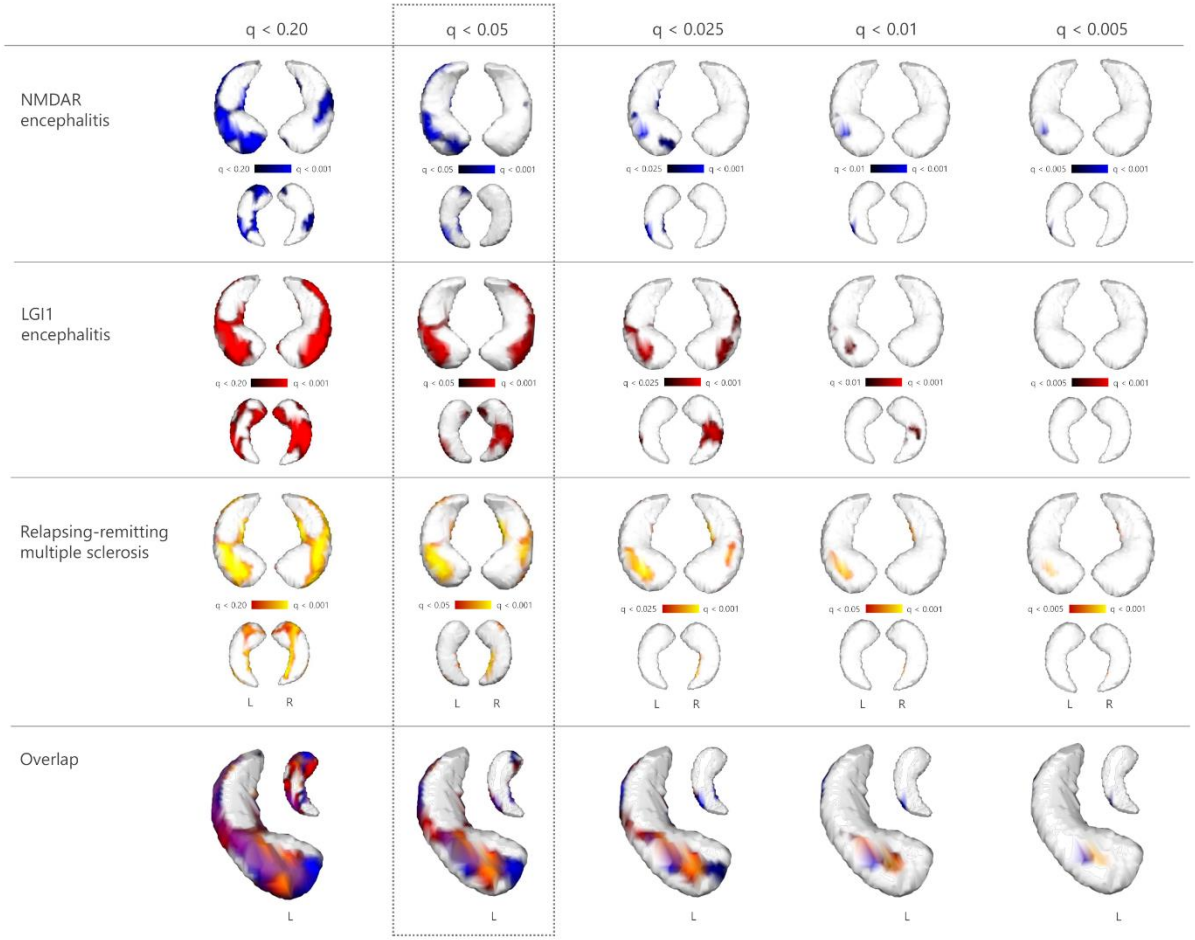

Fig. S1. Statistically significant shape deformations at different FDR-thresholds. For reference, vertex-wise t-maps are presented with FDR-thresholds at q<.20, q<.05, q<.025, q<.01, and q<.005. Between-group comparisons were performed using FSL Randomise with threshold-free cluster enhancement (TFCE).

Implications & future directions

The following section will discuss the aims, results, and implications of this work in the order of their appearance in the introduction. This section will synthesise the insights of this thesis and outline avenues for future research.

Cognitive profiles of NMDAR and LGI1 encephalitis

The findings of *publications II & V* of this thesis provide comprehensive descriptions of the neuropsychological profiles of patients with NMDAR and LGI1 encephalitis after the acute hospital stay. *Publication II* identifies deficits in verbal and visual learning and recall as the hallmark cognitive sequelae after LGI1 encephalitis. Additionally, many patients show impaired working memory and verbal fluency, together with increased error susceptibility on test of attention and executive function. *Publication V* follows a longitudinal approach to cognitive dysfunction several years after NMDA receptor encephalitis. Despite improvement in neuropsychological test performance and substantial physical recovery, about 2/3 of the patients showed persistent deficits in at least one domain. Deficits in executive functions, working and episodic memory frequently occurred together.

These studies have important implications for the post-acute care of patients with autoimmune encephalitis and are the to-date most comprehensive neuropsychological descriptions of this rare disease. However, several limitations that arise from working with clinical samples need to be considered. Disease courses in autoimmune encephalitis differ from patient to patient, e.g. with respect to diagnostic procedures, treatment regimen, or delay of diagnosis. We cannot fully exclude that some patients may have undergone neuropsychological assessment in clinical or rehabilitation settings before their inclusion in our study sample. We therefore controlled the impact of practice effects in neuropsychological follow-up tests by using parallel versions or randomization of trials wherever applicable.

Lastly, despite all advances and stories of recovery, autoimmune encephalitis is still a severe disease that is potentially fatal or causes severe disability if no treatment response can be achieved. As discussed recently,[307] severe symptoms can complicate or make the neuropsychological assessment during the acute phase impossible – thereby shifting the opportunity for structured, quantitative testing to the post-acute phase. There are, nonetheless, several case studies which describe cognition in severely impaired patients using individually adapted neuropsychological protocols.[269–271] Taken

together, the results of *publications II & V* highlight the importance of fast treatment initiation to achieve a better cognitive outcome.

During the initial inflammatory phase of autoimmune encephalitis, cognitive alterations can in some cases be less visible to medical professionals involved in the acute care. If the first presenting symptom is a seizure or hallucination, co-existing working memory alterations may be overlooked in face of more prominent symptoms that demand immediate medical attention. Other circumstances, such as mechanical ventilation in the intensive care unit, downright exclude any possibility of cognitive testing during the initial inflammatory phase. To date, not all clinical centres to which patients with probable autoimmune encephalitis are admitted include a structured neuropsychological assessment of cognitive complaints in their standard diagnostic protocol. Here, advances made in other diseases, such as multiple sclerosis, could inform the management of cognitive deficits in autoimmune encephalitis as well. Both fields face similar practical challenges: self-reported complaints do not always reflect objective deficits, and clinician-rated dysfunction has limited precision compared to standardised neuropsychological assessments.[308] At the same time, cognitive impairment has a detrimental effect on day-to-day independence and occupational life in both patient groups, with possible consequences for the patients' quality of life, social interactions, or financial independence. Options for the treatment and prevention of cognitive impairment in MS currently include cognitive rehabilitation, cognitive training, metacognitive approaches, and additional interventions like cognitive behavioural therapy, counselling, or exercise-based trainings.[308,309] These approaches may be beneficial for patients with autoimmune encephalitis as well. Future studies will moreover investigate accompanying psychosocial outcomes, quality of life, and subjective cognitive outcomes to fully understand the sequelae of autoimmune encephalitis.

In an attempt to evaluate the clinical utility of neuroimaging for autoimmune encephalitis, *publication I* synthesises insights from previous studies to provide specific imaging profiles for common cell-surface and synaptic antigens. This approach follows the general endeavour to channel the knowledge gained from case descriptions to larger cohort studies into the description of distinctive syndromes. For instance, it was previously common to test a patient for antibodies against the voltage-gated potassium channel (VGKC). With new insights into the disease mechanisms and specialised antibody tests, we now know that the target is not the VGKC itself. Instead, antibodies bind to at least two specific proteins located on the channel. The LGI1[4] and CASPR2[110] proteins have already been identified as such antigens and are now known to give rise to different clinical presentations. Together with the limited clinical use of double negative test results (i.e. tests which turn out positive for non-pathogenic VGKC antibodies, but negative for either LGI1 and CASPR2 antibodies), this evidence has led leading clinical experts to appeal for testing exclusively for LGI1 and CASPR2 antibodies during diagnosis.[199,310] In the research setting, unspecific VKGC positive cases may still help to identify new antibody targets in the future. *Publications II & III* of this thesis investigate the structural and functional imaging correlates

of patients with LGI1-positive encephalitis. In light of differences in disease course and clinical presentation, future research will shed light on the characteristics of cognitive impairment in CASPR2-positive encephalitis and provide insights into differences and commonalities of its imaging correlates.

Advances in treatment options and long-term outcomes

Publication IV investigates therapeutic apheresis as a treatment option in autoimmune encephalitis. The observational case control study evaluated efficacy and safety of two apheresis methods – plasma exchange and immunoadsorption. Both interventions significantly reduced the disease severity as assessed using the modified Rankin Score. The best treatment response was observed for patients with neuronal surface antibodies (i.e. NMDA receptor, LGI1, CASPR2, and mGluR5), while patients with intracellular antigens (anti-Hu) showed no improvement. These findings corroborate the hypothesis of better treatment response for autoimmune encephalitis with cell surface antibodies based on their directly pathogenic features.

A fast clinical improvement is highly desirable as it is closely tied to long-term outcomes. In light of heterogeneous disease courses, it remains a challenge to predict a patient's long-term outcome very early in the disease. A recent systematic review of more than 40 studies followed a qualitative approach to determine early clinical and paraclinical factors related to patient outcomes.[311] A poor prognosis following NMDA receptor encephalitis was frequently observed in patients who received no or delayed immunotherapy, showed alterations of consciousness, or required admission to the intensive care unit. Another study reviewed 382 patient records to build a 5-point score predictive of functional status 1 year after diagnosis.[27] In addition to the (1) need for ICU admission and a (2) treatment delay >4 weeks, the score also includes (3) abnormal MRI, (4) an elevated white blood cell count in the CSF (>20 cells/µL), and (5) a lack of clinical improvement within 4 weeks as predictors of poor functional status (mRS≥3). The outcome measure, the modified Rankin Scale, was initially developed to assess physical disability after stroke.[247] It therefore has limited sensitivity for the effects of cognitive impairment. *Publications II* and *V* identified predictors specifically for cognitive outcomes in LGI1 and NMDA receptor encephalitis, including delayed treatment, longer hospitalization, and need for second-line therapy.

Besides cognitive alterations, emotional and behavioural changes frequently persist beyond the acute phase of autoimmune encephalitis. A recent systematic review identified behavioural alterations, psychosis, mood, catatonia, and sleep problems as the most common psychiatric features of acute

NMDA receptor encephalitis.[312] To date, little is known about how these psychopathological features develop beyond the acute phase and how they interact with recovery from cognitive dysfunction. It has recently been proposed that the autoimmune response may likewise influence inhibitory and excitatory neuronal networks within the amygdala.[313] As part of the limbic system, the amygdala is highly interconnected with the hippocampal formation. The view of amygdalar function was long dominated by its role in fear processing. Nonetheless, accumulating evidence establishes a wider array of associated functions, including social cognition, emotion recognition, controlling positive and negative affects in response to external stimuli, reward processing, or adaptive, flexible behaviour towards stress.[314] Aberrant neuronal communication of the amygdala may therefore account for at least a part of the affective symptoms in patients with autoimmune encephalitis. Anxiety and depressive symptoms are common neuropsychiatric presentations during the acute phase.[221,312] These symptoms can persist during recovery and demand therapeutic attention in face of compromised well-being and potential impact on cognitive performance, which is substantial for regaining day-to-day independence after acute treatment, and returning to work or school. In this line of research, future studies will therefore elucidate the mechanisms of aberrant excitability in amygdalar circuits, their neuroimaging correlates, as well as their interactions with cognitive performance.

The utility of advanced MR postprocessing

Our systematic review of imaging findings (*publication I)* analysed MRI findings from ~800 patients with NMDA receptor encephalitis. Only 23-50% of the patients had abnormalities on their clinical MRI scans during the early acute stage, and if they occurred, they were mostly discrete and non-specific. Nevertheless, advanced postprocessing of MRI scans revealed pathological features after the acute illness. These include the hippocampal shape alterations and reduced volumes observed in *publication VI*, volume loss in hippocampal subfields and microstructural damage,[92] white matter changes seen on diffusion imaging,[101,267] and aberrant connectivity of functional networks.[101,217]

Publications II and *III* applied these advanced postprocessing techniques to LGI1 encephalitis. As summarized in *publication I*, MRI changes in the medial temporal lobe are much more common during the acute illness here and contribute to the clinical picture of limbic encephalitis. Overt hippocampal atrophy is a frequent finding on follow-up clinical MRI scans. Acquiring MRI sequences which are not typically included in standard clinical imaging protocols, such as diffusion or resting-state sequences, and the computational postprocessing thereof have several benefits:

— *Observer independence:* For instance, techniques like volumetry with highly automated segmentation streams provide reliable estimates of hippocampal size.[172,315] These are independent of the level of neuroradiological expertise in rating grades of hippocampal atrophy or, as in the case of manual labelling of subregion boundaries, less susceptible to interobserver variability.
— *Quantifiable values:* In addition to the qualitative visual assessment, postprocessing allows the collection of quantifiable values which facilitate the precise tracking of pathology progression over time.
— *Hidden correlates:* As the amount of information obtained from visual inspection is limited, postprocessing provides new insights into the hidden disease correlates that are not visually assessable, e.g. changes in correlated activation patterns in functional brain networks.
— *Association with cognition:* Imaging variables can be set in relation to scores from standardised cognitive testing in a meaningful and biologically plausible way. The modelling of cognitive covariates can thus be used to understand the pathophysiology of cognitive dysfunction.

The use of volumetry and resting-state MRI in the scope of this thesis has revealed several mechanisms of memory impairment in LGI1 encephalitis. *Publication II* focused on structural correlates and described decreased microstructural integrity and volume reductions in major subfields, including CA2/3 and CA4/dentate gyrus. These imaging markers correlated with performance on classic neuropsychological paradigms, such as word-list learning or retrieving a complex geometrical figure from memory. In addition to this first report of standardised neuropsychological assessment in a relatively large cohort of LGI1 encephalitis patients, subsequent studies have started to use experimental paradigms. For instance, a recent study[316] investigated behavioural pattern separation in a sample of LGI1 encephalitis patients that was partially overlapping with that reported in *publication II* and *III*. In this study, a group of 15 patients performed the mnemonic similarity task. This computer-based task requires participants to successfully identify lure images – i.e. similar images that were modified from their originals – among previously presented (old) and completely new images. The marked pattern separation deficits were strongly related to the dentate gyrus volume loss which was observed using automated volumetry in this group of patients with LGI1 encephalitis.

Another recent study investigated medial temporal lobe pathology in patients with LGI1 encephalitis at a field strength of 7 Tesla.[201] This higher field strength allows the acquisition of MR images at submillimeter resolution. Using a manual segmentation protocol, Miller et al. found volume reductions across several subfields in the absence of, as described in *publication II*, further cortical grey matter loss. Interestingly, the encephalitis patients in this study also performed an autobiographical interview. While patients with LGI1 encephalitis were able to recall personal semantics about postmorbid events, they

showed a severe amnesia during the recollection of episodic event details. Moreover, a case series observed reduced dream frequency and a less episodic-like dream quality in four patients with selective bilateral hippocampal damage due to LGI1 encephalitis.[317] Given the evidence for localised atrophy in LGI1 encephalitis, these findings corroborate the role of the hippocampus in the formation and retrieval of rich, detailed, personal episodes of one's own experiences. *Publication III* showed that functional alterations can also occur outside the hippocampal formation and contribute to memory impairment through aberrant functional interactions of distributed brain areas. These changes in network connectivity may have a compensatory or disruptive role, which require further investigation in future longitudinal designs.

Mechanisms of hippocampal vulnerability and neuroplasticity

Publications II and *VI* described hippocampal volume loss, decreased microstructural integrity, and surface deformations as pathological substrates of the cognitive dysfunction in LGI1 encephalitis. Around 66-89% of the patients experience temporal lobe seizures during the acute phase of LGI1 encephalitis.[318] Recent in-vitro investigations observed that an injection of patient CSF containing LGI1 antibodies into the hippocampus of mice increased the probability of CA1-CA3 glutamate release from the synapse, resulting in epileptiform activity in CA1 pyramidal neurons.[319] Another study suggests that apoptosis of hippocampal neurons and reduced calcium currents contribute to the neurotoxicity of LGI1 antibodies.[320] Seizure-related activity can thus contribute to cornu ammonis damage. As reported in *publication II*, 50% of the patients in our sample showed hippocampal sclerosis around 2 years after the acute phase. Hippocampal sclerosis is a pathological finding common to classic temporal lobe epilepsy and originates from gliosis and neuronal cell loss in the hippocampus. On MRI scans, signs of hippocampal sclerosis are volume reduction, a disturbed internal architecture of the hippocampal formation, and high signal intensity on T2-weighted images.[321] There is an ongoing debate whether it is a consequence of ongoing seizures, the cause of new epileptic activity, or both.[322] In the case of LGI1 encephalitis, the development of hippocampal sclerosis during the course of the disease is very likely contributing to chronic memory impairment.

Neuroplasticity is generally understood as the potential of the brain to dynamically reorganize itself.[323] Following damage, structural or functional reshaping can occur at short-term or long-term level and support clinical recovery. While the adaptive reorganization of hippocampal structure and function is crucial for memory processing in the healthy brain, its high degree of plasticity may also come at a cost in face of disease. The hippocampus is markedly vulnerable to the pathological influences that occur in the context of various neurological diseases.[48]

It is currently not well characterised how the correlates of hippocampal damage in LGI1 encephalitis develop longitudinally. Progressive or chronic volume reductions would point to an atrophic process that may interact with age-related changes in this older patient cohort. The same question applies to NMDA receptor encephalitis. *Publication VI* showed that hippocampal surface deformations, in addition to the classic volume measures, are a macroscopic marker of cognitive impairment. *Publication V* employs such a longitudinal design for cognitive variables. At a median follow-up of 4.3 years after symptom onset, 55% of the patients still experienced verbal episodic memory dysfunction. Despite a significant improvement in individual test scores since the first study visit, their scores were still significantly lower than those of healthy control participants. Recovery following NMDA receptor encephalitis seems to follow highly individual trajectories. Delayed routes to diagnosis and individually adapted treatment regimens are only two of the factors that can vary among patients. Future neuroimaging studies should therefore track to what extent the recovery of cognitive function described in this work is reflected in macroscopic changes of, for instance, gains in hippocampal volume or reshaping of functional networks. If the NMDA receptor dysfunction is indeed reversible,[32] this could potentially be reflected in macroscopically observable changes over time. Candidate mechanisms of neuroplasticity on the microscopic level have been described elsewhere and include the activity-dependent synaptic mechanisms, such as the NMDA receptor-mediated long-term potentiation, remyelination of white matter damage, or dentate gyrus neurogenesis and re-modelling of neural circuits.[323]

Taken together, the findings of *publications II* and *VI* corroborate the view that hippocampal subfields have a dissociable vulnerability to disease. Previous research emphasized that lesions which are initially considered 'selective' to one subfield may over time deteriorate the function of surrounding areas.[e.g.43] A conceivable mechanism is that upstream lesions propagate defects to areas further down the intricate hippocampal circuitry.

A network perspective on brain damage in autoimmune encephalitis

Complex cognitive processes, such as those involved in the processing of memory, are based on the continuous interaction between spatially distributed brain areas.[324] A macroscopic perspective on this integrative communication has evolved from methodological advances in functional connectivity MRI. The analysis of spontaneous low-frequency BOLD oscillations (~0.01-0.1Hz)[324] in resting-state brain scans is of particular interest in the clinical context. From a practical perspective, some patient populations with acute symptoms may have motor or sensory impairments which make task-based functional MRI difficult. This can potentially lead to a sampling bias when studies only test the least

affected participants of a patient group.[325] In patients with marked cognitive symptoms, performing an fMRI scan at rest makes minimal demands, reduces discomfort for the patient, and thus enhances compliance during the scan. From a theoretical perspective, resting-state networks of functionally linked brain areas are consistently identified across studies and their alterations have been linked to clinical and cognitive symptoms in many different neurological and neuropsychiatric diseases. When local information processing is interrupted, e.g. through a lesion in a critical brain area, the aberrant activation can influence the function of anatomically separate brain areas through functional network interactions. Within the reciprocal networks of cortical and subcortical regions, the hippocampus is one of the major network hubs and preferentially targeted by the pathological processes seen in autoimmune encephalitis.

Publication III investigated how functional networks adapt to the isolated hippocampal volume loss which was observed in patients with LGI1 encephalitis in *publication II*. Here, one mechanism of functional plasticity is increased within-network connectivity, as seen in the default-mode network. The recruitment of additional brain areas to circumscribed networks, such as the co-activation of the inferior temporal lobe to the default-mode network, was associated with better memory performance and points to a potential compensatory mechanism. In fact, a study in multiple sclerosis found increased activation of parahippocampal and anterior cingulate areas during an episodic memory task in patients who were cognitively preserved.[291] In patients with progressive MS, reduced activation in anterior default-mode network areas was related to impaired performance on a word-list learning test and the paced auditory serial addition test (PASAT).[326] As a consequence, it has been proposed that the initially small structural damage gives rise to finite mechanisms of functional reorganization through enhanced activation and synchronization of brain areas and networks.[215] While these network adaptations may initially support an adequate cognitive performance, their compensatory power is thought to expire over time as the structural damage accumulates.

In contrast, co-activation of the insula, a part of the salience network, to default-mode areas was related to worse performance. At this point, it has not yet been conclusively clarified whether the latter observation is a disruptive mechanism or represents an exhausted compensatory mechanism after the acute disease when memory deficits have manifested. To this extent, the cross-sectional design of the study allows limited conclusions. Future longitudinal study designs will reveal whether the functional network alterations are persistent or temporary, and how they relate to memory impairment several years after the acute disease.

Concluding remarks

The findings in this thesis add to the expanding research on the long-term sequelae of autoimmune encephalitis. Apart from contributing to the diagnostic process during the acute phase, magnetic resonance imaging can be a useful tool to describe post-acute structural and functional connectivity changes. In both LGI1 and NMDA receptor encephalitis, hippocampal vulnerability plays a crucial role in the emergence of long-term cognitive symptoms. Here, focal and quantifiable hippocampal damage not only relates to persistent memory impairment, but can likewise induce more widespread functional network changes. Autoimmune encephalitis thus also provides an opportunity to study the mechanisms of brain plasticity in patients with hippocampal damage. An increased understanding of the trajectories of recovery may be beneficial to define relevant imaging markers, inform the long-term prognosis in these patients, and ultimately guide clinical decision making in the acute and post-acute care.

Abbreviations

Ab	*antibody*
aCC	*anterior cingulate cortex*
AD	*axial diffusivity*
AMPA	*α-amino-3-hydroxy-5-methyl-4-isoxazolepropionic acid (receptor)*
AQP4	*aquaporin-4*
BOLD	*blood oxygen level dependent*
CA	*cornu ammonis*
CASPR2	*contactin-associated protein-like 2*
CI	*confidence interval*
CNS	*central nervous system*
CSF	*cerebrospinal fluid*
CT	*computed tomography*
DG	*dentate gyrus*
DMN	*default mode network*
DOF	*degree of freedom*
DPPX	*dipeptidyl-peptidase-like protein 6*
DTI	*diffusion tensor imaging*
DWI	*diffusion-weighted imaging*
EEG	*electroencephalography*
EPI	*echo-planar imaging*
FA	*fractional anisotropy*
FBDS	*faciobrachial dystonic seizure*
FDG-PET	*fluorodeoxyglucose positron emission tomography*
FFP	*fresh frozen plasma*
FLAIR	*fluid-attenuated inversion recovery*
FPN	*frontoparietal network*
$GABA_A$	*γ-aminobutyric acid A (receptor)*
$GABA_B$	*γ-aminobutyric acid B (receptor)*
GAD	*glutamic acid decarboxylase*
GLM	*general linear model*
GlyR	*glycine receptor*

HA	*human albumin*
IA	*immunoadsorption*
IC	*independent component*
ICA	*independent component analysis*
ICU	*intensive care unit*
123I-IMP	*N-isopropyl-(123I)-p-iodoamphetamine*
IQR	*interquartile range*
IV	*intravenous*
IVIG	*intravenous immunoglobulins*
LGI1	*leucine-rich glioma-inactivated 1 protein*
MD	*mean diffusivity*
mGlu5	*metabotropic glutamate receptor 5*
MNI152	*Montreal Neurosciences Institute-152*
MOG	*myelin oligodendrocyte glycoprotein*
mPFC	*medial prefrontal cortex*
MPRAGE	*magnetization-prepared rapid gradient-echo*
MRI	*magnetic resonance imaging*
mRS	*modified Rankin scale*
MTL	*medial temporal lobe*
NMDAR	*N-methyl d-aspartate receptor*
NMOSD	*neuromyelitis optica spectrum disorder*
pCC	*posterior cingulate cortex*
PE	*plasma exchange*
PERM	*progressive encephalomyelitis, rigidity and myoclonus*
PET	*positron emission tomography*
RAVLT	*Rey Auditory Verbal Learning Test*
RD	*radial diffusivity*
ROCF	*Rey-Osterrieth Complex Figure Test*
RSN	*resting-state network*
SAE	*subcortical arteriosclerotic encephalopathy*
SD	*standard deviation*
SE	*standard error of the mean*
SN	*salience network*
SPECT	*single photon emission tomography*
TAP	*Testbatterie zur Aufmerksamkeitsprüfung*

TBSS	*tract-based spatial statistics*
TE	*echo time*
TFCE	*threshold-free cluster enhancement*
TR	*repetition time*
VBM	*voxel-based morphometry*
VGKC	*voltage-gated potassium channel*

Glossary of clinical & immunological terms

Antigen	The target structure of an antibody, e.g. a neuronal receptor or secreted protein
Autoimmune encephalitis	Encephalitis caused by autoimmune processes, including the production of autoantibodies and cytotoxic t-cell response, resulting in inflammation of the brain parenchyma and corresponding neurological and psychiatric symptoms
Cell-based assays	A technique to study cellular mechanisms in living cells
Cross-linking	In this context: process of binding of an antibody to a cell surface receptor
CSF pleiocytosis	An increased white blood cell count in the cerebrospinal fluid, indicative of inflammatory processes within the CNS
Cyclophosphamide	An immunosuppressive medication for autoimmune diseases, also used during chemotherapy
Epitope	The specific part of the antigen that is recognised by the antibody and to which the antibody binds
Fresh frozen plasma	A plasma product generated from donor blood, administered as replacement during plasma exchange
Gliosis	Unspecific neuropathological response of glial cells to damage to the central nervous system
Human albumin	A serum protein in the human blood, administered as replacement solution during plasma exchange
Immunohistochemistry	A technique to visualize antibodies in a tissue sample
IVIG	Immunoglobulin therapy in which an immunotherapeutic blood plasma product is administered to suppress pathogenic immune responses
Limbic encephalitis	A clinical syndrome which can occur in some patients with autoimmune encephalitis. Inflammation of limbic brain structures leads to a characteristic presentation of marked memory deficits, disorientation, psychiatric features, and temporal lobe seizures.
Oligoclonal bands	Bands of plasma call proteins detected in the CSF, indicative of inflammatory processes within the CNS
Paraneoplastic syndrome	A clinical syndrome in which the presence of a tumour triggers autoantibody production and the associated brain inflammation, and thus causes the neurological symptoms of encephalitis
Prodrome	Early, frequently unspecific signs of a disease that emerge before the onset of the distinctive symptoms that lead to a diagnosis
Receptor internalisation	A process of endocytosis in which the receptor moves from the cell surface to the inside of the cell
Rituximab	A monoclonal antibody therapy directed against the protein CD20 on the surface of B cells

Acknowledgements

I would like to express my sincere gratitude to my first supervisor, *Prof. Dr. Carsten Finke*, for sharing the curiosity about memory and the brain throughout the years. I appreciate your invaluable contribution of time and ideas, and your trust in my work and research ideas. I sincerely enjoyed discussing results and crafting the research articles bringing our findings into the world.

I am equally thankful towards my second supervisor *Prof. Dr. Rasha Abdel Rahman* for the guidance, the time, and feedback throughout the process of working on this thesis. I am likewise grateful for the expertise that *Prof. Dr. Isabel Dziobek*, *Dr. Mareike Bayer, and Dr. Amit Lampit* contribute to the examination committee of this dissertation.

I greatly appreciate the contributions of my collaborators *Prof. Dr. Harald Prüß, Dr. Ute Kopp, and Prof. Dr. Friedemann Paul* for providing their clinical and neuropsychological insights and essential infrastructure that made this work possible. The success of this project is equally based on the work of the research assistants *Dimitra M. Kandia, Johanna Klag, and Leonie Maier* – each of them an aspiring scientist and clinician. Thank you for your conscientious support in data acquisition and study organisation. At the *Berlin Center for Advanced Neuroimaging (BCAN),* I received invaluable support by *Andrea Hassenpflug, Yvonne Kamm, and Dr. Stefan Hetzer,* who provided my training at the MRI scanner, technical support, and overall advice on data quality and MR safety. It is always a pleasure to work with you. *Dr. Frederik Bartels and Julia Heine* have been the most fantastic editors of this thesis.

This work would not have been possible without the generous support of the *Studienstiftung des deutschen Volkes (German Academic Scholarship Foundation)*. Thank you for funding my research over the years and for invaluable experiences at meetings and summer schools, broadening my perspective on science and giving me the opportunity to meet inspiring people and wonderful new friends like you, *Friedrich and Katharina*. Moreover, I am thankful to all participants and their caregivers for their time and cooperation, for travelling to Berlin, and for sharing their stories that inspired and motivated me throughout the years. I hope this work helps you and future patients.

My sincere gratitude goes to my dear friends and colleagues from the *Cognitive Neurology Lab Berlin*, a pack of talented, determined, and genuinely kind people. *Darko, Deetje, Frederik, Graham, Harry, Joseph, Maron, Martina, Nina, Patrizia, Sophia, Stephan – ship ahoy!* Being in science is so much nicer when you are around.

My sincere gratitude goes to my sister *Julia*, a brilliant mind, for sharing her thoughts, critical analysis, and loving company. I would equally like to thank my parents for their support and trust in me and my work. Thanks to my grandmother, who danced through life, and to my grandparents, who sparked my curiosity in science. *Line, Franzi, and Anne* – your company throughout the last years was invaluable. Lastly, thank you, *Ani*, for being a wonderful friend for more than 20 years, for your encouraging and always enthusiastic spirit. You make me laugh at the ups and even more at the downs, and help me put things into perspective. *Obrigada*.

References

1. Oppenheim, H. Über Hirnsymptome bei Carcinomatose ohne nachweisbare Veränderungen im Gehirn. *Charité-Annalen (Berlin)* **13**, 335–344 (1888).

2. Schulz, P. & Prüss, H. "Hirnsymptome bei Carcinomatose" — Hermann Oppenheim and an Early Description of a Paraneoplastic Neurological Syndrome. *J. Hist. Neurosci.* **24**, 371–377 (2015).

3. Dalmau, J. *et al.* Paraneoplastic anti-N-methyl-D-aspartate receptor encephalitis associated with ovarian teratoma. *Ann. Neurol.* **61**, 25–36 (2007).

4. Lai, M. *et al.* Investigation of LGI1 as the antigen in limbic encephalitis previously attributed to potassium channels: a case series. *Lancet Neurol.* **9**, 776–785 (2010).

5. Kreye, J. *et al.* Human cerebrospinal fluid monoclonal N -methyl-D-aspartate receptor autoantibodies are sufficient for encephalitis pathogenesis. *Brain* **139**, 2641–2652 (2016).

6. Leypoldt, F., Armangue, T. & Dalmau, J. Autoimmune encephalopathies. *Ann. N. Y. Acad. Sci.* 1–21 (2014). doi:10.1111/nyas.12553

7. Fukata, Y. *et al.* Disruption of LGI1-linked synaptic complex causes abnormal synaptic transmission and epilepsy. *Proc. Natl. Acad. Sci.* **107**, 3799–3804 (2010).

8. Hughes, E. G. *et al.* Cellular and Synaptic Mechanisms of Anti-NMDA Receptor Encephalitis. *J. Neurosci.* **30**, 5866–5875 (2010).

9. Titulaer, M. J. *et al.* Treatment and prognostic factors for long-term outcome in patients with anti-NMDA receptor encephalitis: an observational cohort study. *Lancet Neurol.* **12**, 157–65 (2013).

10. Dalmau, J. & Graus, F. Antibody-Mediated Encephalitis. *N. Engl. J. Med.* **378**, 840–851 (2018).

11. Prüss, H. *et al.* N-methyl-D-aspartate receptor antibodies in herpes simplex encephalitis. *Ann. Neurol.* **72**, 902–911 (2012).

12. Mueller, S. H. *et al.* Genetic predisposition in anti-LGI1 and anti-NMDA receptor encephalitis. *Ann. Neurol.* **83**, 863–869 (2018).

13. Hebert, J., Riche, B., Rabilloud, M. & Honnorat, J. Epidemiology of paraneoplastic neurologic disorders and autoimmune encephalitides in France. *J. Neurol. Sci.* **405**, 5–8 (2019).

14. Dubey, D. *et al.* Autoimmune encephalitis epidemiology and a comparison to infectious encephalitis. *Ann. Neurol.* **83**, 166–177 (2018).

15. Dalmau, J. *et al.* Review An update on anti-NMDA receptor encephalitis for neurologists and psychiatrists : mechanisms and models. **4422**, 1–13 (2019).

16. Gable, M. S., Sheriff, H., Dalmau, J., Tilley, D. H. & Glaser, C. A. The Frequency of Autoimmune N-Methyl-D-Aspartate Receptor Encephalitis Surpasses That of Individual Viral Etiologies in Young Individuals Enrolled in the California Encephalitis Project. *Clin. Infect. Dis.* **54**, 899–904 (2012).

17. Dalmau, J. *et al.* Anti-NMDA-receptor encephalitis: case series and analysis of the effects of antibodies. *Lancet Neurol.* **7**, 1091–1098 (2008).

18. van Sonderen, A. *et al.* Anti-LGI1 encephalitis: Clinical syndrome and long-term follow-up. *Neurology* **87**, 1449–1456 (2016).

19. Global Burden of Disease Study 2015 (GDB 2015). ghdx.healthdata.org/gbd-2015

20. Dalmau, J., Lancaster, E., Martinez-Hernandez, E., Rosenfeld, M. R. & Balice-Gordon, R. Clinical experience and laboratory investigations in patients with anti-NMDAR encephalitis. *Lancet Neurol.* **10**, 63–74 (2011).

21. Gadoth, A. *et al.* Expanded phenotypes and outcomes among 256 LGI1/CASPR2-IgG-positive patients. *Ann. Neurol.* **82**, 79–92 (2017).

22. Irani, S. R. *et al.* Faciobrachial dystonic seizures precede Lgi1 antibody limbic encephalitis. *Ann. Neurol.* **69**, 892–900 (2011).

23. Graus, F. *et al.* A clinical approach to diagnosis of autoimmune encephalitis. *Lancet Neurol.* **15**, 391–404 (2016).

24. Vincent, A. *et al.* Potassium channel antibody-associated encephalopathy: a potentially immunotherapy-responsive form of limbic encephalitis. *Brain* **127**, 701–712 (2004).

25. Thompson, J. *et al.* The importance of early immunotherapy in patients with faciobrachial dystonic seizures. *Brain* **141**, 348–356 (2018).

26. Baumgartner, A. *et al.* Admission diagnoses of patients later diagnosed with autoimmune encephalitis. *J. Neurol.* **266**, 124–132 (2019).

27. Balu, R. *et al.* A score that predicts 1-year functional status in patients with anti-NMDA receptor encephalitis. *Neurology* **92**, 244–252 (2019).

28. Herken, J. & Prüss, H. Red Flags: Clinical Signs for Identifying Autoimmune Encephalitis in Psychiatric Patients. *Front. Psychiatry* **8**, 1–9 (2017).

29. Blinder, T. & Lewerenz, J. Cerebrospinal Fluid Findings in Patients With Autoimmune Encephalitis—A Systematic Analysis. *Front. Neurol.* **10**, (2019).

30. Hébert, J. *et al.* Searching for autoimmune encephalitis: Beware of normal CSF. *J. Neuroimmunol.* **345**, 577285 (2020).

31. Rössling, R. & Prüss, H. SOP: antibody-associated autoimmune encephalitis. *Neurol. Res. Pract.* **2**, 1 (2020).

32. Dalmau, J., Geis, C. & Graus, F. Autoantibodies to Synaptic Receptors and Neuronal Cell Surface Proteins in Autoimmune Diseases of the Central Nervous System. *Physiol. Rev.* **97**, 839–887 (2017).

33. Scoville, W. B. & Milner, B. Loss of recent memory after bilateral hippocampal lesions. *J. Neurol. Neurosurg. Psychiatry* **20**, 11–21 (1957).

34. Annese, J. *et al.* Postmortem examination of patient H.M.'s brainbased on histological sectioning and digital 3Dreconstruction. *Nat. Commun.* 1–9 (2014). doi:10.1038/ncomms4122

35. Damasio, A. R., Eslinger, P. J., Damasio, H., Van Hoesen, G. W., & Cornell, S. Multimodal amnesic syndrome following bilateral temporal and basal forebrain damage. *Arch. Neurol.* **42**, 252–259 (1985).

36. Witt, J.-A. *et al.* The overall pathological status of the left hippocampus determines preoperative verbal memory performance in left mesial temporal lobe epilepsy. *Hippocampus* **24**, 446–454 (2014).

37. Alessio, A. *et al.* Memory and language impairments and their relationships to

hippocampal and perirhinal cortex damage in patients with medial temporal lobe epilepsy. *Epilepsy Behav.* **8**, 593–600 (2006).

38. Bartsch, T. *et al.* Selective Neuronal Vulnerability of Human Hippocampal CA1 Neurons: Lesion Evolution, Temporal Course, and Pattern of Hippocampal Damage in Diffusion-Weighted MR Imaging. *J. Cereb. Blood Flow Metab.* **35**, 1836–1845 (2015).

39. Monaghan, D. & Cotman, C. Distribution of N-methyl-D-aspartate-sensitive L-[3H]glutamate-binding sites in rat brain. *J. Neurosci.* **5**, 2909–2919 (1985).

40. Palomero-Gallagher, N., Amunts, K. & Zilles, K. Transmitter Receptor Distribution in the Human Brain. in *Brain Mapping* **2**, 261–275 (Elsevier, 2015).

41. Herranz-Pérez, V., Olucha-Bordonau, F. E., Morante-Redolat, J. M. & Pérez-Tur, J. Regional distribution of the leucine-rich glioma inactivated (LGI) gene family transcripts in the adult mouse brain. *Brain Res.* **1307**, 177–194 (2010).

42. Flores, R. *et al.* Characterization of hippocampal subfields using ex vivo MRI and histology data: Lessons for in vivo segmentation. *Hippocampus* **30**, 545–564 (2020).

43. Small, S. A., Schobel, S. A., Buxton, R. B., Witter, M. P. & Barnes, C. A. A pathophysiological framework of hippocampal dysfunction in ageing and disease. *Nat. Rev. Neurosci.* **12**, 585–601 (2011).

44. Newmark, R. E., Schon, K., Ross, R. S. & Stern, C. E. Contributions of the hippocampal subfields and entorhinal cortex to disambiguation during working memory. *Hippocampus* **23**, 467–475 (2013).

45. Grande, X. *et al.* Holistic Recollection via Pattern Completion Involves Hippocampal Subfield CA3. *J. Neurosci.* **39**, 8100–8111 (2019).

46. Leutgeb, J. K., Leutgeb, S., Moser, M.-B. & Moser, E. I. Pattern Separation in the Dentate Gyrus and CA3 of the Hippocampus. *Science (80-.).* **315**, 961–966 (2007).

47. Zhao, C., Deng, W. & Gage, F. H. Mechanisms and Functional Implications of Adult Neurogenesis. *Cell* **132**, 645–660 (2008).

48. Bartsch, T. & Wulff, P. The hippocampus in aging and disease: From plasticity to vulnerability. *Neuroscience* **309**, 1–16 (2015).

49. Brierley, J. B., Corsellis, J. A. N., Hierons, R. & Nevin, S. Subacute encephalitis of later adult life. Mainly affecting the limbic areas. *Brain* **83**, 357–368 (1960).

50. Corsellis, J. A. N., Goldberg, G. J. & Norton, A. R. "Limbic encephalitis" and its association with carcinoma. *Brain* **91**, 481–496 (1968).

51. Russell, D. S. Encephalomyelitis and carcinomatous neuropathy. *Enceph.* **13**, 1–5 (1961).

52. Wilkinson, P. C. Serological findings in carcinomatous neuromyopathy. *Lancet* **283**, 1301–1303 (1964).

53. Trotter, J. L. Cerebellar Degeneration With Hodgkin Disease. *Arch. Neurol.* **33**, 660 (1976).

54. Graus, F., Cordon-Cardo, C. & Posner, J. B. Neuronal antinuclear antibody in sensory neuronopathy from lung cancer. *Neurology* **35**, 538–538 (1985).

55. Dalmau, J. & Rosenfeld, M. R. Autoimmune encephalitis update. *Neuro. Oncol.* **16**, 771–8 (2014).

56. Irani, S. R., Gelfand, J. M., Al-Diwani, A. & Vincent, A. Cell-surface central nervous system autoantibodies: clinical relevance and emerging paradigms. *Ann. Neurol.* **76**, 168–

184 (2014).

57. Irani, S. R., Gelfand, J. M., Bettcher, B. M., Singhal, N. S. & Geschwind, M. D. Effect of Rituximab in Patients With Leucine-Rich, Glioma-Inactivated 1 Antibody-Associated Encephalopathy. *JAMA Neurol.* (2014). doi:10.1001/jamaneurol.2014.463

58. Bartsch, T. *et al.* Focal lesions of human hippocampal CA1 neurons in transient global amnesia impair place memory. *Science (80-.).* **328**, 1412–1415 (2010).

59. Bartsch, T., Dohring, J., Rohr, A., Jansen, O. & Deuschl, G. CA1 neurons in the human hippocampus are critical for autobiographical memory, mental time travel, and autonoetic consciousness. *Proc. Natl. Acad. Sci.* **108**, 17562–17567 (2011).

60. Finke, C., Bruehl, H., Düzel, E., Heekeren, H. R. & Ploner, C. J. Neural correlates of short-term memory reorganization in humans with hippocampal damage. *J. Neurosci.* **33**, 11061–11069 (2013).

61. Lancaster, E. & Dalmau, J. Neuronal autoantigens—pathogenesis, associated disorders and antibody testing. *Nat. Rev. Neurol.* **8**, 380–390 (2012).

62. Bien, C. G. & Bauer, J. Autoimmune epilepsies. *Neurotherapeutics* **11**, 311–8 (2014).

63. Varley, J., Vincent, A. & Irani, S. R. Clinical and experimental studies of potentially pathogenic brain-directed autoantibodies: current knowledge and future directions. *J. Neurol.* 1–15 (2014). doi:10.1007/s00415-014-7600-8

64. Gultekin, S. H. *et al.* Paraneoplastic limbic encephalitis: Neurological symptoms, immunological findings and tumour association in 50 patients. *Brain* **123**, 1481–1494 (2000).

65. Lawn, N. D., Westmoreland, B. F., Kiely, M. J., Lennon, V. A. & Vernino, S. Clinical, Magnetic Resonance Imaging, and Electroencephalographic Findings in Paraneoplastic Limbic Encephalitis. *Mayo Clin. Proc.* **78**, 1363–1368 (2003).

66. Ances, B. M. *et al.* Treatment-responsive limbic encephalitis identified by neuropil antibodies: MRI and PET correlates. *Brain* **128**, 1764–77 (2005).

67. Urbach, H. *et al.* Serial MRI of limbic encephalitis. *Neuroradiology* **48**, 380–6 (2006).

68. Dirr, L. Y., Elster, A. D., Donofrio, P. D. & Smith, M. Evolution of brain MRI abnormalities in limbic encephalitis. *Neurology* **40**, 1304–1306 (1990).

69. Bartsch, T. The hippocampus in neurological disease. in *The Clinical Neurobiology of the Hippocampus: An Integrative View* 200 (Oxford University Press, 2012).

70. Scheid, R., Lincke, T., Voltz, R., Von Cramon, D. Y. & Sabri, O. Serial 18F-fluoro-2-deoxy-D-glucose positron emission tomography and magnetic resonance imaging of paraneoplastic limbic encephalitis. *Archives of Neurology* **61**, 1785–1789 (2004).

71. Basu, S. & Alavi, A. Role of FDG-PET in the clinical management of paraneoplastic neurological syndrome: Detection of the underlying malignancy and the brain PET-MRI correlates. *Molecular Imaging and Biology* **10**, 131–137 (2008).

72. Granerod, J. *et al.* Causes of encephalitis and differences in their clinical presentations in England: a multicentre, population-based prospective study. *Lancet Infect. Dis.* **10**, 835–44 (2010).

73. Irani, S. R. *et al.* N-methyl-D-aspartate antibody encephalitis: temporal progression of clinical and paraclinical observations in a predominantly non-paraneoplastic disorder of both sexes. *Brain* **133**, 1655–67 (2010).

74. Heine, J. *et al.* Imaging of autoimmune encephalitis - Relevance for clinical practice and

hippocampal function. *Neuroscience* **309**, 68–83 (2015).

75. Wegner, F. *et al.* Anti-leucine rich glioma inactivated 1 protein and anti-N-methyl-D-aspartate receptor encephalitis show distinct patterns of brain glucose metabolism in 18F-fluoro-2-deoxy-d-glucose positron emission tomography. *BMC Neurol.* **14**, 136 (2014).

76. Tojo, K. *et al.* A Young Man with Anti-NMDAR Encephalitis following Guillain-Barré Syndrome. *Case Rep. Neurol.* **3**, 7–13 (2011).

77. Vitaliani, R. *et al.* Paraneoplastic encephalitis, psychiatric symptoms, and hypoventilation in ovarian teratoma. *Ann. Neurol.* **58**, 594–604 (2005).

78. Maqbool, M. *et al.* Novel FDG-PET findings in anti-NMDA receptor encephalitis: a case based report. *J. Child Neurol.* **26**, 1325–1328 (2011).

79. Hacohen, Y. *et al.* NMDA receptor antibodies associated with distinct white matter syndromes. *Neurol. Neuroimmunol. neuroinflammation* **1**, e2 (2014).

80. Tobin, W. O. *et al.* NMDA receptor encephalitis causing reversible caudate changes on MRI and PET imaging. *Neurol. Clin. Pract.* **4**, 470–473 (2014).

81. Tzoulis, C. *et al.* Progressive striatal necrosis associated with anti-NMDA receptor antibodies. *BMC Neurol.* **13**, 55 (2013).

82. Rubio-Agusti, I. *et al.* Peripheral nerve hyperexcitability: a clinical and immunologic study of 38 patients. *Neurology* **76**, 172–8 (2011).

83. Gumbinger, C., Hametner, C., Wildemann, B., Veltkamp, R. & Bösel, J. Administration of isoflurane-controlled dyskinetic movements caused by anti-NMDAR encephalitis. *Neurology* **80**, 1997–8 (2013).

84. Labate, A., Quattrone, A., Dalmau, J. & Gambardella, A. Anti-N-methyl-D-aspartate-glutamic-receptor encephalitis presenting as paroxysmal exercise-induced foot weakness. *Mov. Disord.* **28**, 820–2 (2013).

85. Aguiar de Sousa, D., Lobo, P. P., Caldas, A. C., Coelho, M. & Albuquerque, L. Pure ataxia associated with N-methyl-D-aspartate receptor antibodies. *Parkinsonism Relat. Disord.* **20**, 568–9 (2014).

86. Hacohen, Y. *et al.* N-methyl-D-aspartate receptor antibody-associated movement disorder without encephalopathy. *Dev. Med. Child Neurol.* **56**, 190–3 (2014).

87. Iizuka, T. *et al.* Anti-NMDA receptor encephalitis in Japan: long-term outcome without tumor removal. *Neurology* **70**, 504–11 (2008).

88. Iizuka, T. *et al.* Reversible brain atrophy in anti-NMDA receptor encephalitis: a long-term observational study. *J. Neurol.* **257**, 1686–91 (2010).

89. Pillai, S. C., Gill, D., Webster, R., Howman-Giles, R. & Dale, R. C. Cortical hypometabolism demonstrated by PET in relapsing NMDA receptor encephalitis. *Pediatr. Neurol.* **43**, 217–220 (2010).

90. Frechette, E. S., Zhou, L., Galetta, S. L., Chen, L. & Dalmau, J. Prolonged follow-up and CSF antibody titers in a patient with anti-NMDA receptor encephalitis. *Neurology* **76**, S64-6 (2011).

91. Thomas, A. *et al.* Anti-N-methyl-D-aspartate receptor encephalitis: a patient with refractory illness after 25 months of intensive immunotherapy. *JAMA Neurol.* **70**, 1566–8 (2013).

92. Finke, C. *et al.* Structural Hippocampal Damage Following Anti-N-Methyl-D-Aspartate

Receptor Encephalitis. *Biol. Psychiatry* **79**, 727–734 (2016).

93. Maeder-Ingvar, M. *et al.* FDG-PET hyperactivity in basal ganglia correlating with clinical course in anti-NDMA-R antibodies encephalitis. *J. Neurol. Neurosurg. Psychiatry* **82**, 235–6 (2011).

94. Leypoldt, F. *et al.* Fluorodeoxyglucose positron emission tomography in anti-N-methyl-D-aspartate receptor encephalitis: distinct pattern of disease. *J. Neurol. Neurosurg. Psychiatry* **83**, 681–6 (2012).

95. Baumgartner, A., Rauer, S., Mader, I. & Meyer, P. T. Cerebral FDG-PET and MRI findings in autoimmune limbic encephalitis: correlation with autoantibody types. *J. Neurol.* **260**, 2744–53 (2013).

96. Mohr, B. C. & Minoshima, S. F-18 fluorodeoxyglucose PET/CT findings in a case of anti-NMDA receptor encephalitis. *Clin. Nucl. Med.* **35**, 461–3 (2010).

97. Fisher, R. E., Patel, N. R., Lai, E. C. & Schulz, P. E. Two different 18F-FDG brain PET metabolic patterns in autoimmune limbic encephalitis. *Clin. Nucl. Med.* **37**, e213-8 (2012).

98. Caballero, P. E. J. Fluorodeoxyglucose positron emission tomography findings in NMDA receptor antibody encephalitis. *Arq. Neuropsiquiatr.* **69**, 409–410 (2011).

99. Abers, M., Zafar, S. & Kass, J. FDG-PET Reveals Reduced Metabolic Activity in the Basal Ganglia of a Patient with Anti-NMDA Receptor Encephalitis. *Neurology* **80**, (2013).

100. Tsuyusaki, Y., Sakakibara, R., Kishi, M., Tateno, F. & Yoshida, T. Downbeat nystagmus as the initial manifestation of anti-NMDAR encephalitis. *Neurological Sciences* **35**, 125–126 (2014).

101. Finke, C. *et al.* Functional and structural brain changes in anti-N-methyl-D-aspartate receptor encephalitis. *Ann. Neurol.* **74**, 284–296 (2013).

102. Lipton, S. A. NMDA receptors, glial cells, and clinical medicine. *Neuron* **50**, 9–11 (2006).

103. Takeda, A. *et al.* A case of anti-N-methyl-d-aspartate receptor encephalitis with multiple sclerosis-like demyelinated lesions. *Mult. Scler. Relat. Disord.* **3**, 391–397 (2014).

104. Titulaer, M. J. *et al.* Overlapping demyelinating syndromes and anti-N-methyl-D-aspartate receptor encephalitis. *Ann. Neurol.* **75**, 411–428 (2014).

105. Kaneko, K. *et al.* Anti-N-methyl-D-aspartate receptor encephalitis with multiphasic demyelination. *Ann. Neurol.* **76**, 462–4 (2014).

106. Fleischmann, R. *et al.* Severe Cognitive Impairment Associated With Intrathecal Antibodies to the NR1 Subunit of the N -Methyl-D-Aspartate Receptor in a Patient With Multiple Sclerosis. *JAMA Neurol.* **72**, 96 (2015).

107. Anticevic, A. *et al.* NMDA receptor function in large-scale anticorrelated neural systems with implications for cognition and schizophrenia. *Proc. Natl. Acad. Sci.* **109**, 16720–5 (2012).

108. Planagumà, J. *et al.* Human N-methyl D-aspartate receptor antibodies alter memory and behaviour in mice. *Brain* **138**, 94–109 (2015).

109. Liguori, R. *et al.* Morvan's syndrome: peripheral and central nervous system and cardiac involvement with antibodies to voltage-gated potassium channels. *Brain* **124**, 2417–2426 (2001).

110. Irani, S. R. *et al.* Antibodies to Kv1 potassium channel-complex proteins leucine-rich, glioma inactivated 1 protein and contactin-associated protein-2 in limbic encephalitis,

Morvan's syndrome and acquired neuromyotonia. *Brain* **133**, 2734–2748 (2010).

111. Kotsenas, A. L. *et al.* MRI findings in autoimmune voltage-gated potassium channel complex encephalitis with seizures: one potential etiology for mesial temporal sclerosis. *Am. J. Neuroradiol.* **35**, 84–9 (2014).

112. Wagner, J. *et al.* Automated volumetry of the mesiotemporal structures in antibody-associated limbic encephalitis. *J. Neurol. Neurosurg. Psychiatry* (2014). doi:10.1136/jnnp-2014-307875

113. Chatzikonstantinou, A., Szabo, K., Ottomeyer, C., Kern, R. & Hennerici, M. G. Successive affection of bilateral temporomesial structures in a case of non-paraneoplastic limbic encephalitis demonstrated by serial MRI and FDG-PET. *J. Neurol.* **256**, 1753–1755 (2009).

114. Kröll-Seger, J., Bien, C. G. & Huppertz, H. Non-paraneoplastic limbic encephalitis associated with antibodies to potassium channels leading to bilateral hippocampal sclerosis in a pre-pubertal girl. *Epileptic Disord.* **11**, 54–9 (2009).

115. Irani, S. R. *et al.* Faciobrachial dystonic seizures: the influence of immunotherapy on seizure control and prevention of cognitive impairment in a broadening phenotype. *Brain* **136**, 3151–3162 (2013).

116. Plantone, D., Renna, R., Grossi, D., Plantone, F. & Iorio, R. Basal ganglia involvement in facio-brachial dystonic seizures associated with LGI1 antibodies. *Neurology* **80**, 183–184 (2013).

117. Boesebeck, F. *et al.* Faciobrachial dystonic seizures arise from cortico-subcortical abnormal brain areas. *J. Neurol.* **260**, 1684–1686 (2013).

118. Fidzinski, P. *et al.* Faciobrachial dystonic seizures and antibodies to Lgi1 in a 92-year-old patient: A case report. *J. Neurol. Sci.* **347**, 404–405 (2014).

119. Andrade, D. M., Tai, P., Dalmau, J. & Wennberg, R. Tonic seizures: A diagnostic clue of anti-LGI1 encephalitis? *Neurology* **76**, 1355–7 (2011).

120. Malter, M. P. *et al.* Outcome of limbic encephalitis with VGKC-complex antibodies: relation to antigenic specificity. *J. Neurol.* **261**, 1695–1705 (2014).

121. Szots, M. *et al.* Natural course of LGI1 encephalitis: 3-5 years of follow-up without immunotherapy. *J. Neurol. Sci.* **343**, 198–202 (2014).

122. Shin, Y.-W. *et al.* VGKC-complex/LGI1-antibody encephalitis: Clinical manifestations and response to immunotherapy. *J. Neuroimmunol.* **265**, 75–81 (2013).

123. Cash, S. S., Larvie, M. & Dalmau, J. Case records of the Massachusetts General Hospital. Case 34-2011: A 75-year-old man with memory loss and partial seizures. *N. Engl. J. Med.* **365**, 1825–33 (2011).

124. Park, S., Choi, H., Cheon, G. J., Wook Kang, K. & Lee, D. S. 18F-FDG PET/CT in Anti-LGI1 Encephalitis. *Clin. Nucl. Med.* **40**, 156–158 (2015).

125. Striano, P. *et al.* Tonic seizures: A diagnostic clue of anti-LGI1 encephalitis? *Neurology* **77**, 2140–3 (2011).

126. Lancaster, E. *et al.* Investigations of CASPR2, an autoantigen of encephalitis and neuromyotonia. *Ann. Neurol.* **69**, 303–311 (2011).

127. Irani, S. R. *et al.* Morvan syndrome: clinical and serological observations in 29 cases. *Ann. Neurol.* **72**, 241–55 (2012).

128. Spinazzi, M. *et al.* Immunotherapy-reversed compulsive, monoaminergic, circadian

rhythm disorder in Morvan syndrome. *Neurology* **71**, 2008–10 (2008).

129. Toosy, A. T. *et al.* Functional imaging correlates of fronto-temporal dysfunction in Morvan's syndrome. *J. Neurol. Neurosurg. Psychiatry* **79**, 734–735 (2008).

130. Loukaides, P. *et al.* Morvan's syndrome associated with antibodies to multiple components of the voltage-gated potassium channel complex. *J. Neurol. Sci.* **312**, 52–6 (2012).

131. Krogias, C. *et al.* Successful treatment of anti-Caspr2 syndrome by interleukin 6 receptor blockade through tocilizumab. *JAMA Neurol.* **70**, 1056–9 (2013).

132. Lai, M. *et al.* AMPA receptor antibodies in limbic encephalitis alter synaptic receptor location. *Ann. Neurol.* **65**, 424–434 (2009).

133. Bataller, L. *et al.* Reversible paraneoplastic limbic encephalitis associated with antibodies to the AMPA receptor. *Neurology* **74**, 265–7 (2010).

134. Dogan Onugoren, M. *et al.* Limbic encephalitis due to GABA B and AMPA receptor antibodies: a case series. *J. Neurol. Neurosurg. Psychiatry* **86**, 965–972 (2015).

135. Spatola, M., Stojanova, V., Prior, J. O., Dalmau, J. & Rossetti, A. O. Serial brain ^{18}FDG-PET in anti-AMPA receptor limbic encephalitis. *J. Neuroimmunol.* **271**, 53–5 (2014).

136. Wei, Y.-C. *et al.* Rapid progression and brain atrophy in anti-AMPA receptor encephalitis. *J. Neuroimmunol.* **261**, 129–33 (2013).

137. Graus, F. *et al.* The expanding clinical profile of anti-AMPA receptor encephalitis. *Neurology* **74**, 857–9 (2010).

138. Petit-Pedrol, M. *et al.* Encephalitis with refractory seizures, status epilepticus, and antibodies to the GABAA receptor: a case series, characterisation of the antigen, and analysis of the effects of antibodies. *Lancet. Neurol.* **13**, 276–286 (2014).

139. Ohkawa, T. *et al.* Identification and characterization of GABA(A) receptor autoantibodies in autoimmune encephalitis. *J. Neurosci.* **34**, 8151–63 (2014).

140. Lancaster, E. *et al.* Antibodies to the GABA(B) receptor in limbic encephalitis with seizures: case series and characterisation of the antigen. *Lancet. Neurol.* **9**, 67–76 (2010).

141. Boronat, A., Sabater, L., Saiz, A., Dalmau, J. & Graus, F. GABA(B) receptor antibodies in limbic encephalitis and anti-GAD-associated neurologic disorders. *Neurology* **76**, 795–800 (2011).

142. Höftberger, R. *et al.* Encephalitis and GABAB receptor antibodies: novel findings in a new case series of 20 patients. *Neurology* **81**, 1500–6 (2013).

143. Jeffery, O. J. *et al.* GABAB receptor autoantibody frequency in service serologic evaluation. *Neurology* **81**, 882–7 (2013).

144. Jarius, S. *et al.* GABAB receptor antibodies in paraneoplastic cerebellar ataxia. *J. Neuroimmunol.* **256**, 94–6 (2013).

145. Mundiyanapurath, S. *et al.* GABA-B-receptor antibodies in paraneoplastic brainstem encephalitis. *J. Neuroimmunol.* **259**, 88–91 (2013).

146. DeFelipe-Mimbrera, A. *et al.* Opsoclonus-myoclonus syndrome and limbic encephalitis associated with GABAB receptor antibodies in CSF. *J. Neuroimmunol.* **272**, 91–3 (2014).

147. Kruer, M. C. *et al.* Aggressive course in encephalitis with opsoclonus, ataxia, chorea, and seizures: the first pediatric case of γ-aminobutyric acid type B receptor autoimmunity. *JAMA Neurol.* **71**, 620–3 (2014).

148. Kim, T.-J. *et al.* Clinical manifestations and outcomes of the treatment of patients with GABAB encephalitis. *J. Neuroimmunol.* **270**, 45–50 (2014).

149. Ohta, K., Seki, M., Dalmau, J. & Shinohara, Y. Perfusion IMP-SPECT shows reversible abnormalities in GABA(B) receptor antibody associated encephalitis with normal MRI. *Brain Behav.* **1**, 70–72 (2011).

150. Dale, R. C. *et al.* Antibodies to surface dopamine-2 receptor in autoimmune movement and psychiatric disorders. *Brain* **135**, 3453–3468 (2012).

151. Boronat, A. *et al.* Encephalitis and antibodies to dipeptidyl-peptidase-like protein-6, a subunit of Kv4.2 potassium channels. *Ann. Neurol.* **73**, 120–128 (2013).

152. Tobin, W. O. *et al.* DPPX potassium channel antibody: Frequency, clinical accompaniments, and outcomes in 20 patients. *Neurology* **83**, 1797–803 (2014).

153. Balint, B. *et al.* Progressive encephalomyelitis with rigidity and myoclonus: a new variant with DPPX antibodies. *Neurology* **82**, 1521–8 (2014).

154. Saiz, A. *et al.* Spectrum of neurological syndromes associated with glutamic acid decarboxylase antibodies: diagnostic clues for this association. *Brain* **131**, 2553–63 (2008).

155. Malter, M. P., Helmstaedter, C., Urbach, H., Vincent, A. & Bien, C. G. Antibodies to glutamic acid decarboxylase define a form of limbic encephalitis. *Ann. Neurol.* **67**, 470–8 (2010).

156. Honnorat, J. *et al.* Cerebellar Ataxia With Anti–Glutamic Acid Decarboxylase Antibodies. *Arch. Neurol.* **58**, 225 (2001).

157. Ariño, H. *et al.* Cerebellar ataxia and glutamic acid decarboxylase antibodies: immunologic profile and long-term effect of immunotherapy. *JAMA Neurol.* **71**, 1009–16 (2014).

158. Wagner, J. *et al.* Quantitative FLAIR analysis indicates predominant affection of the amygdala in antibody-associated limbic encephalitis. *Epilepsia* **54**, 1679–87 (2013).

159. Hutchinson, M. *et al.* Progressive encephalomyelitis, rigidity, and myoclonus: a novel glycine receptor antibody. *Neurology* **71**, 1291–2 (2008).

160. McKeon, A. *et al.* Glycine Receptor Autoimmune Spectrum With Stiff-Man Syndrome Phenotype. *Arch. Neurol.* 1–9 (2012). doi:10.1001/jamaneurol.2013.574

161. Carvajal-González, A. *et al.* Glycine receptor antibodies in PERM and related syndromes: characteristics, clinical features and outcomes. *Brain* **137**, 2178–92 (2014).

162. Wuerfel, E., Bien, C. G., Vincent, A., Woodhall, M. & Brockmann, K. Glycine receptor antibodies in a boy with focal epilepsy and episodic behavioral disorder. *J. Neurol. Sci.* **343**, 180–182 (2014).

163. Flanagan, E. P. *et al.* Basal ganglia T1 hyperintensity in LGI1-autoantibody faciobrachial dystonic seizures. *Neurol. - Neuroimmunol. Neuroinflammation* **2**, e161 (2015).

164. Rankin, J. Cerebral vascular accidents in patients over the age of 60. II. Prognosis. *Scott. Med. J.* **2**, 200–215 (1957).

165. Helmstaedter, C., Lendt, M. & Lux, S. *VLMT: Verbaler Lern-und Merkfähigkeitstest*. (Beltz Test, 2001).

166. Stern, R. A. *et al.* The Boston qualitative scoring system for the Rey-Osterrieth complex figure: Description and interrater reliability. *Clin. Neuropsychol.* **8**, 309–322 (1994).

167. Zimmermann, P., & Fimm, B. *Testbatterie zur Aufmerksamkeitsprüfung-Version 2.2: TAP [Handbuch]*. (Psytest, 2009).

168. Aschenbrenner, S., Tucha, O. & Lange, K. W. *Regensburger Wortflüssigkeits-Test: RWT*. (Hogrefe, Verlag für Psychologie, 2000).

169. Lehrl, S. *Mehrfachwahl-Wortschatz-Intelligenztest: MWT-B*. (1999).

170. Horn, W. *Leistungsprüfsystem*. (Hogrefe, 1983).

171. Morey, R. A. *et al.* A comparison of automated segmentation and manual tracing for quantifying hippocampal and amygdala volumes. *Neuroimage* **45**, 855–866 (2009).

172. Leemput, K. Van *et al.* Automated segmentation of hippocampal subfields from ultra-high resolution in vivo MRI. *Hippocampus* **9**, 549–557 (2009).

173. Fisher, R. S. *et al.* Operational classification of seizure types by the International League Against Epilepsy. *Epilepsia* **58**, 522–530 (2017).

174. Blume, W. T. *et al.* Glossary of descriptive terminology for ictal semiology: report of the ILAE Task Force on Classification and Terminology. *Epilepsia* **42**, 1212–1218 (2001).

175. Klein, C. J. *et al.* Insights from LGI1 and CASPR2 potassium channel complex autoantibody subtyping. *JAMA Neurol.* **70**, 229–34 (2013).

176. Toledano, M. *et al.* Utility of an immunotherapy trial in evaluating patients with presumed autoimmune epilepsy. *Neurology* **82**, 1578–1586 (2014).

177. Finke, C. *et al.* Cognitive deficits following anti-NMDA receptor encephalitis. *J. Neurol. Neurosurg. Psychiatry* **83**, 195–198 (2012).

178. Flanagan, E. P. *et al.* Autoimmune dementia: clinical course and predictors of immunotherapy response. *Mayo Clin. proceedings.* **85**, 881–97 (2010).

179. Quek, A. M. L. *et al.* Autoimmune epilepsy: clinical characteristics and response to immunotherapy. *Arch. Neurol.* **69**, 582–593 (2012).

180. Wieser, S. *et al.* Pilomotor seizures and status in non-paraneoplastic limbic encephalitis. *Epileptic Disord.* **7**, 205–211 (2005).

181. Rocamora, R. *et al.* Pilomotor seizures: an autonomic semiology of limbic encephalitis? *Seizure* **23**, 670–3 (2014).

182. Symvoulakis, E. K., Anyfantakis, D. & Zaganas, I. Pilomotor seizures: an unusual presentation of limbic encephalitis. *Acta Neurol. Belg.* **116**, 365–367 (2016).

183. Bien, C. G. *et al.* Limbic encephalitis as a precipitating event in adult-onset temporal lobe epilepsy. *Neurology* **69**, 1236–1244 (2007).

184. Zeineh, M. M., Engel, S. A., Thompson, P. M. & Bookheimer, S. Y. Dynamics of the hippocampus during encoding and retrieval of face-name pairs. *Science (80-.).* **299**, 577–580 (2003).

185. Suthana, N., Ekstrom, A., Moshirvaziri, S., Knowlton, B. & Bookheimer, S. Dissociations within human hippocampal subregions during encoding and retrieval of spatial information. *Hippocampus* **21**, 694–701 (2011).

186. Bakker, A., Kirwan, C. B., Miller, M. & Stark, C. E. L. Pattern Separation in the Human Hippocampal CA3 and Dentate Gyrus. *Science (80-.).* **319**, 1640–1642 (2008).

187. Bonnici, H. M., Chadwick, M. J. & Maguire, E. A. Representations of recent and remote autobiographical memories in hippocampal subfields. *Hippocampus* **23**, 849–854 (2013).

188. Le Bihan, D. *et al.* Diffusion tensor imaging: concepts and applications. *J. Magn. Reson. Imaging* **13**, 534–546 (2001).

189. Carlesimo, G. A., Cherubini, A., Caltagirone, C. & Spalletta, G. Hippocampal mean diffusivity and memory in healthy elderly individuals: A cross-sectional study. *Neurology* **74**, 194–200 (2010).

190. Den Heijer, T. *et al.* Structural and diffusion MRI measures of the hippocampus and memory performance. *Neuroimage* **63**, 1782–1789 (2012).

191. Demey, I. *et al.* Hippocampal mean diffusivity is a biomarker of neuronal injury in patients with mild cognitive impairment and Alzheimer's disease dementia. *Alzheimer's Dement.* **11**, 802 (2015).

192. Navarro, V. *et al.* Motor cortex and hippocampus are the two main cortical targets in LGI1-antibody encephalitis. *Brain* **139**, 1079–1093 (2016).

193. Smith, S. M. *et al.* Tract-based spatial statistics: voxelwise analysis of multi-subject diffusion data. *Neuroimage* **31**, 1487–505 (2006).

194. Behrens, T. E. J. *et al.* Non-invasive mapping of connections between human thalamus and cortex using diffusion imaging. *Nat. Neurosci.* **6**, 750–757 (2003).

195. Patenaude, B., Smith, S. M., Kennedy, D. N. & Jenkinson, M. A Bayesian model of shape and appearance for subcortical brain segmentation. *Neuroimage* **56**, 907–922 (2011).

196. Smith, S. M. *et al.* Advances in functional and structural MR image analysis and implementation as FSL. *Neuroimage* **23 Suppl 1**, S208-19 (2004).

197. Fischl, B. *et al.* Whole Brain Segmentation : Neurotechnique Automated Labeling of Neuroanatomical Structures in the Human Brain. *Neuron* **33**, 341–355 (2002).

198. Fischl, B. *et al.* Sequence-independent segmentation of magnetic resonance images. *Neuroimage* **23**, 69–84 (2004).

199. van Sonderen, A., Petit-Pedrol, M., Dalmau, J. & Titulaer, M. J. The value of LGI1, Caspr2 and voltage-gated potassium channel antibodies in encephalitis. *Nat. Rev. Neurol.* **13**, 290–301 (2017).

200. Finke, C. *et al.* Evaluation of Cognitive Deficits and Structural Hippocampal Damage in Encephalitis With Leucine-Rich, Glioma-Inactivated 1 Antibodies. *JAMA Neurol.* (2017). doi:10.1001/jamaneurol.2016.4226

201. Miller, T. D. *et al.* Focal CA3 hippocampal subfield atrophy following LGI1 VGKC-complex antibody limbic encephalitis. *Brain* **140**, 1–8 (2017).

202. Arino, H. *et al.* Anti-LGI1 – associated cognitive impairment Presentation and long-term outcome. *Neurology* **78**, 1–8 (2016).

203. Biswal, B., Zerrin Yetkin, F., Haughton, V. M. & Hyde, J. S. Functional connectivity in the motor cortex of resting human brain using echo-planar MRI. *Magn. Reson. Med.* **34**, 537–541 (1995).

204. Raichle, M. E. Two views of brain function. *Trends Cogn. Sci.* **14**, 180–190 (2010).

205. Beckmann, C. F. & Smith, S. M. Probabilistic Independent Component Analysis for Functional Magnetic Resonance Imaging. *IEEE Trans. Med. Imaging* **23**, 137–152 (2004).

206. Filippini, N. *et al.* Distinct patterns of brain activity in young carriers of the APOE-epsilon4 allele. *Pnas* **106**, 7209–7214 (2009).

207. Zhang, Y., Brady, M. & Smith, S. Segmentation of brain MR images through a hidden

Markov random field model and the expectation-maximization algorithm. *IEEE Trans. Med. Imaging* **20**, 45–57 (2001).

208. Winkler, A. M., Ridgway, G. R., Webster, M. A., Smith, S. M. & Nichols, T. E. Permutation inference for the general linear model. *Neuroimage* **92**, 381–397 (2014).

209. Smith, S. & Nichols, T. Threshold-free cluster enhancement: Addressing problems of smoothing, threshold dependence and localisation in cluster inference. *Neuroimage* **44**, 83–98 (2009).

210. Shirer, W. R., Ryali, S., Rykhlevskaia, E., Menon, V. & Greicius, M. D. Decoding Subject-Driven Cognitive States with Whole-Brain Connectivity Patterns. *Cereb. Cortex* **22**, 158–165 (2012).

211. Beckmann, C. F., DeLuca, M., Devlin, J. T. & Smith, S. M. Investigations into resting-state connectivity using independent component analysis. *Philos. Trans. R. Soc. Lond. B. Biol. Sci.* **360**, 1001–1013 (2005).

212. Raichle, M. E. *et al.* A default mode of brain function. *Proc. Natl. Acad. Sci.* **98**, 676–682 (2001).

213. Buckner, R. L., Andrews-Hanna, J. R. & Schacter, D. L. The Brain's Default Network: Anatomy, Function, and Relevance to Disease. *Ann. N. Y. Acad. Sci.* **1124**, 1–38 (2008).

214. Damoiseaux, J. S., Prater, K. E., Miller, B. L. & Greicius, M. D. Functional connectivity tracks clinical deterioration in Alzheimer's disease. *Neurobiol. Aging* **33**, 828-e19 (2012).

215. Schoonheim, M. M., Geurts, J. J. G. & Barkhof, F. The limits of functional reorganization in multiple sclerosis. *Neurology* **74**, 1246–1247 (2010).

216. Bettus, G. *et al.* Decreased basal fMRI functional connectivity in epileptogenic networks and contralateral compensatory mechanisms. *Hum. Brain Mapp.* **30**, 1580–91 (2009).

217. Peer, M. *et al.* Functional connectivity of large-scale brain networks in patients with anti-NMDA receptor encephalitis: An observational study. *The Lancet Psychiatry* **4**, (2017).

218. Menon, V. & Uddin, L. Q. Saliency, switching, attention and control: a network model of insula function. *Brain Struct. Funct.* **214**, 655–667 (2010).

219. Seeley, W. W. *et al.* Dissociable Intrinsic Connectivity Networks for Salience Processing and Executive Control. *J. Neurosci.* **27**, 2349–2356 (2007).

220. Menon, V. Large-scale brain networks and psychopathology: a unifying triple network model. *Trends Cogn. Sci.* **15**, 483–506 (2011).

221. Prüss, H. & Lennox, B. R. Emerging psychiatric syndromes associated with antivoltage-gated potassium channel complex antibodies. *J. Neurol. Neurosurg. Psychiatry* **87**, 1242–1247 (2016).

222. Pollak, T. & Moran, N. Emergence of new-onset psychotic disorder following recovery from LGI1 antibody-associated limbic encephalitis. *BMJ Case Rep.* (2017).

223. Brown, J. W. L. *et al.* Long-term remission with rituximab in refractory leucine-rich glioma inactivated 1 antibody encephalitis. *J. Neuroimmunol.* **271**, 66–68 (2014).

224. Naasan, G., Irani, S. R., Bettcher, B. M., Geschwind, M. D. & Gelfand, J. M. Episodic Bradycardia as Neurocardiac Prodrome to Voltage- Gated Potassium Channel Complex/Leucine-Rich, Glioma Inactivated 1 Antibody Encephalitis. *JAMA Neurol.* **71**, 1300–1304 (2015).

225. Butler, C. R. *et al.* Persistent anterograde amnesia following limbic encephalitis associated with antibodies to the voltage-gated potassium channel complex. *J. Neurol.*

Neurosurg. Psychiatry **85**, 387–91 (2014).

226. Dodds, C. M., Morein-Zamir, S. & Robbins, T. W. Dissociating Inhibition, Attention, and Response Control in the Frontoparietal Network Using Functional Magnetic Resonance Imaging. *Cereb. Cortex* **21**, 1155–1165 (2011).

227. Graus, F. *et al.* Neuronal surface antigen antibodies in limbic encephalitis: Clinical & immunologic associations. *Neurology* **71**, 930–936 (2008).

228. Gresa-Arribas, N. *et al.* Antibody titres at diagnosis and during follow-up of anti-NMDA receptor encephalitis: A retrospective study. *Lancet Neurol.* **13**, 167–177 (2014).

229. Yücesan, C. *et al.* Therapeutic plasma exchange in the treatment of neuroimmunologic disorders: Review of 50 cases. *Transfus. Apher. Sci.* **36**, 103–107 (2007).

230. Weinshenker, B. G. *et al.* A randomized trial of plasma exchange in acute central nervous system inflammatory demyelinating disease. *Ann. Neurol.* **46**, 878–886 (1999).

231. Trebst, C., Bronzlik, P., Kielstein, J. T., Schmidt, B. M. W. & Stangel, M. Immunoadsorption Therapy for Steroid-Unresponsive Relapses in Patients with Multiple Sclerosis. *Blood Purif.* **33**, 1–6 (2012).

232. Pham, H. P., Daniel-Johnson, J. A., Stotler, B. A., Stephens, H. & Schwartz, J. Therapeutic plasma exchange for the treatment of anti-NMDA receptor encephalitis. *J. Clin. Apher.* **26**, 320–325 (2011).

233. Jaben, E. A. & Winters, J. L. Plasma exchange as a therapeutic option in patients with neurologic symptoms due to antibodies to voltage-gated potassium channels: A report of five cases and review of the literature. *J. Clin. Apher.* **27**, 267–273 (2012).

234. DeSena, A. D. *et al.* Intravenous methylprednisolone versus therapeutic plasma exchange for treatment of anti-n-methyl-d-aspartate receptor antibody encephalitis: A retrospective review. *J. Clin. Apher.* **30**, 212–216 (2015).

235. Köhler, W. *et al.* Tryptophan immunoadsorption for the treatment of autoimmune encephalitis. *Eur. J. Neurol.* 203–206 (2014). doi:10.1111/ene.12389

236. Dogan Onugoren, M. *et al.* Immunoadsorption therapy in autoimmune encephalitides. *Neurol. Neuroimmunol. Neuroinflammation* **3**, (2016).

237. Sprenger, K. B., Huber, K., Kratz, W. & Henze, E. Nomograms for the prediction of patient's plasma volume in plasma exchange therapy from height, weight, and hematocrit. *J. Clin. Apher.* **3**, 185–190 (1987).

238. Batchelor, T. T., Platten, M. & Hochberg, F. H. Immunoadsorption therapy for paraneoplastic syndromes. *J. Neurooncol.* **40**, 131–136 (1998).

239. Klingel, R., Heibges, A. & Fassbender, C. Neurologic diseases of the central nervous system with pathophysiologically relevant autoantibodies--perspectives for immunoadsorption. *Atheroscler. Suppl.* **14**, 161–5 (2013).

240. Mazzi, G., de Roia, D., Cruciatti, B., Matà, S. & Catapano, R. Plasma exchange for anti GAD associated non paraneoplastic limbic encephalitis. *Transfus. Apher. Sci.* **39**, 229–233 (2008).

241. Mori, M. *et al.* Successful immune treatment for non-paraneoplastic limbic encephalitis. *J. Neurol. Sci.* **201**, 85–88 (2002).

242. Magana, S. M. *et al.* Beneficial Plasma Exchange Response in Central Nervous System Inflammatory Demyelination. *Arch. Neurol.* **68**, 870–878 (2011).

243. Köhler, W., Bucka, C. & Klingel, R. A Randomized and Controlled Study Comparing

Immunoadsorption and Plasma Exchange in Myasthenic Crisis. *J. Clin. …* **28**, 349–355 (2011).

244. Hewitt, P. E. *et al.* Hepatitis E virus in blood components: a prevalence and transmission study in southeast England. *Lancet* **384**, 1766–1773 (2014).

245. Keegan, M. *et al.* Plasma exchange for severe attacks of CNS demyelination: predictors of response. *Neurology* **58**, 143–146 (2002).

246. McKeon, G. L. *et al.* Cognitive outcomes following anti-N-methyl-D-aspartate receptor encephalitis: A systematic review. *J. Clin. Exp. Neuropsychol.* **40**, 234–252 (2018).

247. Farrell, B., Godwin, J., Richards, S. & Warlow, C. The United Kingdom transient ischaemic attack (UK-TIA) aspirin trial: final results. *J. Neurol. Neurosurg. Psychiatry* **54**, 1044–1054 (1991).

248. Schubert, J. *et al.* Management and prognostic markers in patients with autoimmune encephalitis requiring ICU treatment. *Neurol. - Neuroimmunol. Neuroinflammation* **6**, e514 (2019).

249. McKeon, G. L. *et al.* Cognitive and Social Functioning Deficits after Anti-N-Methyl-D-Aspartate Receptor Encephalitis: An Exploratory Case Series. *J. Int. Neuropsychol. Soc.* **22**, 828–838 (2016).

250. Bach, L. J. Long term rehabilitation management and outcome of anti-NMDA receptor encephalitis: case reports. *NeuroRehabilitation* **35**, 863–75 (2014).

251. Hinkle, C. D. *et al.* Neuropsychological characterization of three adolescent females with anti-NMDA receptor encephalitis in the acute, post-acute, and chronic phases: an inter-institutional case series. *Clin. Neuropsychol.* **31**, 268–288 (2017).

252. Urakami, Y. Neurocognitive rehabilitation following anti-NMDA-receptor encephalitis. *Act. Nerv. Super. Rediviva* **58**, 73–76 (2016).

253. Chen, Z., Wu, D., Wang, K. & Luo, B. Cognitive Function Recovery Pattern in Adult Patients With Severe Anti-N-Methyl-D-Aspartate Receptor Encephalitis: A Longitudinal Study. *Front. Neurol.* **9**, (2018).

254. Nicolle, D. C. M. & Moses, J. L. A Systematic Review of the Neuropsychological Sequelae of People Diagnosed with Anti N-Methyl-D-Aspartate Receptor Encephalitis in the Acute and Chronic Phases. *Arch. Clin. Neuropsychol.* **33**, 964–983 (2018).

255. Bäumler, G. *Farbe-Wort-Interferenztest nach Stroop*. (Hogrefe, 1985).

256. Wechsler, D. *Wechsler adult intelligence scale–Fourth Edition (WAIS–IV)*. (NCS Pearson, 2008).

257. Beck, A. T., Steer, R. A. & Brown, G. K. *Beck Depression Inventory - Second Edition (BDI-II)*. (1996).

258. Steer, R. A. & Beck, A. T. Beck Anxiety Inventory. *Eval. Stress A B. Resour.* 23–40 (1997).

259. Bates, D., Mächler, M., Bolker, B. & Walker, S. Fitting Linear Mixed-Effects Models Using lme4. *J. Stat. Softw.* **67**, (2015).

260. Xu, X. *et al.* Anti-NMDAR encephalitis: A single-center, longitudinal study in China. *Neurol. Neuroimmunol. Neuroinflammation* **7**, (2020).

261. de Bruijn, M. A. A. M. *et al.* Long-term neuropsychological outcome following pediatric anti-NMDAR encephalitis. *Neurology* **90**, e1997–e2005 (2018).

262. Riedel, G., Platt, B. & Micheau, J. Glutamate receptor function in learning and memory.

Behav. Brain Res. **140**, 1–47 (2003).

263. Grunze, H. *et al.* NMDA-dependent modulation of CA1 local circuit inhibition. *J. Neurosci.* **16**, 2034–2043 (1996).

264. Dudek, S. M. & Bear, M. F. Homosynaptic long-term depression in area CA1 of hippocampus and effects of N-methyl-D-aspartate receptor blockade. *Proc. Natl. Acad. Sci.* **89**, 4363–4367 (1992).

265. Malhotra, A. K. *et al.* NMDA receptor function and human cognition: The effects of ketamine in healthy volunteers. *Neuropsychopharmacology* **14**, 301–307 (1996).

266. Krystal, J. H. *et al.* Dissociation of ketamine effects on rule acquisition and rule implementation: Possible relevance to NMDA receptor contributions to executive cognitive functions. *Biol. Psychiatry* **47**, 137–143 (2000).

267. Phillips, O. R. *et al.* Superficial white matter damage in anti-NMDA receptor encephalitis. *J. Neurol. Neurosurg. Psychiatry* 1–8 (2017). doi:10.1136/jnnp-2017-316822

268. Matute, C. *et al.* N-Methyl-D-Aspartate Receptor Antibodies in Autoimmune Encephalopathy Alter Oligodendrocyte Function. *Ann. Neurol.* 1–7 (2020). doi:10.1002/ana.25699

269. Vahter, L. *et al.* Cognitive dysfunction during anti-NMDA-receptor encephalitis is present in early phase of the disease. *Oxford Med. Case Reports* **2014**, 74–76 (2014).

270. Parfene, C., Lipira, C., Gunning, F. & Gordon-Elliott, J. S. The Neurocognitive Profile of an Anti- N -Methyl-D-Aspartate Receptor Encephalitis Patient Presenting With Neuropsychiatric Symptoms. *J. Neuropsychiatry Clin. Neurosci.* **28**, 255–256 (2016).

271. Leypoldt, F., Gelderblom, M., Schöttle, D., Hoffmann, S. & Wandinger, K.-P. Recovery from severe frontotemporal dysfunction at 3years after N-methyl-d-aspartic acid (NMDA) receptor antibody encephalitis. *J. Clin. Neurosci.* **20**, 611–613 (2013).

272. Gold, S. M. *et al.* Detection of altered hippocampal morphology in multiple sclerosis-associated depression using automated surface mesh modeling. *Hum. Brain Mapp.* **35**, 30–37 (2014).

273. Sicotte, N. L. *et al.* Regional hippocampal atrophy in multiple sclerosis. *Brain* **131**, 1134–1141 (2008).

274. Calabrese, M. *et al.* No MRI evidence of cortical lesions in neuromyelitis optica. *Neurology* **79**, 1671–1676 (2012).

275. Finke, C. *et al.* Normal volumes and microstructural integrity of deep gray matter structures in AQP4+ NMOSD. *Neurol. - Neuroimmunol. Neuroinflammation* **3**, e229 (2016).

276. Husain, M. Transdiagnostic neurology: neuropsychiatric symptoms in neurodegenerative diseases. *Brain* **140**, 1535–1536 (2017).

277. Csernansky, J. G. *et al.* Preclinical detection of Alzheimer's disease: Hippocampal shape and volume predict dementia onset in the elderly. *Neuroimage* **25**, 783–792 (2005).

278. Gerardin, E. *et al.* Multidimensional classification of hippocampal shape features discriminates Alzheimer's disease and mild cognitive impairment from normal aging. *Neuroimage* **47**, 1476–1486 (2009).

279. Postma, T. S. *et al.* Hippocampal Shape Is Associated with Memory Deficits in Temporal Lobe Epilepsy. *Ann. Neurol.* **88**, 170–182 (2020).

280. Schmidt, P. *et al.* An automated tool for detection of FLAIR-hyperintense white-matter

lesions in Multiple Sclerosis. *Neuroimage* **59**, 3774–3783 (2012).

281. Smith, S. M. *et al.* Accurate, Robust, and Automated Longitudinal and Cross-Sectional Brain Change Analysis. *Neuroimage* **17**, 479–489 (2002).

282. Heine, J. *et al.* Beyond the limbic system: disruption and functional compensation of large-scale brain networks in patients with anti-LGI1 encephalitis. *J. Neurol. Neurosurg. Psychiatry* jnnp-2017-317780 (2018). doi:10.1136/jnnp-2017-317780

283. Filippi, M. *et al.* The contribution of MRI in assessing cognitive impairment in multiple sclerosis. *Neurology* **75**, 2121–2128 (2010).

284. Sumowski, J. F. *et al.* Cognition in multiple sclerosis. *Neurology* **90**, 278–288 (2018).

285. Rocca, M. A. *et al.* The hippocampus in multiple sclerosis. *Lancet Neurol.* **17**, 918–926 (2018).

286. Papadopoulos, D. *et al.* Substantial Archaeocortical Atrophy and Neuronal Loss in Multiple Sclerosis. *Brain Pathol.* **19**, 238–253 (2009).

287. Anderson, V. *et al.* Hippocampal atrophy in relapsing-remitting and primary progressive MS: a comparative study. *Mult. Scler.* **16**, 1083–1090 (2010).

288. Gold, S. M. *et al.* Smaller Cornu Ammonis 2–3/Dentate Gyrus Volumes and Elevated Cortisol in Multiple Sclerosis Patients with Depressive Symptoms. *Biol. Psychiatry* **68**, 553–559 (2010).

289. Planche, V. *et al.* Hippocampal microstructural damage correlates with memory impairment in clinically isolated syndrome suggestive of multiple sclerosis. *Mult. Scler. J.* **23**, 1214–1224 (2017).

290. Di Filippo, M., Portaccio, E., Mancini, A. & Calabresi, P. Multiple sclerosis and cognition: synaptic failure and network dysfunction. *Nat. Rev. Neurosci.* **19**, 599–609 (2018).

291. Hulst, H. E. *et al.* Functional adaptive changes within the hippocampal memory system of patients with multiple sclerosis. *Hum. Brain Mapp.* **33**, 2268–2280 (2012).

292. Longoni, G. *et al.* Deficits in memory and visuospatial learning correlate with regional hippocampal atrophy in MS. *Brain Struct. Funct.* **220**, 435–444 (2015).

293. Hyun, J.-W. *et al.* Deep gray matter atrophy in neuromyelitis optica spectrum disorder and multiple sclerosis. *Eur. J. Neurol.* **24**, 437–445 (2017).

294. Liu, Y. *et al.* Structural MRI substrates of cognitive impairment in neuromyelitis optica. *Neurology* **85**, 1491–1499 (2015).

295. Chen, X. *et al.* Altered volume and microstructural integrity of hippocampus in NMOSD. *Mult. Scler. Relat. Disord.* **28**, 132–137 (2019).

296. Popescu, B. F. G. *et al.* Absence of cortical demyelination in neuromyelitis optica. *Neurology* **75**, 2103–2109 (2010).

297. Wang, Q. *et al.* Gray Matter Volume Reduction Is Associated with Cognitive Impairment in Neuromyelitis Optica. *AJNR. Am. J. Neuroradiol.* **36**, 1822–9 (2015).

298. Pittock, S. J. *et al.* Neuromyelitis Optica Brain Lesions Localized at Sites of High Aquaporin 4 Expression. *Arch. Neurol.* **63**, 964 (2006).

299. Kesner, R. P. & Hunsaker, M. R. The temporal attributes of episodic memory. *Behav. Brain Res.* **215**, 299–309 (2010).

300. Gee, C. E. *et al.* NMDA receptors and the differential ischemic vulnerability of hippocampal neurons. *Eur. J. Neurosci.* **23**, 2595–2603 (2006).

301. Li, S. *et al.* Hippocampal shape analysis of Alzheimer disease based on machine learning methods. *Am. J. Neuroradiol.* **28**, 1339–1345 (2007).

302. Achterberg, H. C. *et al.* Hippocampal shape is predictive for the development of dementia in a normal, elderly population. *Hum. Brain Mapp.* **35**, 2359–2371 (2014).

303. Gold, A. E. & Kesner, R. P. The role of the CA3 subregion of the dorsal hippocampus in spatial pattern completion in the rat. *Hippocampus* **15**, 808–814 (2005).

304. Sapolsky, R., Uno, H., Rebert, C. & Finch, C. Hippocampal damage associated with prolonged glucocorticoid exposure in primates. *J. Neurosci.* **10**, 2897–2902 (1990).

305. Csernansky, J. G. *et al.* Hippocampal Deformities in Schizophrenia Characterized by High Dimensional Brain Mapping. *Am. J. Psychiatry* **159**, 2000–2006 (2002).

306. Shenton, M. E., Gerig, G., McCarley, R. W., Székely, G. & Kikinis, R. Amygdala-hippocampal shape differences in schizophrenia: The application of 3D shape models to volumetric MR data. *Psychiatry Res. - Neuroimaging* **115**, 15–35 (2002).

307. Gibson, L. L., McKeever, A., Coutinho, E., Finke, C. & Pollak, T. A. Cognitive impact of neuronal antibodies: encephalitis and beyond. *Transl. Psychiatry* **10**, 304 (2020).

308. DeLuca, J., Chiaravalloti, N. D. & Sandroff, B. M. Treatment and management of cognitive dysfunction in patients with multiple sclerosis. *Nat. Rev. Neurol.* **16**, 319–332 (2020).

309. Lampit, A. *et al.* Computerized Cognitive Training in Multiple Sclerosis: A Systematic Review and Meta-analysis. *Neurorehabil. Neural Repair* **33**, 695–706 (2019).

310. Michael, S., Waters, P. & Irani, S. R. Stop testing for autoantibodies to the VGKC-complex: only request LGI1 and CASPR2. *Pract. Neurol.* **1**, practneurol-2019-002494 (2020).

311. Broadley, J. *et al.* Prognosticating autoimmune encephalitis: A systematic review. *J. Autoimmun.* **96**, 24–34 (2019).

312. Al-Diwani, A. *et al.* The psychopathology of NMDAR-antibody encephalitis in adults: a systematic review and phenotypic analysis of individual patient data. *The Lancet Psychiatry* **6**, 235–246 (2019).

313. Melzer, N., Budde, T., Stork, O. & Meuth, S. G. Limbic Encephalitis: Potential Impact of Adaptive Autoimmune Inflammation on Neuronal Circuits of the Amygdala. *Front. Neurol.* **6**, 1–10 (2015).

314. Gothard, K. M. Multidimensional processing in the amygdala. *Nat. Rev. Neurosci.* **21**, 565–575 (2020).

315. Whelan, C. D. *et al.* Heritability and reliability of automatically segmented human hippocampal formation subregions. *Neuroimage* **128**, 125–137 (2016).

316. Hanert, A. *et al.* Hippocampal Dentate Gyrus Atrophy Predicts Pattern Separation Impairment in Patients with LGI1 Encephalitis. *Neuroscience* **400**, 120–131 (2019).

317. Spanò, G. *et al.* Dreaming with hippocampal damage. *Elife* **9**, 1–15 (2020).

318. Vogrig, A. *et al.* Seizure specificities in patients with antibody-mediated autoimmune encephalitis. *Epilepsia* **60**, 1508–1525 (2019).

319. Romoli, M. *et al.* Hippocampal epileptogenesis in autoimmune encephalitis. *Ann. Clin. Transl. Neurol.* **6**, 2261–2269 (2019).

320. Ayşit-Altuncu, N., Ulusoy, C., Öztürk, G. & Tüzün, E. Effect of LGI1 antibody-positive

IgG on hippocampal neuron survival. *Neuroreport* **29**, 932–938 (2018).

321. Malmgren, K. & Thom, M. Hippocampal sclerosis-Origins and imaging. *Epilepsia* **53**, 19–33 (2012).

322. Mathern, G. W., David Adelson, P., Cahan, L. D. & Leite, J. P. Hippocampal neuron damage in human epilepsy: Meyer's hypothesis revisited. in *Progress in Brain Research* **135**, 237–251 (2002).

323. Duffau, H. Brain plasticity: From pathophysiological mechanisms to therapeutic applications. *J. Clin. Neurosci.* **13**, 885–897 (2006).

324. van den Heuvel, M. P. & Hulshoff Pol, H. E. Exploring the brain network: a review on resting-state fMRI functional connectivity. *Eur. Neuropsychopharmacol.* **20**, 519–534 (2010).

325. Fox, M. D. & Greicius, M. Clinical applications of resting state functional connectivity. *Front. Syst. Neurosci.* **4**, 19 (2010).

326. Rocca, M. A. *et al.* Default-mode network dysfunction and cognitive impairment in progressive MS. *Neurology* **74**, 1252–1259 (2010).